WIICT2018

Proceedings of the Workshop on Innovation on Information and Communication Technologies 2018

Institute ITACA
Information and Communication Technologies

Editors:
Dr. Carlos Fernandez-Llatas
Dra. Maria Guillen

Committees

Organizing Committee

- **Chair:**Maria Guillem, Universitat Politècnica de València, Spain
- Alberto Bonastre, Universitat Politècnica de València, Spain
- Jose Manuel Catala, Universitat Politècnica de València, Spain
- Montserrat Robles, Universitat Politècnica de València, Spain
- Carlos Fernández-Llatas, Universitat Politècnica de València, Spain
- Jose Mariano Dahoui, Universitat Politècnica de València, Spain
- Isidora Navarro, Universitat Politècnica de València, Spain
- Manuel Traver Salcedo, Universitat Politècnica de València, Spain
- Lucia Aparici, Universitat Politècnica de València, Spain

Scientific Committee

- **Chair**: Carlos Fernandez-Llatas, Universitat Politècnica de València, Spain
- Paulo de Carvalho, University of Coimbra, Portugal
- Anna-Maria Bianchi, Politecnico di Milano, Italy
- Jorge Munoz-Gama, Pontificia Universidad Catolica de Chile
- Fernando Seoane, Karolinska Institutet
- Jorge Henriques, University of Coimbra, Portugal
- Cenk Demiroglu, Ozyegin University, Turkey
- Johan Gustav Bellika, National Center of Telemedicine, Norway
- Yigzaw Kassaye Yitbarek, University of Tromso, Norway
- Raymundo Barrales, Universidad Autónoma Metropolitana de México
- Frank Y. Li, University of Agder, Norway
- Pilar Sala, MySphera., Spain
- Alvaro Martinez, MySphera, Spain
- Jose Carlos Campelo, Universitat Politècnica de València, Spain
- Juan Vicente Capella, Universitat Politècnica de València, Spain
- Antonio Mocholí, Universitat Politècnica de València, Spain
- Sara Blanc, Universitat Politècnica de València, Spain
- Juan-Carlos Baraza-Calvo, Universitat Politècnica de València, Spain
- Juan Carlos Ruiz, Universitat Politècnica de València, Spain
- Joaquin Gracia, Universitat Politècnica de València, Spain
- David De Andres, Universitat Politècnica de València, Spain
- Ricardo Mercado, Universitat Politècnica de València, Spain
- Miguel Rodrigo Bort, Universitat Politècnica de València, Spain
- Alejandro Liberos, Universitat Politècnica de València, Spain
- Jorge Pedrón, Universitat Politècnica de València, Spain
- Lenin Lemus, Universitat Politècnica de València, Spain
- Vicente Traver, Universitat Politècnica de València, Spain
- Antonio Martinez-Millana, Universitat Politècnica de València, Spain
- Jose Luis Bayo-Monton, Universitat Politècnica de València, Spain
- Lucia Aparici-Tortajada, Universitat Politècnica de València, Spain
- Juan Miguel García-Gomez, Universitat Politècnica de València, Spain
- Elies Fuster, Universitat Politècnica de València, Spain
- Carlos Saez, Universitat Politècnica de València, Spain
- Miguel Angel Rodriguez-Hernandez, Universitat Politècnica de València, Spain
- Canek Portillo Jimenez, Universitat Politècnica de València, Spain
- Ángel Perles, Universitat Politècnica de València, Spain
- Julian Camilo Romero-Chavarro, Universitat Politècnica de València, Spain
- Diego Boscá Tomás, Universitat Politècnica de València, Spain
- Luis Tello-Oquendo, Universitat Politècnica de València, Spain

- Israel Leyva-Mayorga, Universitat Politècnica de València, Spain
- Ángel Sanchis-Cano, Universitat Politècnica de València, Spain
- Luis José Saiz Adalid, Universitat Politècnica de València, Spain
- Gema Ibañez, Universitat Politècnica de València, Spain
- Pedro Yuste, Universitat Politècnica de València, Spain
- Daniel Gil Tomàs, Universitat Politècnica de València, Spain
- Conrado Javier Calvo Saiz, Universitat Politècnica de València, Spain
- Sabina Asensio, Universitat Politècnica de València, Spain
- Beatriz Garcia-Baños, Universitat Politècnica de València, Spain
- Diogo Nunes, University of Coimbra, Portugal
- Adriana Leal, University of Coimbra, Portugal
- Zoe Valero Ramón, Universitat Politècnica de València, Spain

Table of Contents

A Review on Information Fusion Techniques with Application to Heart Failure Decompensation Prediction

Diogo Nunes[1], César Teixeira[1], Paulo Carvalho[1], Simão Paredes[2], Anna Bianchi[3], Teresa Rocha[2], Vicente Traver[4], and Jorge Henriques[1]

[1] Centre for Informatics and Systems, Polo II Coimbra, 3030-290, Portugal
{dbnunes, cteixei, carvalho, jh}@dei.uc.pt
[2] Coimbra Polytechnic - ISEC, Coimbra, Portugal
{sparedes, teresa}@isec.pt
[3] Department of Electronics, Information and Bioengineering, Politecnico di Milano, Piazza Leonardo da Vinci 32, 20133 Milan, Italy
Annamaria.bianchi@polimi.it
[4] Institute for Information and Communication Technologies, Universitat Politècnica de València, Valencia, 46022, Spain
vtraver@itaca.upv.es

Abstract. Cardiac function deterioration of heart failure patients is frequently manifested by the occurrence of decompensation events. One relevant step to adequately prevent cardiovascular status degradation is to predict decompensation episodes in order to allow preventive medical interventions. As this deterioration is reflected in several physiological parameters, information fusion techniques may provide an effective framework to develop more accurate prediction schemes. In this work is presented a review on information fusion techniques that may be useful on the prediction of decompensation events and finally, a possible fusion scheme and some preliminary results are presented on the prediction of heart failure decompensation events resorting to feature spaces that perform the fusion of different physiological parameters.

1 Introduction

Information fusion is known as the integration of data and knowledge from several sources. Through information fusion a system can be better characterized by exploring the redundancies and complementarities of the data that is produced from that system. The term information fusion in this review encompasses the fusion processes at all the abstraction levels, i.e., from the sensor/data fusion to higher levels of information, such as features, events, decisions or expert knowledge.

Before some main methods used in information fusion are described it is important to give some definitions of the concept. One of the most accepted definitions by researchers is from the Joint Directors Laboratories (JDL), which states: "*A multi-level process dealing with the association, correlation, combination of data and information from single and multiple sources to achieve refined position, identify estimates*

C.Fernandez-Llatas and M.Guillen (Ed.):
Workshop on Innovation on
Information and Communication Technologies
(ITACA-WIICT 2018)

ISBN 978-84-09-07373-3

and complete and timely assessments of situations, threats and their significance." [1]. Another well-known definition is from [2]: "*data fusion techniques combine data from multiple sensors and related information from associated databases to achieve improved accuracy and more specific inferences than could be achieved by the use of a single sensor alone*." One particular definition that fits the research interest of this work is: "*Information fusion encompasses the theory, techniques, and tools conceived and employed for exploiting the synergy in the information acquired from multiple sources (sensor, databases, information gathered by humans etc.) such that the resulting decision or action is in some sense better (qualitatively and quantitatively, in terms of accuracy, robustness and etc.) than would be possible, if these sources were used individually without such synergy exploitation*.", from [3].

Information fusion as a multidisciplinary area that it is, contains several categorizations of the existing methods. In this work is not intended to do an exhaustive review in all the existing methods neither in all possible categorizations of such methods. It will be focused in a few techniques that are common in most of the applications, and in categorizations that are suitable for the chosen techniques.

2 Categorization of Information Fusion Techniques

As referred before that are possible ways to categorize the fusion methods, depending on the given application and field of implementation. In the next list are presented some, that are differentiated by the type of sources and level of analysis:

- Based on the relation between sources [4];
- According to the input/output abstraction level [3];
- Following the abstraction level of the employed data [5].
- Based on data-related fusion aspects [6].

Other categorizations could be considered, namely the ones based on the architectures of fusion, or the ones more appropriate to the design of data fusion systems. However, these ones will not be considered since this work is more concerned in understanding the relations between the fusion tasks and employed data.

2.1.1 Based on the Relation Between Sources

In this categorization the fusion methods are divided by the relations of the sources, and three main category of data fusion applications are proposed, which are the situations where the sources are:

- **Complementary:** When the sources that describe a given process have different perspectives and are of the same type. For example, two cameras filming an object from two different angles, or two different leads of an Electrocardiogram (ECG), or even two microphones at different spatial positions. Through the fusion of the information is possible to obtain a more complete knowledge about the process.

- **Redundant:** When the sources that describe a given process are at the same perspective and are of the same type. For example, two cameras at the same perspective. This fusion can provide improved knowledge by exploring the redundancy of data and reduce the intrinsic errors and noise of the recording instruments.
- **Cooperative:** When data from sources of different data types/modalities are fused together. For example, the fusion of information of multi-modal physiologic data, i.e. the fusion of data coming from an, e.g., ECG and Phonocardiogram (PCG), both are recording the same process (the cardiac function) but recording it from different ways.

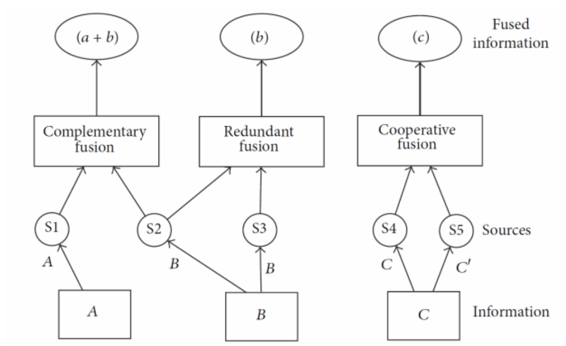

Figure 1. Categorization based on the relations between the sources [7].

2.1.2 According to the Input/Output Abstraction Level

In [3] is described how to differentiate the processes of information fusion based on its inputs and outputs. It was the first categorization that differentiated the methods and techniques based on the abstraction level of application.

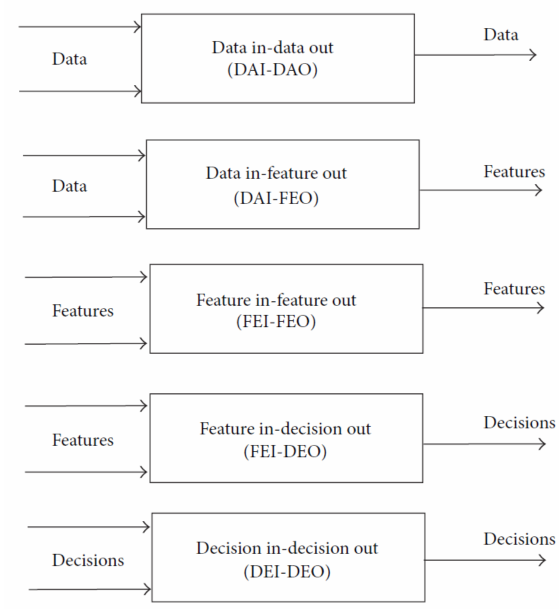

Figure 2. Categorization according to the input/output data types and nature [7].

2.1.3 Following the Abstraction Level of the Employed Data

As in [3], the following work also categorized the methods based on the abstraction levels, but with a few nuances between them. In this work, the methods are divided in the following way:

- **Signal level:** Addresses the fusion at the level of one-dimensional signals, e.g. one lead ECG, PCG, Arterial Blood Pressure, and so on.
- **Pixel level:** The methods used at the raw level on image data.
- **Characteristic:** Addresses fusion mechanism employed in level of features of multiple sources, be them images or signals.
- **Symbol:** It is respective to fusion at the decision level, i.e., the fusion of the results of several models that intent to represent a given system or process.

2.1.4 Based on Data-Related Fusion Aspects

In [6] the categorization is focused on the data characteristics provided by the sensors, particularly in the fusion challenges of different input data. It was identified four main challenges related to multi-sensor data fusion.

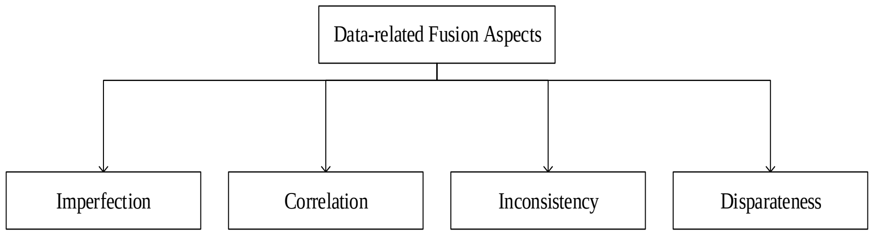

Figure 3. Categorization based on Data-Related Fusion Aspects.

- **Imperfection:** Imperfection in this context refers to the uncertainty associated with the measures from the sensors, as also the stochasticity of the process being recorded. One fusion technique must be able to consider these uncertain phenomena in order to provide more accurate estimates.
- **Correlation:** This problem is present when different sensors are exposed to the same external noise, introducing a bias in the measurements. The obtained results for the fusion methodology may suffer from under/over confidence if these dependencies between sensors are not accounted for.
- **Inconsistency:** Inconsistency refers to the problem of having conflicting data from different sensors, or even the problem of having spurious data with outliers or missing values. The challenge in this aspect resides in the problem of fusing several sources of information that contradicts each other or that present abnormal measurements due to systems' failure. Another challenge that resides in the inconsistency challenge is the one of having different source of data that present different sampling frequencies.
- **Disparateness:** Fusing information from different modalities, e.g. an fMRI with an EEG, can be a challenge due to the difference of the sensors nature.

2.1.5 Categorization Used in this Work

The categorization used in this work also follows a differentiation based on the abstraction levels, namely:

- **Measurements:** Comprises all fusion mechanism that perform at the level of raw measurements coming from sensors, without distinguish if the produced data is images or one-dimensional signals;
- **Features:** Methods used at the fusion of features from different sources;
- **Decisions:** Respective to the combination of several decision models that describe a process or system.

Our categorization does not intend to depart from the presented ones, but find a consensus/synthesis between all of them. For example, in measurements level is addressed the DAI-DAO and DAI-FEO of the categorization presented in [3] and the signal and pixel level from the categorization in [5]. Our characteristics level comprises the FEI-FEO and FEI-DEO levels and is the same as the characteristic level from [5]. The Decisions level corresponds to the DEI-DEO and the symbol levels from the previous categorizations. The categorization presented in [4] based on the relation between sources is also considered, by considering that at each abstraction level, the information sources can be complementary, redundant or cooperative. Moreover, the suitability of each method will be considered regarding the challenges present in [6].

2.2 Information Fusion: Measurement Level

The fusion at the level of measurements normally focus on the preprocessing phase, by estimating the state of a variable of interest. These techniques are used to fuse redundant information in order to obtain a better parameter estimation, or even to fuse complementary information if the system that describes the interactions between the measurements is possible to be defined. However, it is difficult to adopt these techniques when facing fusion problems with inconsistent or disparate data [6]. Among the techniques at this level, the weighted averages and state estimators are the most common to be employed.

2.2.1 Weighted Averages

This method performs the average of all available sensor measurements at each time. Despite being simple, it is useful when the sensors are of the same type and recording the same process (redundant fusion). By taking the mean value, uncertainty can be reduced [8].

2.2.2 State Estimators

The Kalman filter [9] is characterized as an optimal linear estimation algorithm, i.e., it is used to estimate the optimal values of a parameter. This method is used in situations where there are multiple measurements (direct or indirect) of a parameter, however these measurements can be biased by noise. By using the Kalman filter, these noises can be considered to produce a more accurate estimation, therefore this method is usually applied in cases where the data is imperfect, or used to consider the correlation challenge, if the errors covariance are taken into account. Additionally, if the state system is known, fusion of complementary sensors' information can be performed, resulting in a refined state estimation. It is a recursive process composed by two phases: (1) predict the next state based on the system definition; (2) update the estimation based on the noisy measurements of the current state.

However, the Kalman filter takes some assumptions that make it inapplicable in some situations, such when the process and observation errors are not drawn from a Gaussian distribution, or the process to be described mathematically is nonlinear. To take into account these situations some variants of the presented methodology were developed known as the nonlinear state estimators, namely the Extended Kalman Filter (EKF), the Unscented Kalman Filter (UKF) and Particle Filter (PF). The EKF assumes that the nonlinear system can be locally approximated by a linear function, and is differentiable. UKF approximates the Gaussian distributions instead of the nonlinear function to take into account highly nonlinear functions that cannot be approximated linearly. These two methods, although taking into account the nonlinearity of the process, still assume that the errors follow a Gaussian distribution. In the case of the non-normality of the errors' probability density function, the PF can be employed.

2.3 Information Fusion: Feature Level

Feature level fusion concerns with the fusion of several features from different sources in order to produce an output, when the latter can be categorical (classification problem) or continuous (regression problem). At this level, features from different sources/sensors are computed and fed to a classifier/regressor which maps the relations between features trough an automatic learning procedure, to obtain a fused output in the end. Due to the higher abstraction level, these methodologies provide a more flexible framework to deal with disparateness and inconsistency fusion problems [10]. The number of classifiers/regressors is enormous due to the always evolving and broad area of Machine Learning, ranging from linear to non-linear, supervised or non-supervised, and parametric or non-parametric techniques. Moreover, there is no general better solutions, as each method can be more appropriate in a given situation.

Tackling the problem of information fusion, K-Nearest Neighbors (K-NNs) have been widely used in the field of activity recognition through fusion of accelerometers signals [11]–[14], as also Support Vector Machines (SVMs) [15]–[17] and Artificial Neural Networks (ANNs) [18]–[20]. In other fields of physiological monitoring, a Linear Discriminant Analysis (LDA) classifier was used to detect stress in driving tasks [21], and in the prediction of Heart Failure (HF) decompensations events Decision Trees (DTs) [22], [23], K-NNs [24], SVMs [22], [23], [25] and Naïve-Bayes (NB) [26] were used.

2.4 Information Fusion: Decision Level

Decision level fusion corresponds to the fusion of several decisions from different models developed for each source. This is the highest abstraction level in the categorization of information fusion, and these techniques facilitate a framework to fuse information that is highly heterogeneous, e.g., an ECG with an fMRI image. However, higher the abstraction level, lesser information is retained and possible dependencies and relations between sources may be lost, which can be preponderant to achieve an effective model [27]. Among the techniques at this level, the Bayesian Inference [28], [29], Fuzzy Logic [30], [31], Dempster-Shaffer [32] and Ensemble Heuristics [33], [34] are the most common to be employed.

3 Information Fusion on the Prediction of Decompensation Events

Heart Failure is characterized by the occurrence of structural or functional abnormalities in the normal filling or ejection of blood in the ventricle. Treatment of HF typically takes place at the hospital as consequence of the repeated occurrence of acute decompensation events reflecting the continuous deterioration of the patient's cardiac function. The poor prognosis and recurrent admissions associated with HF can help explain why the diagnosis of HF is, in fact, the commonest among all hospitalizations, with related treatment costs accounting for 2-3% of total expenditure of healthcare systems in developed countries [35]–[37].

Based on the above, it is pertinent to analyze HF data towards the exhaustive identification and characterization of predictors and this way, ultimately improve treatment, decrease the number of readmissions and reduce healthcare costs [35], [37]. In other words, monitoring physiological indicators able to reflect the progress of the decompensation (such as alterations in the ventricular filling pressures, in the body weight (BW), in the heart rate (HR) and the presence of arrhythmias, among others) might be a key factor in improving risk stratification of patients [35].

Studies reporting HF predictors of morbidity, mortality, destabilizations (sudden alternating periods of apparent stability) and re-hospitalizations can be found in literature [35], [38]. Many of these report the use of blood pressure (BP) as predictor, which is in accordance with the characterization of cardiovascular diseases, particularly hypertension, that is typically associated with high BP [38]–[48]. BW, another feature widely reported in HF prediction studies, was observed to increase before the occurrence of an acute decompensation event [40], [49]. Furthermore, intracardiac impedance has also been recently reported to decrease as result of HF worsening being a strong candidate as HF decompensation predictor [50], [51].

Based on the aforementioned, it is crucial the existence of approaches that are able to fuse relevant information from the physiological parameters in order to predict and prevent HF decompensation events and consequently the worsening of HF patients. In the next sub-sections is proposed a fusion scheme for decompensated HF oriented data, with the goal of combining information that can be useful in the prognosis of HF decompensation events.

3.1 A Possible Fusion Scheme

Due to the ambulatory nature of physiological monitoring, the acquired data may be subject to uncertainty and inconsistency, with the presence of missing values and outliers. Furthermore, depending on the data acquisition system, signals with different sampling rates may also be present. Based on the referred possibilities, a fusion scheme at the level of features may be more appropriate, once the higher abstraction level provides a more flexible framework. Another consequence of fusing the information at this level is the loss of information present in the raw data which may be relevant to obtain relationships between sources, to tackle this issue the features obtained from the signals must be the most representative of the problem at hand. In the

HF decompensation context, studies suggest that modifications and trend onsets can be observed on HR, BW, BP, thoracic impedance, or respiratory rate (RR) weeks before a decompensation event occurs. Given this, the proposed methodology aims to find relevant feature's spaces that have predictive value in HF decompensation events. To find the relevant features to be fused, the following procedure is performed:

- **Preprocessing:** Imputation of missing data through linear interpolation and obtainment of the 20 last daily measurements prior to the event in the case of the decompensation patients, and random 20 consecutive daily measurements in the case of the control group. The time window of 20 days was chosen based on the hypothesis that it has a sufficient length to capture all the modifications and trends caused by an incoming decompensation event [52].
- **Feature computation:** For each physiological parameter four features are calculated with the intention of capturing the state of the 20 days measurements, namely the mean, the standard deviation, the slope, and the absolute value of the slope. The mean is used in order to capture the level of magnitude of the physiological parameter, the standard deviation its variability, the slope its trend and evolution in the past 20 days, and finally, the absolute value of the slope, based on the hypothesis that a positive or negative slope against a zero slope may have discriminant power to differentiate between prior decompensation class (high risk) and normal condition class (low risk), i.e., the presence of a trend (positive or negative) against a null trend. The slope value is obtained by a linear regression.
- **Feature selection and classification:** As a consequence of calculating 4 features for each physiological time-series, the number of obtained features becomes increasingly high as the number of sensors being used increase. Due to this, a feature selection procedure must be employed in order to keep the relevant features, eliminating the non-useful, and reducing the feature space dimensionality. Using the best feature subset encountered, a classification system can be used in order to emit alarms if incoming decompensation events are detected.

3.2 Preliminary Results on the MyHeart Dataset

The MyHeart dataset [46], is a heart failure telemonitoring study with annotated heart failure episodes, which is a private dataset composed by daily physiological parameters such as body weight (BW), systolic blood pressure (BP), heart rate (HR), respiratory rate (RR), external and internal thoracic impedance, (RE) and (RI), respectively.

This study enrolled 148 patients from six clinical centers in Germany and Spain that agreed with data acquisition and processing under anonymous conditions. During the study the patients were requested to measure the physiological measurements referred above. As a consequence of the ambulatory nature of the study, the data produced is composed by missing values and noise. Consequently, only 39 patients were used in this present study (the ones who have at least one measurement of all the physiological parameters 20 days preceding a decompensation event). This selection was performed in order to find the relevant and discriminatory features that precede a decompensation event. Additionally, six cardiologists have analyzed the data, identifying which patients had experienced a decompensation event (14 patients) and which patients had not (25 patients).

A genetic algorithm (GA) was used for the feature selection procedure. The used fitness function is based on the maximization of the geometric mean (Gmean) of Fisher Discriminant Classifiers (FD) on a Leave-One-Out (LOO) validation. FD classifiers, which are linear classifiers, were used to prevent high degrees of freedom in the training procedure and obtain models with generalization capabilities. The feature subsets were limited to a maximum of three features and a minimum of one. This choice was made to prevent overfitting and for interpretability purposes. The interpretability in this study is taken as an important characteristic, because in the case of the development of a clinical application, as a decision support method that it is, the clinicians may require observing and understand why decompensation alarms occurred, or did not.

The best feature combination achieved is the mean of the weight, the standard deviation of the blood pressure and the mean of the intrathoracic bio impedance, with a geometric mean of 88.32%, and a sensitivity and specificity of 92.86% and 84%, respectively.

4 Conclusion

In this work was presented a review on information fusion techniques that may be useful on the prediction of decompensation events. Based on the advantages and disadvantages of the different types of information fusion techniques, a possible framework to fuse physiological measurements with application to HF decompensation prediction was proposed. In future work, is intended to perform a more in-depth exploration on the advantages and limitations of the proposed fusion framework for HF decompensation prediction, as also test new approaches.

References

[1] F. E. White, “Data Fusion Lexicon,” *Data Fusion Subpanel Jt. Dir. Lab. Tech. Panel C3*, vol. 15, no. 0704, p. 15, 1991.

[2] D. L. Hall and J. Llinas, “An introduction to multisensor data fusion,” *Proc. IEEE*, vol. 85, no. 1, pp. 6–23, 1997.

[3] B. V. Dasarathy, “Sensor fusion potential exploitation-innovative architectures and illustrative applications,” *Proc. IEEE*, vol. 85, no. 1, pp. 24–38, 1997.

[4] H. F. Durrant-Whyte, “Sensor Models and Multisensor Integration,” *Int. J. Rob. Res.*, vol. 7, no. 6, pp. 97–113, Dec. 1988.

[5] R. C. Luo, Chih-Chen Yih, and Kuo Lan Su, “Multisensor fusion and

integration: approaches, applications, and future research directions," *IEEE Sens. J.*, vol. 2, no. 2, pp. 107–119, Apr. 2002.

[6] B. Khaleghi, A. Khamis, F. O. Karray, and S. N. Razavi, "Multisensor data fusion: A review of the state-of-the-art," *Inf. Fusion*, vol. 14, no. 1, pp. 28–44, Jan. 2013.

[7] F. Castanedo, "A Review of Data Fusion Techniques," *Sci. World J.*, vol. 2013, pp. 1–19, 2013.

[8] R. C. Luo and M. G. Kay, "A tutorial on multisensor integration and fusion," in *[Proceedings] IECON '90: 16th Annual Conference of IEEE Industrial Electronics Society*, pp. 707–722.

[9] R. E. Kalman, "A New Approach to Linear Filtering and Prediction Problems," *J. Basic Eng.*, vol. 82, no. 1, p. 35, Mar. 1960.

[10] R. C. King, E. Villeneuve, R. J. White, R. S. Sherratt, W. Holderbaum, and W. S. Harwin, "Application of data fusion techniques and technologies for wearable health monitoring," *Med. Eng. Phys.*, vol. 42, pp. 1–12, Apr. 2017.

[11] S. Thiemjarus, "A Device-Orientation Independent Method for Activity Recognition," in *2010 International Conference on Body Sensor Networks*, 2010, pp. 19–23.

[12] H. Ghassemzadeh, E. Guenterberg, S. Ostadabbas, and R. Jafari, "A motion sequence fusion technique based on PCA for activity analysis in body sensor networks," in *2009 Annual International Conference of the IEEE Engineering in Medicine and Biology Society*, 2009, vol. 2009, pp. 3146–3149.

[13] Shaopeng Liu, R. X. Gao, D. John, J. W. Staudenmayer, and P. S. Freedson, "Multisensor Data Fusion for Physical Activity Assessment," *IEEE Trans. Biomed. Eng.*, vol. 59, no. 3, pp. 687–696, Mar. 2012.

[14] L. Atallah, B. Lo, R. King, and G.-Z. Yang, "Sensor Positioning for Activity Recognition Using Wearable Accelerometers," *IEEE Trans. Biomed. Circuits Syst.*, vol. 5, no. 4, pp. 320–329, Aug. 2011.

[15] D. Rodriguez-Martin, A. Samà, C. Perez-Lopez, A. Català, J. Cabestany, and A. Rodriguez-Molinero, "SVM-based posture identification with a single waist-located triaxial accelerometer," *Expert Syst. Appl.*, vol. 40, no. 18, pp. 7203–7211, Dec. 2013.

[16] A. Mannini and A. M. Sabatini, "On-line classification of human activity and estimation of walk-run speed from acceleration data using support vector machines," in *2011 Annual International Conference of the IEEE Engineering in Medicine and Biology Society*, 2011, pp. 3302–3305.

[17] O. Banos, M. Damas, H. Pomares, A. Prieto, and I. Rojas, "Daily living activity recognition based on statistical feature quality group selection," *Expert Syst. Appl.*, vol. 39, no. 9, pp. 8013–8021, Jul. 2012.

[18] K. Altun, B. Barshan, and O. Tunçel, "Comparative study on classifying human activities with miniature inertial and magnetic sensors," *Pattern Recognit.*, vol. 43, no. 10, pp. 3605–3620, Oct. 2010.

[19] S. H. Roy, M. S. Cheng, S.-S. Chang, J. Moore, G. De Luca, S. H. Nawab, and C. J. De Luca, "A Combined sEMG and Accelerometer System for Monitoring Functional Activity in Stroke," *IEEE Trans. Neural Syst. Rehabil. Eng.*, vol. 17, no. 6, pp. 585–594, Dec. 2009.

[20] J.-Y. Yang, J.-S. Wang, and Y.-P. Chen, “Using acceleration measurements for activity recognition: An effective learning algorithm for constructing neural classifiers,” *Pattern Recognit. Lett.*, vol. 29, no. 16, pp. 2213–2220, Dec. 2008.

[21] J. A. Healey and R. W. Picard, “Detecting Stress During Real-World Driving Tasks Using Physiological Sensors,” *IEEE Trans. Intell. Transp. Syst.*, vol. 6, no. 2, pp. 156–166, Jun. 2005.

[22] A. Candelieri, D. Conforti, F. Perticone, A. Sciacqua, K. Kawecka-Jaszcz, and K. Styczkiewicz, “Early detection of decompensation conditions in heart failure patients by knowledge discovery: The HEARTFAID approaches,” in *2008 Computers in Cardiology*, 2008, vol. 35, pp. 893–896.

[23] A. Candelieri, D. Conforti, A. Sciacqua, and F. Perticone, “Knowledge discovery approaches for early detection of decompensation conditions in heart failure patients,” in *ISDA 2009 - 9th International Conference on Intelligent Systems Design and Applications*, 2009, pp. 357–362.

[24] J. Henriques, P. Carvalho, S. Paredes, T. Rocha, J. Habetha, M. Antunes, and J. Morais, “Prediction of Heart Failure Decompensation Events by Trend Analysis of Telemonitoring Data,” *IEEE J. Biomed. Heal. Informatics*, vol. 19, no. 5, pp. 1757–1769, Sep. 2015.

[25] A. Candelieri, “A Hyper-Solution Framework for SVM Classification: Application for Predicting Destabilizations in Chronic Heart Failure Patients,” *Open Med. Inform. J.*, vol. 4, no. 1, pp. 136–140, Jul. 2010.

[26] G. Koulaouzidis, D. K. Iakovidis, and A. L. Clark, “Telemonitoring predicts in advance heart failure admissions,” *Int. J. Cardiol.*, vol. 216, pp. 78–84, Aug. 2016.

[27] R. Gravina, P. Alinia, H. Ghasemzadeh, and G. Fortino, “Multi-sensor fusion in body sensor networks: State-of-the-art and research challenges,” *Inf. Fusion*, vol. 35, no. October 2017, pp. 68–80, May 2017.

[28] P. Zappi, T. Stiefmeier, E. Farella, D. Roggen, L. Benini, and G. Troster, “Activity recognition from on-body sensors by classifier fusion: sensor scalability and robustness,” in *2007 3rd International Conference on Intelligent Sensors, Sensor Networks and Information*, 2007, pp. 281–286.

[29] L. Atallah, B. Lo, R. Ali, R. King, and G.-Z. Guang-Zhong Yang, “Real-Time Activity Classification Using Ambient and Wearable Sensors,” *IEEE Trans. Inf. Technol. Biomed.*, vol. 13, no. 6, pp. 1031–1039, Nov. 2009.

[30] H. Medjahed, D. Istrate, J. Boudy, and B. Dorizzi, “Human activities of daily living recognition using fuzzy logic for elderly home monitoring,” in *2009 IEEE International Conference on Fuzzy Systems*, 2009, pp. 2001–2006.

[31] B. Yuan and J. Herbert, “Fuzzy CARA - A Fuzzy-Based Context Reasoning System For Pervasive Healthcare,” *Procedia Comput. Sci.*, vol. 10, pp. 357–365, Jan. 2012.

[32] C. Chen, R. Jafari, and N. Kehtarnavaz, “Improving Human Action Recognition Using Fusion of Depth Camera and Inertial Sensors,” *IEEE Trans. Human-Machine Syst.*, vol. 45, no. 1, pp. 51–61, Feb. 2015.

[33] L. Mo, S. Liu, R. X. Gao, and P. S. Freedson, “Energy-efficient and data synchronized body sensor network for physical activity measurement,” in

2013 IEEE International Instrumentation and Measurement Technology Conference (I2MTC), 2013, pp. 1120–1124.

[34] N. Ravi, N. Dandekar, P. Mysore, and M. L. Littman, “Activity recognition from accelerometer data,” *Proc. 17th Conf. Innov. Appl. Artif. Intell. - Vol. 3*, pp. 1541–1546, 2005.

[35] E. E. Tripoliti, T. G. Papadopoulos, G. S. Karanasiou, K. K. Naka, and D. I. Fotiadis, “Heart Failure: Diagnosis, Severity Estimation and Prediction of Adverse Events Through Machine Learning Techniques,” *Comput. Struct. Biotechnol. J.*, vol. 15, pp. 26–47, Jan. 2017.

[36] M. Metra and J. R. Teerlink, “Heart failure,” *Lancet*, vol. 390, no. 10106, pp. 1981–1995, Oct. 2017.

[37] V. L. Roger, “Epidemiology of Heart Failure,” *Circ. Res.*, vol. 113, no. 6, pp. 646–659, Aug. 2013.

[38] B. W. Sahle, A. J. Owen, K. L. Chin, and C. M. Reid, “Risk Prediction Models for Incident Heart Failure: A Systematic Review of Methodology and Model Performance,” *J. Card. Fail.*, vol. 23, no. 9, pp. 680–687, Sep. 2017.

[39] A. Candelieri, D. Conforti, F. Perticone, A. Sciacqua, K. Kawecka-Jaszcz, and K. Styczkiewicz, “Early detection of decompensation conditions in heart failure patients by knowledge discovery: The HEARTFAID approaches,” in *2008 Computers in Cardiology*, 2008, vol. 35, pp. 893–896.

[40] H. Khan, A. P. Kalogeropoulos, F. Zannad, C. N. Marti, P. W. F. Wilson, V. V Georgiopoulou, A. M. Kanaya, A. B. Newman, E. Schelbert, T. B. Harris, S. Kritchevsky, C. Yancy, M. Gheorghiade, G. C. Fonarow, and J. Butler, “Incident heart failure in relation to vascular disease: Insights from the Health, Aging, and Body Composition Study,” *Eur. J. Heart Fail.*, vol. 16, no. 5, pp. 526–534, May 2014.

[41] A. Candelieri, D. Conforti, A. Sciacqua, and F. Perticone, “Knowledge Discovery Approaches for Early Detection of Decompensation Conditions in Heart Failure Patients,” in *2009 Ninth International Conference on Intelligent Systems Design and Applications*, 2009, pp. 357–362.

[42] A. Candelieri, “A Hyper-Solution Framework for SVM Classification: Application for Predicting Destabilizations in Chronic Heart Failure Patients,” *Open Med. Inform. J.*, vol. 4, no. 1, pp. 136–140, Jul. 2010.

[43] G. Guidi, M. C. Pettenati, P. Melillo, and E. Iadanza, “A Machine Learning System to Improve Heart Failure Patient Assistance,” *IEEE J. Biomed. Heal. Informatics*, vol. 18, no. 6, pp. 1750–1756, Nov. 2014.

[44] G. Guidi, L. Pollonini, C. C. Dacso, and E. Iadanza, “A multi-layer monitoring system for clinical management of Congestive Heart Failure,” *BMC Med. Inform. Decis. Mak.*, vol. 15, no. S3, p. S5, Dec. 2015.

[45] S. Basu Roy, A. Teredesai, K. Zolfaghar, R. Liu, D. Hazel, S. Newman, and A. Marinez, “Dynamic Hierarchical Classification for Patient Risk-of-Readmission,” in *Proceedings of the 21th ACM SIGKDD International Conference on Knowledge Discovery and Data Mining - KDD ’15*, 2015, pp. 1691–1700.

[46] J. Henriques, P. Carvalho, S. Paredes, T. Rocha, J. Habetha, M. Antunes, and J. Morais, “Prediction of Heart Failure Decompensation Events by Trend

Analysis of Telemonitoring Data," *IEEE J. Biomed. Heal. Informatics*, vol. 19, no. 5, pp. 1757–1769, Sep. 2015.

[47] G. Koulaouzidis, D. K. Iakovidis, and A. L. Clark, "Telemonitoring predicts in advance heart failure admissions," *Int. J. Cardiol.*, vol. 216, pp. 78–84, Aug. 2016.

[48] B. F. McBride and C. M. White, "Acute Decompensated Heart Failure: A Contemporary Approach to Pharmacotherapeutic Management," *Pharmacotherapy*, vol. 23, no. 8, pp. 997–1020, Aug. 2003.

[49] S. I. Chaudhry, Y. Wang, J. Concato, T. M. Gill, and H. M. Krumholz, "Patterns of Weight Change Preceding Hospitalization for Heart Failure," *Circulation*, vol. 116, no. 14, pp. 1549–1554, Oct. 2007.

[50] J. P. Boehmer, R. Hariharan, F. G. Devecchi, A. L. Smith, G. Molon, A. Capucci, Q. An, V. Averina, C. M. Stolen, P. H. Thakur, J. A. Thompson, R. Wariar, Y. Zhang, and J. P. Singh, "A Multisensor Algorithm Predicts Heart Failure Events in Patients With Implanted Devices," *JACC Hear. Fail.*, vol. 5, no. 3, pp. 216–225, Mar. 2017.

[51] H. Suzuki, M. Nodera, M. Kamioka, T. Kaneshiro, Y. Kamiyama, and Y. Takeishi, "Intracardiac impedance after cardiac resynchronization therapy is a novel predictor for worsening of heart failure," *Heart Vessels*, vol. 32, no. 8, pp. 926–931, Aug. 2017.

[52] G. D. Schiff, S. Fung, T. Speroff, and R. a. McNutt, "Decompensated heart failure: Symptoms, patterns of onset, and contributing factors," *Am. J. Med.*, vol. 114, no. 8, pp. 625–630, 2003.

Social Technological Transference: A Case Study

Sara Blanc[1], Juan Vicente Capella[1], Sara Ibañez[1], José V. Benlloch
[1] Universitat Politècnica de València, Camino de Vera s/n
46022 Valencia, Spain
{sablacla, jcapella, sibanez, jbenlloc}@upv.es

Abstract. Much of the responsibility for technology to reach society is from researchers. Through financial tools and collaborative projects, technology transfer becomes a reality. This is the case of the paper which describes a technology transfer on-going project. The work started as an experience of collation ApS (Service-based Learning). However, after the initial analysis, the experience has become a technology transfer project involving the Universitat Politècnica de València along with other European universities and educational centers.

Collaborating partners: Centro de Cooperación al Desarrollo (Universitat Politècnica de València); Escola Tècnica Superior d'Enginyeria Informàtica (Universitat Politècnica de València); Colegio la Purísima-Hnas. Franciscanas de Valencia, Spain; Fundación Caja Mar de la Comunidad Valenciana, Spain; Universitatea Tehnica Cluj-Napoca, Romania; Universidade do Porto, Portugal; Agrupaçao Paredes, Portugal; TBAgrosensors, SME; Osnovna sola Smartno pod Smarno goro, Slovenia; Directorate of Primary School Educatio, Greece.

1 Introduction

"School Gardens for Future Citizens" is a project which aims to improve inclusive quality education and students' skills, cultural diversity, sustainable growth social citizenship and its education throughout a transversal integration of technology at all school levels around a real-life use case in ecologic school gardens.
The defense, of school gardens and its advantages in education is not new. For example, the network Eco-Schools.org groups 51.000 schools of 61 countries. Erasmus+ has also funded several initiatives such as "Erasmus Gardening: Culture and Science" [1] or "GARDENStoGROW: Urban Horticulture for Innovative and Inclusive Early Childhood Education" [2]. These examples highlight school gardens as a students' learning vehicle to different goals, such as social inclusion or nutrition. A holistic learning approach encourages knowledge of social, economic and cultural understanding in which students live. It will promote learning competences, critical thinking and prepare them for a global world in continuous change. Adding the ecological approach, schools' gardens also promotes values for future citizenship towards respect for the environment and responsible behavior, sustainable production of food or healthy food.

C.Fernandez-Llatas and M.Guillen (Ed.):
Workshop on Innovation on
Information and Communication Technologies
(ITACA-WIICT 2018)

ISBN 978-84-09-07373-3

For example, FAO, in its document “New School Garden Policy” [3] promotes to use of school gardens and the application of GBL methodology (Garden Based Learning).

General speaking, school gardens deal with many sustainable development targets (SDGs) such as ensuring healthy lives and promote well-being for all at all ages, inclusive and equitable quality education, gender equality or responsible consumption.

Under this context, school gardens need to take a step forward. The potential of ICT is very high but scarcely materialized in schools except for the use of tablets or computers for accessing to external educational resources.

Technology is well received by the new digital generations. However, the use of technology in schools is still a challenge. ICT can be incorporated in formats better accepted by all students and levels as a means of observing the reality, sharing knowledge, stimulating creativity, stoking the initiative and empowering students in their own learning.

This project proposes an innovative technology transferring pilot which pretends to transfer to the classroom activities the garden through the creation of a virtual environment that transform garden observation and work in data and information which allow the teacher to, on the one hand, build own educational resources and on the other hand, establish a connection between the physical world (garden) and the digital (virtual), linking non-formal activities outside the classroom with the content of the programs of the teaching guides. It eases the integral development of the students, helping to improve their self-esteem and personal satisfaction because the activities carried out are highly motivating and link the process of learning with the development of both personal and academic skills. Moreover, school gardens improve the relationship between the community and the school, since social and educative networks are created, fostering the feeling of belonging to a bigger community. On a pilot experience it is possible to define targets, to observe deficiencies on needs and to create a suitable and adapted ICT environment accepted by the students, teachers and in general, throughout the educational community.

The school gardens combine technological needs for managing and control with education in values of environmental sustainability [4], social inclusion and citizenship, transmission of tradition and the promotion of digital culture in both girls and boys from the early school stages. It is a challenge to carry out the integration so that it can be extended to other schools throughout Europe with the same interests and impact, taking into account cultural diversity and climate differences.

In summary, the project mission is to work on good practices, tools and resources which help to a broad community to create and produce adapted educational resources to their own needs to improve students’ basic and soft skills, language skills and social education. It will bring advancement on a new digital project-based learning methodology by adopting an inclusive real-life learning programme supported by teachers’ good practices and activities within an ICT specific developed approach.

2 Objectives

Research, innovation and now we must add social transfer. These are the primary objectives of a research project. The technological evolution has brought knowledge and applicability to many public and business sectors. However, its impact on schools and their educational programmes is below their current potential many times limited to specific subjects few hours a month. Although ICT transference could be much more extensive, on a pilot experience it is possible to define specific objectives, to observe deficiencies on needs and to create a suitable and adapted environment accepted by the students, teachers and in general, throughout the educational community.

In summary, this project "School Gardens for Future Citizens" will bring advancement on digital project-based learning methodologies by adopting an inclusive real-life learning programme supported by teachers' good practices and activities within an ICT specific developed approach [5-6]. The study and results will be focused on a pilot set around school gardens that joint real-life learning with tradition, SDG values, quality education and socio-cultural European opening. Three schools participate as pilots to research on good cross-curricular practices to the overall school levels and subjects, adopting a technological approach to build new activities than combine gardening and technology.

2.1 Technological Objectives

The technological objectives are based on the adaptation of wireless sensor networks for the monitoring of field values to the concept of IoT (Internet of Things) or IoF (Internet of Farming). The values measured with different types of sensors are treated syntactically and semantically to be sent to an *information concentrator* that serves clients to display parameters in the cloud.

Post information treatment derives in user resources, such as a library of software resources to complete an ICT tool to control, virtualize and manage information related to school gardens. Students, teachers and staff necessities should be translated into control, management and interaction requirements attending to the variety of plots, agro-uses and agro- specific planning of schools. The ICT tool supports teachers and staff to promote gardens sustainability, while it becomes a continue source of input data usable and available to design and share learning resources to different subjects and age. Output will provide with core components and examples of human/children interfaces to interact with information, to observe and care the garden.

2.2 Social Objectives

Promoting the acquisition of skills and competences

The project will promote learning competences, critical thinking and prepare students for a global world in continuous change. Besides, the project will promote values for future citizenship. It will also contribute to the improvement of the knowledge students have of English, since it will be the language used during the project. It will also contribute to the development of their ICT competence / skills since students will interact with technology and will use technology to observe reality, transform the garden information and work in data, and share that information and their work with other students.

Open education and innovative practices in a digital era

The project will promote innovative practices connecting both virtual and real worlds with the aim of motivating students learning. Moreover, the project pretends to transfer to the students the creation of a digital environment transforming the garden observation and work in data observation, so that teachers can create own educational resources. The students will learn to use new applications and coding for the real life. Students will discover knowledge through orchards and environment and they will give to this a digital treatment.

Social inclusion

Students will improve their self- esteem and personal satisfaction because the activities carried out are highly motivating and link the process of learning with the development of both personal and academic skills. It will improve the relationship between the community and the school. The project will be based on an inclusive perspective which promotes equality of opportunities giving an individual education. Groups of work will be established through cooperative methodology in order to mix students with different qualities and necessities (gender, special educational needs, etc.) so that all members can help each other to improve their knowledge and abilities. Teachers will adapt the activities to the students in order that the cooperative learning is effective.

3 Impact

Impact will be largely seen at the teachers, students and parents involvement and at the shift of curricula development fostering very significant issues such as a increased quality of education and training, more strategic and integrated use of ICTs and open educational resources in education systems, an increased use of learning outcomes, the improvement of the quality of life for the school communities, the development of curriculum for the communities of the organization, the increasing cooperation between schools in local/national level, a long-term adoption of the program by the majority of schools, the facilitation of the implementation of the project in schools by means of production of supporting material, new and increased inter-regional and transnational cooperation of public authorities in the fields of education, the strengthening the relations with local stakeholders and a education system closer links to business and the community. For non-school partners impact will be evident by the enhancing of ability to support schools' innovation and by enlarging its proficiency regarding technology transference and projects' evaluation competences.

4 Conclusion

This paper presents an on-going technological transference project aims to improve inclusive quality education and students' skills.

Ecological school gardens deal with many sustainable development targets (SDGs) such as ensuring healthy lives and promote well-being for all at all ages, inclusive and equitable quality education, gender equality or responsible consumption.

The project makes a step forward in School Gardens with an innovative technology transferring pilot which pretends to transfer to the classroom activities the garden through the creation of a virtual environment that transform garden observation and work in data and information which allow the teacher to, on the one hand, build own educational resources and on the other hand, establish a connection between the physical world (garden) and the digital (virtual), linking non-formal activities outside the classroom with the content of the programs of the teaching guides. It eases the integral development of the students, helping to improve their self-esteem and personal satisfaction because the activities carried out are highly motivating and link the process of learning with the development of both personal and academic skills. Moreover, school gardens improve the relationship between the community and the university and the school, since social and educative networks are created, fostering the feeling of belonging to a bigger community, encouraging cultural exchange, sustainability values, social integration and digital responsible use in a globalized Europe.

References

1. https://erasmusgardening.poli.hu/ Accessed in June 2018.
2. http://www.gardenstogrow.eu/en/ Accessed in June 2018.
3. http://www.fao.org/docrep/013/i1689e/i1689e00.pdf Accessed in June 2018.
4. United Nations; https://sustainabledevelopment.un.org/sdgs
5. I. Zonda, J. Martins; International conference on Intelligent Technologies for Interactive Entertainment “Grüt: A gardening sensor kit for children: A digital application that helps children develop ownership for their plants”, June 2015.
6. V. Tomkova, I. Zemberova; International conference on Application of Information and Communication Technologies “Development of the educational skills of primary school learners through ICT”, October 2015.

Energy-aware Design Space Exploration for Optimal Implementation Parameters Tuning

Ilya Tuzov, David de Andrés, and Juan Carlos Ruiz

ITACA, Universitat Politècnica de València
Camino de Vera s/n, 46022 Valencia, Spain
{tuil, ddandres, jcruizg}@disca.upv.es

Abstract. Determining the optimum configuration of semicustom implementation tools to simultaneously optimize the energy consumption, maximum clock frequency, and area of the target circuit requires navigating through millions of configurations. Existing design space exploration approaches, like genetic algorithms, try to reduce as much as possible the number of configurations that must be implemented to find the (close to) optimum configuration. However, these approaches are not suitable when dependability-related properties must be also taken into account. To accurately estimate these properties, extensive simulation-based fault injection experiments must be executed for each configuration, leading to unfeasible experimentation times. This work proposes an alternative approach, based on statistical and operational research artifacts, to drastically reduce the design space while preserving the accuracy of results, thus, enabling the energy-aware design space exploration for semicustom implementation of logic circuits.

Research Area: Fault Tolerant Systems

1 Introduction

Modern Electronic Design Automation (EDA) tools offer a wide range of optimization options to fine tune each of the stages of the hardware design flow. They allow designers to meet their required implementation goals in terms of performance, power consumption, area (PPA) and dependability attributes [9]. As these tools operate in a daisy chain fashion, optimizations applied at the first stage of the design flow, i.e the logic synthesis, are of prime importance towards achieving the implementation goals. However, and in spite of their importance, the exact impact of these optimization options is usually very hard to predict [3].

Accordingly, determining the best possible configuration of the logic synthesis tool to optimise the power consumption for a given hardware design, while keeping a fair balance among the rest of implementation goals, would require implementing that system once for each combination of the available optimization options at all their possible levels. Taking into account that modern logic synthesis tools usually provide tenths of different optimization options, it is unfeasible

C.Fernandez-Llatas and M.Guillen (Ed.):
Workshop on Innovation on
Information and Communication Technologies
(ITACA-WIICT 2018)

ISBN 978-84-09-07373-3

to perform a full design space exploration (DSE) in a reasonable time frame. For instance, [4] focused only on the impact of just 5 different optimization options on the power consumption of security algorithms.

Existing approaches to explore just a subset of the whole design space, like genetic algorithms and evolutionary approaches [7], cannot be used when not only power consumption but also dependability-related attributes are taken into account. Firstly, simulating the implementation model of the system is a timing consuming process and, secondly, a large number of fault injection experiments are required to take into account all the fault models, injection times, and targets to ensure the accuracy and representativeness of obtained results. Accordingly, it can be seen that the impact of simulation-based fault injection experiments on the speed at which a single configuration is evaluated will require a drastic pruning of the design space to reduce the runtime of the process and, thus, the quality of the resulting configuration will be very low.

This paper addresses this challenging problem by proposing an alternative combination of statistical and operational research techniques to greatly reduce the design space in a controlled manner, so that the confidence on the provided configuration is not compromised and the procedure can be executed within a reasonable time frame. The proposed approach is detailed in Section 2. Section 3 applies this procedure to an embedded processor model (MC8051) synthesized by means of the Xilinx XST tool. Then Section 4 performs a study of the results obtained for this processor. Finally, Section 5 summarizes the results of the study.

2 Proposed Methodology

The proposed methodology to reduce the power consumption of the circuit while keeping a tradeoff among the rest of implementation goals is depicted in Fig. 1. The different phases comprising this methodology are described next.

2.1 Design of Experiments

The goal of this stage is to determine the precise configurations that will be taken into account as a representative sample of the whole design space. This design space will be defined by the considered optimization flags (factors) of the selected synthesis tool and the levels at which these flags can be set up.

Fractional factorial design of experiments **??** can be used to select this sample in such a way that any combination of factors at any level has the same number of observations (balanced design), and the effects of any factor balance out across the effects of the other factors (orthogonal design). Additionally, the resolution of the design will determine the degree to which estimated main effects will be confounded with estimated low-level interactions. Fractional factorial designs are denoted as I_R^{K-P}, where I is the number of possible levels of each factor, K is the total number of considered factors, R is the design resolution, and $1/I^P$ is the size of the fraction of the full factorial design space to explore.

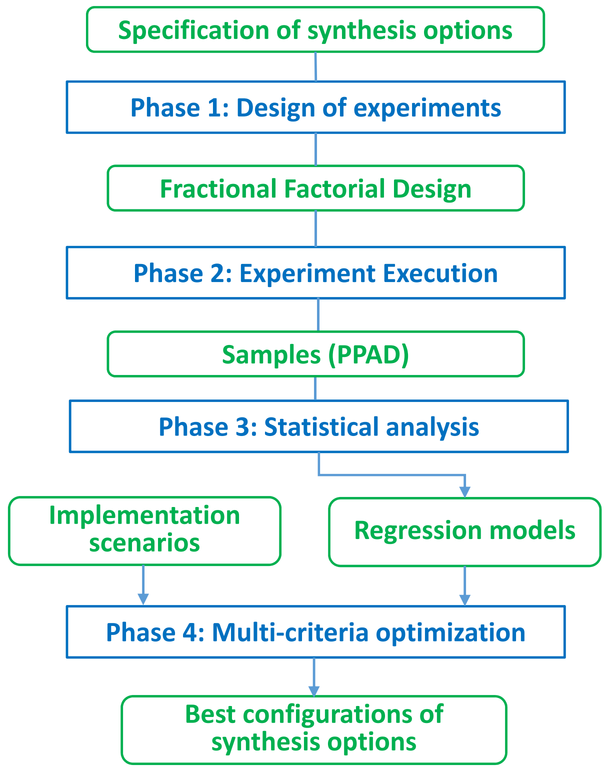

Fig. 1. Methodology overview

2.2 Experiment Execution

Each of the configurations determined by the fractional factorial design is used in this stage to configure the selected synthesis tool and run the common semi-custom implementation flow for each configuration.

As a result of this implementation process it is possible to obtain:

- The maximum attainable clock frequency of the final implementation via static timing analysers.
- The number of sequential and combinational resources required to implement the circuit in the selected technology.
- The power consumption of the circuit, estimated by the power analyser after a detailed simulation in which the switching activity of all the nets of the circuit is computed.
- The robustness of the final implementation, computed after executing the required number of simulation-based fault injection experiments according to the number of considered faults, injection times, and injection targets.

2.3 Statistical Analysis

The actual value of the different implementation goals obtained for each sample configuration are then statistically processed in order to derive a model to estimate the value of these implementation goals for the rest of configurations of the whole design space.

First, an analysis of variance (ANOVA) [5] process is used to determine which of the considered factors have a statistically significant impact on the implementation goals. These selected factors are used to build a linear regression model, which assumes that the relationship between the implementation goal and the factors is linear ($y = \beta_0 + \beta_1 X_1 + \ldots + \beta_n X_n$) [2]. The coefficient of determination (R^2) explains the proportion of the variance in the implementation goal that can be explained by the factors, i.e. how well the model fits the data.

2.4 Multi-criteria optimization

These regression models can now be used to estimate the value of all implementations goals for any possible configuration within the whole design space. In such a way, it is easy to find the best configuration for a given implementation goals, like power consumption. Nevertheless, different techniques could be applied when more than one goal should be taken into account.

In case that no information is provided related to the relative importance of each implementation goal, then a set of optimal configurations can be obtained through the Pareto frontier [1] of the design. This frontier is the set of configurations in which none of the implementation goals could be improve without degrading the others. Hence, any of those configurations can be considered as equally good as the others, and it is the responsibility of the designer to select the most suitable one.

However, when information about the importance of each implementation goal is available, then multiple-criteria decision-making techniques can be applied to determine the best candidate according to this information. Among the existing techniques, this proposal promotes the use of the Weighted Sum Model (WSM) [8], due to its simplicity and widespread use in different domains. The score for each configuration is computed by normalising the estimated values for each implementation goal (a) and aggregating them together according to their respective weight (ω) as shown in Equation 1. The configuration with the higher score will be that obtaining the best tradeoff among all implementation goals.

$$WSM = \sum_{i=1}^{n} \omega_i a_i \tag{1}$$

3 Case Study

The MC8051 core [6] developed by Oregano Systems, which is compatible with the industry standard 8051, has been selected as the design to be implemented in this case study. The Xilinx ISE Design Suite framework, which provides all the required toolchain for design entry, synthesis, mapping, placement, routing, and simulation, has been used to implement this design on a Xilinx XC6VCX240T-FF784-2 FPGA. The integrated Xilinx Synthesis Technology (XST) tool [10] presents a total of 31 flags that can be configured to optimise different aspects of the resulting implementation.

As implementing the whole set of 2 billions of possible configurations is unfeasible, the proposed approach has been deployed to drastically reduce the space to be explore while keeping the statistical significance of the results. A 2_{IV}^{31-24} fractional factorial design, listed in Table 1, has been defined to consider just 128 sample configurations.

Table 1. XST synthesis optimization options under study

Factor	Synthesis option	Low/High levels
X01	Optimization Goal	Speed/Area
X02	Optimization Effort	Normal/High
X03	Power Reduction	No/Yes
X04	Keep Hierarchy	No/Yes
X05	Global Optimization Goal	AllClockNets/Maximum Delay
X06	Cross Clock Analysis	No/Yes
X07	BRAM Utilization Ratio	0%/100%
X08	DSP Utilization Ratio	0%/100%
X09	Automatic FSM Extraction	No/Yes
X10	FSM Encoding Algorithm	Auto/Compact
X11	Safe Implementation	No/Yes
X12	FSM Style	LUT/BRAM
X13	RAM Extraction	No/Yes
X14	RAM Style	Auto/Distributed
X15	ROM Extraction	No/Yes
X16	ROM Style	Auto/Distributed
X17	Automatic BRAM Packing	No/Yes
X18	Shift Register Extraction	No/Yes
X19	Shift Register Minimum Size	2/8
X20	Resource Sharing	No/Yes
X21	Use DSP Blocks	Auto/Automax
X22	Max Fanout	100/100000
X23	Register Duplication	No/Yes
X24	Equivalent Register Removal	No/Yes
X25	Pack I/O Registers into IOBs	No/Auto
X26	LUT Combining	Auto/Area
X27	Reduce Control Sets	No/Auto
X28	Use Clock Enable	No/Auto
X29	Use Synchronous Set	No/Auto
X30	Use Synchronous Reset	No/Auto
X31	Optimize Instantiated Primitives	No/Yes

For each of these configurations, the following implementation goals have been measured: power consumption (mW), maximum clock frequency (MHz), flip-flops (#), look-up tables (#), and mission time (h). The mission time is defined as the time in which the reliability ($R(t)$) of the system reaches a given threshold (0.98 in this case study). The reliability of the system has been computed as: $R(t) = e^{-12\times10^{-9}\times f\times t}$, being f the experimentally obtained probability of a fault leading to a failure.

This failure rate has been experimentally estimated by means of fault injection experiments, which injected a single fault in one of the possible fault targets. The fault models considered in this case study include stuck-at-0 and stuck-at-1 (permanent faults) in combinational and sequential logic, and bit-flip (transient fault) in sequential logic. One fault injection experiment was conducted for each type of stuck-at fault, in which the fault was injected just at the beginning of the experimentation, whereas three different experiments with different injection times were conducted for bitflips.

4 Results

Once all the configurations have been implemented and the fault injection experiments have taken place, we have available the information related to the power consumption, clock frequency, area, and robustness for each considered configuration. This information must be now processed in order to build the models that will enable the estimation of these implementation goals for any configuration within the design space.

According to the ANOVA, depicted in Table 2, the only factors that statistically significantly impact the power consumption of the MC8051 microcontroller are X_01 (Optimization Goal), X_04 (Keep Hierarchy), X_19 (Shift Register Minimum Size), and X_25 (Pack I/O Registers into IOBs).

Hence, the linear regression model that estimates the power consumption (mW) of any of the possible configurations within the design space is represented by Equation 2.

$$Power = 121.73 - 30.41X_{01} - 3.00X_{04} - 2.42X_{19} - 3.44X_{25} \qquad (2)$$

From this information, the configuration that decreases the power consumption to just 74.46 mW is encoded as $\{1011000110011100111011111101000\}$ (X_{01}–X_{31}), whereas the worst possible configuration in terms of power consumption reaches 129.28 mW.

However, if power consumption should not be considered in isolation but together with the rest of implementation goal, different tradeoffs can be found. As an example, Fig. 2 displays the Pareto frontier obtained when considering both the power consumption and the mission time in an out of context scenario.

As can be seen in Fig. 2, there is one configuration that optimises the power consumption in detriment of the mission time, another configuration that gets the best mission time at the expense of an increased power consumption, and another configuration that balances both goals. It is the responsibility of designers

Table 2. Impact of factors on power consumption. Significant factors are highlighted in blue

Factor	Estimator (mW)	Factor	Estimator (mW)	Factor	Estimator (mW)
X01	-30.41	X12	-0.24	X23	-1.01
X02	1.40	X13	-0.44	X24	-0.36
X03	-0.61	X14	-0.58	X25	-3.44
X04	-3.00	X15	0.28	X26	-0.21
X05	0.96	X16	0.72	X27	1.47
X06	0.19	X17	-0.49	X28	-0.54
X07	0.45	X18	-0.95	X29	0.03
X08	-0.70	X19	-2.42	X30	0.07
X09	-0.14	X20	0.90	X31	0.78
X10	0.25	X21	-0.63		
X11	0.05	X22	-1.10	Intercept	121.73

to select which one of this configurations is the most suitable for their purposes. It is worth noting that the default configuration provided by the synthesis tool is far from optimising any of these goals.

However, when the context of use of the implemented circuit is know, it is possible to take into account the relative importance of each implementation goal to guide the search for the most suitable configuration. Let us assume two different contexts of use in which the MC8051 microcontroller could be used: a consumer electronics scenario, like a set-top box, and a mobile scenario, like a smartphone. Clearly the priorities in these scenarios differ, as designers for consumer electronic devices could be more focused on improving the maximum attainable clock frequency, whereas they could be more interested in reducing the power consumption for mobile devices. Table 3 lists the weights considered for the different implementation goals in these two scenarios.

Table 3. Relative importance of each implementation goal for the consumer electronics and mobile scenarios

Scenario	Mission time	Clock frequency	Power consumption	Look-up tables	Flip-flops Flip-flops
Consumer	0.167	0.500	0.000	0.167	0.167
Mobile	0.125	0.250	0.375	0.125	0.125

These weights have been used in Equation 1 to determine the score of each configuration within the design space. Table 4 lists the score and estimations obtained for the best, worst, and default configurations.

In this case, as the relative importance of each implementation goal is explicitly stated, it is possible to determine the score of each configuration that

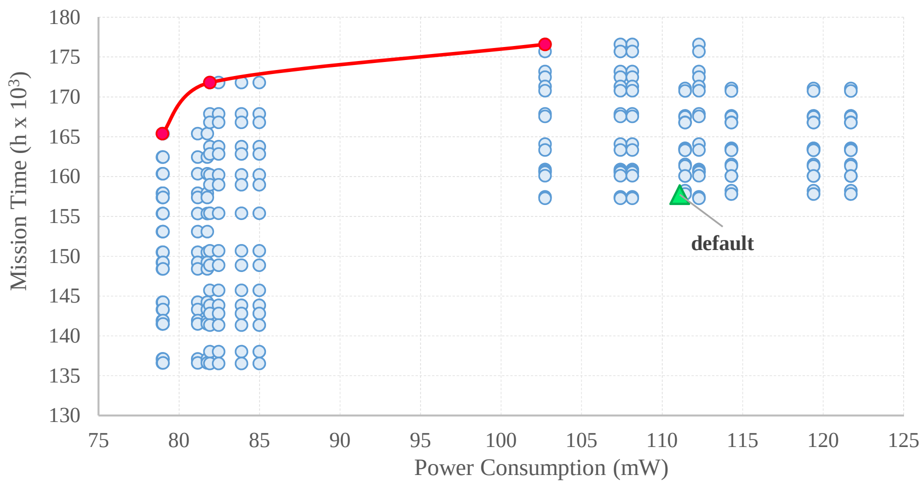

Fig. 2. Pareto optimal configurations when considering both power consumption and mission time

Table 4. Estimated values for each implementation goal and WSM scores for the best, worst, and default configurations for the consumer electronics and mobile scenarios

Scenario		WSM score	Mission time	Clock frequency	Power consumption	Look-up tables	Flip-flops
Consumer	Best	0.96	7384202	64.37	112.28	571	2404
	Worst	0.74	6372938	41.90	82.47	581	2699
	Default	0.81	6753621	59.05	111.09	610	2901
Mobile	Best	0.91	6553768	45.76	78.97	544	2026
	Worst	0.77	6756442	59.29	119.41	616	3362
	Default	0.80	6753621	59.05	111.09	610	2901

represents the quality of this configuration with respect to the priorities stated in the model. As in the context-less case, the default configuration is closer to the worst configuration than to the best one.

5 Conclusions

As Electronic Design Automation tools are increasing their complexity to alleviate the task of hardware designers, selecting the proper configuration of the synthesiser to optimise a set of implementation goals become more and more troublesome. These tools present tenths of different optimisation flags with no clear indication of their particular purpose, their impact on the design, and their interaction.

This paper has presented a methodology to precisely determine the impact of each flag on each implementation goal (particularly the power consumption), and determining the best possible configuration according when searching for a balance among different and often conflicting goals.

Results for our particular case study show that the default configuration provided by the XST synthesiser is mainly focused on improving the clock frequency of the final implementation, at the expense of the power consumption and silicon area. Accordingly, by proper configuring the synthesizer, it is possible to improve up to 42% the power consumption, 30% de mission time, 56% the clock frequency, 12% the flip-flops utilisation, and 35% the look-up tables utilisation.

Our future work will focus on extending this approach to all EDA tools (placer and router), not just the synthesiser, and studying a large number of benchmark circuits to extract common configuration patterns and define generic guidelines for the configuration of these tools for different scenarios.

Acknowledgment

This work has been partially funded by the Ministerio de Economía, Industria y Competitividad de España under grant agreement no TIN2016-81075-R, and the "Programa de Ayudas de Investigación y Desarrollo" (PAID) of the Universitat Politècnica de València.

References

1. Branke, J., Deb, K., Miettinen, K., Słowiński, R. (eds.): Multiobjective Optimization: Interactive and Evolutionary Approaches. Springer Berlin Heidelberg, Berlin, Heidelberg (2008)
2. Freedman, D.A.: Statistical Models: Theory and Practice. Cambridge University Press (2009)
3. Kilts, S.: Advanced FPGA Design: Architecture, Implementation, and Optimization. Wiley-IEEE Press (2007)
4. Meidanis, D., Georgopoulos, K., Papaefstathiou, I.: FPGA Power Consumption Measurements and Estimations Under Different Implementation Parameters. In: International Conference on Field-Programmable Technology. pp. 1–6 (2011)
5. NIST/SEMATECH: NIST/SEMATECH e-Handbook of Statistical Methods (2013), http://www.itl.nist.gov/div898/handbook/
6. Oregano Systems GmbH: MC8051 IP Core, Synthesizeable VHDL Microcontroller IP-Core, User Guide (V 1.2), 2013 (2013), http://www.oreganosystems.at/download/mc8051_ug.pdf
7. Pilato, C., Loiacono, D., andFabrizio Ferrandi, A.T., Lanzi, P.L., Sciuto, D.: Computational Intelligence in Expensive Optimization Problems, chap. Speeding-Up Expensive Evaluations in High-Level Synthesis Using Solution Modeling and Fitness Inheritance, pp. 701–723. Springer-Verlag Berlin Heidelberg (2010)
8. Triantaphyllou, E.: Multi-Criteria Decision Making Methods. In: Multi-criteria Decision Making Methods: A Comparative Study, Applied Optimization, vol. 44, pp. 5–21. Springer US (2000)
9. Wolf, W.: FPGA-Based System Design. Prentice Hall (2004)
10. Xilinx Inc.: XST User Guide for Virtex-6, Spartan-6, and 7 Series Devices (v 14.5) (2013), http://www.xilinx.com/support/documentation/sw_manuals/xilinx14_7/xst_v6s6.pdf

On the Efficiency of Random Linear Network Coding for Ultra-reliable and Low Latency Communications in 5G

Israel Leyva-Mayorga[1], Vicent Pla[1], Jorge Martinez-Bauset[1], and Frank H.P. Fitzek[2]

[1] ITACA Research Institute,
Universitat Politècnica de València, 46022, Valencia, Spain
Email: {isleyma, vpla, jmartinez}@upv.es
[2] Deutsche Telekom Chair of Communication Networks
Technische Universität Dresden, 01062 Dresden, Germany
Email: frank.fitzek@tu-dresden.de

Abstract. Ultra-low latency, high reliability and increased throughput are three of the main requirements of 5G networks. As such, 5G will bring us a step closer to the realization of the Tactile Internet, an evolution of the Internet of Things (IoT) in which humans and machines interact in a real-time fashion. Random linear network coding (RLNC) is a promising technique that can potentially enhance each of the three above mentioned requirements simultaneously by randomly creating linear combinations of the source data packets at the transmitter. As a result, the concept of individual data packets is lost and data transmission can be seen as a flow of information. In this paper, we assess the efficiency of two of the most common RLNC schemes, namely full-vector and systematic, in terms of the probability of successfully decoding a batch of packets (i.e., a generation) and packet delay. We also present our novel analytical model used for obtaining the packet delay in systematic RLNC. Results show that systematic RLNC clearly outperforms full-vector RLNC when few wireless channel errors occur. On the other hand, the superiority of systematic over full-vector RLNC is concealed when a large number of wireless channel errors occur.

1 Introduction

We are in the edge of a revolution in communication networks. 5G networks have attracted the attention of both the industry and academia during the past few years and everyday we are getting closer their real implementation.

5G is expected to clearly outperform 4G LTE-A in several aspects, with the most important being energy efficiency, throughput, and packet latency. As such, one of the major use cases for 5G systems, as defined by the International Telecommunication Union (ITU) is ultra-reliable and low latency communications (URLLC) [6]. Needless to say, URLLC combined with a high security leads to the Tactile Internet, an evolution of the Internet of things (IoT) in which

C.Fernandez-Llatas and M.Guillen (Ed.):
Workshop on Innovation on
Information and Communication Technologies
(ITACA-WIICT 2018)

ISBN 978-84-09-07373-3

humans and machines interact in a real-time fasion regardless of the distance between them [8]. Examples of URLLC-enabled applications are remote tactile control and autonomous driving.

Network coding (NC) is a technique introduced in [2] that has proven to be highly valuable to ensure high data rates with low error ratios. In NC, coded packets are transmitted, which are linear combinations of the source packets, created according to the selected coding coefficients. Random linear network coding (RLNC) is one of the most widely used variants of NC [5], in which these combinations are performed by choosing the coding coefficients coefficients at random from a Galois-field of size q, GF(q).

Full-vector and systematic RLNC are two of the most widely used RLNC schemes that are characterized by their simplicity and efficiency. In full-vector RLNC every transmitted packet is coded, whereas in systematic RLNC the source packets are first transmitted and then coded packets are transmitted to recover the errors that may have occurred.

In this paper, we assess the efficiency of full-vector and systematic RLNC in terms of the number of packet transmissions needed to decode the generation, hereafter referred to as the probability of successful delivery, and packet delay. We consider a point-to-point communication with strict in-order delivey. That is, a packet is only decoded and sent to upper layers if each and every one of the previous packets have been decoded correctly.

We use the formulations provided in [9] for the exact decoding probability under full-vector RLNC. Then we extend these formulations to calculate the packet delay under this scheme.

The main contribution of this paper is the Markov model to calculate packet latency under systematic RLNC. While the exact decoding probability under this RLNC scheme has been obtained in [7], to the best of our knowledge no study has presented a model for packet delay.

Other popular RLNC schemes include telescopic and sparse RLNC. Telecopic codes were introduced in [4] and the basic idea is to reduce the coding overhead in the first transmission and increase the reliability in the last packet transmissions. This is achieved by combining a small numbe of packets for the first transmissions and a large number of packets for the last transmissions. Sparse RLNC on the other hand thrives to reduce the coding overhead throughout the whole process by combining a reduced number of packets [10]. Nevertheless, the analytical modeling of the probability of successful delivery under these two RLNC schemes is complicated; hence developing a model to obtain the packet delay is a daunting task. For instance, authors in [3] developed a Markov model to obtain the decoding probability under sparse RLNC. However, some of the transition probabilities had to be obtained by curve fitting. That is, performing a large number of simulations and then finding an expression that fits the obtained curves.

The rest of the paper is organized as follows. In Secction 2 we describe the RLNC basic principles and the characteristics of full-vector and systematic RLNC. Then in Section 3 we present the analytical models for both RLNC

$$\begin{bmatrix} 1 & X & X & X \\ 0 & 1 & X & X \\ 0 & 0 & 1 & X \\ 0 & 0 & 0 & 1 \end{bmatrix}$$

Fig. 1. Example of a full-rank 4×4 matrix.

schemes, followed by the results obtained in Section 4. We conclude the paper in Section 5.

2 Random Linear Network Coding (RLNC)

Random Linear Network Coding is a novel technique that has the potential to increase throughput and reduce energy consumption in wireless networks [2]. The basic idea behind RLNC is to segment the content in batches of g source data packets called generations; hence the generation size is g packets. Then the source sends coded packets to the destination. Each of these coded packets is a linear combination of the source packets.

For this, the source node generates random numbers distributed uniformly in the Galois-field of size q, (i.e., GF(q)) to form a coding matrix $\mathbf{M}$ of size $t \times g$. The coding vector for the nth coded packet is the nth row of $\mathbf{M}$, $\mathbf{m}_n$, where $\{n \in \mathbb{Z}_+ \mid n \leq t\}$. On itself, $\mathbf{m}_n$ is a row vector with g elements. The matrix that contains the source packets $\mathbf{G} = [\mathbf{p}_1; \mathbf{p}_2; \ldots; \mathbf{p}_g]$ is multiplied by $\mathbf{M}$ to create coded packets as

$$\mathbf{C} = \mathbf{M}\,\mathbf{G}. \tag{1}$$

The nth coding vector $\mathbf{m}_n$ is appended to the nth row of $\mathbf{C}$, $\mathbf{c}_n$, to create the nth coded packet that will be transmitted by the source.

The destination stores the received packets in matrix $\mathbf{C}'$ and creates the decoding matrix $\mathbf{D}$ with the received coding vectors. Please observe that matrix $\mathbf{C}'$ is equal to $\mathbf{C}$ only if no errors occur in the wireless link. The destination can decode the generation when sufficient coded packets have been received so $\mathbf{D}$ is full rank (i.e., when matrix $\mathbf{D}$ has exactly g linearly independent rows, also known as degrees of freedom). The rank of $\mathbf{D}$ can be calculated by performing Gaussian elimination so that the matrix is in reduced row echelon form and counting the number of pivots (i.e., number of ones in the diagonal). Fig. 1 illustrates a 4×4 matrix that is full-rank.

At this point, the destination decodes the packets as

$$\mathbf{G} = \mathbf{D}^{-1}\ \mathbf{C}' \tag{2}$$

Two of the most simple and widely used RLNC schemes are full-vector and systematic RLNC. The difference between these two schemes relies in the contents of their coding matrices. That is, in full-vector RLNC every packet transmission is coded, whereas in systematic RLNC the g source packets are first

$$\begin{bmatrix} 1&1&0&1 \\ 1&1&1&1 \\ 1&1&1&0 \\ 0&0&1&1 \\ 1&0&1&1 \\ 0&1&1&0 \end{bmatrix} \qquad \begin{bmatrix} 1&0&0&0 \\ 0&1&0&0 \\ 0&0&1&0 \\ 0&0&0&1 \\ 1&0&1&1 \\ 0&1&1&0 \end{bmatrix}$$

(a) (b)

Fig. 2. Example of coding matrices $\mathbf{M}$ to transmit six packets under (a) full-vector and (b) systematic RLNC given $g = 4$.

transmitted in sequence; only then coded packets are transmitted. Fig. 2 illustrates the contents of the coding matrices for full-vector and for systematic RLNC for a generation size $g = 4$.

One of the main advantages of systematic over full-vector RLNC is that the source node can transmit the source packets as soon as these are generated; this is because packets are first transmitted in sequence. On the other hand, the source node must wait until the g packets have been generated in order to start coding. Yet another advantage of systematic over full-vector is that the probability that the first g transmitted packets are linearly dependent is zero. As it will be seen in Section 4, this increases the probability of successful content delivery. In other words, systematic RLNC reduces the number of transmissions needed to decode the generation at the destination.

3 Analytical models

In this section we present the models used for the analysis of the two selected RLNC schemes: full-vector and systematic for a point-to-point communication. We study the efficiency of these RLNC schemes under a wireless erasure channel with a constant packet error ratio (PER), ϵ, between source and destination. That is, each packet transmission is received at the destination with probability $1 - \epsilon$ and an erasure (i.e., wireless channel error) occurs with probability ϵ.

We assess the packet delay as the number of time slots elapsed between the transmission of the ith data packet and its decoding at the destination. For this, we consider a time-slotted channel, where one packet transmission is performed at each time slot. Therefore we define the RV D as the packet delay, given in time slots. In this study we assume strict in-order delivery, hence a source packet is sent to upper layers if and only if each and every one of the previous packets has been decoded correctly.

3.1 Full-vector RLNC

In full-vector RLNC every packet transmission is coded. Let X_n be the stochastic process that defines the rank of the decoding matrix at the destination $\mathbf{D}$

after n packet transmissions, whose support is $\{x \in \mathbb{Z}_{\geq 0} \mid x \leq g\}$. Given that the transmitter is the source node, the probability that a coded packet transmission towards the destination is innovative (i.e., linearly independent to any packet received previously) depends on the rank of $\mathbf{D}$, X_n, on the selected field size q, and on the generation size g as

$$p_{x \to x+1} = 1 - q^{x-g} \tag{3}$$

The probability that a packet is linearly dependent is simply given as

$$p_{x \to x} = q^{x-g} \tag{4}$$

Building on this, the probability that a matrix $\mathbf{D}$ of size $n \times g$ whose elements have been generated uniformly at random from the GF(q) is full rank, is given as [9]

$$F(n, g) = \Pr[X_n = g \mid \epsilon = 0] = \begin{cases} 0 & \text{for } n < g, \\ \prod_{j=0}^{g-1} \left(1 - q^{j-n}\right) & \text{otherwise.} \end{cases} \tag{5}$$

Now let S be the RV that defines the number of packets transmissions needed to decode the generation at the destination. Clearly S is a phase-type distribution, so hereafter we refer to S as the probability of successful delivery. The generalization of (16) for any PER $\epsilon \in [0, 1]$ gives the CDF of S under full-vector RLNC, S_{fv}, as

$$F_{S_{\text{fv}}}(n) = \sum_{k=g}^{n} \binom{n}{k} (1 - \epsilon)^k \epsilon^{n-k} F(k, g). \tag{6}$$

The destination can only start decoding the generation under full-vector RLNC when its decoding matrix $\mathbf{D}$ is full rank. Hence, the distribution of packet delay can be calculated by means of the following convolution

$$p_{D_{\text{fv}}}(d) = \Pr[D_{\text{fv}} = d] = p_{S_{\text{fv}}}(d) * \sum_{k=0}^{g} \delta_{dk}; \tag{7}$$

where $p_{S_{\text{fv}}}(n) = F_{S_{\text{fv}}}(n) - F_{S_{\text{fv}}}(n-1)$ and δ_{dk} is the kronecker delta defined as

$$\delta_{dk} := \begin{cases} 1 & \text{if } d = k, \\ 0 & \text{otherwise.} \end{cases} \tag{8}$$

3.2 Systematic RLNC

We obtain the packet delay under systematic RLNC by means of a two-dimensional and a one-dimensional absorbing discrete-time Markov chain (DTMC). Let Y_n be the RV that defines the source packet transmission in which the first erasure

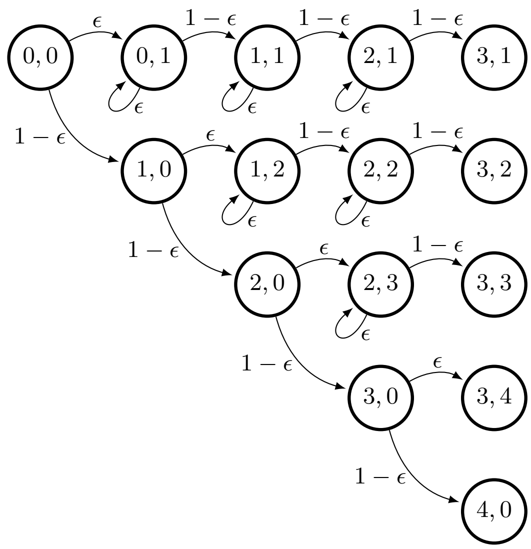

Fig. 3. Example of the two-dimensional DTMC that models the source packet transmissions under systematic RLNC given $g = 4$.

occurs. The two-dimensional DTMC is used to calculate the joint pmf of X_g and Y_g. That is, the state of the system after the g source packet transmissions. Then the one dimensional DTMC is used to calculate the CDF of T given X_g.

Let $\mathscr{I} = \{(x, y) \in \mathbb{Z}_{\geq 0} \mid x, y \leq g\}$ be the state space of the two-dimensional DTMC. Therefore, each state is defined by the index pair (x, y), where x denotes the source packets received so far (i.e., the rank of $\mathbf{D}$) and y denotes the first step in which an erasure occurs. That is, the system is in state $(x, 0)$ if the first x packets have been successfully transmitted. Then, the system transitions to state $(x, x+1)$ if an erasure occurs at the $(x+1)$th transmission. An example of the two-dimensional DTMC for $g = 4$ is illustrated in Fig. 3. Transitions from states $(3, y \geq 1)$ and from state $(4, 0)$ have been omitted as these are not possible since only $g = 4$ transitions occur (i.e., $g = 4$ source packets are transmitted) and at least five transitions are required to reach these states.

Clearly, transitions between states only depend on the PER ϵ suring the source packet transmissions. Hence, the substochastic matrix $\mathbf{T}$ that represents the transitions between transient states can be easily constructed given the following transition probabilities:

$$p_{x,y \to x+1,y} = 1 - \epsilon \tag{9}$$

$$p_{x,y \to x,y} = \begin{cases} \epsilon & \text{for } y \neq 0, \\ 0 & \text{otherwise,} \end{cases} \tag{10}$$

$$p_{x,0 \to x,x+1} = \epsilon; \tag{11}$$

$$
\mathbf{T} = \begin{bmatrix}
0 & \epsilon & 0 & 0 & 0 & 1-\epsilon & 0 & 0 & 0 & 0 & \\
0 & \epsilon & 0 & 0 & 0 & 0 & 1-\epsilon & 0 & 0 & 0 & \\
0 & 0 & \epsilon & 0 & 0 & 0 & 0 & 1-\epsilon & 0 & 0 & \\
0 & 0 & 0 & \epsilon & 0 & 0 & 0 & 0 & 1-\epsilon & 0 & \\
0 & 0 & 0 & 0 & \epsilon & 0 & 0 & 0 & 0 & 1-\epsilon & \\
0 & 0 & 0 & 0 & 0 & 0 & 0 & \epsilon & 0 & 0 & \\
0 & 0 & 0 & 0 & 0 & 0 & \epsilon & 0 & 0 & 0 & \\
0 & 0 & 0 & 0 & 0 & 0 & 0 & \epsilon & 0 & 0 & \\
0 & 0 & 0 & 0 & 0 & 0 & 0 & 0 & \epsilon & 0 & \\
0 & 0 & 0 & 0 & 0 & 0 & 0 & 0 & 0 & \epsilon & \ddots \\
 & & & & & & & & & \ddots & \ddots
\end{bmatrix}
$$

Fig. 4. First rows and columns of the transition matrix $\mathbf{T}$ given $g = 4$.

Fig. 4 illustrates the elements of the transition matrix $\mathbf{T}$ given $g = 4$. As it can be seen, transitions are similar to those in a traditional negative binomial distribution, except for states $(x, 0)$.

Let $\boldsymbol{\alpha}^{(n)} = \left[\alpha^{(n)}_{0\,0}, \alpha^{(n)}_{0\,1}, \ldots, \alpha^{(n)}_{1\,0}, \alpha^{(n)}_{1\,1}, \ldots, \alpha^{(n)}_{4\,0}\right]$ be the state probability vector at time n. At time zero we have the vector of initial states $\boldsymbol{\alpha}^{(0)}$ with every entry $\alpha^{(0)}_{x\,y} = 0$ except $\alpha^{(0)}_{0\,0} = 1$. The state probability vector at the end of the source packet transmissions (i.e., at time g) can be easily calculated with the following recursion

$$\boldsymbol{\alpha}^{(g)} = \boldsymbol{\alpha}^{(g-1)}\mathbf{T} \tag{12}$$

Now let $\boldsymbol{\beta}^{(0)}_y = \left[\alpha^{(g)}_{0\,y}, \alpha^{(g)}_{1\,y}, \ldots, \alpha^{(g)}_{g-1\,y}\right]$ be the state probability vector at the end of the source packet transmissions, given that an erasure occurred at the yth source packet transmission. Then the state probability matrix during the coded packet transmissions is given as $\boldsymbol{\beta}^{(s)} = \left[\boldsymbol{\beta}^{(s)}_1; \boldsymbol{\beta}^{(s)}_2, \ldots, \boldsymbol{\beta}^{(s)}_g\right]$. That is, the time index s represents the number of coded packet transmissions under the systematic RLNC, hence $s = n - g$.

The substocastic matrix that represents the transitions between transient states during coded packet transmissions $\mathbf{T}_c$ is the result of a one-dimensional absorbing DTMC. The transition probabilities are derived from (3) and (4) by including the PER ϵ. Fig. 5 illustrates $\mathbf{T}_c$ for $g = 4$.

The state probability matrix after s coded packet transmissions is given as

$$\boldsymbol{\beta}^{(s)} = \boldsymbol{\beta}^{(s-1)}\,\mathbf{T}_c \tag{13}$$

The vector $\mathbf{t}_c$ that represents the transitions from a transient state to the absorbing state g is a column vector of zeros except its gth entry is $\left(1 - q^{-1}\right)\epsilon$. For example, for $g = 4$ we have $\mathbf{t}_c = \left[0; 0; 0; \left(1 - q^{-1}\right)\epsilon\right]$.

$$\mathbf{T}_c = \begin{bmatrix} q^{-g}(1-\epsilon)+\epsilon & \left(1-q^{-g}\right)\epsilon & 0 & 0 \\ 0 & q^{1-g}(1-\epsilon)+\epsilon & \left(1-q^{1-g}\right)\epsilon & 0 \\ 0 & 0 & q^{2-g}(1-\epsilon)+\epsilon & \left(1-q^{2-g}\right)\epsilon \\ 0 & 0 & 0 & q^{3-g}(1-\epsilon)+\epsilon \end{bmatrix}$$

Fig. 5. Transition matrix during coded packet transmissions $\mathbf{T}_c$ given $g = 4$.

Next we define the RV S_{sys} as the probability of successful delivery under systematic RLNC. The joint pmf of S_{sys} and Y_g for a given y can be obtained as

$$p_{S_{\text{sys}},Y_g}(s,y) = \begin{cases} 1-\boldsymbol{\alpha}^{(g)}\,\mathbf{1} & \text{for } y=0 \text{ and } s=0, \\ \boldsymbol{\beta}_y^{(s-1)}\,\mathbf{t}_c & \text{otherwise;} \end{cases} \tag{14}$$

where $\mathbf{1}$ is a column vector of ones with the same dimension as $\boldsymbol{\alpha}^{(g)}$. Clearly, the pmf of S_{sys} alone can be easily obtained as

$$p_{S_{\text{sys}}}(s) = \sum_{y=0}^{g} p_{S_{\text{sys}},Y_g}(s,y) \tag{15}$$

Finally, the joint pmf of packet delay under systematic RLNC, D_{sys} and Y_g can be calculated as

$$p_{D_{\text{sys}},Y_g}(d,y) = \begin{cases} p_{S_{\text{sys}},Y_g}(0,0) & \text{for } y=0 \text{ and } d=0, \\ 0 & \text{for } y=0 \text{ and } d\geq 1 \\ \dfrac{y}{g}\,\boldsymbol{\beta}_y^{(0)}\,\mathbf{1} & \text{for } y\geq 1 \text{ and } d=0, \\ p_{S_{\text{sys}},Y_g}(d,y) * \displaystyle\sum_{k=0}^{g+1-y}\frac{\delta_{dk}}{g} & \text{otherwise;} \end{cases} \tag{16}$$

and the pmf of D_{sys} alone is calculated as

$$p_{D_{\text{sys}}}(d) = \sum_{y=0}^{g} p_{D_{\text{sys}},Y_g}(d,y)\,. \tag{17}$$

4 Results

In this section we present the most relevant results derived from our performance analysis of both RLNC schemes. As a starting point, we compare the probability of successful delivery for the most typical generation sizes $g \in \{32, 64\}$ and field sizes $q \in \{2, 2^8\}$ in Fig. 6. The number of redundant packet transmissions is simply given as the total number of transmissions n minus the generation size g. A relatively high PER $\epsilon = 0.1$ has been selected, which is the highest

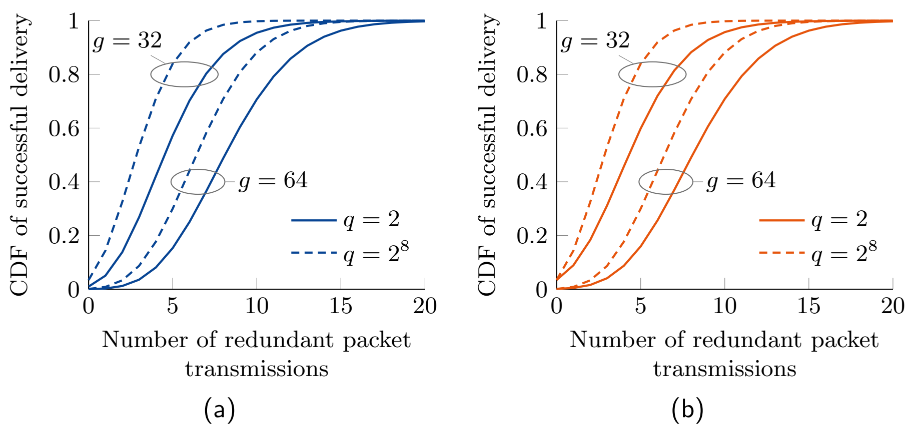

Fig. 6. CDF of successful delivery given $g = 32$ and $g = 64$ for the: (a) full-vector, S_{fv}, and (b) systematic, S_{sys}, RLNC schemes; $\epsilon = 0.1$.

PER permitted in LTE-A. That is, the eNB changes the modulation and coding scheme (MCS) if $\epsilon \geq 0.1$ is reported by a UE [1, Sec. 7.2.3].

As Fig. 6 shows, the probability of successful delivery is considerably higher for $q = 2^8$ than for $q = 2$; also a small generation size (e.g., $g = 32$ instead of 64) increases this probability. This is mainly due to two factors: (a) large field sizes increase the probability of linear independence between packets and (b) fewer errors occur during the transmission of fewer packets. As a result, fewer redundant transmissions are needed to successfully deliver a generation of size $g = 32$ than a generation of size $g = 64$. Nevertheless, it is important to observe that two generations of size $g = 32$ have to be transmitted for each generation of size $g = 64$ to achieve the same number of transmitted packets.

Yet another important characteristic is revealed by comparing Fig. 6a with Fig. 6b: the probability of successful delivery for full-vector, S_{fv}, and for systematic RLNC, S_{sys}, is greatly similar for $\epsilon = 0.1$. The reason for this is that the effect of such a high PER is much more relevant than the effect of linear dependencies in the first g packet transmissions. That is, the probability of linear dependence between coded packets increases with the rank of the decoding matrix at the destination and the maximum probability of linear dependence occurs when only one packet is missing and is $p_{g-1 \to g} = q^{-1}$. The probability of a packet being linearly dependent during the first packet transmissions is much lower.

To showcase the benefits of systematic RLNC and of large field sizes, we compare the probability of successful delivery with full-vector and systematic RLNC given a low PER $\epsilon = 0.01$ in Fig. 7. As it can be seen, the difference between: (a) full-vector and systematic RLNC, and (b) $q = 2$ and $q = 2^8$ is much more noticeable with a low PER. Clearly, in this case the best performance is achieved with systematic RLNC and $q = 2^8$, as less redundant packet transmissions are

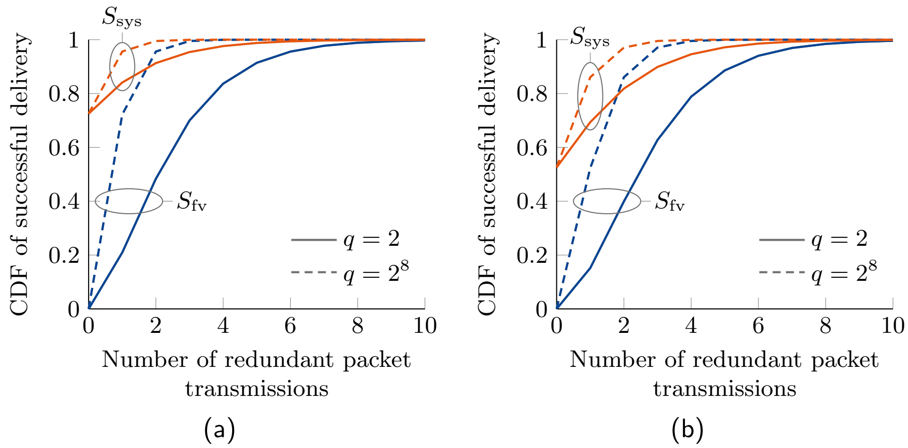

Fig. 7. CDF of successful delivery for the full-vector, S_{fv}, and systematic, S_{sys}, RLNC schemes given: (a) $g = 32$ and (b) $g = 64$; $\epsilon = 0.01$.

needed. As a consequence, high energy savings and a high throughput increase can be achieved with this combination.

Contrary to what is observed in Fig. 6, Fig. 7 shows that the probability of successful delivery for $g = 32$ and for $g = 64$ are highly similar with a low PER. This effect can be clearly observed by comparing the CDF of successful delivery for full-vector RLNC in Fig. 7a with the one in Fig. 7b. That is, the number of redundant packet transmissions performed for $g = 32$ and for $g = 64$ with a low PER are much closer than with a high PER. As a consequence, selecting $g = 64$ leads to a higher ratio of received source packets to total packet transmissions when the wireless channel has low errors. In other words, the benefits of large generation sizes are more evident with a low PER.

Finally, we compare the distribution of packet delay obtained with full-vector and with systematic RLNC for $\epsilon \in \{0.01, 0.1\}$, $g \in \{32, 64\}$, and $q \in \{2, 2^8\}$ in Fig. 8. Similarly as in Fig. 6 and in Fig. 7, the difference between systematic and full-vector RLNC is more noticeable for $\epsilon = 0.01$ (i.e., a low PER) than for $\epsilon = 0.1$. Also, by comparing Fig. 8a with Fig. 8b, and Fig. 8c with Fig. 8d, it can be observed that large generation sizes increase the packet delay. Hence a tradeoff exists between throughput and packet delay with respect to the generation size.

Naturally, large field sizes reduce packet delay as these increase the probability of linear independence of packets and in turn, the probability of successful delivery. However, the difference in packet delay between $q = 2$ and $q = 2^8$ is minimal under systematic RLNC and $\epsilon = 0.01$. On the other hand, the benefits in terms of packet delay of selecting $q = 2^8$ over $q = 2$ under full-vector RLNC are similar for $g = 32$ and $g = 64$, and for $\epsilon = 0.01$ and $\epsilon = 0.1$.

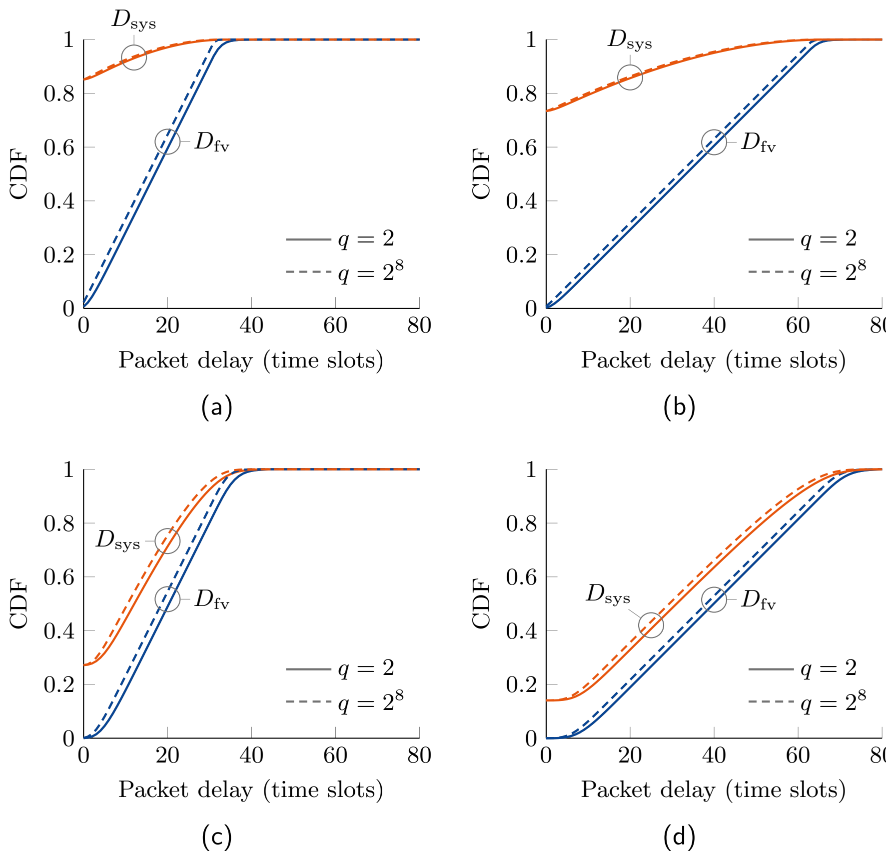

Fig. 8. CDF of packet delay for the full-vector, D_{fv}, and systematic, D_{sys}, RLNC schemes given: (a) $g = 32$ and (b) $g = 64$ with $\epsilon = 0.01$; (b) $g = 32$ and (c) $g = 64$ with $\epsilon = 0.1$.

5 Conclusion

In this paper we assessed the efficiency of two of the most widely used RLNC schemes, namely full-vector and systematic RLNC, in terms of probability of successful delivery and packet delay. We considered a point-to-point communication with strict in-order delivery. Our analysis revealed that if the PER is low, systematic RLNC greatly outperforms full-vector. On the other hand, the difference between these two schemes in terms of probability of successful delivery is minimal if the PER is high. The main reason for this similarity is that we assume in-order delivery. Systematic RLNC would clearly outperform full-vector in terms of probability of successful delivery for any given PER if losses are allowed. On the other hand, systematic RLNC is always better than full-vector in terms of packet delay.

As a result, systematic RLNC is a better candidate for 5G networks than full-vector RLNC as it can provide with a higher reliability (i.e., probability of successful delivery) and throughput in combination with a reduced energy consumption. All these three are among the main requirements for 5G. However, there exists a tradeoff between probability of successful delivery and packet delay. Specifically, large generation sizes increase the probability of successful delivery and packet delay when compared to small generation sizes. Hende, the generation size is a parameter that must be selected according to the requirements of the application.

A relevant aspect that was not taken into account in our analysis and hence is considered for future work is the computational complexity of encoding and decoding processes. That is, the number of operations that must be performed under each of the selected RLNC schemes to create coded packets and to decode the generation. Clearly this is a relevant aspect because it increases the energy consumption for communication.

References

1. 3GPP. Physical layer procedures. TS 36.213 V13.0.0, May 2016.
2. R. Ahlswede, Ning Cai, S. Y. R. Li, and R. W. Yeung. Network Information Flow. *IEEE Trans. Inf. Theory*, 46(4):1204–1216, 2000.
3. P. Garrido, D. E. Lucani, and R. Agüero. Markov Chain Model for the Decoding Probability of Sparse Network Coding. *IEEE Trans. Commun.*, 65(4):1675–1685, 2017.
4. J. Heide and D. Lucani. Composite Extension Finite Fields for Low Overhead Network Coding: Telescopic Codes. In *IEEE Int. Conf. Commun. (ICC)*, pages 4505–4510, 2015.
5. T. Ho, M. Medard, J. Shi, M. Efiros, and D. R. Karger. On randomized network coding. In *Proc. Annu. Allerton Conf. Commun., Control, Comput.*, pages 11–20, 2003.
6. ITU-R. IMT Vision – Framework and Overall Objectives of the Future Development of IMT for 2020 and Beyond. Rec. M.2083, 2015.
7. A. L. Jones, I. Chatzigeorgiou, and A. Tassi. Binary systematic network coding for progressive packet decoding. In *Proc. IEEE Int. Conf. Commun. (ICC)*, pages 4499–4504, 2015.
8. M. Simsek, A. Aijaz, M. Dohler, J. Sachs, and G. Fettweis. 5G-Enabled Tactile Internet. *IEEE J. Sel. Areas Commun.*, 34(3):460–473, 2016.
9. O. Trullols-Cruces, J. M. Barcelo-Ordinas, and M. Fiore. Exact Decoding Probability Under Random Linear Network Coding. *IEEE Commun. Lett.*, 15(1):67–69, 2011.
10. M. Wang and B. Li. How Practical is Network Coding? In *Proc. IEEE International Workshop on Quality of Service*, pages 274–278, 2006.

Automation of the System Responsible for Carrying Out Compatibility Tests to Traffic Regulators and Communication Centers According to the Standard UNE 135401-5:2003 IN

Raúl Sahuquillo Valle[1], Antonio Mocholí Salcedo[1], and Ferran Mocholí Belenguer[1]

[1] Instituto ITACA, Universitat Politècnica de València, Camino de vera s/n
46022 Valencia, Spain
raul_sahuquillo@hotmail.com
amocholi@eln.upv.es
fermocbe@upv.es

Abstract. Although the smart cities boom tries to promote public transport and reduce the private one, the reality is that movement with private cars is still a widespread practice in our society. This causes that the vehicle population and the number of drivers increases every year, which translates into the need to install new infrastructure for traffic management and control. However, prior to their installation, all these elements must be homologated. In this way, as traffic regulators are in charge of controlling traffic lights and a failure in these systems could cause serious incidents, the standards applied to these are the strictest. In the case of Valencia, traffic regulators use Protocol V (UNE 135401-5: 2003 IN) and the City Council requires that before their installation, these have been approved by trusted entities. Nevertheless, the current equipment used to perform this homologation was from 1996 and its realization was manual, complex and took a long time. For this reason, with the aim of facilitating the accomplishment of the different compatibility tests and speeding up the process, an automated procedure that allows and facilitates the systematic performance of mandatory compliance tests in the city of Valencia was proposed as a solution.

1 Introduction

The transformation of transport is already underway and at a much faster pace than expected. New technologies applied to the automotive industry, big data and shared economy are changing the way people move. These advances, together with the growth of the world population and technology, will contribute to an increase in the number of cars that will possibly translate into unsustainable traffic. Currently, it is estimated that there are 1.2 billion vehicles worldwide, but the forecast is that in 2035, this figure will exceed 2.000 million [2]. The main consequences of this growth in traffic will probably be the loss of productivity, the increase in accidents and pollution

C.Fernandez-Llatas and M.Guillen (Ed.):
Workshop on Innovation on
Information and Communication Technologies
(ITACA-WIICT 2018)

ISBN 978-84-09-07373-3

and its negative impact on public health. Therefore, with the purpose of minimizing these effects, increasing road safety, improving traffic efficiency, facilitating user mobility and protecting the environment, traffic management and control emerges as a priority these days in Intelligent Transportation Systems (ITS) [3].

All of the above implies a continuous installation and improvement of the road infrastructure, which is being redefined nowadays. If years ago it was limited to physical components, such as barriers, traffic signals, or regulators, it now includes components such as wireless networks and artificial intelligence. Furthermore, as roads cover a large proportion of the earths land surface, especially in cities, the idea is that the large number of emerging technologies can turn this element, previously passive, into something more productive.

However, regardless of the installed infrastructure, it is clear that for the proper functioning of the system and the safety of all users, this must be approved according to the standards before its installation. This regulation, which can vary depending on the city, community or country in which the traffic equipment is installed, sets a series of specifications that must be overcome by the corresponding equipment. In addition, these tests must ensure that although the most recent equipment implements more advanced functionalities, these must be totally compatible with the technology currently in operation.

The Traffic Control Systems Group of the Polytechnic University of Valencia (ITACA Institute) is cataloged by the Valencia City Council as a trusted entity and thus has the capacity to carry out this certification for regulators and traffic centers according to UNE 135401-5:2003 IN. Nevertheless, the material destined to perform these compatibility tests had never been updated and the realization of any test plan was an arduous task due to the large number of manual operations required, which were prone to generate errors because of the long duration and the necessary knowledge for its realization. Therefore, the automation of the whole process emerged as a necessity.

2 Standardization

In the fifties, the universalization of markets and the concern for increasing the competitiveness of products and services promoted the development of standardization. The purpose of this activity was to develop technical specifications which were used voluntarily as a reference to improve the quality and safety of any activity, whether technological, scientific, industrial or service. In this way, normalization was seen as the way to create consensus, achieve the internationalization of companies and provide them with greater relevance and transparency and impartiality, which finally translated into a final increase in quality.

This standardization is carried out these days by both national and international organizations. In Spain, the entity in charge of standardization is the Spanish Association for Standardization and Certification (AENOR) [4]. This is a private, independent and non-profit organization founded in 1986 by order of the Ministry of Industry and Energy, whose main functions are to improve the quality of products and services of companies and to protect the environment.

The standardization activity by AENOR is developed by areas through the different Technical Standardization Committees (AEN / CTN). In each of these committees are represented all the agents involved in the same sector, such as consumers, users, manufacturers or service companies, although the administration, research laboratories or professional associations are also invited to join. Participation in these technical committees is totally voluntary and disinterested, and all the agents mentioned in the standardization are only rewarded by the benefits that the standards generate for the welfare of society, as there is no type of economic compensation.

AENOR is currently composed of 215 standardization technical committees, but that one related to the creation of standards for road infrastructure and therefore, responsible for UNE 135401-5:2003 IN standard, is the Technical Committee 199. This is called 'Equipment for traffic management' [5] and its secretariat and presidency are respectively ‘La Asociación Española de la Carretera’ and ‘La Dirección General de Tráfico’.

This standardization allows that all road users in their everyday life can take the least possible time to get from one place to another and they can do it in the simplest and safest way, which is achieved thanks to what in traffic terminology is called 'green wave', a situation in which vehicles find all the traffic lights of a street or the vast majority of them in green. However, this fact is only possible due to traffic plans designed by road engineering and the communication between all the road elements. For this reason, interoperability, which is obtained through the application of regulations and standards, is essential in this type of systems.

If one imagines a situation in which there are two traffic regulators from different manufacturers and two vehicles approaching a crossing as shown in Fig. 1A, the ideal case would be that both regulators were connected to a traffic central capable of sending orders in order to provide the situation of Fig. 1B, in which there is a traffic light in green and another in red. Nevertheless, if the traffic regulators had been implemented according to different standards, they could not communicate with each other or with the traffic centers, which could cause situations like the one shown in Fig. 1C.

Hence all regulators of the same city must use the same protocol, which means that they must be implemented under the technical specifications described in the corresponding UNE standard. This is how the understanding and correct operation between all the installed elements is achieved.

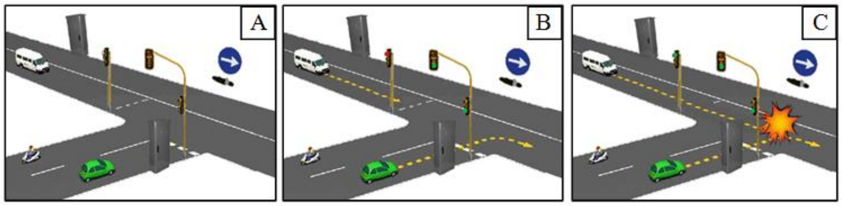

Fig. 1. Common intersection. (A) Intersection with two regulators. (B) Situation in which traffic is managed correctly. (C) Uncontrolled situation in which traffic is not managed correctly.

2.2 Valencia (UNE 135401-5:2003 IN)

The city of Valencia has about 800,000 inhabitants, a metropolitan area close to one and a half million, an automobile fleet of half a million vehicles and a main road network of 300 kilometers in length [6]. This implies the existence of a large number of intersections in which all the agents involved in traffic control are present, which means pedestrians, cyclists, private vehicles, public transport and priority vehicles such as firemen or ambulances.

Unlike Madrid or Barcelona where protocols M and B respectively are used, traffic regulators in the city of Valencia use Protocol V (UNE 135401-5: 2003 IN). This protocol establishes the form and syntax of the frames and commands exchanged by traffic regulators and centrals but it does not detail what tests are necessary to verify that these equipment have been implemented according to this standard. Therefore, the City Council together with the group of Traffic Control Systems (ITACA Institute) and the company ETRA, created a testing plan with some compatibility test in order to validate equipment according to this regulation [7-9]. This testing plan was based on the way traffic regulators work in the city of Valencia and established different tests related to communications, interpreter of commands, alarms, detectors, general functionality, incompatibilities, synchronism, lighting, timetable and SDCTU (Distributed Urban Traffic Control System) tests.

The equipment available in the laboratory to test manually the protocol UNE 135401-5: 2003 IN before the automation was composed by a test console, a communications center (CMC), an internal regulator (CD), a panel of lamps and the software used in the control room of Valencia and Alicante (SDCTU). All these elements are shown in Fig. 2.

Fig. 2. Technician operating in the Traffic Control Systems Group Laboratory. The lamp panel is on the upper left and the regulator under test on the right side behind the test console, which includes a communications center (CMC) and an internal regulator (CD).

However, to carry out each of the tests described in the Valencia testing plan it was necessary to activate and deactivate some of the thirty-eight switches shown in Fig. 3, to make constant RS-232 connections between the different elements as shown in Fig. 4, to send, receive and interpret commands through serial communications and to program each equipment with the appropriate configuration, since each test needed a specific programming.

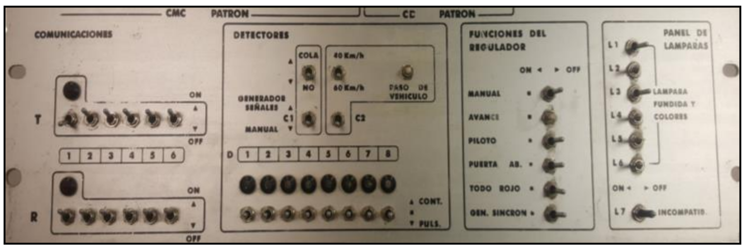

Fig. 3. Test console switches

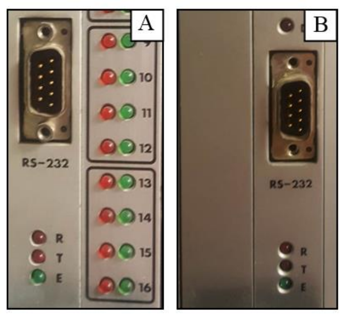

Fig. 4. RS-232 Serial Port. (A) Communications center serial port. (B) Regulator serial port.

Switches of Fig. 3 were necessary to simulate situations similar to those that occur on the roads. These can be grouped into four blocks:

- Communications. With these switches it is possible to select the different connections between the central, regulator and sub-regulator in order to simulate communication losses and restoration.
- Detectors. To simulate detector signals there are 8 switches / pushbuttons corresponding to detectors 1 to 8. In addition, three of them can be connected to the output of a signal generator that simulates queue situation, fluid traffic, and vehicle passage to different speeds.
- General functionalities. With these switches we can simulate different inputs to the regulator such as: guard key, open door, step by manual, advance ...
- Panel of lamps. These switches are available to simulate incompatibility alarm and different situations of blown bulbs.

The panel of lamps consists of 4 groups, which are connected to the outputs of groups 1, 3, 10 and 27 of the regulator. Furthermore, each group has a different configuration of lamps in order to get as close as possible to real installations. In this way, the function of each of these switches is:

- L1 Short-circuits the red of group 1 with the amber of the same group.
- L2 Disconnects the incandescent lamp from group 1 red.
- L3 Short-circuits the red of group 1 with the red of group 3.
- L4 Disconnects a lamp from group 3 red.
- L5 Disconnects a lamp from group 10 red.
- L6 Disconnects the halogen lamp from group 27 red.
- L7 Short-circuits the green of group 1 with the green of group 10.

3 Process Automation

The test console shown in Fig. 5 is the main element to test equipment according to UNE 135401-5: 2003 IN. It was created by the Group of Traffic Control Systems together with ETRA and the City Council of Valencia and is a very complex system that includes different elements. In fact, in the vertical panel, four sections are distinguished:

- Power supply (from ETRA company)
- Communication center (CMC from ETRA company)
- Standard Regulator (CD from ETRA company)
- Power supply control module

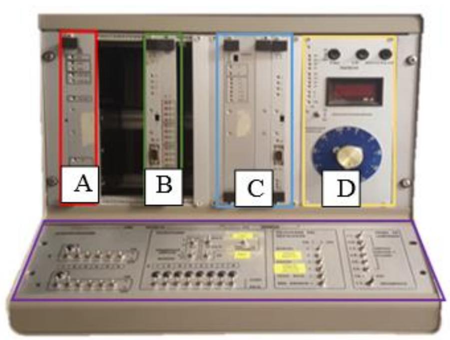

Fig. 5. Test console. (A) Power supply. (B) Communications center. (C) Internal regulator. (D) Voltage controller with switches capable of turning on or off the different elements.

The connection scheme used to perform these tests is shown in Fig. 6.

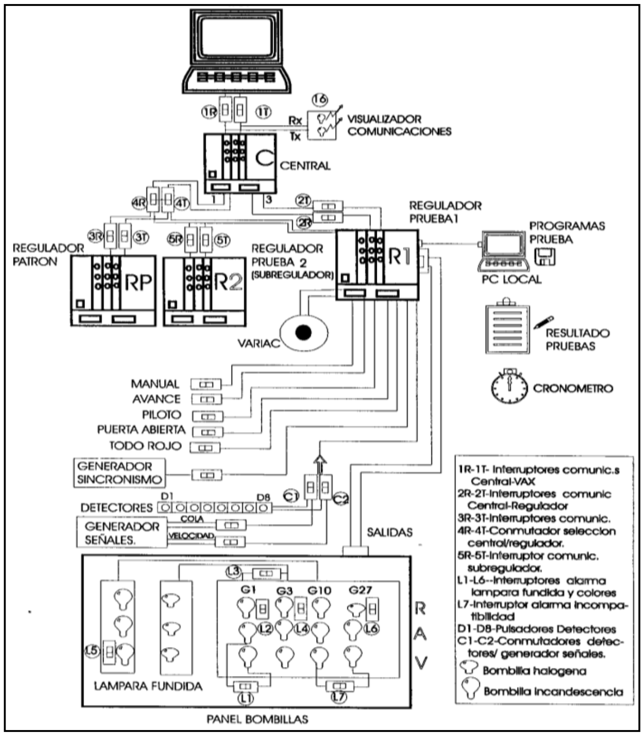

Fig. 6. Connection scheme.

Until now, the element used to enter commands through serial communication was a laptop. This communication required USB-RS-232 connection with the equipment to which it was being interrogated. Therefore, depending on the test, it was necessary to change the connections manually as seen in Fig. 4. In addition, as each test block was trying to check different functionalities, the programming of each equipment for each test was different and also needed to be changed constantly. For this reason, there was a program capable of programming the different regulators according to the necessary requirements.

To replace the manual system existing in the laboratory, two totally differentiated processes were required. On the one hand, it was necessary to carry out the tasks related to assembling and replacing the old wiring and switches by the three relay boards, which entailed cutting the cables, soldering them and equipping them with DB-9, DB-15 and DB-25 pins. On the other hand, with the purpose of avoiding having to make constant RS-232 connections, programming the equipment and sending and interpreting commands, a software capable of running tests automatically was designed in Matlab©.

Consequently, the switches from the test console were replaced by three USB 16 Channel Relay Boards as shown in Fig.7. These relays are now controlled via PC USB port and are configured adequately to emulate each of the tests. They simply emulate the behavior of the previous switches but with the advantage of not doing manually.

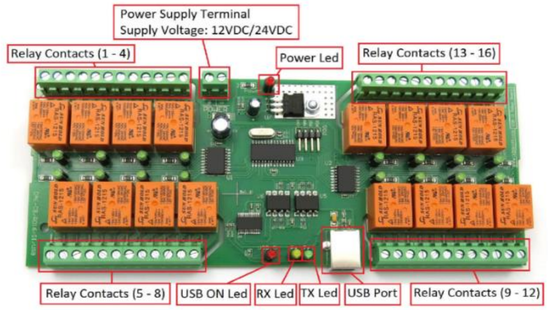

Fig. 7. USB 16 Channel Relay Board – Serial Port

Finally, some of the graphic interfaces of the designed program are shown in Fig. 8. This software allows to select between performing some block of tests or performing the entire test plan. The expected result and the result obtained are displayed on the screen in real time, so that the user can check whether the test is suitable or not. In any case, the program has a function in which it decides for itself if the test is overcome or not by comparing both results.

Fig. 8. Software designed by the group of traffic control systems to test equipment

4 Results

In order to analyze the procedure to perform the Valencia testing plan with the manual system and observe the advantages of having automated this process, the performance of a random test is shown manually and automatically.

When trying to perform the testing plan in the old way, the user first needed the document "Validation Test Plan" [7] in which the procedure of all the tests classified into categories is explained. At the beginning of each of the tests, the programs with which each device must be configured were specified, and then the test was divided into steps in which it was shown in which device the RS-232 cable must be connected at all times, the switches variations, the commands that must be sent and the response that the device must provide. In addition, the user must use a stopwatch in order to respect the waiting times, also specified in this document.

In this manner, Fig. 9 shows the procedure of a random test with the purpose of having a better understanding.

The commands sent by the user through the serial communication have been highlighted in yellow. The responses coming from the devices are shown in red. In addition, since during the test commands are sent both to the traffic regulator under test and to the communications center, some blue and orange brackets have been included to indicate the device with which the command exchange is taking place and therefore, the device where the RS232 cable is connected at all times.

On the other hand, some pink boxes have been introduced to indicate what changes are necessary to make on the switch plate. After these changes, the user must wait before sending the next command due to the waiting times established in the testing plan, which have been highlighted in green.

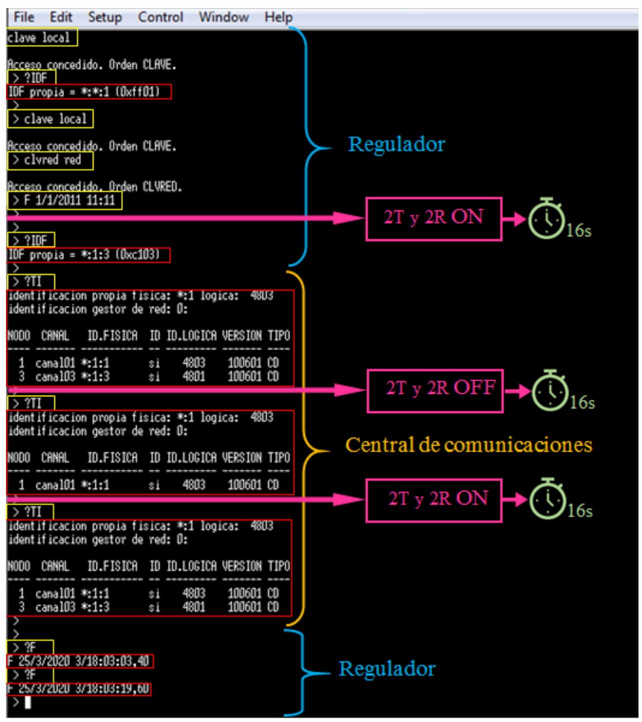

Fig. 9. Operating mode before automation

However, although this system worked properly, it was not entirely efficient. In fact, with this new system it is only necessary to register the regulator, or choose it if it has already been discharged, perform a connection test in order to verify that all devices are properly configured, and choose the test or the block of tests to be performed. In this way, the need to enter commands, interpret them, program equipment and make connections changes is eliminated. In addition, all the tasks that previously were carried out by different software, now have been implemented in the same software designed in Matlab. Fig. 10 shows different program interfaces.

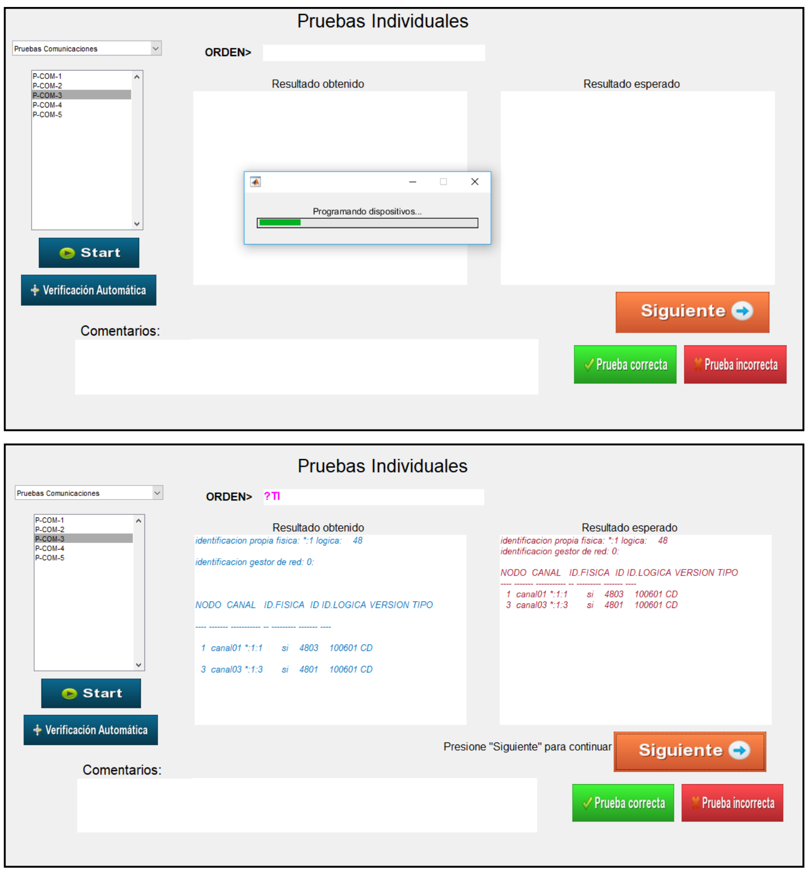

Fig. 10. Operating mode after automation

5 Conclusions

The municipality of Valencia has a test plan consisting of eleven different types of tests. In the event that everything worked as it should, these tests took around 10 hours, although this time could increase to several days if possible failures arise. In addition, the large number of operations required for each test increased the possibility of making mistakes.

However, with this new automated procedure, errors associated with mechanical failures have been minimized and the entire process has been simplified. This avoids introducing and interpreting commands while performing the tests, although highly qualified personnel continue to be required. In addition, this new method is able to generate reports and indicate which tests have been passed and which have not. Thus, it facilitates the interpretation of results and saves time in the customized elaboration of reports for the different companies.

References

1. Antonio Randulfe – Director de Comunicación de la Asociación Española de Fabricantes de Automóviles y Camiones (ANFAC), "La fabricación de vehículos en España sube el 2,9% entre enero y abril", Nota de prensa, 2018.
2. Sperling, D., and D. Gordon. Two Billion Cars: Driving Toward Sustainability. Oxford University Press, 2009.
3. R. H. Goudar; H. N. Megha: Next generation intelligent traffic management system and analysis for smart cities: International Conference On Smart Technologies For Smart Nation (SmartTechCon) IEEE Conferences, pp 999-1003, 2017.
4. Asociación Española de Normalización y Certificación (AENOR) – Web page: http://www.aenor.es/
5. Angel J. Muñoz Suárez, Miembro del Comité de Normalización AEN/CTN199 "Equipamiento para la gestión del tráfico": Potencialidad de la tecnología de gestión de tráfico en la mejora de la Seguridad Vial.
6. Ayuntamiento de Valencia – Movilidad – Centro de gestión de tráfico. Web page: http://www.valencia.es/ayuntamiento/trafico.nsf
7. Regulador de Tráfico – Plan de Pruebas de Validación - Mayo de 1997 - Universidad Politécnica de Valencia – A.Mocholí Salcedo.
8. Estudio de Sistemas de Control de Tráfico – Revisión de la normativa nacional e internacional – Desarrollo de un Sistema de Validación para Reguladores y Centrales de Control de Tráfico - Trabajo conducente a obtención de DEA - Universitat Politècnica de València – Pineda Castillo Ubaldo Augusto - 26/07/2006.
9. Desarrollo de Herramientas Hardware y Software para Ejecutar Test Automatizado a Controladores según los Estándares de la Industria del Tráfico Vial - 1er Congreso Internacional de Mecatronica (CIM 08) - Chiapas, México - 02/04/2008 -U. Pineda C.; A. Mocholi S.; V. Traver S- "Proceedings".pp. 73 - 79. COCyTECH.

Telecom Traffic Characterization & Quality of Service in a Smart City: Municipal Heritage Management Service

Zhuhan Jiang[1], Angel Gomez-Sacristan[2], Miguel A. Rodriguez-Hernandez[3]

[1] Beijing University of Posts and Telecommunication, 100876 Beijing, China
z.jiang@se14.qmul.ac.uk
[2] Instituto ITACA, Universitat Politècnica de València, Camino de Vera s/n, 46022, Valencia, Spain
agomez@dcom.upv.es
[3] Instituto ITACA, Universitat Politècnica de València, Camino de Vera s/n, 46022, Valencia, Spain
marodrig@upvnet.upv.es

Abstract. This paper aims to define characterization of telecom traffic sources in intelligent municipal heritage management service inside smart sustainable city (SSC) and to find out a proper quality of service (QoS) mechanism for this communication network using Valencia City as background. Four traffic heterogenous sources were defined according to real-life requirements and datasheet of sensors suitable. Different simulation has been made to find proper CIR (Committed Information Rate) and PIR (Peak Information Rate) values for this network. Network's performance was checked through its packet loss, throughput, delay and jitter. As the result, we defined minimum values for PIR and CIR, and thus traffic telecom costs.

1 Introduction

Smart sustainable city (SSC) is a kind of city combing devices able to utilize information and communication technology (ICT) with the existing infrastructures (such as building and lights) in a city [1]. By using ICTs, SSC is capable to converge all systems and able to control all resources in this city. Therefore, the consequence that saving cost and energy can be achieved.
This paper is based on an existing network structure and simulator, aiming to solve a problem that heterogeneous sensors in the existing telecommunication networks are needed to be implemented. In case of the study, intelligent heritage management, consisting of multiple sensors, is included in municipality network that is going to be analyzed. The intelligent heritage management is a kind of service protecting heritages from deterioration causes that will damage the durability of art work [2]. Deterioration causes are those physical factors and human-made destructions. For example, artworks can be influenced by surrounding environment agents such as temperature, humidity, ultraviolet and chemical agents (e.g., SO_2, O_3, NO, etc.) [3]. Therefore, to protect heritages from those destructive agents all the time, an intelligent system is

C.Fernandez-Llatas and M.Guillen (Ed.):
Workshop on Innovation on
Information and Communication Technologies
(ITACA-WIICT 2018)

ISBN 978-84-09-07373-3

required to provide art heritages with real-time monitoring and recording of historical data.

The objective of this paper is to simulate the behavior of municipal communication network including intelligent heritage management, analyzing the bandwidth consumed, delay, packet loss, etc. The work included is an application of Internet-of-things (IoT) allowing heterogeneous sensors to be applied together [4]. The goal is to find how to ensure an adequate quality of service (QoS) in a network of heterogenous devices.

In the scenario of smart city shown in Fig1, there are city council internal network, MPLS network and city platform servers. Inside the city council internal network, there are traffic sources and output trunk. The sources refer to heterogenous sources included in the intelligent municipal heritage management service, and the output link is responsible for collecting all generated data and transferring them forward to outside network. MPLS network is multiprotocol packet label switching network that is used between hosts and servers [5], transmitting packets from the city council internal network to corresponding remote servers. City platform servers are controllers receiving all data from sources and monitoring services.

The network also has QoS mechanism to ensure that important information is not delayed too much or dropped in the network, making sure the network is operating under a high efficiency and quality. QoS mechanism includes five steps: classification, marking, policing, queueing and scheduling [6]. Classifications used are multimedia, gold and silver that defined based on a Macrolan of smart hospital [7]. The policer used is two rates Three Color Meters (trTCM).

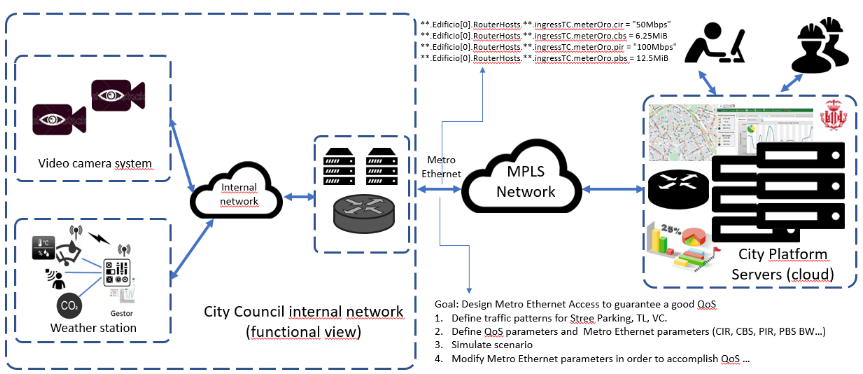

Fig. 1. Scenario of smart city in functional view

This paper is written in five parts: Section 2 introduces the simulation tool OMNET++; Section 3 introduces the intelligent municipal heritage service and heterogenous sources included inside; Section 4 shows the results of simulations implementing smart city network; Section 5 concludes the work and lists further work.

2 OMNET++ Introduction

OMNET++ is a network simulator programmed and compiled in C++, based on which we can create and test telecommunication network simulations with many different structures and configurations. This tool has a huge number of basic libraries and it is extensive enough to satisfy different requirements, we can use it to establish many kinds of networks. For easy operations and designs, OMNET++ also provides an Eclipse-based IDE, the network is described in high-level language [8].

2.1 Components of one simulation

In OMNET++ simulator, one simulation consists of five main parts: network description file (.ned, which describe the structure of this network), network definition file (.cc, which define the communication mode), message definition file (.msg), simulation kernel library and user interface library(.lib/ .a) and profile (.ini).
Among them, NED and INI file are main parts of one simulation that we need to define: NED file describes the structure of network including modules and connections. There can be multiple NED files in one simulation; INI file defines the configuration of one simulation, such as defining communication rules and matching sources with destinations. Besides, we use XML file to add complementation to one simulation.

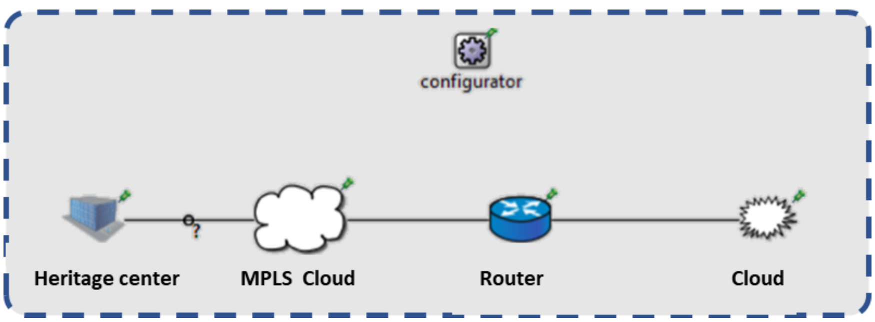

Fig. 2. NED file of the simulation defining the topology of smart city communication network implemented in OMNET++

2.2 Run the Simulation

After defining all three kinds of files, we can start the simulation by running the "ini" file by clicking "Run As OMNeT++ Simulation" button. Then the window of simulation is generated, we can click on the "run" or "express" button to start it. After one simulation arrives the time limitation, it will finish and generate results in result list. Then any analyzation and evaluation based on results can be applied.

3 Intelligent Municipal Heritage Management

In order to protect heritage from deterioration causes, three kinds of sensors and a video surveillance system are concluded inside. Video surveillance system is applied to monitor surrounding situation, in case that someone may damage art work. Sensors are temperature and humidity sensor, lighting and ultraviolet sensor and gas sensor, used to detect physical agents around art work and provide real-time data of physical agents to city council. In this section, traffic sources characterizations are defined.

3.1 General Characterization of Video and Data Sources

Traffic sources can be divided into three classes in content: voice, video and data sources. Voice and video sources belong to human type communication, having active and inactive time. Data sources belong to machine type communication, having burst intervals and huge number of sources. In definition of one source, there are four parts: start time, class of service, quality or data size and profile. Start time is the time when this service begins to transmit information, commonly a random variable. Class of service is the priority of one source (multimedia, gold and silver). Quality or data size define the packet size. Profile stores the configuration of one source, different kinds of source have different parameters included. Tables 1 and 2 show the general model of data and video source.

Table 1. General Characterization of Data Source

Parameter	Type	Description
Text resource size	Data size	Size of each text packet (in bytes)
Image resource size		Size of each image packet (in bytes)
Number of text resource		Number of text resource in the file
Number of image resource		Number of image resource in the file
Number of packets	Profile	Number of packets in one session
Send interval		Time between two packets
Number of bursts		Number of sessions in total
Burst interval		Time between two sessions

Table 2. General Characterization of Video Source

Parameter	Type	Description
Res X	Video Quality	Frame width (in pixels)
Res Y		Frame height (in pixels)
Duration	Profile	Duration of a video (minutes)
Time inactive		Time when no video generated (minutes)
Movement		The level of movement in a video (1 to 4)
Frame per second(fps)		Number of frames in one second

3.2 Video sources definition

In order to define video sources of video surveillance system, we compared several cameras according to requirements of this service at first to find the most proper terminal for this system. Table 3 shows the comparison.

From the comparison, we found everyone has its pros and cons. But, according to the importance of each function, we chose the third one, “TV-IP450P”. The reasons are: 1) The motion detection is one of the most important function for surveillance. 2) The requirements for shutter speed is between 1/1 – 1/1,000s, the second one’s shutter speed is too much. After the selection, we defined video sources characterization from its data sheet and real-life condition, which is shown in Table 4.

Table 3. Comparison of four cameras. “IP2M-846EB”[9] and “IP2M-850E”[10] come from Amcrest company, “TV-IP450P”[11] and “TV-IP450PI”[12] come from TRENDnet company.

Parameter	IP2M-846EB	IP2M-850E	TV-IP450P	TV-IP450PI
Minimum illumination (Lux)	Color: 0.05 B/W: 0.005	Color: 0.05 B/W: 0.005	Color: 0.05 B/W: 0.01	Color: 0.05 B/W: 0.01
Shutter speed (s)	1/1–1/30000	1/3–1/30000	1/1–1/10000	1/1–1/10000
Zoom	Digital: 16x Optical: 4x	Digital: 16x Optical: 20x	Digital: 16x Optical: 20x	Digital: 16x Optical: 20x
Viewing angle	H:116.5-34.5° V: N/A	H: 54.1-3.2° V: N/A	H: 54° V: N/A	H: 54° V: N/A
Focal length(mm)	2.7– 11mm	4.7– 94mm	4.7– 94mm	4.7 – 94mm
Max Aperture	F 1.6 – 2.8	F 1.4 – 2.6	F1.4 – 3.5	F1.4 – 3.5
Rotation angle/ inclination	Pan: 0 – 360° Tilt: 0 – 90°	Pan:0 – 360° Tilt: -15–90°	Pan: 0–360° Tilt: -5– 90°	Pan: 0 – 360° Tilt: -5 – 90°
Day/ Night	Yes	Yes	Yes	Yes
Resolution	1280x720	1280x720	1280x960	1280x960
Video encoding	H.264/MJPEG	H.264/MJPEG	H.264/MJPEG	H.264/MJPEG
Max frame rate	30fps	30fps	30fps	30fps
Motion detection	N/A	Yes	Yes	N/A
Alarm handling	2/1 channel in/out	2/1 channel in/out	External alarm	External alarm
Audio detection	Yes	Yes	Yes	Yes
Microphone input	N/A	N/A	External	External
Network Port	RJ-45	RJ-45	100Base-T	100Base-T

Table 4. Characterization of Video Source in video surveillance system

Video Surveillance					
Number		10			
Start time		Uniform(0s,900s)			
Class of service		Gold			
Video Profile	Duration	Type: Exponential	Mean: 5	Min: 3	Max: 7
	Time Inactive	Type: Exponential	Mean: 15	Min: 10	Max: 20
	Movement	2			
	fps	25			
Video Quality		1280 x 720			

3.3 Data sources definition

Similar as video sources, three different sensors should be selected firstly to define corresponding characterizations. Due to their corresponding requirements, we select several candidates and finally defined three proper sensors.

For temperature and humidity, we select one sensor that can detect both of them. After comparing range of measurements and their accuracy with requirements, we select "Humidity and Temperature Transmitter EE33-M"[13] finally. Because this sensor has higher accuracy than requirements and larger measuring range. For lighting and ultraviolet, sensor should capable to detect ambient brightness and sunlight strength on the surface. Due to those needs, we choose "UVB+UVA Sensor PMA1107"[14] as corresponding sensor. For gas sensor, we chose the one that can measure NO_2, O_3, CO and SO_2 of environment and the particle PM2.5 and PM10 in the environment [15]. Because this sensor should be used indoor to protect heritage, we chose the one having highest accuracy and bigger range than others. Table 5 show characterizations of data source from gas sensor, the other sensors are modulated in a similar way.

Table 5. Characterization of data source from gas sensor

Number		8
Start Time		Uniform(0s,180s)
Class of Service		Silver
Data Profile	numPackets	1
	SendInterval	1
	numBursts	1
	burstInterval	3600s
Data Size	textResourceSize	20 Bytes
	numResources	4

4 Simulations and results

This section shows the results of simulations. This section is divided into two parts. In the first part, we simulate this service to find our proper value of CIR and PIR. Then we simulated to find the proper bandwidth that should be assigned to this network in output link.

4.1 Test CIR and PIR

Table 6. QoS mechanism parameters and corresponding results for video source (gold class)

	CIR (Mbps)	CBS (MiB)	PIR (Mbps)	PBS (MiB)	Packet loss
CIR<PIR<Max throughput	10	1.25	20	2.5	140520
CIR<Max throughput<PIR	20	2.5	30	3.75	0
Max throughput<CIR<PIR	50	6.25	60	7.5	0

For the four sources included in this service, we firstly classified them based on their characterization. Video source is classified into gold class for its high time sensibility. Data source is classified into silver class for its lower importance and time sensibility. Therefore, we test CIR and PIR of gold and silver class communications. CIR is the guaranteed communication speed for important data in one connection, PIR is the limitation of one connection to define the maximal speed. Tests are divided into three conditions:

1) CIR < PIR < maximal throughput,
2) CIR < maximal throughput < PIR,
3) maximal throughput < CIR < PIR.

Table 6 and Table 7 show the parameters we assigned for two classes.

Table 7. QoS mechanism parameters and corresponding results for data source (silver class)

No.	Condition	CIR (kbps)	CBS (KiB)	PIR (kbps)	PBS (KiB)	Packet loss
1	CIR<PIR<Max throughput	0.4	0.05	0.8	0.1	90
2	CIR<Max throughput<PIR	0.8	0.1	2	0.25	0
3	Max throughput<CIR<PIR	20	2.5	30	3.75	0

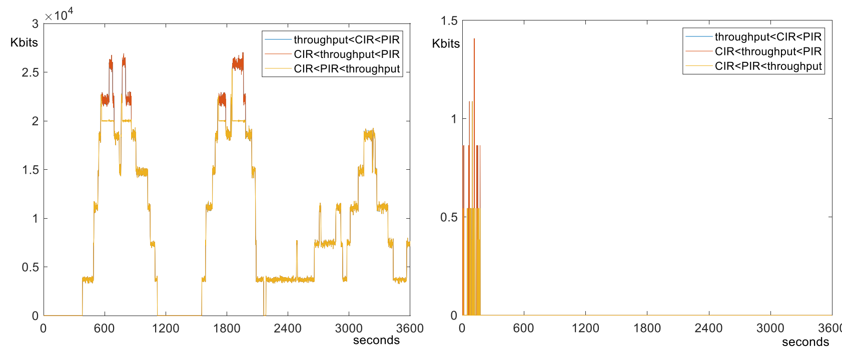

Fig. 3 Throughput of 10 video (*left, kbits/sec*) and 37 data sources (*right, kbits/sec, 21 temperature and humidity sensors, 8 lighting and ultraviolet sensor, 8 gas sensor*) under three conditions (*Blue line for condition 3, orange line for condition 2, yellow line for condition 1*).

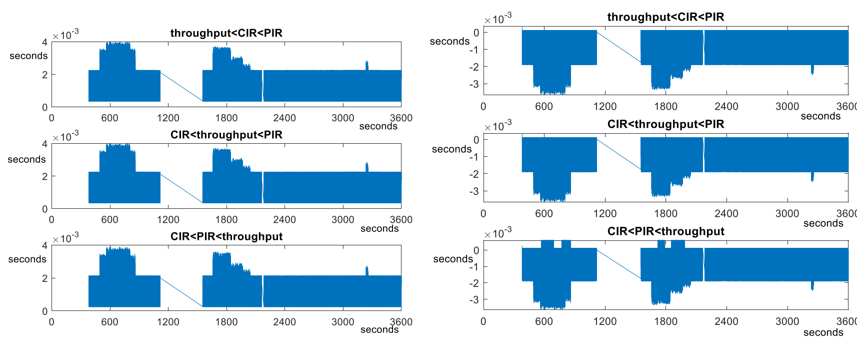

Fig. 4 Delay (*left, sec/sec*) and jitter (*right, sec/sec*) of 10 video sources under three conditions. (*Top one for condition 3, middle one for condition 2, bottom one for condition 1*).

After simulating each condition for 1 hour, we got results shown in figure 3, figure 4 and figure 5.

Because three data sensors have similar characterization, we showed result of temperature and humidity sensor as an example of data source. From figure 3, the throughput of 20 video sources is from about 0 Mbps to 32 Mbps, and the throughput of data sources generated from temperature and humidity sensor is around 1.1 Kbps. For both data and video sources, the throughput under condition 1 is obviously limited under 20Mbps, that difference happened when throughput exceeds PIR value and caused huge packet losses.

The throughput under condition 2 is not influenced so much by low CIR because the packet sizes and throughput of this service are not big enough to cause obvious distance. From figure 4, the delay and jitter of video source under condition 2 is slightly higher than condition 3 but the delay and jitter under condition 1 is obviously lower than other two conditions.

That showed that many packets are dropped directly instead of waiting in the queue, causing lower delay and jitter. The delay and jitter of data source shown in figure 5 are in a similar result.

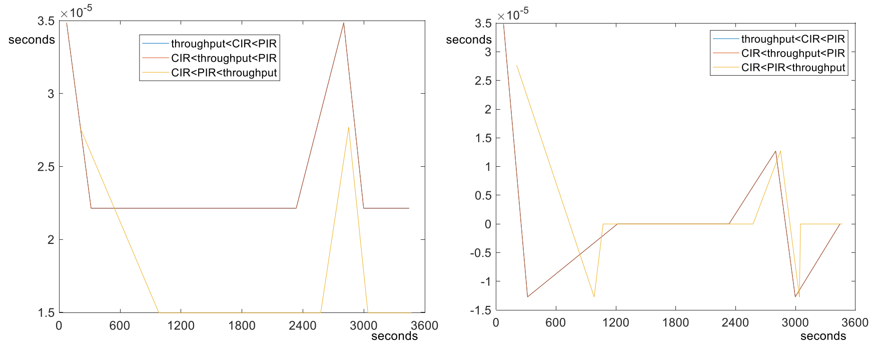

Fig. 5 Delay (*middle, sec/20s*) and jitter (*right, sec/20s*) of 21 temperature and humidity sources under three conditions. (*Blue line for condition 3, orange line for condition 2, yellow line for condition 1*).

4.2 Test total bandwidth

Three levels were tested for this simulation, 10M, 100M and 1G. The result of three two-hour-simulations are shown in figure 6, figure 7 and figure 8. Temperature and humidity sensor was still used as the example of data source.

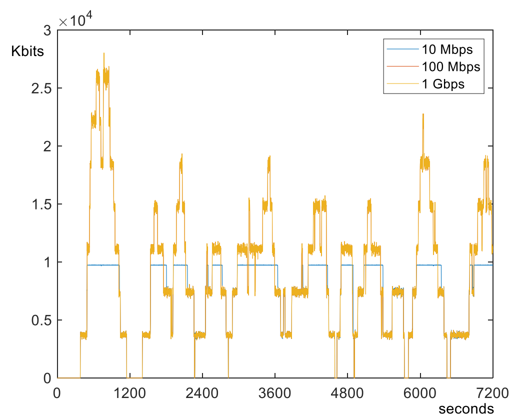

Fig. 6 Throughput (*kbits/sec*) in output link (*10 video sources and 37 data sources*) under three different bandwidths (*Blue line is for 10M, orange line is for 100M, yellow line is for 1G*).

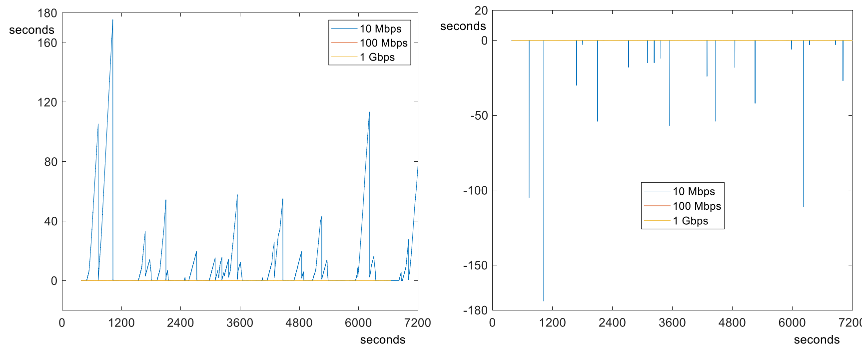

Fig. 7 Delay (*left, sec/sec*) and jitter (*right, sec/sec*) of 10 video sources under three bandwidths (*Blue line is for 10M, orange line is for 100M, yellow line is for 1G*).

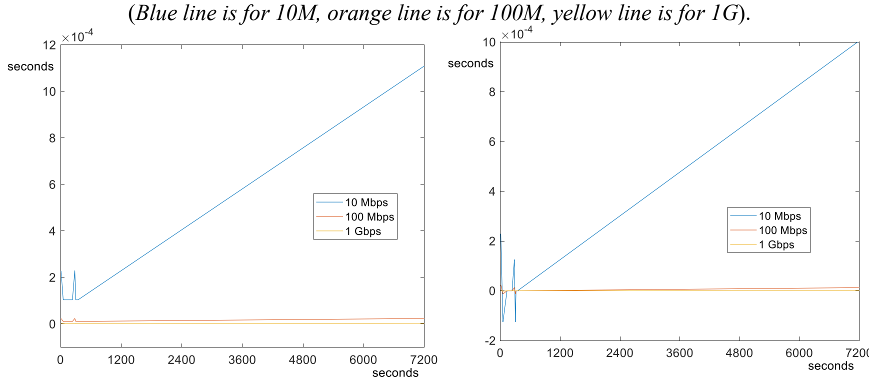

Fig. 8 Delay (*left, sec/ 2s*) and jitter (*left, sec/ 2s*) of 21 temperature and humidity sensor under three conditions (*Blue line is for 10M, orange line is for 100M, yellow line is for 1G*).

The results showed that the throughput under 10M is obviously lower than other two bandwidths, causing 1,205,120 packets lost. And the delay of both video and data sources are also larger than other two bandwidths. Due to large throughput of video sources, the bandwidth assigned must larger than 32Mbps. Therefore, 10M is definitely not large enough.

For 100M and 1G, there are almost no differences in throughput of video and data sources, delay and jitter of video source, but small differences in delay and jitter part for data sources. However, that small difference doesn't influence normal communication for sources in lowest priority. Because that bandwidth is very important source, 100M is the better choice for this service than 1G in order to save bandwidth.

5 Conclusions and Further Work

From all tests of simulation, following conclusions about QoS mechanism and bandwidths were achieved:

1. The simulation tools provide a flexible and economical mechanism to evaluate the network impact of projects that generate heterogeneous traffic with finite sources.
2. Lower CIR or PIR limits the throughput and cause delay, jitter and packet losses.
3. It is necessary to perform an iterative process to get calculate the appropriate parameters of bandwidth, CIR & PIR and in this way to minimize the costs of the necessary communications for this project.

As future lines of work, it may be of interest to evaluate the impact on the municipal network of the implementation of new projects that share the available bandwidth and the resulting aggregate traffic. Besides, after intelligent municipal heritage management system has been established in the future, more accurate and exact real data can be achieved to test the behavior and performance of this network.

References

1. ITU-T Y.4250 series. Smart sustainable cities – Overview of smart sustainable cities infrastructure. ITU-T Y-series Recommendations – Supplement 30 (2016)
2. Mesas-Carrascosa, F., Santano, D., Larriva, J., Cordero, R., Fernández, R. and García-Ferrer, A. (2016). Monitoring Heritage Buildings with Open Source Hardware Sensors: A Case Study of the Mosque-Cathedral of Córdoba. *Sensors 2016*, 16, 1620
3. Garcia Diego, F., Esteban, B., Merello, P. (2015). Design of a Hybrid (Wired/Wireless) Acquisition Data System for Monitoring of Cultural Heritage Physical Parameters in Smart Cites. *Sensors*. pp. 7246-7266.
4. Gribaudo, M., Lacono, M. And Levis, A. (2017). An IoT-based monitoring approach for cultural heritage sites: The Matera case. *Wiley*. 2017;29;e4153. John Wiley & Sons, Ltd.
5. Heron, G., Martini, L. (2008). 'MPLS'. In: Kasim, A. (eds.). *Delivering carrier ethernet*. The McGraw-Hill Companies. pp. 421-467.
6. Evans, J., Filsfils, C. (2007). 'Data Plane QOS Mechanisms', pp. 99-100, In: *Deploying IP and MPLS QOS for multiservice Networks*. USA: Elsevier Inc.
7. Gomez-Sacristan, A., Rodriguez-Hernandez, M. and Sempere, V. (2015). Evaluation of Quality of Service in Smart-Hospital Communications. *Journal of Medical Imaging and Health informatics*. 5, pp. 1-6
8. OMNET++, *What is OMNET++?* [online] Available from: https://omnetpp.org/intro [Accessed 20 January 2018]
9. Amcrest, *Amcrest ProHD Indoor PTZ (4x Optical Zoom) 1080P POE IP Camera, 98ft Night Vision, Pan/Tilt/4x Motorized Zoom, Wide 116° Viewing Angle, 2-Megapixel (1920TVL), Sentinel, IP2M-846E (Black)* [online] Available from: https://amcrest.com/amcrest-prohd-indoor-2-megapixel-poe-ptz-dome-ip-security-camera-4x-optical-zoom-wide-116-viewing-angle-2mp-1920tvl-ip2m-846e-black.html [Accessed 2 March 2018]
10. Amcrest, *Amcrest ProHD PTZ (20x Optical Zoom) Outdoor POE IP Camera Speed Dome 1080P, 328ft Night Vision, POE+ (802.3at) - IP66 Weatherproof, Pan/Tilt/20x Motorized Zoom, 2-Megapixel (1920TVL), Goliath IP2M-850E (Black)* [online] Available from: https://amcrest.com/amcrest-prohd-outdoor-2-megapixel-poe-ptz-ir-speed-dome-ip66-

weatherproof-remnote-360-field-of-view-2mp-1920tvl-ip2m-850e-black.html [Accessed 2 March 2018]

11. Trendnet, *Outdoor 1.3 MP HD PoE+ Speed Dome Network Camera* [online] Available from: http://www.trendnet.com/products/proddetail?prod=220_TV-IP450P [Accessed from 3 March 2018]
12. Trendnet, *Outdoor 1.3 MP HD PoE IR Speed Dome Network Camera* [online] Available from:http://www.trendnet.com/products/proddetail?prod=105_TV-IP450PI#tabs-solution02 [Accessed from 3 March 2018]
13. E+E Elektronik, *EE33-M Humidity and Temperature Transmitter for High-end Meteorological Applications* [online] Available from: https://www.epluse.com/en/products/humidity-instruments/industrial-humidity-transmitters/ee33-m/ [Accessed from 4 March 2018]
14. Solar light, *Model PMA1107 Analog Non-Weighted UVA+B Sensor* [online] Available from: https://solarlight.com/product/uvauvbsensorpma1107/
15. Vaisala, *Air Quality Transmitter AQT400 Series* [online] Available from: https://www.vaisala.com/sites/default/files/documents/AQT400-Series-Datasheet-B211581EN.pdf

Interactive Data Modeling for Pancreas Transplantation Decision Support in Type 1 Diabetes Patients

Pilar Moreno-Alfaro[1], Antonio Martinez-Millana *[1], Maria Argente-Pla[2], Juan-Francisco Merino-Torres[2] and Vicente Traver[2]

[1] ITACA. Universitat Politècnica de València, Camino de Vera S/N, Valencia 46022, Spain
[2] Servicio de Endocrinología y Nutrición del Hospital Universitario y Politécnico La Fe, Bulevar Sur S/N, Valencia 46026, Spain

Abstract. The following communication describes the interactive development and implementation of a web-based clinical decision support system to help doctors on the assessment of pancreas and kidney transplant in patients with type 1 Diabetes Mellitus. An exploratory data analysis has been performed using a group of 82 patients, which have been transplanted in University Hospital La Fe (Valencia, Spain) between 2002 and 2015. This analysis allows to describe the sample population and 134 variables acquired during the study. Among them, the most significant indicators were used for developing a classification model to predict the transplant success and failure. An ensemble model of k-Nearest Neighbors enables to predict the pancreas loss with a 82,9% accuracy using ten input variables. The model was implemented in runtime engine and integrated into a distributed service oriented architecture.

1 Introduction

Diabetes Mellitus (DM) is a chronic disease that occurs when the pancreas does not produce enough insulin or when the body does not efficiently use it.[1]. Type 1 Diabetes Mellitus (T1DM) management requires a daily administration of exogenous insulin [2]. The main therapeutic strategy for T1DM is based on maintaining blood glucose levels within values considered normal with the injection of insulin [3], and the combination of carbohydrate intake and moderate physical activity [4].

An effective control of blood glucose levels minimizes the prognosis as a continuous exposure to high glucose levels is associated in the long term with macro- and micro-vascular complications that decrease the quality and life expectancy of patients [5]. A new therapeutic option is the simultaneous kidney and pancreas transplant [6]. The first pancreas transplant in animals was performed in 1892 when a portion of pancreas was implanted in a dog, preventing the development of diabetes. In 1922, with the discovery of insulin, research on

* *Corresponding author: anmarmil@itaca.upv.es

C.Fernandez-Llatas and M.Guillen (Ed.):
Workshop on Innovation on
Information and Communication Technologies
(ITACA-WIICT 2018)

ISBN 978-84-09-07373-3

pancreas transplantation decreased since the use of insulin allowed to increase the survival of diabetic patients [7]. However, chronic complications derived from T1DM stood and in the decade of the 60s the advances in the suppression allowed to successfully undertake the first transplant of pancreas in humans. The main benefits of pancreas transplantation are the decrease in mortality and the improvement of the quality of life of the patient [8]. The decrease in mortality is due to kidney transplantation, since patients on dialysis have a higher mortality compared to those who do not transplant [9]. The improvement in the quality of life is derived, not only due to dialysis drop off, but also from the abandonment of insulin, avoiding daily injections. The improvement in the results of the pancreas transplant has been progressively increasing as donor and recipient selection criteria, surgical techniques, immune-suppressants and graft monitoring have improved, so that the average survival of the patient and the pancreatic and renal grafts have increased progressively [10].Moreover, patient survival at 5 years after transplantation has reached an impressive 89.8 % [11]. Therefore, pancreas transplantation in any of its modalities entails a notable increase in patient survival, of around 10 years, compared to those who remain on the waiting list.

Despite surgical techniques and drugs for this type of intervention have improved, the rate of transplanted pancreas loss is still high. A study conducted by E.B.Finger [12] focused on the analysis of risk factors directly related to the short-term loss of the pancreas. Finger and colleagues found statistically significant risk factors associated with the graft donor, among which are the donor's age, creatinine levels and Body Mass Index. The study concluded that donors who present only one of these risk factors did not have a relevant influence on the final result, while the presence of at least 3 risk factors can decrease graft survival up to 50%. In this manuscript we analyze a group of 82 patients who were transplanted and followed-up for 13 years. A retrospective data analysis is conducted to assess different modeling techniques and predictors selection to build and validate a prediction model for the success/failure in the reappearance of T1DM in transplant receivers. After comparing state-of-the-art modeling techniques, the best prediction performance (Accuracy=82.9%) was achieved for an ensemble k-Nearest Neighbors model which needed the following input predictors of the receiver: Body Mass Index, Systolic Blood Glucose, Fasting Glucose, Urea, HDL, Units of insulin per day and Number of cigarettes per day.

2 Materials and methods

2.1 Data and modeling analysis pipeline

The initial stage of the study methodology was based on a comprehensive Exploratory Data Analysis (EDA) and a bivariate statistical analysis. Parametric tests (t-Student test, Pearson correlation analysis and ANOVA test) and non-parametric tests (Mann-Whitney-Wilcoxon and Kruskal-Wallis tests) were applied depending on the variable distribution goodness-to-fit. After the identification of significant variables, different classification algorithms were trained and validated subsequently to compare the statistical performance in an iterative variable selection process [13].

Table 1. Classification methods

Modeling Technique	**Description**
Linear/Logistic Regression	Linear or non-linear relationship among predictors and responses, which can be numerical or categorical [14]
Decision Trees	Consecutive divisions of data into roots and leaves(the result) [15]
k-Nearest Neighbors (KNN)	Classification according to the most frequent class of its k closer data (with less distance) [16]
Support Vector Machines (SVM)	Classification of data by building a hyperplane that separates the samples according to the class to which they belong [17]
Discriminant Analysis	Method to establish a boundary between prediction and response distributions that allows to properly classify the samples [18].
Ensemble Classifiers	Divides the dataset into similar sub-datasets which are used for training and testing a the model performance [19]

2.2 Classification Models

Classification models aim to analyze the simultaneous effect of the relationships on a set of more than two variables in a numerical way [20]. For the development of the models it is necessary to have known data, that is, to include both the input variables and its classification. Once the model is produced, it can be used to predict results based on new input data. Within these categories there is a wide variety of models and techniques, however, in this study only the spread-used models are trained and validated to compare its performance in the current problem (Table 1).

The performance of the models was assessed by classical performance indicators: Sensitivity, Specificity, Area Under the ROC curve, Accuracy and Predictive Positive Value according to the TRIPOD Statement [21].

2.3 Statistical software

Data analysis and models development and validation was done using Matlab 2017a software with the Academic license of the Universitat Politècnica Valéncia. In addition to the basic functions of Matlab, this study was done using the Classification Learner toolbox.

2.4 Reduction of dimensionality

Principal Components Analysis (PCA) was used to identify principal characteristics in which groupings of variables moved in similar directions. Matlab allows the use of this dimensionality reduction technique in the Classification Learner toolbox however, this tool has the limitation that it does not apply to categorical variables. Therefore, we implemented another extensively used feature extraction method, the Neighborhood Component Analysis (NCA) based on Euclidean distances. This method calculates the probability of a variable to influence the final result.

2.5 Validation of the models

All models were validated with a 5 layer cross-validation method. Moreover, the iterative validation of the models consisted of the three subsequent tasks: i) Dimensionality reduction methods in case the set of predictor variables is very high ($>$ 10 variables). ii) Modification of the set of input variables used, according to the interest that their contribution to the class determination. iii) Significance analysis and variable elimination.

classification performance was assessed as regards to the following indicators:

- Sensitivity (the ability to correctly identify successful transplants).
- Specificity (the ability to correctly identify failed trasplants)
- Area under the Receiving Operator Characteristic (C statistic)
- Accuracy, defined as the ratio of correctly identified cases (True Positives + True Negatives) and the overall cases (True Positives + False Positives + True Negatives + False Negatives).

The criteria for selecting the best performing model was based on the higher accuracy.

3 Results

3.1 Descentralized Decision Support System

The system architecture is presented using the service-oriented architecture pattern, where services are provided and shared between the components. Based on the architecture of an orchestrated system defined previously by the authors [22], a system composed of three modules has been proposed to build a clinical decision support system which will integrate the iterative model development framework:

1. Data Storage Module: contains a database to store clinical data and a history of the results of the predictions obtained by the user by executing the classification model.

2. Control and Prediction Module: consists of two components. The orchestrator component, which is the functional director that controls the service flow of the system. And the predictive component, which contain the engine to run the model and obtain the prediction results based on input data.
3. Communication Module with the User: designed to provide end users with a web application to enter data of the ten selected variables and receive the results of the execution of the prediction model.

According to the functional scheme of the clinical decision support system described, the orchestration system was adapted to integrate the best performing classification model and a web interface. Figure 1 shows the structure of the solution adopted for the orchestrated system.

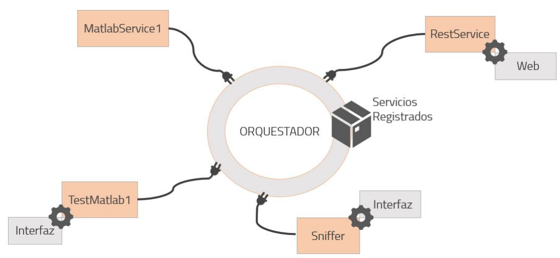

Fig. 1. Orchestrated system for the model execution

3.2 Interactive Data Modeling

The data of the study was taken in the Hospital La Fe (Valencia, Spain) during 13 years of patients follow-up, beginning in September 2002 and ending in August 2015. 81 patients who have undergone a pancreas transplant and kidney, either simultaneously (SPK) and signed the informed consent were included into the dataset (Table 2). 56 subjects retained the pancreatic graft, whereas 17 lose it and 8 died, therefore 69.13% of the the subjects where labeled with the successful event.

The selection and compilation of the study variables was defined by the clinical staff of the hospital, and they included several phenotype variables and clinical laboratory tests. The set of study variables had a total of 134 variables (62 quantitative), which were divided according to this classification to make the analysis more appropriate in each case based on this classification. The graphical descriptive analysis contributed to the detection of erroneous values in the samples by using box-whisker charts. Errors and outliers due to special patient circumstances (e.g.: use of steroids alters fasting glucose) were eliminated.

Using the Classification Learner toolbox, different prediction models were developed and validated with a 5 layer cross-fold validation. After 4 iterations,

Table 2. Descriptive information of the study sample

Variable	**Distribution // Mean±SD**
Sex	Male(58.5%) - Female(41,5%)
Age at transplant (years old)	37.4±5.7
Body Mass Index (Kgm^2)	24.0±3.4
Duration of T1DM (years	25.5±6.5
HbA1C	8.2±1.6
Insulin Bolus (U/day)	37.6±19.6
Insulin intake/day	3.5±0.9
Success of pancreatic transplant	69.13%

Table 3. Influencing variables and their relative weight after NCA analysis

Variable	**Weight**	**Variable**	**Weight**	**Variable**	**Weight**
Sys. BP	0.34	Fasting Glucose	1.35	HBA1C	0.32
UREA	0.18	C-peptide	0.04	Trygliceride	0.31
Waist	0.33	Cigarettes/day	0.15	Years since onset	0.27
Creatinine	0.34	Donor Age	0.34		

we have obtained a model based on KNN with a precision of 82.9 % and 11 predictors. In the following sections, the results obtained in each iteration are detailed.

The first iteration excluded the variables with a low number of observations (less than 30%). From the original 134 variables, only 49 were kept for the next iteration. This complete set of variables was used for the training of the models, obtaining a maximum level of precision of 80 %.

The second iteration focused on reducing the number of input variables, since it is unsustainable and impractical for a prediction model to have such a high number of input variables. PCA was used to discard non-influent variables, obtaining a set of components, whose first main component was sufficient to determine more than 95 % of the variance of the data set. With this training, a maximum precision of 80 % was obtained again. Therefore, NCA was applied obtaining the influence of the predictors on the result of the classification (Table 3). The results of this table show the importance of these variables with respect to the observed class and do not state the direction of the effect (eg.: and increased Systolic Blood pressure does not indicate a higher probability of transplant success). This work was left for the classification models, which were trained the 10 variables which achieved the greater relative weight. The best precision was obtained for the Ensemble Classifier model of the KNN Subspace type, reaching 81.4%.

The third iteration aimed to remove the age of the donor variable, so the model could be used without demanding external information from the patient. With this subset of variables, we launched the four and final iteration. From all the trained models, the Ensemble Classifier model of the KNN Subspace achieved a 82.9 % of classification accuracy (Table 4). This model achieved a sensitivity of 96% and a specificity of 21%. The area under the curve (AUC) was 59%.

Table 4. Accuracy of the classification models for the 10 selected predictors

Model	**Algorithm**	**Accuracy**
Decision tree	Complex Tree	71.4 %
	Medium Tree	71.4 %
	Simple Tree	77.1 %
Discriminant	Linear discriminant	72.9 %
	Quadratic Discriminant	72.9 %
Regression	Logistic Reg.	71.4 %
SVM	Linear SVM	80.0%
	Quad. SVM	68.6 %
	Cubic SVM	71.4 %
	Gaussian SVM	80.0 %
KNN	Fine KNN	74.3 %
	Medium KNN	80.0 %
	Coarse KNN	80.0 %
	Cosine KNN	80.0 %
	Cubic KNN	80.0 %
	Weighted KNN	80.0 %
Ensemble	Boosted Trees	80.0 %
	Bagged Trees	80.0 %
	Sub. Discriminant	81.4 %
	Subspace KNN	**82.9 %**

4 Conclusion

A model for the prediction of pancreatic grasp was developed and validated using data modeling techniques and dimensionality reduction on a sample population of 81 patients who have undergone thorugh a pancreas transplant in University Hospital La Fe. After a descriptive analysis and bivariate comparisons, no significant variables were found with respect to the success of pancreatic transplant. The prediction problem has been then approached using classification models with the total set of available variables and applying dimensionality reduction techniques. An ensemble model of subspace KNN achieved the best accuracy performance with an 82.9% which needed the following input predictors of the receiver: Systolic Blood Glucose, Fasting Glucose, Urea, Waist, creatinine, C-peptide, number of cigarettes per day, HBA1C, triglyceride and onset year. State of the art model proposed by Finger et altres [12] included donor information, however, after the dimensionality reduction iteration any of the donors variable did not achieved a significant weight with respect to the transplant success.

The selected model, which has a high sensitivity (98%) will help clinicians to maximize the chances of transplant success in T1DM therapies [23] as it classifies almost perfectly the patients who truly maintain the pancreas. The system will allow to identify the patients with higher chances of maintaining the graft, and thus, not to erroneously exclude potential patients from a transplant. In contrast, this model has a very low specificity (21.0%). Of the total number of patients who have truly lost their pancreas, the model has classified very few as a loss. This suggests that the model determines as apt for the transplant to great amount of patients unless it is very evident that the patient is going to lose the pancreas, which may be derived by the class unbalance (patients with the event are the 69.13%). Further work including new prospective data is needed to ensure a model with a more balanced derivation data set.

References

1. Association, A.D., et al.: Report of the expert committee on the diagnosis and classification of diabetes mellitus. Diabetes care **26**(suppl 1) (2003) s5–s20
2. ADA: Classification and diagnosis of diabetes. Diabetes Care **40**(Supplement 1) (dec 2016) S11–S24
3. Association, A.D., et al.: 2. classification and diagnosis of diabetes. Diabetes Care **40**(Supplement 1) (2017) S11–S24
4. Association, A.D., et al.: Physical activity/exercise and diabetes mellitus. Diabetes care **26**(suppl 1) (2003) s73–s77
5. : Definition, diagnosis and classification of diabetes mellitus and its complications. Report of a WHO Consultation **1**(1) (2003)
6. Trusler, L.: Simultaneous kidney-pancreas transplantation. ANNA journal/American Nephrology Nurses' Association **18**(5) (1991) 487–491
7. Banting, F., Best, C.: The internal secretion of the pancreas. Translational Research **80**(4) (1972) 465–480
8. Reddy, K.S., Stablein, D., Taranto, S., Stratta, R.J., Johnston, T.D., Waid, T.H., McKeown, J.W., Lucas, B.A., Ranjan, D.: Long-term survival following simultaneous kidney-pancreas transplantation versus kidney transplantation alone in patients with type 1 diabetes mellitus and renal failure. American journal of kidney diseases **41**(2) (2003) 464–470
9. Venstrom, J.M., McBride, M.A., Rother, K.I., Hirshberg, B., Orchard, T.J., Harlan, D.M.: Survival after pancreas transplantation in patients with diabetes and preserved kidney function. Jama **290**(21) (2003) 2817–2823
10. Sung, R.S., Zhang, M., Schaubel, D.E., Shu, X., Magee, J.C.: A reassessment of the survival advantage of simultaneous kidney-pancreas versus kidney-alone transplantation. Transplantation **99**(9) (2015) 1900
11. Gruessner, R.W., Gruessner, A.: Pancreas after islet transplantation: A first report of the international pancreas transplant registry. American Journal of Transplantation **16**(2) (2016) 688–693
12. Finger, E.B., Radosevich, D.M., Dunn, T.B., Chinnakotla, S., Sutherland, D.E., Matas, A.J., Pruett, T.L., Kandaswamy, R.: A composite risk model for predicting technical failure in pancreas transplantation. American Journal of Transplantation **13**(7) (2013) 1840–1849

13. Fernández-Llatas, C., Meneu, T., Traver, V., Benedi, J.M.: Applying evidence-based medicine in telehealth: An interactive pattern recognition approximation. International Journal of Environmental Research and Public Health **10**(11) (2013) 5671–5682
14. Hosmer, D.W., Lemesbow, S.: Goodness of fit tests for the multiple logistic regression model. Communications in statistics-Theory and Methods **9**(10) (1980) 1043–1069
15. Karaolis, M.A., Moutiris, J.A., Hadjipanayi, D., Pattichis, C.S.: Assessment of the risk factors of coronary heart events based on data mining with decision trees. IEEE Transactions on information technology in biomedicine **14**(3) (2010) 559–566
16. Hall, P., Park, B.U., Samworth, R.J.: Choice of neighbor order in nearest-neighbor classification. The Annals of Statistics (2008) 2135–2152
17. Polat, K., Güneş, S., Arslan, A.: A cascade learning system for classification of diabetes disease: Generalized discriminant analysis and least square support vector machine. Expert systems with applications **34**(1) (2008) 482–487
18. McLachlan, G.: Discriminant analysis and statistical pattern recognition. Volume 544. John Wiley & Sons (2004)
19. Bahler, D., Navarro, L.: Methods for combining heterogeneous sets of classifiers. In: 17th Natl. Conf. on Artificial Intelligence (AAAI), Workshop on New Research Problems for Machine Learning. (2000)
20. Bellazzi, R., Zupan, B.: Predictive data mining in clinical medicine: current issues and guidelines. International journal of medical informatics **77**(2) (2008) 81–97
21. Collins, G.S., Reitsma, J.B., Altman, D.G., Moons, K.G.: Transparent reporting of a multivariable prediction model for individual prognosis or diagnosis (tripod): the tripod statement. BMC medicine **13**(1) (2015) 55
22. Martinez-Millana, A., Bayo-Monton, J.L., Argente-Pla, M., Fernandez-Llatas, C., Merino-Torres, J., Traver-Salcedo, V.: Integration of distributed services and hybrid models based on process choreography to predict and detect type 2 diabetes. Sensors **18**(1) (dec 2017) 79
23. Martinez-Millana, A., Fernández-Llatas, C., Sacchi, L., Segagni, D., Guillén, S., Bellazzi, R., Traver, V.: From data to the decision: A software architecture to integrate predictive modelling in clinical settings. In: Engineering in Medicine and Biology Society (EMBC), 2015 37th Annual International Conference of the IEEE, IEEE (2015) 8161–8164

A comparison of two different matrix Error Correction Codes*

J. Gracia-Morán[1], L.J. Saiz-Adalid[1], D. Gil-Tomás[1], P.J. Gil-Vicente[1]

[1] Instituto ITACA. Universitat Politècnica de València. Camino de Vera s/n.
46022 Valencia, España.
{ jgracia, ljsaiz, dgil, pgil } @ itaca.upv.es

Abstract. Due to the continuous increment in the integration scale, the fault rate in computer memory systems has augmented. Thus, the probability of occurrence of *Single Cell Upsets* (SCUs) or *Multiple Cell Upsets* (MCUs) also increases. A common solution is the use of Error Correction Codes (ECCs). However, when using ECCs, a good balance between the error coverage, the redundancy introduced and the area, power and delay overheads of the encoders and decoders circuits must be achieved.

In this sense, there exist different proposals to tolerate MCUs. For example, matrix codes are codes able to detect and/or correct MCUs using a two-dimensional format. However, these codes introduce a great redundancy, which leads to an excessive area, power and delay overhead.

In this paper we present a complete comparison of two recently introduced matrix codes.

1 Introduction

Currently, the continued size reduction of CMOS technology provides memory systems with a large storage capacity. However, this size decrement also causes an increment in the memory error rate [1], [2]. In this sense, the impact of a cosmic radiation particle can provoke the change in a single memory cell (known as *Single Cell Upset* or SCU), or, as shown in different experiments, in several memory cells (*Multiple Cell Upsets* or MCUs). An MCU can be defined as simultaneous errors in more than one memory cell induced by a single particle [3], [4], [5], [6], [7].

Traditionally, Error Correction Codes (ECCs) have been used to protect memory systems. The most common ECCs used have been SEC or SEC-DED codes [8], [9], [10]. SEC codes can correct an error in a single memory cell, while SEC-DED codes can correct an error in a memory cell, as well as they can detect two errors in two independent cells.

In critical applications, more complex and sophisticated codes are used [11], [12], [13], [14], [15], [16], [17]. For example, Column-Line-Code (CLC code) [15] combines extended Hamming codes (a SEC-DED code) and parity checks to correct different error patterns.

* This work has been supported in part by the Spanish Government under the research project TIN2016-81075-R.

C.Fernandez-Llatas and M.Guillen (Ed.):
Workshop on Innovation on
Information and Communication Technologies
(ITACA-WIICT 2018)

ISBN 978-84-09-07373-3

However, when adding an ECC to a memory system, a number of factors must be taken into account. Firstly, the required redundancy, that is, the additional bits used to detect and/or correct the possible errors. These bits are added to each word of data stored in the memory. In this way, the amount of storage occupied by the redundant bits is scaled with the memory capacity. For example, if an ECC with 100% of redundancy is used in a 2GB memory, only 1GB will be available to store the "clean" data; the remaining 1GB is required for the code bits.

And secondly, another factor to take into account is the complexity of the encoding and decoding circuits, as this complexity will affect the area, power and delay overheads of encoder and decoder circuits.

In this work, we present a complete comparison between two matrix codes: the CLC code [15] and a matrix code designed by the authors and recently presented in [18]. This new ECC greatly decreases the redundancy introduced, reducing also the overhead of the encoding and decoding circuits. In this way, we will compare the error coverage of both codes, as well as the area, power and delay overheads of the encoder and decoder circuits.

The new code has been designed by using the FUEC (Flexible Unequal Error Control Codes) methodology, developed by the authors in [19], where an algorithm (and a tool) was introduced to design FUEC codes. FUEC codes are an improvement of the Unequal Error Control Codes (UEC) [8]. An advantage of the FUEC methodology is that it can be employed to design other codes, just selecting the error vectors to be corrected.

This work is organized as follows. Section 2 presents a brief introduction to the design of ECCs, as well as it introduces the most common errors produced in memories. Section 3 summarizes the behavior of the two matrix codes that we will evaluate in Section 4. Finally, Section 5 concludes this work.

2 Error Correction Codes

2.1 Introduction to the design of Error Correction Codes

An (n, k) binary ECC encodes a k-bit input word in an n-bit output word [20]. The input word $\mathbf{u} = (u_0, u_1, ..., u_{k-1})$ is a k-bit vector that represents the original data. The code word $\mathbf{b} = (b_0, b_1, ..., b_{n-1})$ is an n-bit vector, where the $(n - k)$ added bits are called parity bits or code bits. $\mathbf{b}$ is transmitted through an unreliable channel that delivers the received word $\mathbf{r} = (r_0, r_1, ..., r_{n-1})$. The error vector $\mathbf{e} = (e_0, e_1, ..., e_{n-1})$ models the error induced by the channel. If no error has occurred in the i-th bit, then $e_i = 0$; otherwise, $e_i = 1$. In this way, $\mathbf{r}$ can be interpreted as $\mathbf{r} = \mathbf{b} \oplus \mathbf{e}$. Fig. 1 synthesizes this coding, transmission and decoding process.

The parity matrix $\mathbf{H}_{(n-k) \times n}$ of a linear code defines the code [8]. For the coding process, $\mathbf{b}$ must meet the requirement $\mathbf{H} \cdot \mathbf{b}^T = \mathbf{0}$. For syndrome decoding, syndrome is defined as $\mathbf{s}^T = \mathbf{H} \cdot \mathbf{r}^T$, and it exclusively depends on $\mathbf{e}$:

$$\mathbf{s}^T = \mathbf{H} \cdot \mathbf{r}^T = \mathbf{H} \cdot (\mathbf{b} \oplus \mathbf{e})^T = \mathbf{H} \cdot \mathbf{b}^T \oplus \mathbf{H} \cdot \mathbf{e}^T = \mathbf{H} \cdot \mathbf{e}^T \qquad \mathbf{(1)}$$

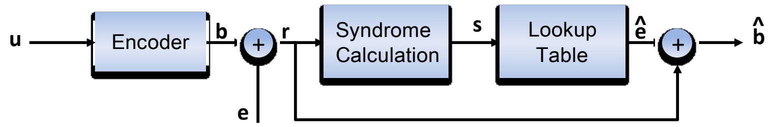

Fig. 1. Encoding, channel crossing and decoding process

There must be a different syndrome **s** for each correctable **e**. If **s** = **0**, we can assume that **e** = **0**. Therefore, **r** is correct. Otherwise, an error has occurred. Syndrome decoding is done through a lookup table that relates each **s** to the decoded error vector $\hat{\mathbf{e}}$. The decoded code word $\hat{\mathbf{b}}$ is calculated as $\hat{\mathbf{b}} = \mathbf{r} \oplus \hat{\mathbf{e}}$. From $\hat{\mathbf{b}}$, it is easy to obtain $\hat{\mathbf{u}}$ by discarding the parity bits. If the fault hypothesis used to design the ECC is consistent with the behavior of the channel, $\hat{\mathbf{u}}$ and **u** must be equal with a very high probability.

2.2 Error Models

In coding theory [8], the term *random error* commonly refers to one or more erroneous bits, randomly distributed in the coded word (data bits plus code bits generated by the ECC). *Random errors* can be *single* or *multiple*. *Single errors* affect a unique memory cell. They are commonly produced by Single Event Upsets (SEU, in RAM) or Single Event Transients (SET, in combinational logic) [21].

As previously mentioned, with the continuous increment of the integration scale, *multiple errors* are more and more frequent [3], [4], [5], [6], [7]. Nevertheless, they commonly appear grouped in neighboring bits, rather than randomly. For example, when a cosmic particle hits a memory cell, a radiation of electron-hole pairs along the transport track is produced [22]. In this way, *adjacent errors* can be generated, that is, multiple errors where all the erroneous bits are contiguous [4], [23].

3 Matrix Codes

3.1 Introduction to Matrix Codes

Matrix codes are ECCs that combine two or more types of error correction methods to detect and/or correct different types of errors [14], [15], [24], [25], [26]. Usually, diverse types of Hamming codes and parity checks are combined. In this way, matrix codes form a two-dimensional scheme.

An example of matrix code is the CLC code [15], whose layout can be seen in Fig. 2 (extracted from [15]). This code divides the primary data input (represented by X_i) into groups of 4 bits. Each group is codified by a SEC-DED (8, 4) Extended Hamming code (marked as C_i and Pa_i). Finally, a set of vertical parity bits (represented by P_i) form the matrix. This matrix code is able to correct all single errors, as well as different types of adjacent errors, as we will see in Section 4.

X_1	X_2	X_3	X_4	C_1	C_2	C_3	Pa_1
X_5	X_6	X_7	X_8	C_4	C_5	C_6	Pa_2
X_9	X_{10}	X_{11}	X_{12}	C_7	C_8	C_9	Pa_3
X_{13}	X_{14}	X_{15}	X_{16}	C_{10}	C_{11}	C_{12}	Pa_4
P_1	P_2	P_3	P_4	P_5	P_6	P_7	P_8

Fig. 2. Layout of a matrix code with 16 data-bit word [15]

The main problem of this ECC is the high number of redundant bits. In fact, this redundancy is 150%. This high score provokes a reduction in the available memory for the payload. Redundancy can be calculated as:

$$Redundancy = \frac{No.\ code\ bits}{No.\ data\ bits} \times 100 \qquad (2)$$

3.2 Our proposal

Recently presented [18], we have proposed a matrix code with a very low redundancy. This code can correct all single errors, as well as all different types of adjacent errors. The layout of our code can be seen in Fig. 3, where X_i represents the data bits and C_i the control bits (calculated using the FUEC methodology [19]).

C_0	C_1	C_2	C_3	C_4
C_5	C_6	C_7	C_8	X_0
X_1	X_2	X_3	X_4	X_5
X_6	X_7	X_8	X_9	X_{10}
X_{11}	X_{12}	X_{13}	X_{14}	X_{15}

Fig. 3. Layout of our matrix code [18]

The main advantage of our proposal is that it only introduces 9 bits of redundancy, instead of the 24 bits used in the previous code. That is, our ECC only presents a 56.25% of redundancy. The importance of this low number comes from the fact that these additional bits must also be stored in memory. In this way, a greater redundancy means less availability for data bits.

For example, for the CLC code presented in Section 3.1, a 1GB memory chip will spend about 614MB to store code bits, so only about 410MB would be available to store data bits. In the case of our proposal, only 370MB are necessary to store the code bits, being the rest, about 655MB, used to store the data bits.

4 Evaluation of Matrix Codes

In this section, we present the results of the evaluation of the matrix codes presented in Section 3. We have carried out two different processes. During the first one, we have injected faults in the C models of the matrix codes. With this injection, we have evaluated the error coverage. In a second step, we have implemented the two matrix codes in VHDL, and we have synthesized them in order to estimate the area, power and delay overheads.

4.1 Error coverage evaluation

Using the tool explained in [18] and [27], we have used fault injection to study the error coverage of the matrix codes introduced in Section 3.

It should be noted that we have not injected errors according to their probability of occurrence. As our objective is to measure the correction coverage, we have injected each type of error (single errors or adjacent errors of different lengths) in all the bits of the codeword. In this way, we have been able to verify the error correction capabilities of both matrix codes.

Thus, we have injected single errors, as well as adjacent errors with different patterns, as it can be seen in Fig. 4. In particular, we have injected adjacent errors with a length between 2 and 5 used a horizontal pattern (Fig. 4-a) and a vertical pattern (Fig. 4-b). In addition, we have also injected adjacent errors with a square pattern (Fig. 4-c), particularly errors with a length of 2x2, 2x3 and 3x2.

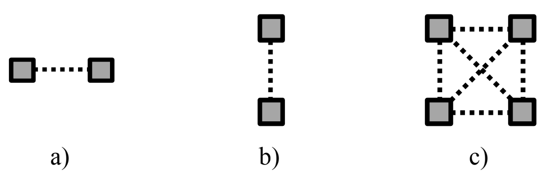

Fig. 4. Error patterns injected

Table 1 shows the correction coverage of both codes. This coverage has been calculated as:

$$C_{correc} = \frac{Errors\_Corrected}{Errors\_Injected} \times 100 \quad (3)$$

where $Errors\_Corrected$ are the number of errors corrected by the ECC, and $Errors\_Injected$ are the total amount of errors injected for a given error type.

With respect to the results obtained, we can see that CLC code presents a good error coverage, as it can correct a high percentage of the adjacent errors that we have injected. This is an expected result, as its redundancy is really high (150%). Nevertheless, a weakness can be found as it only corrects 50% of 2-bit adjacent errors in the vertical pattern.

On the other hand, matrix code from [18] can correct all single faults, as well as all 2-bit horizontal and vertical adjacent errors and the 2x2 error square pattern. So, our matrix code is a good alternative when these types of faults are predominant, as our proposal introduces a lower redundancy.

Table 1. Error correction coverage

	CLC [15]	Matrix Code [18]
Horizontal Error Pattern		
Error Length	% Corrected Errors	% Corrected Errors
1	100,00	100,00
2	100,00	100,00
3	100,00	0,00
4	68,00	0,00
5	100,00	0,00
Vertical Error Pattern		
Error Length	% Corrected Errors	% Corrected Errors
1	100,00	100,00
2	50,00	100,00
3	100,00	6,67
4	50,00	0,00
5	100,00	0,00
Square Error Pattern		
Error Length	% Corrected Errors	% Corrected Errors
2x2	42,86	100,00
3x2	100,00	0,00
2x3	33,33	0,00

4.2 Synthesis results

We have synthesized the encoders and decoders of both matrix codes. To do this, we have implemented them in VHDL, and using the CADENCE software [28], we have carried out a logical synthesis for the 45 nm technology, by using the NanGate FreePDK45 library [29], [30].

As it can be seen in Fig. 5, matrix code from [18] presents a lower area overhead. This is an expected result, as the redundancy introduced by CLC code and its decoding schema requires a greater number of logic gates.

On the other hand, Fig. 6 shows the power overhead of both codes. Although the decoding mechanisms are quite different, both decoders show similar power consumption. The lower redundancy of matrix code from [18] is balanced with more complex operations. In any case, the general power overhead is higher for CLC code.

Finally, Fig. 7 presents the delay overhead of both ECCs. This overhead follows a similar trend than the power overhead, that is, the delay's decoders are very similar. Also, as in the power overhead, the encoders' delay for our proposal is lower.

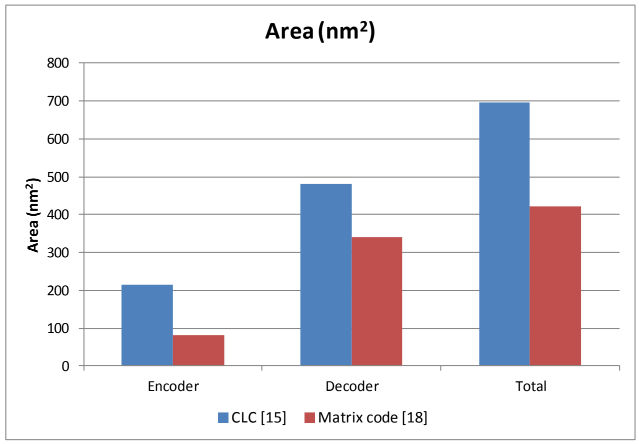

Fig. 5. Area overhead

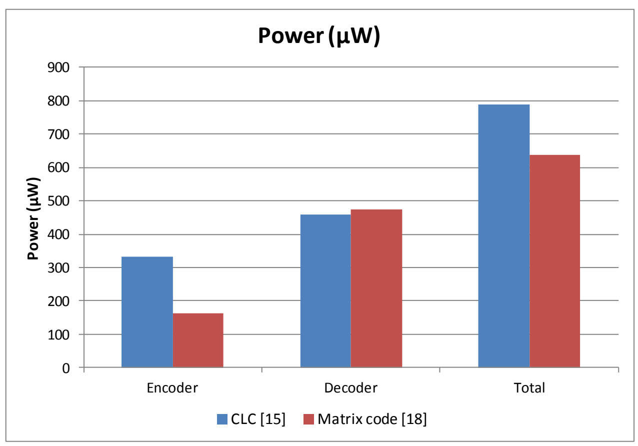

Fig. 6. Power overhead

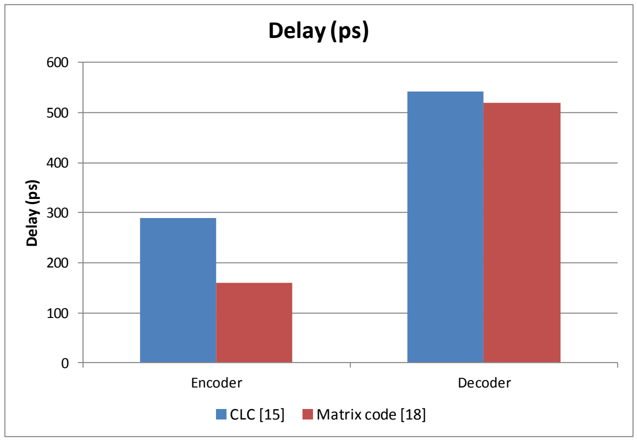

Fig. 7. Delay overhead

5 Conclusions

In this work, we have compared two matrix Error Correction Codes with respect to their error correction coverage and area, power and delay overheads.

Regarding the correction coverage, our proposal is able to correct 100% of single errors, as well as all adjacent double errors, with different patterns of occurrence. On the other hand, the low redundancy of our proposal also causes a low area, power consumption and delay overhead.

In general, our proposal is an appropriate option for applications where double adjacent errors are expected. Beyond this type of errors, the performance of our code decreases significantly due to its low redundancy. If these errors are expected to occur, more powerful ECCs should be used.

In future works, we want to continue developing ECCs in order to reduce area, power and delay overheads, and maintaining, or even improving, the error coverage. On the other hand, we also want to develop other ECCs focused on long length errors, which are expected to have an increasing impact.

References

1. The International Technology Roadmap for Semiconductors 2013. [Online]. Available at: http://www.itrs2.net/2013-itrs.html
2. S.K. Kurinec and K. Iniewsky. Nanoscale Semiconductor Memories: Technology and Application, CRC Press, Taylor & Francis Group, 2014.
3. E. Ibe, H. Taniguchi, Y. Yahagi, K. Shimbo, and T. Toba, “Impact of scaling on neutron-induced soft error in SRAMs from a 250 nm to a 22 nm design rule”, IEEE Trans. Electron Devices, vol. 57, no. 7, pp. 1527–1538, July 2010.

4. G. Tsiligiannis et. al., “Multiple Cell Upset Classification in Commercial SRAMs”, IEEE Transactions on Nuclear Science, vol. 61, no. 4, August 2014.
5. G.I. Zebrev, “Multiple Cell Upset Cross-Section Uncertainty in Nanoscale Memories: Microdosimetric Approach”, 15th European Conference on Radiation and its Effects on Components and Systems (RADECS 2015), September 2015.
6. N.G. Chechenin and M. Sajid, “Multiple cell upsets rate estimation for 65 nm SRAM bit-cell in space radiation environment”, 3rd International Conference and Exhibition on Satellite & Space Missions, May 2017.
7. N.N. Mahatme, B.L. Bhuva, Y.P. Fang, and A.S. Oates, “Impact of strained-Si PMOS transistors on SRAM soft error rates”, IEEE Trans. on Nuclear Science, vol. 59, no. 4, pp. 845–850, August 2012.
8. E. Fujiwara, Code Design for Dependable Systems: Theory and Practical Application, Ed. Wiley-Interscience, 2006.
9. R. W. Hamming, “Error detecting and error correcting codes,” Bell System Technical Journal, vol. 29, pp. 147–160, 1950.
10. C.L. Chen and M.Y. Hsiao, “Error-correcting codes for semiconductor memory applications: a state-of-the-art review”, IBM Journal of Research and Development, vol. 58, no. 2, pp. 124–134, March 1984.
11. G.C. Cardarilli, M. Ottavi, S. Pontarelli, M. Re, and A. Salsano, “Fault Tolerant Solid State Mass Memory for Space Applications”, IEEE Trans. on Aerospace and Electronic Systems, vol. 41, no. 4, pp. 1353–1372, October 2005.
12. S. Pontarelli, G.C. Cardarilli, M. Re and A. Salsano, “Error correction codes for SEU and SEFI tolerant memory systems”, 24th IEEE International Symposium on Defect and Fault Tolerance in VLSI Systems (DFT 2009), pp. 425-430, 2009.
13. A. Sánchez-Macián, P. Reviriego, J. Tabero, A. Regadío, and J.A. Maestro, “SEFI protection for Nanosat 16-bit Chip On-Board Computer Memories”, IEEE Transactions on Device and Materials Reliability, DOI 10.1109/TDMR.2017.2750718, 2017.
14. C. Argyrides, D.K. Pradhan, and T. Kocak, “Matrix codes for reliable and cost efficient memory chips”, IEEE Transactions on Very Large Scale Integration (VLSI) Systems, vol. 19, nº 3, pp.420–428, March 2011.
15. H.S. de Castro, et al. “A correction code for multiple cells upsets in memory devices for space applications”, 2016 14th IEEE International New Circuits and Systems Conference (NEWCAS 2016), pp.1–4, June 2016.
16. S. Ahmad, M. Zahra. S.Z. Farooq, and A. Zafar, “Comparison of EDAC schemes for DDR memory in space applications”, 2013 International Conference on Aerospace Science & Engineering (ICASE 2013), August 2013.
17. D.E. Muller, “Application of boolean algebra to switching circuit design and to error detection”, IRE Transactions on Electronic Computers, vol. 3, pp. 6–12, 1954.
18. J. Gracia-Morán, L.J. Saiz-Adalid, D-Gil-Tomás, P.J. Gil-Vicente, “Un nuevo Código Corrector de Errores de tipo matricial con una baja redundancia”, Submitted to Jornadas SARTECO, 2018.
19. L.J. Saiz-Adalid et al., “Flexible Unequal Error Control Codes with Selectable Error Detection and Correction Levels”, 32th International Conference on Computer Safety, Reliability and Security (SAFECOMP 2013), pp. 178-189, September 2013.
20. A. Neubauer, J. Freudenberger, and V. Kühn, Coding Theory: Algorithms, Architectures and Applications. John Wiley & Sons, 2007.
21. K.A. LaBel, “Proton single event effects (SEE) guideline” submitted for publication on the NASA Electronic Parts and Packaging (NEPP) Program web site, August 2009. Available online at https://nepp.nasa.gov/files/18365/Proton_RHAGuide_NASAAug09.pdf
22. M. Murat, A. Akkerman, and J. Barak, “Electron and ion tracks in silicon: Spatial and temporal evolution,” IEEE Transactions on Nuclear Science, vol. 55, no. 6, pp. 3046–3054, December 2008.

23. M. Wirthlin, D. Lee, G. Swift, and H. Quinn, "A method and case study on identifying physically adjacent multiple-cell upsets using 28-nm, interleaved and SECDED-protected arrays," IEEE Transactions on Nuclear Science, vol. 61, no. 6, pp. 3080–3087, Dec. 2014.
24. S. Liu, L. Xiao, J. Li, Y. Zhou, and Z. Mao, "Low Redundancy Matrix-Based codes for Adjacent Error Correction with Parity Sharing", 2017 18th International Symposium on Quality Electronic Design (ISQED 2017), March 2017.
25. P. Reviriego and J.A. Maestro, "Efficient Error Detection Codes for Multiple-Bit Upset Correction in SRAMs with BICS", ACM Transactions on Design Automation of Electronic Systems (TODAES) Vol. 14 nº 1, January 2009.
26. M. Zhu, L. Xiao, S. Li, and Y. Zhang, "Efficient Two-Dimensional Error Codes for Multiple Bit Upsets Mitigation in Memory", 2010 25th International Symposium on Defect and Fault Tolerance in VLSI Systems (DFT 2010), pp. 129-135, October 2010.
27. J. Gracia-Moran, L.J. Saiz-Adalid, D. Gil-Tomás, and P.J. Gil-Vicente, "Improving Error Correction Codes for Multiple Cell Upsets in Space Applications", IEEE Transactions on Very Large Scale Integration (VLSI) Systems, DOI: 10.1109/TVLSI.2018.2837220, 2018.
28. https://www.cadence.com/
29. J.E Stine et al., "FreePDK: An Open-Source Variation-Aware Design Kit", IEEE International Conference on Microelectronic Systems Education (MSE'07), June 2007.
30. http://www.nangate.com/?page_id=2325

Flow differences between patients with and without Stroke code activation with Process Mining discovery and enhancement

Lucia Aparici-Tortajada[1], Vicente Traver[1], and Carlos Fernandez-Llatas[1]

ITACA. Universitat Politècnica de València
Camino de Vera S/N, Valencia 46022, Spain luaptor@itaca.upv.es

Abstract. Stroke is a major public health issue worldwide. Its diagnosis and treatment should be provided as soon as possible to avoid further patient's complications. In this paper we report novel findings on the application of process mining algorithms to log of data collected in the Emergency Room and the Stroke Unit services of a reference hospital. Our approach is to include discovery and enhancement algorithms into an iterative process with hospital healthcare professionals to enable experts in the identification and knowledge extraction from the automatically collected data. We used the Question-Driven methodology to identify the real challenges of hospital healthcare professionals to discover problematic processes and their intrinsic features in a dataset containing 2283 appointments of 8 years (2010-2017) from 1835 patients, with 7 time milestones (Start, Arrival, CT realization, Neurologist Assessment, SU hospitalization, SU Departure, Hospital Departure). Our results present a way of identifying patients' flows during the beginning of their stroke and their stay in the hospital and a dynamic way to estimate the times and delays in patient care delivery.

Keywords: Process Mining, Question Driven methodology, patient flow.

1 Introduction

A clinical pathway is a complex process which reflects the organization of a care process based on collected clinical and administrative data in a defined cohort of patients for a limited period of time [1]. These pathways may be represented as business processes which can draw actions and results and correlate them with the actual performance of patients across the care process [2].

Stroke is a major public health issue worldwide and especially in industrialized countries [3]. Incidence rates range from 73 to 223 cases/100,000 citizens/year according to region [4],[5]. The disease is the second, sometimes even leading, cause of death in many countries [6],[7]. It is also a major cause of disability and cognitive decline, of worsening of quality of life, and of dependency in one in two patients [8]. Trying to mitigate the problems associated with stroke, clinical pathways have been set up in several European countries [9], [10], [11], [12].

C.Fernandez-Llatas and M.Guillen (Ed.):
Workshop on Innovation on
Information and Communication Technologies
(ITACA-WIICT 2018)

ISBN 978-84-09-07373-3

Intravenous thrombolysis with tissue plasminogen activator administered early in acute ischemic stroke has been shown to improve the prognosis of patients in clinical trials [13], [14]. The therapeutic window established for its administration is 4.5 h, however, the treatment effectiveness is time dependent and decreases as increases the time from the onset of symptoms to its administration. Therefore, it is necessary to dispense the thrombolytic treatment as soon as possible, avoiding unnecessary delays, since every minute can be decisive for the functional prognosis of the patient [15]. Thus, the stroke code activation is crucial since, if it is not activated or activated late, it will influence the emergency service response time and therefore the patient's affectation and recovery probabilities.

Patient access to well-organized, multidisciplinary care in stroke units has been shown to improve quality of service and ultimately to reduce stroke morbidity/mortality rates [16]. The traditional approach of analyzing operational processes with data-driven models has failed and organizations are moving to work with process-driven models [2]. To discover and analyze the operational processes it is crucial to gather information related to the process itself. Interview-based data acquisition involves a huge load of resources to perform observations, which may be subject to bias [17].

Pattern Recognition Algorithms [18] allows discovering and appraising the performance of hospital processes. Moreover, the Interactive Pattern Recognition (IPR) [19] allows experts to evaluate incrementally the operative set up as they introduce modifications in the process. However, in the healthcare area IPR require other technologies that provide human understandable models, such are Process Mining (PM)techniques.

Applying Interactive PM techniques needs a specific framework based on the collaboration of field experts and technicians. Question-Driven methodology presented by Rojas et altres [20] allows reducing the spaghetti effect through the use of specific questions for each specific healthcare field: Emergency Room. The present paper shows that it is possible applying that methodology to analyze the processes performed in other hospital environments like, such in our case, the services related to Stroke process (Emergency Room and the Stroke Unit services).

2 Methods

2.1 Drilling down into the process

A Question-Driven methodology have been applied. It uses the most Frequently-Posed Questions (FPQs) by the clinicians to guide the search for an in-depth knowledge of the process [20]. The premise of this methodology is that when a FPQ answer is achieved, the knowledge acquired causes the generation of new questions. This new issues will lead to a deeper understanding of the processes and, thereby, find the strategic points to place improvements.

Question-Driven Methodology consists of six stages, shown in Figure 1, which has proved its efficacy in an Emergency Room context [20]. In our experiment data is extracted from the Health Information System (HIS) by technical staff in the hospital (Stage 1 in Figure 1).It is performed in collaboration with hospital healthcare professionals since they can guide the extraction for the selection of the most relevant fields for the posed questions study. The most appropriate inclusion and exclusion criteria have been determined according to each question to build different event logs specific for each FPQ (Stage 2).

Stage 3 consists of generating a specific event log according to the requirements of each question that requires an answer. In our case, as will be presented in the results section, it has been filtered between those patients in which the ICTUS protocol has been activated and those in which it has not.

A comprehensive Data Analysis (Stage 4) of the included episodes is performed by data analysts to check data consistency (data characteristics, its quality, missed data that can be inferred, data types, time intervals, data values). Stage 5 is performed by Process Mining experts who discover and enhance the different flows and prepare the reports in Stage 6.These reports are shared and analyzed together with the hospital healthcare professionals to pose questions that may re-launch the entire process depending on the posed questions.

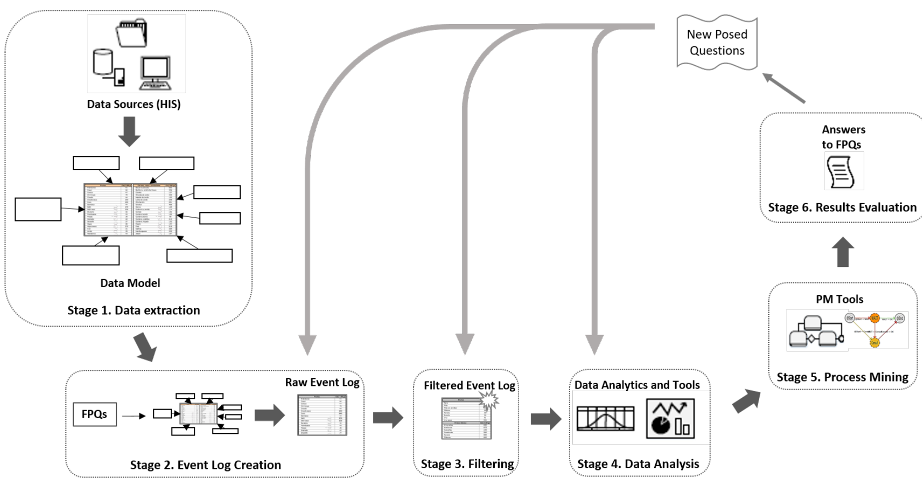

Fig. 1. Question-Driven Methodology

We used PALIA algorithm [21] to perform the discovery and enhancement analysis by means of PALIA suite tool[22]. In front of other popular tools such as Disco (https://fluxicon.com), [23] and ProM (http://www.processmining.org/) [24], we chose PALIA Suite because of its simplicity and effectiveness.

Work flows discovered with PALIA are a formal graphical representation of the relationships between activities in a given process. Such work flows are inferred from logs of data which are stored as observations which occur in a specific time stamp or a timespan (they should have an Start and End time). In our research we assume an observation as an activity which takes a finite categorical value. An activity (A) may have predecessor (P) and/or a successor (S). P should happen in a time interval before A, and S should happen after. The complexity and heterogeneity of processes in health care needs a flexible and efficient mechanism for process representation. Despite their potential, Petri Nets have failed to deliver understandable models to health care professionals [25]. The Time Parallel Automaton in PALIA representation copes with such limitations, enabling to infer work flows in a simple, fast and understandable way [26, 27].

2.2 Stroke Code protocol

Our study is developed in the Emergency Room and the Stroke Unit services form Hospital General Universitario in Valencia (Spain). Hospital General Universitario is one of the four reference hospitals of the Valencian capital and the reference clinical setting of its Health Department, a geographical district that covers a population around 350,000 inhabitants. This health department accounts for more than 3,700 healthcare professionals, 503 beds, 27 operating theaters, more than 130,000 emergency cares and more than 21.800 hospital admissions each year.

The emergencies service staff registers each patient on each stage of the visit process. The information collected by the system is:

1. **Start time (St)**. When the Stroke starts. It is recorded regarding what the patient or a relative reports.
2. **Arrival time (At)**. When the patient arrives to the Emergency room the arrival time is recorded.
3. **CT realization time (CTt)**. When the Computerized Tomography is performed.
4. **Neurologist Assessment time(NAt)**. When the patient's status is evaluated by the doctor o guard.
5. **SU hospitalization time(SUht)**. When the patient is hospitalized in the Stroke Unit.
6. **SU Departure time(SUDt)**. When the patient departs from the Stroke Unit.
7. **Hospital Departure time(HDt)**. When the patient departs from the Hospital.

2.3 Study data

We used data from 8 years, form 2010 until 2017. The study dataset contains 67 variables of 2283 appointments from 1835 patients.

Table 1 shows an explanation of the events recorded. The first column shows the recorded attributes, in which each attribute is a recorded time (St: Stroke Starting time; At: Arrival time; CTt: CT realization time; NAt: Neurologist

Assessment time, SUht: Stroke Unit hospitalization time, SUDt: Stroke Unit Departure time and HDt: Hospital Departure time) as described in the protocol. The second column shows the number of events recorded containing each atributes and the third the percentage regarding the total number of events. The less relevant events (those with a low number of occurrences) are presented in the last row.

For each of the events the distribution of the Accomplishment variable have been calculated (Table 1). 31.14% of all the recorded visits have values for each of the seven observed attributes, 12.09% for all except the neurologist assessment and 11.82% for all except the SU departure time. The rest of events have much lower percentages. 9.6% have only the hospital departure time.

Table 1. Number of recorded events

Attributes	**No. of events**	**%**
St-At-CTt-NAt-SUht-SUDt-HDt	710	31.1
St-At-CTt-SUht-SUDt-HDt	276	12.1
St-At-CTt-NAt-SUht-HDt	270	11.8
HDt	218	9.6
At-CTt-NAt-SUht-SUDt-HDt	163	7.4
St-At-CTt-SUht-HDt	98	4.3
At-CTt-SUht-SUDt-HDt	87	3.8
At-CTt-NAt-SUht-HDt	52	2.3
St-At-NAt-SUht-SUDt-HDt	38	1.7
St-At-SUht-SUDt-HDt	27	1.2
At-CTt-SUht-HDt	25	1.1
St-At-SUht-HDt	20	0.9
At-SUht-SUDt-HDt	20	0.9
Other combinations	279	12.2

An analysis of data quality was performed to ensure the results reliability. They were preprocessed under Quality Department Managers supervision for its improvement.

3 Results

Work flows have been discovered on the basis of the recorded times on the visits of each patient to the Emergencies and Stroke Unit Service. The steps in the process are represented as nodes, a circular shape identified with a name, and an arrow, which represent the transition between nodes. There are two special nodes added to all the observations: @Start node to indicate the start of the observations for a visit and @End, to indicate the patient left the hospital.

Enhancement tools are used to intensify both nodes and arrows using the traffic light protocol, as it is shown in Figure 2. Node color represents the relative time patients are therein (Green ⇒ short time/ Red ⇒ long time). Arrow color represents the relative number of patients who perform that node transition (Green ⇒ a few patients/ Red ⇒ all patients)

Transitions are represented by an arrow from the origin to the destination node. The arrow has a label with the following format "Origin node name = Destination node name". Table 2 defines all the possible stages (node names) in which a patient can be at a given time.

Table 2. States definition

Name of the State	Start Time	End Time
PreUrg	Start time	Arrival time
WaitCT	Arrival time	CT realization time
	Neurologist Assessment time	CT realization time
WaitNeur	Arrival time	Neurologist Assessment time
	CT realization time	Neurologist Assessment time
WaitUI	CT realization time	SU hospitalization time
	Neurologist Assessment time	SU hospitalization time
UI	SU hospitalization time	SU Departure time
Hosp	SU Departure time	Hospital Departure time

Both events, the CT realization and the Neurologist Assessment could be after the Arrival time, depending on the availability. That's why in the Table 2 the states "WaitCT", "WaitNeur" and "WaitUI" has 2 possibilities.

The first iteration of the Question-Driven Methodology involves discovering paths followed by the patients. Figure 2 shows at a glance the flow of patients across the different stages defined in Table 2. The work flow is enhanced to show the time spent on each stage an the busiest transitions.

The most remarkable thing on Figure 2 is that Regarding the averaged hospitalization time (UI+Hosp = 8 days and 14 hours), it is shown that it is much greater than the patient's averaged time in Emergency room (around 7 hours). In addition, you can also see the path that most patients follow, since the arrows are a more red color.

Healthcare experts of the hospital were involved in the analysis of the workflows. Experts posed 2 main questions related to the process performance:

- Q1:Do patients with Stroke code activated and those who do not follow the same flow?
- Q2:Is the time in the emergency room different if the Stroke code is activated than if it is not?

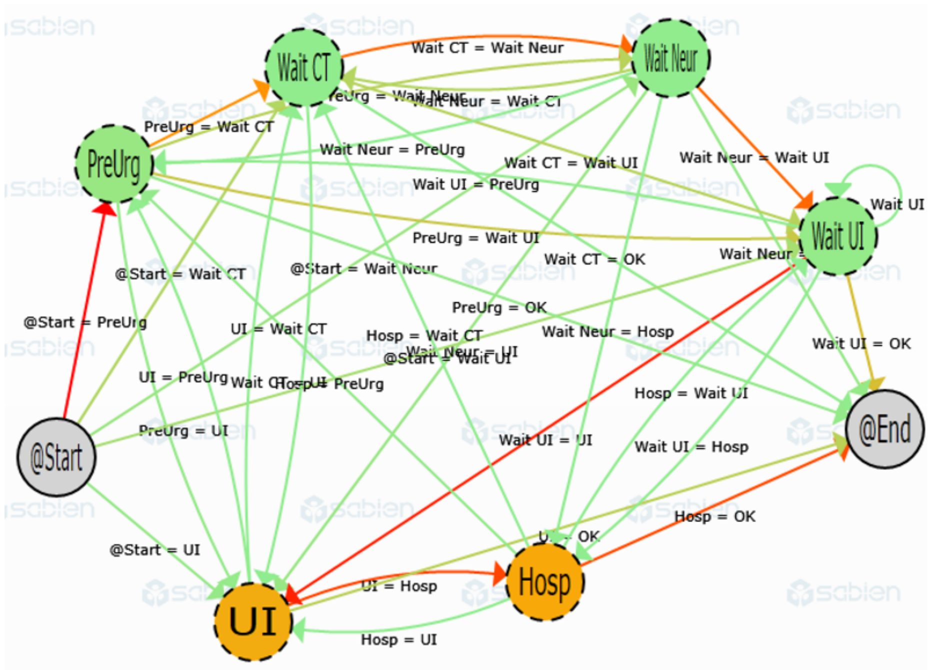

Fig. 2. All the studied patients' flow

3.1 Q1:Do patients with Stroke code activated and those who do not follow the same flow?

To answer this question two figures are presented. The first one (Figure 3 shows the patients' flow for whom the Stroke code has not been activated. This is an illustrative example of the potential of the application of Process Mining techniques and the presented methodology to draw in an easy and understandable way clinical processes. The arrows color denotes the number of times that a patient makes that path, varying from green (less times) to red (more times). The states color indicates the average time that patients spend in each state.

In Figure 3 we discover that patients without Stroke code activated usually follow the same flow: When the stroke starts, they go to the emergency room (PreURG), wait until a TC could be performed (WaitCT), wait until a neurologist can asses them (WaitNeur), wait until they could be hospitalized in the Stroke Unit (WaitUI) and then they get in the Stroke Unit (UI); When they are better, they remain some time hospitalized until their departure (Hosp). In addition, we found some expected findings, like that the averaged time in hospitalization (UI+Hosp) is higher than the averaged time in Emergency room (WaitCT+waitNeur+WaitUI).

The second figure (Figure 4) shows the patients' flow for whom the Stroke code has been activated. As could be sown, these patients do not always follow the same flow in Emergency service. From PreUrg state they go mainly to two

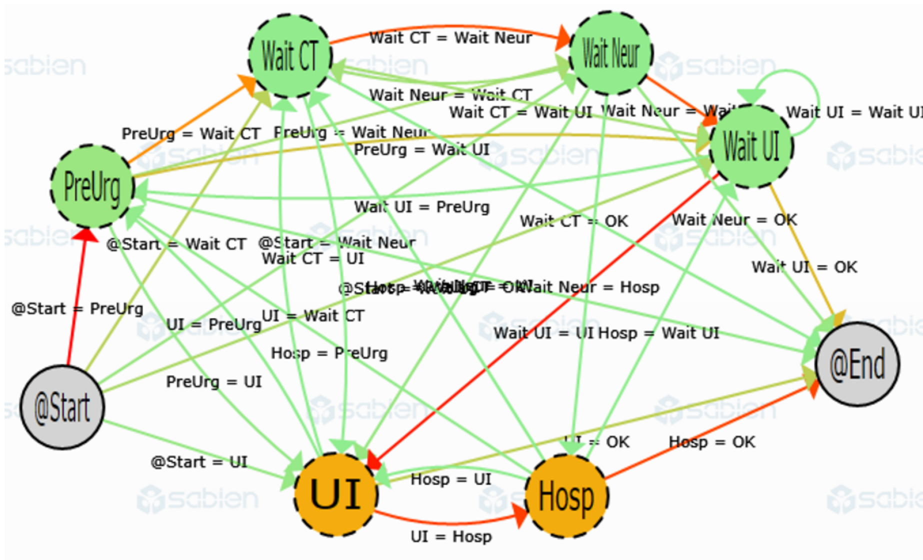

Fig. 3. Patients flow without Stroke code activated

sates: some of them to WaitCT state and some others to WaitNeur state; then patients in WaitCT go mainly to WaitNeur and vice-versa; from both states patients go to WaitUI state and finally to UI and to Hosp, as in the non-activated Stroke code case. Therefore, differences between this flow and the previous one have been appreciated.

3.2 Q2:Is the time in the emergency room different if the Stroke code is activated than if it is not?

Regarding the time in each service, it has been checked that the average time in emergencies when the Stroke code is activated (around 3:15 hours) is notably less than in case of patients without stroke code activation (around 9 hours). The hospitalization time, however, is quite similar in both cases, so conclusions can not be drawn about whether the activation of the stroke code is influencing or not on the patients' recovery.

4 Discussion and conclusion

The present work shows the potential of the discovery and time-based enhancement algorithms when they are applied in health care, allowing professionals to know the operation of their departments.

This technique allowed to test a dataset containing 2283 appointments from 1835 patients of 8 years (2010-2017) in the Emergency Room and the Stroke Unit services from Hospital General Universitario in Valencia.

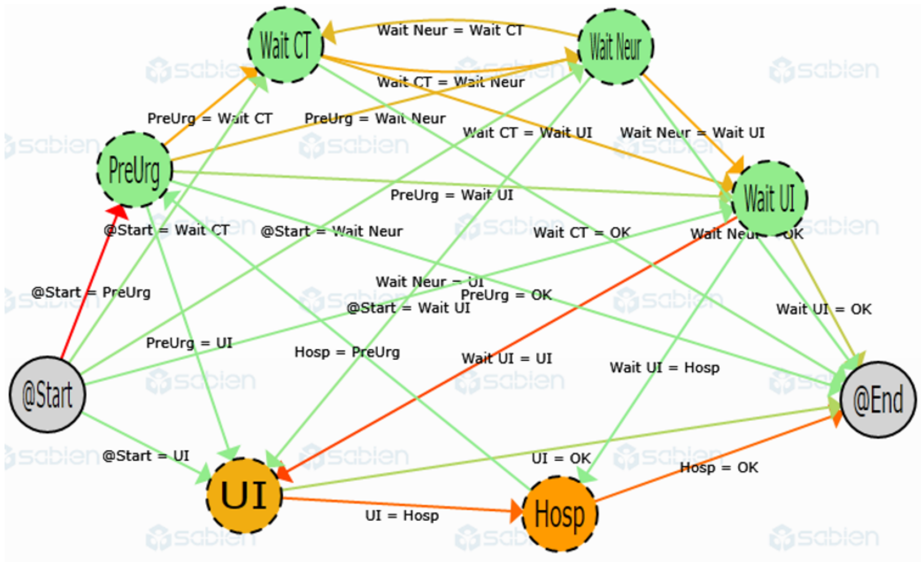

Fig. 4. Patients flow with Stroke code activated

Patients follow different paths if they have activated the stroke code than if not. If they do not have it activated, the most of patients follow a well defined path between states, whereas if they have it activated, the paths of patients in the emergency room vary from one to the other. It appears that this is probably due to the need for diagnostic confirmation shortly to apply the treatment as soon as possible.

In addition, this is likely to influence the second result, where the average time in emergencies in the first case is less than in the second. At the moment, no significant differences have been found in the time they remain in the hospital in both cases. In future works it will be tried to see if the time in the emergency room until they are hospitalized influences on the recovery time.

In addition, the activation or not of the stroke code is indicated in a binary value box. For this study have been used that box to determine if the stroke code have been activated or not. However, it has been observed that in some cases the staff does not activate this box but in the describing the patient's condition section, it is referenced the activation of the stroke code. Thus, for future work, data will be refined to find those in which the stroke code has been activated but is not reflected in the corresponding box.

References

1. Vanhaecht, K., Panella, M., van Zelm, R., Sermeus, W.: An overview on the history and concept of care pathways as complex interventions. International Journal of Care Pathways **14**(3) (2010) 117–123

2. van der Aalst, W.M.P. In: Business Process Management Demystified: A Tutorial on Models, Systems and Standards for Workflow Management. Springer Berlin Heidelberg, Berlin, Heidelberg (2004) 1–65
3. Donnan, G.A., Fisher, M., Macleod, M., Davis, S.M.: Stroke. Lancet **371**(9624) (may 2008) 1612–1623
4. Feigin, V.L., Lawes, C.M., Bennett, D.A., Barker-Collo, S.L., Parag, V.: Worldwide stroke incidence and early case fatality reported in 56 population-based studies: a systematic review. The Lancet Neurology **8**(4) (2009) 355–369
5. Zhang, Y., Chapman, A.M., Plested, M., Jackson, D., Purroy, F.: The incidence, prevalence, and mortality of stroke in france, germany, italy, spain, the uk, and the us: a literature review. Stroke research and treatment **2012** (2012)
6. Bejot, Y., Benatru, I., Rouaud, O., Fromont, A., Besancenot, J.P., Moreau, T., Giroud, M.: Epidemiology of stroke in europe: geographic and environmental differences. Journal of the neurological sciences **262**(1) (2007) 85–88
7. Roger, V.L., Go, A.S., Lloyd-Jones, D.M., Adams, R.J., Berry, J.D., Brown, T.M., Carnethon, M.R., Dai, S., De Simone, G., Ford, E.S., et al.: Heart disease and stroke statistics2011 update: a report from the american heart association. Circulation **123**(4) (2011) e18
8. Miller, E.L., Murray, L., Richards, L., Zorowitz, R.D., Bakas, T., Clark, P., Billinger, S.A., et al.: Comprehensive overview of nursing and interdisciplinary rehabilitation care of the stroke patient: a scientific statement from the american heart association. Stroke **41**(10) (2010) 2402–2448
9. Party, I.S.W., et al.: National clinical guideline for stroke (2012)
10. Panella, M., Marchisio, S., Barbieri, A., Di Stanislao, F.: A cluster randomized trial to assess the impact of clinical pathways for patients with stroke: rationale and design of the clinical pathways for effective and appropriate care study [nct00673491]. BMC health services research **8**(1) (2008) 223
11. de Leciñana-Cases, M.A., Gil-Núñez, A., Díez-Tejedor, E.: Relevance of stroke code, stroke unit and stroke networks in organization of acute stroke care–the madrid acute stroke care program. Cerebrovascular Diseases **27**(Suppl. 1) (2009) 140–147
12. Bussel, E.F., Jeerakathil, T., Schrijvers, A.J.: The process flow and structure of an integrated stroke strategy. International journal of integrated care **13**(2) (2013)
13. Marier, J.: The national institute of neurological disorders and stroke rt-pa stroke study group tissue plasminogen activator for acute ischemic stroke. N Engl J Med **333**(24) (1995) 1581–1587
14. Hacke, W., Kaste, M., Bluhmki, E., Brozman, M., Dávalos, A., Guidetti, D., Larrue, V., Lees, K.R., Medeghri, Z., Machnig, T., et al.: Thrombolysis with alteplase 3 to 4.5 hours after acute ischemic stroke. New England Journal of Medicine **359**(13) (2008) 1317–1329
15. Mohedano, A.I., Pastor, A.G., Arratibel, A.G., García, P.S., Otero, F.D., Delgado, F.R., Rubio, R.D., González, A.M., Alen, P.V., Bullido, Y.F., et al.: Identificación de los factores que influyen en el retraso intrahospitalario del inicio de trombólisis intravenosa en el ictus agudo en un hospital terciario. Neurologia **31**(7) (2016) 452–458
16. TrialistsCollaboration, S.U.: Organised inpatient (stroke unit) care for stroke. Cochrane Database Syst Rev **9**(9) (2013)
17. Scheffer, J.: Data mining in the survey setting: Why do children go off the rails? (2002)
18. Duda, R.O., Hart, P.E., Stork, D.G., et al.: Pattern classification. 2th edn. John Wiley & Sons, New York, USA

19. Fernández-Llatas, C., Meneu, T., Traver, V., Benedi, J.M.: Applying evidence-based medicine in telehealth: An interactive pattern recognition approximation. International Journal of Environmental Research and Public Health **10**(11) (Oct 2013) 5671–5682
20. Rojas, E., Sepúlveda, M., Munoz-Gama, J., Capurro, D., Traver, V., Fernandez-Llatas, C.: Question-driven methodology for analyzing emergency room processes using process mining. Applied Sciences **7**(3) (2017) 302
21. Fernandez-Llatas, C., Valdivieso, B., Traver, V., Benedi, J.M.: Using process mining for automatic support of clinical pathways design. In Fernández-Llatas, C., García-Gómez, J.M., eds.: Data Mining in Clinical Medicine. Number 1246 in Methods in Molecular Biology. Springer New York (January 2015) 79–88
22. Fernandez-Llatas, C., Lizondo, A., Monton, E., Benedi, J.M., Traver, V.: Process mining methodology for health process tracking using real-time indoor location systems. Sensors **15**(12) (November 2015) 29821–29840
23. Rojas, E., Munoz-Gama, J., Sepúlveda, M., Capurro, D.: Process mining in healthcare: A literature review. Journal of biomedical informatics **61** (2016) 224–236
24. Van Dongen, B.F., de Medeiros, A.K.A., Verbeek, H., Weijters, A., Van Der Aalst, W.M.: The prom framework: A new era in process mining tool support. In: International Conference on Application and Theory of Petri Nets, Springer (2005) 444–454
25. Mendling, J., Reijers, H.A., Cardoso, J.: What makes process models understandable? In: International Conference on Business Process Management, Springer (2007) 48–63
26. Fernndez-Llatas, C., Pileggi, S.F., Traver, V., Benedi, J.M.: Timed parallel automaton: A mathematical tool for defining highly expressive formal workflows. In: Proceedings of the 2011 Fifth Asia Modelling Symposium, IEEE Computer Society (2011) 56–61
27. Fernandez-Llatas, C., Martinez-Millana, A., Martinez-Romero, A., Benedi, J.M., Traver, V.: Diabetes care related process modelling using process mining techniques. lessons learned in the application of interactive pattern recognition: Coping with the spaghetti effect. In: Engineering in Medicine and Biology Society (EMBC), 2015 37th Annual International Conference of the IEEE, IEEE (2015) 2127–2130

Overweight and Obesity: review of medical conditions and risk factors for Process Mining approach

Zoe Valero-Ramon[1], Antonio Martinez-Millana[1], Vicente Traver-Salcedo[1], and Carlos Fernandez-Llatas[1]

SABIEN group at ITACA Institute, Universitat Politecnica de Valencia, Spain
{zoevara,anmarmil,vtraver,cfllatas}@itaca.upv.es

Abstract. WHO (World Health Organization) classifies overweight and obesity based on BMI (Body Mass Index). BMI is considered a rough guide because it fails to discriminate between body fat percent and lean mass in both sexes. Obesity is considered a chronic disease associated comorbidities and risk factors. This review considers a variety of medical conditions and risk factors and their association with overweight and obesity, including type of evidence, their presence in Health Electronic Records of Health Department La Fe in Valencia, and their potential to be included in a novel study. This study will use comorbidities and risk factors associated to obesity and Process Mining techniques, to predict obesity in population, without BMI measure, as part of systematic detection model.

Keywords: Comorbidities of Obesity · risks of obesity · BMI · systematic detection.

1 Introduction

WHO (World Health Organization) defines overweight and obesity as abnormal or excessive fat accumulation that represents a risk to health. A crude population measure of obesity is the body mass index (BMI), a person's weight (in kilograms) divided by the square of his or her height (in meters) [49]. Obesity is considered a chronic disease that is increasing in prevalence [5] to the point of being considered an international epidemic, not only in adults, but also in children. Obesity and overweight is associated with increased risk of comorbidities such as type 2 diabetes mellitus, cardiovascular diseases, respiratory disorders, infertility, some cancers, psychological and social problems that negative impact on quality of life [35], moreover overweight and obesity are inside the five leading global risks for mortality in the world [50]. It is therefore vital to identify those population overweight and obese in order to design more efficient interventions. In this context, Crowdhealth study is developing a use case focused on obesity at population level in Health Department La Fe in Valencia with data from Primary Care, Telemedicine and Endocrinology, that compound an integrated

C.Fernandez-Llatas and M.Guillen (Ed.):
Workshop on Innovation on
Information and Communication Technologies
(ITACA-WIICT 2018)

ISBN 978-84-09-07373-3

system based on Big Data. The problem is considered important since despite the numerous interventions supporting healthy diet and exercise, the prevalence of obesity in Valencian community both, for children and adults, still grows. Considering an obesity prevalence of 16% in the region [16], the study will directly point about 45,000 people who could benefit from more efficient policies and interventions. The objectives are, on the one hand, to perform a systematic detection of obesity and overweight based on risk of commorbidities due to obesity thanks to data collected in HER and Process Mining paradigm, and on the other hand, to sensitize the professionals of the National Health System to promote the systematic detection of obesity and overweight in the population thanks to this new approach. In the current work, we review scientific evidence about comorbidities associated to obesity and overweight and other risk factors aiming to be used in identifying obese and overweight population without diagnosis, thanks to data of Health Electronic Records (HER) with a novel approach based on Process Mining techniques.

2 Materials and Methods

BMI is an anthropocentric method to measure body fat based on height and weight that applies to adult men and women. WHO classifies BMI into four categories: underweight (¡ 18.5 kg/m2), normal (18.5 - 24.9 kg/m2), overweight (25.0 - 29.9 kg/m2), and obese (¿= 30.0 kg/m2). BMI provides one of the most useful population-level measure of overweight and obesity as it is the same for both sexes and for all ages of adults. However, it should be considered a rough guide because BMI failed to discriminate between body fat percent and lean mass in both sexes [39]. For the past 40 years obesity has been primarily diagnosed using BMI, but it presents two problems, the limited diagnosis accuracy of BMI in detecting obesity for individuals in the intermediate BMI ranges, in men and in the elderly, and the availability of data in health data systems, that not always include BMI (or height and weight), but many other parameters that could act as risk factors (comorbilities of overweight and obesity). However, the BMI indicates weight-for-height without considering differences in body composition and the distribution of body fat to overall body height. Other measurements of fat distribution include waist circumference and body fat percentage. The body fat percentage (BF%) is total body fat expressed as a percentage of total body weight, but unlike in the case of BMI, there is no generally definition of obesity based on total body fat. Most researchers have defined obesity according to BF% as BF% ¿ 30 in female and ¿ 25 in males [30]. There are numerous formulas to predict BF% from gender, age and BMI, providing easy and non-invasive prediction of BF% [8]. Waist circumference is also used to define central obesity, with cut-off points in Europe of ¿ 94cm for men and ¿ 80 cm in women [46]. All the previous measures and methods to predict obesity and overweight are based on static measures and do not include variability over time, not only of the variable but also of the person health status. One of the challenges for patients and clinicians is that excessive body fat is classified into overweight and obesity on the basis of previous measures (BMI, waist circumference or prediction of BF%), rather than on presence of comorbidities, consequences and evolution.

2.1 Process Mining

Process Mining is applicable to a wide range of systems, such as hospital information systems, as they provide very detailed information about activities executed from different departments. The goal of Process Mining is to extract information from these systems, discovering, monitoring and improving real processes, by extracting knowledge from data over time [27]. This is the case of Crowdhealth study that includes Health Department La Fe in Valencia , that wants to extract knowledge from three different departments: Primary Care, Telemedicine and Endocrinology and try to predict obesity based on available data.

3 Results

The evidence is overwhelming on the association of obesity to a number of medical conditions and socioeconomic factors. A bibliographic review was performed in order to find evidence about prevalence and association of overweight and obesity with other medical conditions (comorbidites) and other risk factors, and that could be retrieved from Health Electronic Records.

3.1 Overweight and obesity: medical factors

Table 1 shows evidence for overweight and obesity regarding medical conditions. Data of Table 1 includes: if the condition is included in HER used in Crowdhealth study; the type of evidence between the medical condition and being obese/overweight (Direct/Indirect/Mild); the type of variable (continuous or static); if the medical condition is feasible obtained (yes/no); if the condition is already included in the study (yes/no); if we have to change the study in order to include the condition (yes/no); and finally the scientific evidence about the association between obesity and the medical condition.

Hypertension or obesity-hypertension The close relationship between excess adipose mass and hypertension is well documented, with population-based studies showing excess adiposity as the strongest known risk factor for hypertension in male and female subjects of different ages and races [17], [44], [47], [32], [38] Hypertension is the most prevalent obesity comorbidity associated with increased cardiovascular risk [48]. Obesity hypertension is a distinct subtype of essential hypertension Excess weight gain, especially when associated with increased visceral adiposity, is a major cause of hypertension, accounting for 65% to 75% of the risk for human primary (essential) hypertension. Obesity-associated hypertension becomes more difficult to control, often requiring multiple antihypertensive drugs and treatment of other risk factors, including dyslipidemia, insulin resistance and diabetes mellitus, and inflammation [15].

Table 1. Medical conditions considered as comorbidities for overweight and obesity.

Medical condition	HER	Type of evidence	Type of var.	Easy obtained	In the study	Modif. the study	Papers
Hypertension	Yes	Direct	Cont.	Yes	Yes	No	[17], [44] [47], [32]
Diabetes and Insulin Resistance [1]	Yes	Direct	Cont.	Yes	Yes	Yes	[19], [12]
Dyslipidemia	Yes	Direct	Cont.	Yes	Yes	Yes	[21], [2], [18]
Coronary heart disease	Yes	Indirect	Cont.	No	Yes	No	[29], [51], [7]
Gallbladder Disease	Yes	Indirect	Cont.	No	Yes	No	[3], [37], [4]
Respiratory Disease	Yes	Indirect	Cont.	No	Yes	No	[26], [41], [33]
Knee osteoarthritis	Yes	Indirect	Cont.	No	Yes	No	[52], [6], [43]
Depression	Yes	Mild	Static	No	No	No	[54], [31], [36]

Diabetes and insulin resistance Obesity is associated with an increased risk of developing insulin resistance and type 2 diabetes. Insulin resistance is the condition where the body does not respond appropriately to circulating insulin. It associates commonly with obesity, hypertension, and cardiovascular disease and typically precedes the onset of Type 2 Diabetes [19].

Obesity induces an inflammation state that is implicated in many clinically important complications, including insulin resistance and diabetes [12] There is increasing evidence showing that inflammation is an important pathogenic mediator of the development of obesity-induced insulin resistance [1]. Overweight and obesity continue to be also prevalent among individuals with T1DM (Type I Diabetes Mellitus). Obesity rates appear to have reached a plateau among children with T1DM in some parts of the world. The risk for development of T1DM is increased by obesity and may occur at an earlier age among obese individuals with a predisposition [34].

Dyslipidemia Dyslipidemia refers to unhealthy levels of one or more kinds of lipids in the blood, as there are three main types of lipid (high-density lipoprotein (LDL), low-density lipoprotein (HDL) and triglycerides), dyslipidemia is usually means LDL level or triglycerides too high or HDL level too low. Accumulating evidence indicates that obesity is closely associated with dyslipidemia: increased levels of triglycerides, decreased levels of HDL and normal or slightly increased LDL [21] - [2]. Although the mechanisms are still unclear, excess adipose tissue and dysfunction can contribute to the development of obesity-related metabolic diseases [18].

Coronary heart disease Coronary Heart Disease (CHD) is a disease in which a waxy substance called plaque builds up inside the coronary arteries. These arteries supply oxygen-rich blood to heart muscle. Over time, plaque can harden or rupture (break open). Hardened plaque narrows the coronary arteries and reduces the flow of oxygen-rich blood to the heart [29]. Obesity and CHD have common risk factors as hypertension, dyslipidemia and type II diabetes mellitus, the independent effect of obesity itself in CHD has been difficult to verify, and its unique contribution to CHD prediction can be difficult to quantify [51]. However, actual data supports the hypothesis that obesity is related to risk of coronary attack [7] or CHD [24].

Gallbladder disease The term gallbladder disease is used for several types of conditions that can affect the gallbladder. There are many different types of gallbladder disease as gallstones, cholecystitis, gallbladder polyps, or gallbladder cancers. According to current studies, obesity is related to various gallbladder diseases and Gallstone disease is more prevalent in the patient with obesity [3], [37], [4]

Respiratory disease There is a gradually increasing impairment of respiratory function with increasing obesity. Obesity, particularly severe central obesity, affects respiratory physiology both at rest and during exercise. Reductions in expiratory reserve volume, functional residual capacity, respiratory system compliance and impaired respiratory system mechanics produce a restrictive ventilatory defect. The combination of ventilatory impairment, excess CO(2) production and reduced ventilatory drive predisposes obese individuals to obesity hypoventilation syndrome [23], [41], [26]. In fact, obesity is the most frequent risk factor for obstructive sleep apnoea [33].

Knee osteoarthritis Gradual onset of knee pain, stiffness and swelling are typical symptoms of knee osteoarthritis. Knee osteoarthritis with obesity are two of the most common diseases and are often comorbidities, as obesity increases the risk of knee osteoarthritis by a variety of mechanisms [52], [6]. In fact, two of the main factors associated with onset of knee pain are being overweight and obesity [43].

Depression Obesity is associated with an increased risk of developing a variety of chronic diseases associated with psychiatric disorders.Studies have showed higher rates of obesity in persons with depression, especially in women with BMI ¿ 25 and men with BMI ¿ 40 [54], [36], so findings suggest that obesity is associated with depression mainly among persons with severe obesity [31]. But there are still disparities in prevalence among people with different BMI levels, so more studies are necessary to clarify obesity - depression relation.

3.2 Overweight and obesity: other risk factors

Table 2 shows evidence on the association of overweight and obesity with other risk factors. Information included is the same as in Table 1.

Table 2. Other risk factors for overweight and obesity.

Risk Factor	HER	Type of evidence	Type of var.	Easy obtained	In the study	Modif. the study	Papers
Poverty and built envirnonment	No	Mild	Static	No	No	Yes	[56] [53], [22]
Ethnic	No	Indirect	Static	No	No	No	[28], [40] [55]
Gender	Yes	More research	Cont.	Yes	Yes	No	[13], [14]
Alcohol	Yes	Direct	Cont.	Yes	Yes	No	[25], [42] [45]
Medication	Yes	Indirect	Cont.	No	Yes	No	[20], [10] [9]

Poverty and built environment Number of people suffering overweight and obesity is increasing, particularly in developed countries. The paradox of obesity and poverty relationship is observed especially in the developed and developing countries [56]. Co-related factors with poverty and obesity are: higher unemployment, lower education level, and irregular meals. Other studies shows the influence of the environment variables in people's behaviour, becoming obesity risk factors (such as urbanicity, fast-food restaurants availability, poverty rate, race heterogeneity) [53]. This situation has even more impact on children and adolescence [22], [11].

Ethnic Obesity is a condition that is especially prevalent among blacks and Latinos [28], causes for this prevalence came from individual-level characteristics and characteristics of the geographic areas in which minority ethnic groups reside [40]. Baseline neighborhood disadvantage is associated with BMI and marginally reduces racial disparities in BMI. BMI differences among ethnics are explained by socioeconomic disadvantages, whereas a range of cultural and family characteristics partially explain disparities for ethnic groups [55].

Gender In most populations, the prevalence of obesity is greater in women than in men, however, the association between global measures of gender inequality and the sex gap in obesity is dependent on the measure used, so studies reveal that is needed more research about mechanisms that underpin the gendered nature of obesity prevalence [13]. This gender inequalities seems to be motivated by spatially influenced processes influencing in obesity prevalence, e.g. policies, societal norms [14].

Alcohol recent prospective studies show that light-to-moderate alcohol intake is not associated with adiposity gain while heavy drinking is more consistently related to weight gain [25], [42]. However, the available evidence is conflicting and hampered by important limitations that preclude a strong conclusion on the effect of alcohol intake on obesity risk [45].

Medication Several studies shows the positive association between obesity and medication use. This medication use come from two reasons, first medication related with obesity itself (appetite-suppressing, drugs for weight reduction) and, secondly medications for managing comorbidities. A revision work in England found that obesity has a statistically significant and positive association with use of a range of medicines for managing diseases associated with obesity [20]. Similar studies in Austria [10] and Netherlands [9] reveal similar results.

4 Discussion

The aim of this work was to perform a bibliographic review about most common comorbidities and risk factors associated to obesity and overweight that there are included in HER, or could be feasible included, and ca be used as predictors of obesity within a systematic detection model using Process Mining paradigm. Our main finding are that there is strong evidence with regards to the relationship of obesity with: hypertension, insulin resistance, dyslipidemia, coronary heart disease, gallbladder disease, respiratory disease and knee osteoarthritis. We also find common risk factors in obesity: poverty and built environment, gender, heavy alcohol consumption and medication use. Comorbidities are dynamic variables that are considered as static values at the time the measurement is made, so we consider that those comorbidities and risk factors could be used as inputs in Process Mining techniques in order to obtain evolution models and to obtain meaningful knowledge about overweight and obesity evolution. Our future work will implement a systematic detection model of obesity based on comorbidities and risk factors found in this work, trying to clinically detect obese people without using the BMI.

References

1. Balsan, G.A., Vieira, J.L.d.C., Oliveira, A.M.d., Portal, V.L.: Relationship between adiponectin, obesity and insulin resistance. Revista da Associação Médica Brasileira **61**(1), 72–80 (2015)
2. Bamba, V., Rader, D.J.: Obesity and atherogenic dyslipidemia. Gastroenterology **132**(6), 2181–2190 (2007)
3. Bonfrate, L., Wang, D.Q., Garruti, G., Portincasa, P.: Obesity and the risk and prognosis of gallstone disease and pancreatitis. Best practice & research Clinical gastroenterology **28**(4), 623–635 (2014)
4. Bray, G., Kim, K., Wilding, J., Federation, W.O.: Obesity: a chronic relapsing progressive disease process. a position statement of the world obesity federation. Obesity Reviews **18**(7), 715–723 (2017)
5. Bray, G.A., Ryan, D.H.: Clinical evaluation of the overweight patient. Endocrine **13**(2), 167–186 (2000)

6. Coggon, D., Reading, I., Croft, P., McLaren, M., Barrett, D., Cooper, C.: Knee osteoarthritis and obesity. International journal of obesity **25**(5), 622 (2001)
7. Dawber, T.R., Moore, F.E., Mann, G.V.: Ii. coronary heart disease in the framingham study. International journal of epidemiology **44**(6), 1767–1780 (2015)
8. Deurenberg, P., Weststrate, J.A., Seidell, J.C.: Body mass index as a measure of body fatness: age-and sex-specific prediction formulas. British journal of nutrition **65**(2), 105–114 (1991)
9. van Dijk, L., Otters, H.B., Schuit, A.J.: Moderately overweight and obese patients in general practice: a population based survey. BMC family practice **7**(1), 43 (2006)
10. Dzien, A., Pfeiffer, K., Dzien-Bischinger, C., Hoppichler, F., Lechleitner, M.: The influence of obesity on the frequency and distribution of medication. Acta Medica Austriaca **30**(2), 51–54 (2003)
11. Ells, L.J., Hancock, C., Copley, V.R., Mead, E., Dinsdale, H., Kinra, S., Viner, R.M., Rutter, H.: Prevalence of severe childhood obesity in england: 2006–2013. Archives of disease in childhood **100**(7), 631–636 (2015)
12. Ferrante, A.: Obesity-induced inflammation: a metabolic dialogue in the language of inflammation. Journal of internal medicine **262**(4), 408–414 (2007)
13. Garawi, F., Devries, K., Thorogood, N., Uauy, R.: Global differences between women and men in the prevalence of obesity: is there an association with gender inequality? European journal of clinical nutrition **68**(10), 1101 (2014)
14. Gartner, D.R., Taber, D.R., Hirsch, J.A., Robinson, W.R.: The spatial distribution of gender differences in obesity prevalence differs from overall obesity prevalence among us adults. Annals of epidemiology **26**(4), 293–298 (2016)
15. Hall, J.E., do Carmo, J.M., da Silva, A.A., Wang, Z., Hall, M.E.: Obesity-induced hypertension: interaction of neurohumoral and renal mechanisms. Circulation research **116**(6), 991–1006 (2015)
16. Jiménez-Talamantes, R., Rizk Hernández, J., Quiles Izquierdo, J.: Diferencias entre la prevalencia de obesidad y exceso de peso estimadas con datos declarados o por medición directa en adultos de la comunidad valenciana. Nutrición Hospitalaria **34**(1), 128–133 (2017)
17. Jones, A., Charakida, M., Falaschetti, E., Hingorani, A.D., Finer, N., Masi, S., Donald, A.E., Lawlor, D.A., Smith, G.D., Deanfield, J.E.: Adipose and height growth through childhood and blood pressure status in a large prospective cohort study. Hypertension **59**(5), 919–925 (2012)
18. Jung, U.J., Choi, M.S.: Obesity and its metabolic complications: the role of adipokines and the relationship between obesity, inflammation, insulin resistance, dyslipidemia and nonalcoholic fatty liver disease. International journal of molecular sciences **15**(4), 6184–6223 (2014)
19. Kahn, S.E., Hull, R.L., Utzschneider, K.M.: Mechanisms linking obesity to insulin resistance and type 2 diabetes. Nature **444**(7121), 840 (2006)
20. Kinge, J.M., Morris, S.: Association between obesity and prescribed medication use in england. Economics & Human Biology **15**, 47–55 (2014)
21. Klop, B., Elte, J.W.F., Cabezas, M.C.: Dyslipidemia in obesity: mechanisms and potential targets. Nutrients **5**(4), 1218–1240 (2013)
22. Lee, H., Andrew, M., Gebremariam, A., Lumeng, J.C., Lee, J.M.: Longitudinal associations between poverty and obesity from birth through adolescence. American journal of public health **104**(5), e70–e76 (2014)
23. LIN, C.K., LIN, C.C.: Work of breathing and respiratory drive in obesity. Respirology **17**(3), 402–411 (2012)

24. Lu, Y., Hajifathalian, K., Ezzati, M., Woodward, M., Rimm, E.B., Danaei, G.: Metabolic mediators of the effects of body-mass index, overweight, and obesity on coronary heart disease and stroke: a pooled analysis of 97 prospective cohorts with 1· 8 million participants. (2014)
25. Lukasiewicz, E., Mennen, L.I., Bertrais, S., Arnault, N., Preziosi, P., Galan, P., Hercberg, S.: Alcohol intake in relation to body mass index and waist-to-hip ratio: the importance of type of alcoholic beverage. Public health nutrition **8**(3), 315–320 (2005)
26. Mandal, S., Hart, N.: Respiratory complications of obesity. Clinical Medicine **12**(1), 75–78 (2012)
27. Mans, R.S., Schonenberg, M., Song, M., van der Aalst, W.M., Bakker, P.J.: Application of process mining in healthcare–a case study in a dutch hospital. In: International joint conference on biomedical engineering systems and technologies. pp. 425–438. Springer (2008)
28. Moloney, K.L., South, S.J.: Ethnic density and obesity: Evidence from fixed-effects models. Health & place **31**, 199–207 (2015)
29. NIH: Nih, coronary heart disease (Jun 2018), https://www.nhlbi.nih.gov/health-topics/coronary-heart-disease
30. Okorodudu, D., Jumean, M., Montori, V.M., Romero-Corral, A., Somers, V., Erwin, P., Lopez-Jimenez, F.: Diagnostic performance of body mass index to identify obesity as defined by body adiposity: a systematic review and meta-analysis. International journal of obesity **34**(5), 791 (2010)
31. Onyike, C.U., Crum, R.M., Lee, H.B., Lyketsos, C.G., Eaton, W.W.: Is obesity associated with major depression? results from the third national health and nutrition examination survey. American journal of epidemiology **158**(12), 1139–1147 (2003)
32. Pausova, Z., Mahboubi, A., Abrahamowicz, M., Leonard, G.T., Perron, M., Richer, L., Veillette, S., Gaudet, D., Paus, T.: Sex differences in the contributions of visceral and total body fat to blood pressure in adolescence. Hypertension **59**(3), 572–579 (2012)
33. Piper, A.J.: Obesity and respiratory diseaseweighing in on the issue: An epilogue. Respirology **18**(1), 5–7 (2013)
34. Polsky, S., Ellis, S.L.: Obesity, insulin resistance, and type 1 diabetes mellitus. Current Opinion in Endocrinology, Diabetes and Obesity **22**(4), 277–282 (2015)
35. Pozza, C., Isidori, A.M.: Whats behind the obesity epidemic. In: Imaging in Bariatric Surgery, pp. 1–8. Springer (2018)
36. Pratt, L.A., Brody, D.J.: Depression and obesity in the us adult household population, 2005–2010. Women **20**, 39 (2014)
37. Radmard, A.R., Merat, S., Kooraki, S., Ashrafi, M., Keshtkar, A., Sharafkhah, M., Jafari, E., Malekzadeh, R., Poustchi, H.: Gallstone disease and obesity: a population-based study on abdominal fat distribution and gender differences. Annals of Hepatology: Official Journal of the Mexican Association of Hepatology **14**(5) (2015)
38. Rahmouni, K.: Obesity-associated hypertension: recent progress in deciphering the pathogenesis. Hypertension **64**(2), 215–221 (2014)
39. Romero-Corral, A., Somers, V.K., Sierra-Johnson, J., Thomas, R.J., Collazo-Clavell, M., Korinek, J., Allison, T.G., Batsis, J., Sert-Kuniyoshi, F., Lopez-Jimenez, F.: Accuracy of body mass index in diagnosing obesity in the adult general population. International journal of obesity **32**(6), 959 (2008)

40. Ruel, E., Reither, E.N., Robert, S.A., Lantz, P.M.: Neighborhood effects on bmi trends: Examining bmi trajectories for black and white women. Health & place **16**(2), 191–198 (2010)
41. Sebastian, J.C.: Respiratory physiology and pulmonary complications in obesity. Best Practice & Research Clinical Endocrinology & Metabolism **27**(2), 157–161 (2013)
42. Shelton, N.J., Knott, C.S.: Association between alcohol calorie intake and overweight and obesity in english adults. American journal of public health **104**(4), 629–631 (2014)
43. Silverwood, V., Blagojevic-Bucknall, M., Jinks, C., Jordan, J., Protheroe, J., Jordan, K.: Current evidence on risk factors for knee osteoarthritis in older adults: a systematic review and meta-analysis. Osteoarthritis and cartilage **23**(4), 507–515 (2015)
44. Suglia, S.F., Clark, C.J., Gary-Webb, T.L.: Adolescent obesity, change in weight status, and hypertensionnovelty and significance: Racial/ethnic variations. Hypertension **61**(2), 290–295 (2013)
45. Traversy, G., Chaput, J.P.: Alcohol consumption and obesity: an update. Current obesity reports **4**(1), 122–130 (2015)
46. Tsigos, C., Hainer, V., Basdevant, A., Finer, N., Fried, M., Mathus-Vliegen, E., Micic, D., Maislos, M., Roman, G., Schutz, Y., et al.: Management of obesity in adults: European clinical practice guidelines. Obesity facts **1**(2), 106–116 (2008)
47. Tu, W., Eckert, G.J., DiMeglio, L.A., Yu, Z., Jung, J., Pratt, J.H.: Intensified effect of adiposity on blood pressure in overweight and obese children. Hypertension **58**(5), 818–824 (2011)
48. Varughese, A.G., Nimkevych, O., Uwaifo, G.I.: Hypercortisolism in obesity-associated hypertension. Current hypertension reports **16**(7), 443 (2014)
49. WHO: Who, obesity (Jun 2018), http://www.who.int/topics/obesity/en/
50. organization (WHO, W.H., et al.: Global health risks-mortality and burden of disease attributable to selected major risks. Cancer (2017)
51. Wilson, P.W., DAgostino, R.B., Levy, D., Belanger, A.M., Silbershatz, H., Kannel, W.B.: Prediction of coronary heart disease using risk factor categories. Circulation **97**(18), 1837–1847 (1998)
52. Wluka, A.E., Lombard, C.B., Cicuttini, F.M.: Tackling obesity in knee osteoarthritis. Nature Reviews Rheumatology **9**(4), 225 (2013)
53. Xu, Y., Wang, F.: Built environment and obesity by urbanicity in the us. Health & place **34**, 19–29 (2015)
54. Zhao, G., Ford, E.S., Dhingra, S., Li, C., Strine, T.W., Mokdad, A.: Depression and anxiety among us adults: associations with body mass index. International journal of obesity **33**(2), 257 (2009)
55. Zilanawala, A., Davis-Kean, P., Nazroo, J., Sacker, A., Simonton, S., Kelly, Y.: Race/ethnic disparities in early childhood bmi, obesity and overweight in the united kingdom and united states. International journal of obesity **39**(3), 520 (2015)
56. Zukiewicz-Sobczak, W., Wróblewska, P., Zwolinski, J., Chmielewska-Badora, J., Adamczuk, P., Krasowska, E., Zagórski, J., Oniszczuk, A., Piatek, J., Silny, W.: Obesity and poverty paradox in developed countries. Annals of Agricultural and Environmental Medicine **21**(3) (2014)

Towards dependability-aware design space exploration using genetic algorithms

Quentin Fabry*, Ilya Tuzov**, Juan-Carlos Ruiz** and David de Andrés**

*ENSEEIHT, Toulouse, 2 Rue Charles Camichel, 31000, France
**ITACA, Universitat Politècnica de València, Campus de Vera s/n, 46022, Spain

Abstract. The development of complex digital systems poses some design optimization problems that are today automatically addressed by Electronic Design Automation (EDA) tools. Deducing optimal configurations for EDA tools attending to specific implementation goals is challenging even for simple HW models. In deed, previous research demonstrates that such configurations may have a non-negligible impact on the performance, power-consumption, occupied area and dependability (PPAD) features exhibited by resulting HW implementations. This paper proposes a genetic algorithm to cope with the selection of appropriate configurations of EDA tools. Regardless statistical approaches, this type of algorithms has the benefit of considering all the effects among all configuration flags and their iterations. Consequently, they have a great potential for finding out tool configurations leading to implementations exhibiting optimal PPAD scores. However, it also exists the risk of incurring in very time-consuming design space explorations, which may limit the usability of the approach in practice. Since the behavior of the genetic algorithm will be strongly conditioned by the initially selected population and the mutation, crossover and filtering functions that will be selected for promoting evolution, these parameters must be determined very carefully on a case per case basis. In this publication, we will rely on a multilinear regression model estimating the impact of synthesis flags on the PPAD features exhibited by the implementation of an Intel 8051 microcontroller model. Beyond reported results, this preliminar research show how and to what extend genetic algorithms can be integrated and use in the semi-custom design flow followed today by major HW manufacturers.

1 Introduction

Electronic Design Automation (EDA) tools are nowadays sophisticated enough to achieve a close-to-optimum implementation of integrated circuits with designer assistance [1]. Hence, designers can reason in terms of functionality and EDA tools take care of the implementation details. It is important to understand that these tools operate in a daisy chain fashion and support all the successive processes within the common semi-custom design flow, the so-called synthesis, mapping, placement and routing processes. These successive steps are in charge of transforming digital design specified at a high-level register-transfer level into

C.Fernandez-Llatas and M.Guillen (Ed.):
Workshop on Innovation on
Information and Communication Technologies
(ITACA-WIICT 2018)

ISBN 978-84-09-07373-3

detailed gate-level netlists. Such refinements require the exploration of a myriad of design implementation alternatives for the considered logic, which is typically referred as a design exploration problem, or DSE for short. It is worth noting that EAD tools offer multitude of parameters (typically called flags) that can be used in order to customize how this exploration is carried out.

Through the aforementioned flags, designers can tune the implementation process according to the specificities of their system, application domain, and a set of expected performance, power consumption, occupied area and dependability goals, the so-called from now on *PPAD goals*. The side effect is that improperly tuning such flags negatively impacts the quality of resulting design implementations. In addition, the larger the number of flags available, the larger the design space to explore, and the more complex its exploration, sometimes falling beyond what even expert designers can manage manually.

There exist a wide variety of state of the art approaches for addressing the multi-objective DSE problem. According to [2], they can be classified into following four classes : i) heuristics and pseudo-random approaches, e.g. simulated annealing [3] ii) statistical techniques with domain knowledge, e.g. techniques relying on Markov Decision Process [4] iii) statistical techniques without domain knowledge, usually based on design of experiments [5], and iv) techniques based on the use of genetic algorithms[6].

Most practical DSE approaches focus only on optimization of performance, power and area (PPA) through tuning of architectural features. For instance, the DESSERT tool [7] optimizes power consumption, targeting HW models in SystemC, while the OCTOPUS tool [8] optimizes performance, targeting HW modeled with Petri nets. The MULTICUBE tool is another example that optimizes performance and power [9] of SoC models described in SystemC. However, very few tools deal with dependability concerns in general, and robustness optimization of designs in particular. And even when they consider dependability, they either do not consider the eventual side effects of dependability optimization on PPA properties [10], or they only focus on the tuning of desing features [11], thus neglecting the impact on implementations of EDA tools' flags.

In a recent paper [5], it has been addressed the complex problem of exploring the design space defined by off-the-shelf synthesis tools to deduce optimal configuration of flags simultaneously attending to PPA and dependability goals. The proposal relied on the use of fractional factorial design of experiments to reduce the number of fault injection experiments to carry out. It made a clever use of statistical and operational research instruments to reduce the design space to a size that allows the experimental estimation of dependability properties through fault injection procedures, so they can be used to determine the best possible configuration for synthesis flags according to designers preferences in terms of PPAD requirements. Such approach not only can guide the implementation process to obtain a faster, cheaper, and more dependable implementations, but it also prevents the really negative effects derived from misconfiguring the selected EDA tools. The obtained results showed that the proper tuning of logic synthesis flags may almost double the mission time of implementations, while simultaneously reducing the area and power consumption. And all of this only relying on the proper tuning of EDA tools' flags. i.e without introducing any modification in original HW designs. The practical implementation of the approach resulted in the DAVOS toolkit [12], which has incorporated various techniques for accurate [13] yet fast [14] robustness assessment of implementation-level HW models.

The above approach paved the way towards the provision of more sophisticated approaches to balance PPAD goals in HW implementations produced by EDA tools. However, under its current formulation, the solution can only estimate the main impact of considered flags in final implementations. According to the principle of hierarchical ordering in the design of experiments [15], the main effect of flags is the one that will more likely have a significant impact on results, but one should not neglect the impact that interactions among flags (the so-called high-order effects) can also have on such results. Consequently, and although in most of the cases the simple consideration of the main effect of flags should be enough to provide close-to globally optimal solutions, higher-order effects must be also taken into consideration to obtain accurate estimations of the impact of such flags on resulting implementations. In order to capture the effect of such interactions using statistical methods, the number of experiments to carry out must be greatly increased, which limits in practice the use of this type of approach for this purpose.

This is where the use of genetic algorithms (GAs) can be of interest, since these algorithms has the potential to simultaneously consider all-order effects of flags on the PPAD features of resulting HW implementations. However, as it is explained in [2] the use of GAs do not guarantee a rapid convergence to a global optimum solution. Typically, GA will only reach reasonable good solutions when the initial population has enough time to evolve [6]. This is mainly why in this paper the effectiveness of a GA will be determined attending to two basic principles: i) the quality of the resulting configuration, that will be determined attending to a PPAD-based score, and ii) the cost of obtaining the resulting configuration, quantified as the total amount of considered configurations until reaching the resulting one. The ideal goal is to provide the best quality configuration at the lowest possible cost, but a more realistic goal, the one adopted in this paper, will be to tune the genetic algorithm in order to find out a configuration with a good-enough quality at a reasonable time-cost. In order to cope with such challenge, the algorithm requires the definition of a number of elements, such as the initial population to consider and the selection, crossover and mutation heuristics to use during the evolution of such population. Obviously, there exist a number of alternatives to consider for each one of these elements. This paper provides the rational behind the definition of a genetic algorithm suitable for supporting the automatic exploration of the design space established by the various EDA tools' flags under consideration. The previous research carried out at [5] will be the one considered as reference for this work.

The rest of this paper is structured as follows. Section 2 provides the background on genetic algorithms used for design space exploration. Section 3 defines particular instance of a GA implementation and presents its parameterization, which is aimed at minimization of optimization cost. Section 4 describes the experimental procedure for calibration of the defined algorithm, using the available regression models. These models relate the PPAD properties of MC8051 soft-core processor implementation (for Virtex6 FPGA) with the parameters of Xilinx XST logic synthesizer. Then section 4 discusses the experimental results, and the calibrated parameters of the GA. Finally, section 5 presents the conclusions drawn from this work.

2 Background on Genetic Algorithms

A Genetic Algorithm (GA) is an optimization method, more specifically, a metaheuristic [16], having a real efficiency to provide high-quality results on many kind of problems. It cannot assure to find the global optimum solution of a problem. In general, GAs are usually a bad choice when addressing simple problems that can be easily solved using methods as exhaustive search or mountain climbing. However, they can be really efficient alternative when deployed on complex problems exploring large research spaces. In that case, this type of algorithms try to explore the research space following a process inspired in biology, where solutions have a genome that evolves over generations.

Using GAs, the data needed to solve the problem is contained in each individual, which is also considered as a potential solution of the problem. Such data can be encoded in different forms in order to be manipulated by GA. Most of the times the genome of each individual is encoded as a bit array, where all choices needed to solve the problem are represented in a bit and take a value of 1 or 0.

Typically, the GA begins with a set of individuals, that are generally randomly generated. Then the algorithm forces the evolution of this population of individuals. This evolution process relies on the use of crossover, mutation and selection functions. A high level view of the process provided in Figure 1.

Evaluation can be seen as the interface between the GA and the addressed problem, as the algorithm will ask the evaluation function to assess the degree of fitness provided by each individual in the population with respect to the considered problem.

There are different way to stop the algorithm, it can be decided to stop it when current individuals are considered good enough: if an individual reaches the expected degree of fitness (typically a previously specified score) it is considered as a solution of the problem and the GA notifies the discovery. Otherwise, it continues with the research of a solution. Or it is also common to run the algorithm until better results are not reasonably expected: the population converge toward a solution, which can be global or local optimum.

The Selection process can be compared to the natural selection process in the nature. Best individuals (i.e. those having a higher fitness score) are those that will be more likely selected. This means that they are more prone to survive and interact together to produce new individuals. There exist many different selection methods. Some relies on the use of probability for the selection of individuals,

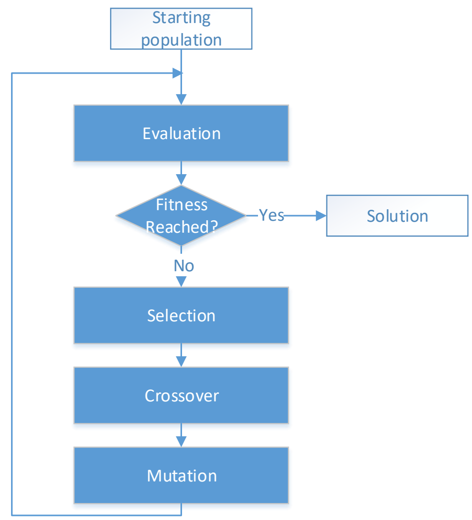

Fig. 1. Architecture of Generic GA

while others renew the whole population at each generation (iteration of the GA algorithm) or they select the individuals in a deterministic way taking only into consideration their features, such as their fitness scores.

Once the set of individuals selected, they interact among them in order to produce new individuals by relying on the use of the so-called crossover functions. The Crossover functions are genetic operators. In biology, two chromosomes cross their chromatids and exchange genes. In GAs, the process, in Figure 2 is similar and basically structured in three successive steps:

1. Parents selection - Two individuals are selected to undergo the crossover process. Remember that their respective genomes are usually encoded as two bit array.
2. Determination of the crossover point - A point is randomly determined in the genome (bit array) of each individual to carry out the crossover, i.e. to split its genome in parts.
3. Data exchange - Attending to the location of the crossover point selected in the genome (bit array) of each individual, the genome is split and then combined with other fragments produced by other individuals.

As also happens in nature, mutation appears from time to time in order to introduce new characteristics in the genome of population individuals. This is carried out following a mutation process, which is defined as another genetic operator of the GA. Since the genome of individuals is encoded as a bit array, a mutation simply consists in flipping one or several bits of the array. Obviously, mutations should the result of chance, i.e. they cannot be systematically applied

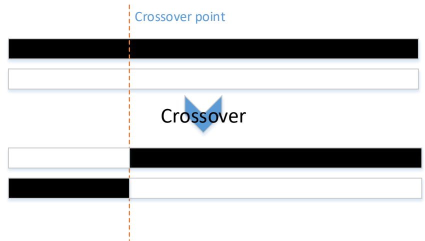

Fig. 2. Single crossover

to all population individuals. This is why a Mutation rate must be fixed. This rate applies not only to the selection of those individuals that should suffer a mutation, but also to determine which bit or bits of their genome must be flipped. This is how new configurations which cannot be reach only by crossover can spontaneously appear in the population under study. This process is illustrated Figure 3

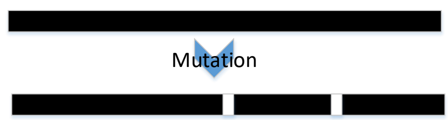

Fig. 3. Mutation

It must be also noted that GAs have to deal with two opposite requirements that must be properly balanced during solution research. The former one is Convergence, which tries to homogenize the population towards a local optimum. The latter is Diversity, which adds new individuals to population in order to enlarge the explored research space, thus avoiding local optimums. If the equilibrium is not correctly managed between these concepts, then a premature convergence towards a local optimum may occur, or the convergence towards a global optimum may become very slow .

3 Use of genetic algorithms for dependability-aware design space exploration

The standard formulation of a genetic algorithm showed in Figure 1 will be refined in this section in order to produce results suitable for properly tuning EDA tools supporting the implementation of HW models. As Figure 5 shows, the first step consists in determining an initial population in order to feed the genetic algorithm. Then, such population is evaluated and if it does not include any solution, it is transformed into a new population by not only applying crossover and mutation, but also filtering resulting new individuals and crowding the finally resulting population. Finally, the algorithm iterates another time. Next subsections detail the aforementioned elements.

3.1 Anatomy of an individual

Since the goal is to properly tune a set of EDA tools, the genome (set of chromosomes) of an individual will be an array of bits (chromosomes) where each bit represents the binary state (0 or 1) of a particular tool parameter. As a result the number of bits in the array will be equal to the number of parameters and tools under consideration. If we consider 1 tool, such a logic synthesizer, for instance, providing 2 parameters, such as *implementaion goal: speed/area* and *implementation effort: normal/high*, then the genome of each individual will contain 2 chromosomes (bits), the first one representing the state of the goal (0 for speed and 1 for area), and the second bit will provide the configuration of the effort flag (0 for normal and 1 for high). If a parameter may have more than two possible values, then the advice is to consider two only two of them, the most representative or interesting one. This is currently a limitation of our proposal that we plan to fix in the near future.

3.2 Initialization process

It is well-known that introducing an initial solution in the initial population can have many beneficial effects. The problem is to know which can be such an initial solution. In the case of EDA tools, most of them are commercialized with a default configuration providing a good balance between performance, power consumption and occupied area. However, considering default configurations as part of the genome of individuals within the initial population is not always a guarantee of improving the space exploration carried out by the genetic algorithm as will be shown in Section 4.

Another aspect to consider is the size of the population, or the number of individuals that the initial population should hold. Providing a value is particularly tough and requires various experiments in order to select a number big enough to enable good evolution, but small enough to avoid an explosion of the population under consideration. Since the consideration of more individuals will imply the realization of more experiments, and thus, the increase of the experimental time, the population size will remain under control during the whole execution of the GA. This means that the number of individuals will not be increased nor reduced from one iteration of the algorithm to another. The experiments leading us to consider a specific number of individuals for the population will be reported in section 4.

3.3 Evaluation through scoring

Providing an score to each individual implies applying the HW design under consideration to the EDA tools under study with the configuration flags provided by each individual. In addition, for each configuration one needs to carry out many (some thousands of) fault injection experiments in order to assess the behavior of the simulated HW implementation i) in the presence of the various considered faults, ii) at all the potential locations of the design that can be affected by such faults, and iii) at all instants of time that this may occur.

Thanks to the research carried out in [5] the effect of a particular configuration over the various performance, power consumption, area and dependability features of a HW design can be statistically estimated without running such a huge number of fault injection experiments. Despite the limited representativeness of the multilinear regression model that was proposed, its accuracy is enough for the purpose of tuning the GA under study. So, this paper will take benefit from this model in order to associate an score for each configuration attending to the PPAD features induced by each configuration. Figure 4 provides an overview of the process followed to compute each individuals' score. This is a three-step approach:

1. The chromosomes of each individual, indeed the set of configurations flags represented by its genome, are provided to the *Davos Toolkit*, a toolkit providing the means to evaluate, among other things, the impact of EDA tools configurations on the PPAD features exhibited by a HW model. Interested readers can found more details on this tool in [12].
2. The estimations of performance, power consumption, area and dependability are returned by *Davos* and normalized for aggregation purposes. This normalization is carried out attending to the maximum values for each one of the considered features that has been obtained so far.
3. The normalized estimations are aggregated attending to the importance provided by designers to each one of the considered parameters. The aggregation technique that is employed is the weighted sum model technique, which requires that the sum of all considered weights should be 1, or 100%.

The resulting score is the one associated to the considered individual. Then, the idea that the higher the score the better, is used in order to rank all the individuals. In other words, the best individuals are those reporting the higher score.

3.4 Limiting the number of iterations of the GA

The fundamental constraint in our case will be the limited number of evaluations that should be carried out, since as earlier mentioned, the experimental time must remain into limited temporal bounds. This is why in the proposed algorithm (see Figure 5) the number of iterations is not only limited by the discovery of an optimal solution, but also by the number of iterations carried out. In a sense, the potential of evolutions will be limited by the number of iterations. This is why the selection of this number is so sensitive in our case, as will be discussed in Section 4.

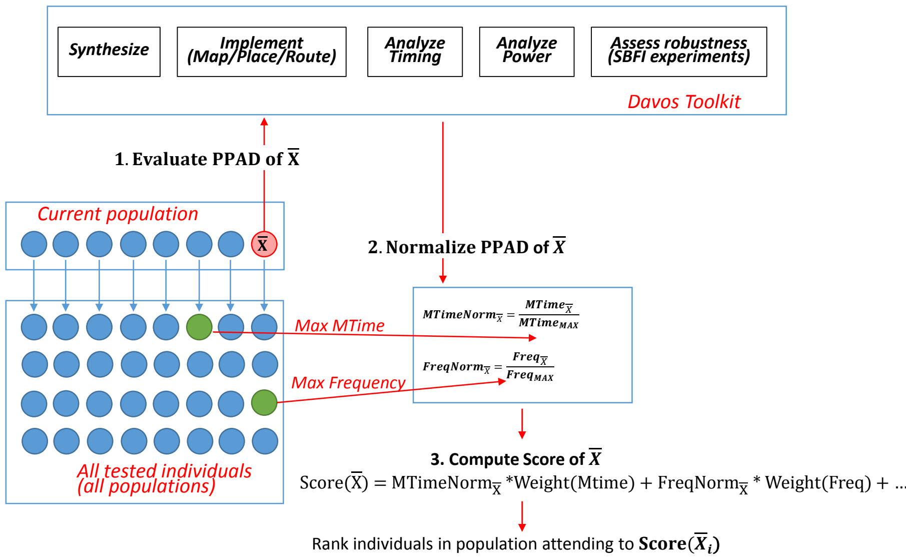

Fig. 4. Procedure to rank the individuals at each iteration of GA

3.5 Selection process

This process directly impacts the ability of the GA to converge towards an optimum (local or global). In our particular case, the Elitism method was selected [17]. This method ensures that the best configurations are kept over generations. From a pure convergence-oriented viewpoint, this approach is the most efficient one. We choose to double the population at each generation (algorithm iteration) with the crossover operation and only half of the existing parents and sons can be selected due to the constraint previously introduced about keeping the size of the population under control. Obviously, the selected ones will be those providing the best evaluations, i.e. PPAD scores.

The global score that will be finally associated to each individual will be computed attending to the aggregated function, detailed in Section 4.1

It must be noted that the elitism selection promoted convergence too much, in the sense that it can lead to a premature convergence around a local optimum, thus missing any other existing (maybe global) optimimum [18]. But this is something very hard to avoid in general when the amount of time for experimentation, and thus for letting the evolution of individuals, is limited.

3.6 Applying crossover

In addition to the simple crossover explained in previous section, two other crossover variants are also taken into consideration: the double crossover and the uniform crossover.

```
Genetic_Algorithm():
    #Initialisation
    Parents=Starting_population_creation(Random)
    *Insert_Specific_configuration_into_population(Parents)
    Evaluation(Parents)
    #Core_loop
    While (no convergence)/*(n iterations):
          #Generation new configurations
          Until population doubles:
                2_Parents_selection(Random)
                Choose_Crossover()
                Sons=Crossover(Parents)
                Sons=Mutation(Sons)
                Filtering_Sons()
                Crowding_process()
                Add_sons_to_population()
          #Scoring
          Evaluation(sons)
          Set_global_score_to_each_configuration(Population)
          #Saving and Discarding
          Selection(Population): Keep the best half population
          #Algorithm End?
          Check_convergence()/*Check_iterations number()
    Return(Population)
```

Fig. 5. Pseudo code of the implemented Genetic Algorithm

On the one hand, the double crossover consists in defining two crossover points and exchange the segment defined by such points between two individuals. The process is graphically explained in Figure 6.

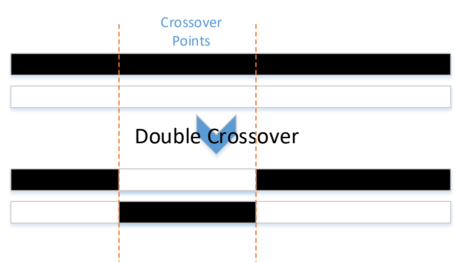

Fig. 6. Double crossover

On the other hand, the uniform crossover randomly cross data among individuals. For each bit in the array of each individual genome it is randomly determined whether the bit is exchange with the corresponding one of the other individual or not. The process is depicted in Figure 7.

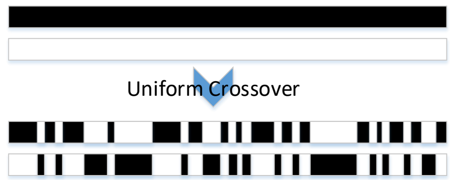

Fig. 7. Uniform crossover

3.7 Applying mutation

As previously commented, mutation relies on the random selection of which individuals, and which bits in their genomes, must be flipped. This random selection is driven by a mutation rate. In our GA each created son is able to undergo mutation, before getting evaluated. For example, with a 0.05 mutation rate, each bit of each son's genome have 5% of probability to flip. Parents a preserved from mutation to avoid the lose of any good solution.

Literature mention the possibility to define an adaptive rate [19]. This means that the algorithm determines whether individuals lead to similar scores, which reflect their potential concentration around a (maybe local) optimum, or their scores are very different, which typically means that individuals are scattered. In the former case, the rate of mutation is increased in order to promote diversity, i.e. the research of a different optimum, while in the latter case, the rate of mutation can be reduced since individuals are scattered enough to guarantee the research of different optimums. This mechanism is implemented in our algorithm, but it is not operational due to co

3.8 Filtering the resulting population

The chromosomes defining the genome of different individuals may be very similar or even identical in situations where the algorithm is converging towards an optimum. In that case, the population can integrate twins, triplets and so on that may prevent evolution. This is why this filtering is necessary in order to ensure the differentiation (diversity) of chromosomes among all population individuals.

Next section explains how the different aspects of the genetic algorithm presented in this section are customized to the specific problem of tuning a commercial off-the-shelf logic synthesizer to explore the design space of an Intel MC8051 processor model

4 Calibration of the Genetic Algorithm using available Regression Models: MC8051 processor as a case study

Let's start with the description of the experimental set-up employed during experimentation. Then the various experiments carried out in order to properly tune the GA under definition will be reported.

4.1 Experimental set-up

Xilinx, one of the major FPGA manufacturers, provides its own framework, the ISE Design Suite, to enable the implementation of HDL designs onto its reconfigurable devices. This framework follows the common semicustom design flow and provides the required toolchain for design entry, synthesis, mapping, placement, routing, and simulation. Accordingly, the integrated Xilinx Synthesis Technology (XST) tool [20] is the synthesizer selected as case study to show the usefulness and feasibility of the proposed approach. The MC8051 core [21] developed by Oregano Systems, which is compatible with the industry standard 8051 microcontroller, has been chosen as the design to be implemented on a Xilinx XC6VCX240T-FF784-2 FPGA. The model will be exercised during the experimentation by an assembly program, distributed as part of the MC8051 package, that activates most paths within the design logic.

The Xilinx XST tool provides more than 60 different parameters (flags) to configure (including paths and the style of generated files), but only 33 of them may have a potential impact onto the design implementation. Table 1 lists all these factors, tagged as X_i, including the flag required to activate this factor through the command line, and the two different values (levels) that have been selected for its configuration. Two-level designs are sufficient for evaluating many production processes [22], and most XST factors are intrinsically two-leveled ('No/Yes'), or can be modeled as being two-level by selecting minimum/maximum thresholds ('0%/100%'), or a reasonable subset of values ('Speed/Area'). It must be noted that factors X_{22} and X_{26}, in combination with some other factors, led to configurations that could not be implemented or to implementations that were not functionally equivalent to the design. Hence, these factors have been left out of this case study and *only* 31 of them are considered.

Another important part of the set-up corresponds to the method followed to estimate the impact of considered configurations on the PPAD properties exhibited by the model under study. Since the purpose is limited to the tuning of the genetic algorithm, the obtention of real estimations of properties from the model is not mandatory. As already underlined in section 3.3, these estimations will be provided by the multilinear regression model defined in [5] for the MC8051 processor. The main benefit is that it is not required to implement the model for each considered configuration and simulate it. The model will directly provide analytical estimations of dependability (mission time), performance (frequency), power consumption and area for each configuration. Even the best possible values (the global maximums and mininums) can be analytically provided by the model. These values will be used to normalize reported estimations that will be then

Table 1. Parameters of logic synthesizer under study, their designation (factors), and selected treatment levels

ID	Factor (*Flag*)	Selected low/high levels – Description
X_{01}	Optimization Goal	*Speed/Area* – reduces the levels of logic/reduces the total amount of logic
X_{02}	Optimization Effort	*Normal* – minimization and algebraic factoring algorithms *High* – additional optimizations dependent on device architecture
X_{03}	Power Reduction	*No/Yes* – consume as little power as possible
X_{04}	Keep Hierarchy	*No/Yes* – design unit is not merged with the design
X_{05}	Global Optimization Goal	*AllClockNets* – optimizes the period of the entire design *Maximum Delay* – the maximum delay for paths that start at an input and end at an output
X_{06}	Cross Clock Analysis	*No/Yes* – timing optimizations across clock domains
X_{07}	BRAM Utilization Ratio	*0%/100%* – percentage of BRAM blocks that can be used
X_{08}	DSP Utilization Ratio	*0%/100%* – percentage of DSP 48 blocks that can be used
X_{09}	Automatic FSM Extraction	*No/Yes* – enables FSM extraction and *FSM Encoding Algorithm* flag
X_{10}	FSM Encoding Algorithm	*Auto/Compact* – selects the *best* coding technique for each FSM/optimizes area
X_{11}	Safe Implementation	*No/Yes* – adds recovery states for any illegal state
X_{12}	FSM Style	*LUT/BRAM* – maps FSM to LUTs/BRAM Blocks
X_{13}	RAM Extraction	*No/Yes* – automatically infers RAM macros
X_{14}	RAM Style	*Auto/Distributed* – selects *best* implementation/uses LUTs for each RAM macro
X_{15}	ROM Extraction	*No/Yes* —automatically infers ROM macros
X_{16}	ROM Style	*Auto/Distributed* – selects *best* implementation/uses LUTs for each ROM macro
X_{17}	Automatic BRAM Packing	*No/Yes* – packs two single–port BRAMs into a dual–port BRAM
X_{18}	Shift Register Extraction	*No/Yes* – automatically infers shift register macros
X_{19}	Shift Register Minimum Size	*2/8* – infers shift registers of at least the selected size
X_{20}	Resource Sharing	*No/Yes* – shares arithmetic operators resources
X_{21}	Use DSP Blocks	*Auto* – selects the best option for each multiplier macro *Automax* – maximizes the utilization of DSP blocks, including adders, counters, accumulators
X_{22}	Asynchronous to Synchronous	*No/Yes* – replaces set/reset signals by synchronous signals
X_{23}	Max Fanout	*100/100000* – limits the fanout of nets to the selected number
X_{24}	Register Duplication	*No/Yes* – duplicates registers to help control fanout
X_{25}	Equivalent Register Removal	*No/Yes* – removes equivalent flip–flops or those with constant inputs
X_{26}	Register balancing	*No/Yes* – moves registers forward and backward through combinatorial logic to evenly distribute the path's delay between registers
X_{27}	Pack I/O Registers into IOBs	*No/Auto* – merges I/O flip–flops into IOBs according to timing specifications
X_{28}	LUT Combining	*Auto* – merges LUT pairs into single dual–output LUT6 trading off area and speed *Area* – merges as much LUTs as possible to provide the smallest implementation
X_{29}	Reduce Control Sets	*No/Auto* – reduces the number of synchronous control signals
X_{30}	Use Clock Enable	*No/Auto* – uses dedicated clock enable pins on inferred registers if they provide a benefit
X_{31}	Use Synchronous Set	*No/Auto* – uses dedicated synchronous set pins on inferred registers if they provide a benefit
X_{32}	Use Synchronous Reset	*No/Auto* – uses dedicated synchronous reset pins on inferred registers if they provide a benefit
X_{33}	Optimize Instantiated Primitives	*No/Yes* – optimizes instantiated primitives in HDL

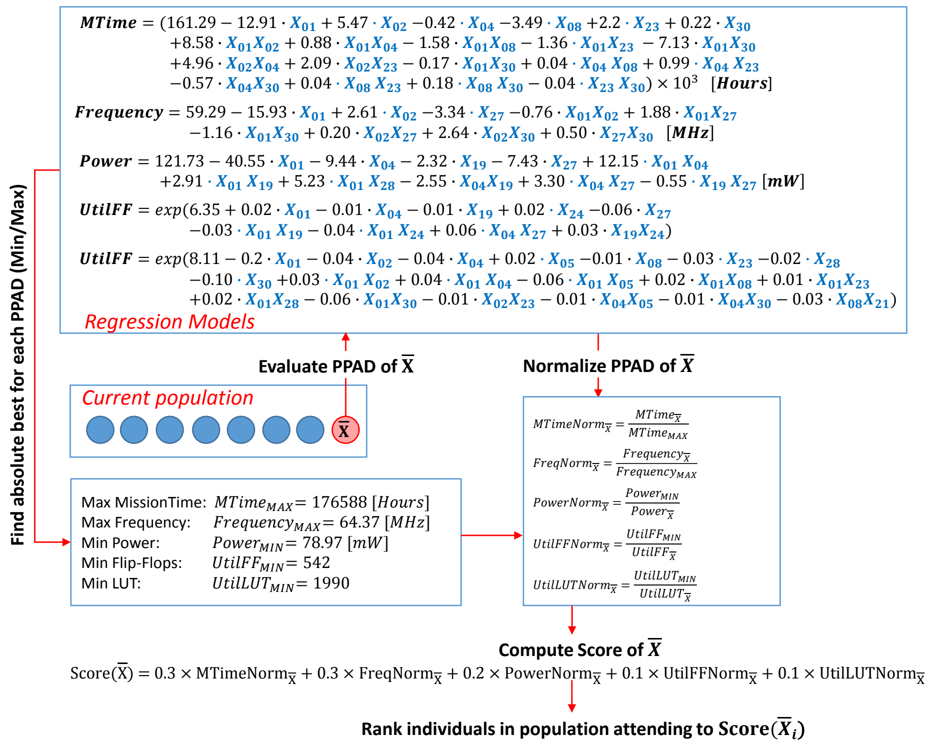

Fig. 8. Evaluation of individuals based on Regression Models

aggregated following the scoring process introduced in Section 3.3. It is worth mentioning that the weights that will be used are the ones reflecting the relative importance that normalized estimations may have for an automotive expert, as proposed in [5].

The following subsections describe the various experiments carried out in order to tune the various parameters of the genetic algorithm under study. These experiments have been carried out on an Intel Core i7-4790, running at 3.60GHz and providing 4 physical cores (8 threads) and 16 GB of RAM.

4.2 Defining the starting population

Figure 9 compares the efficiency of an initial population including the default configuration specified by the considered EDA tool with respect to an initial population randomly generated. As can be seen, in our particular case, although both populations converge to the maximum possible score of 0.918 (after aggregation of PPAD estimations), their behavior is not so different. Indeed, the full randomly generated population behaves better than the other one when a small number of iterations is considered

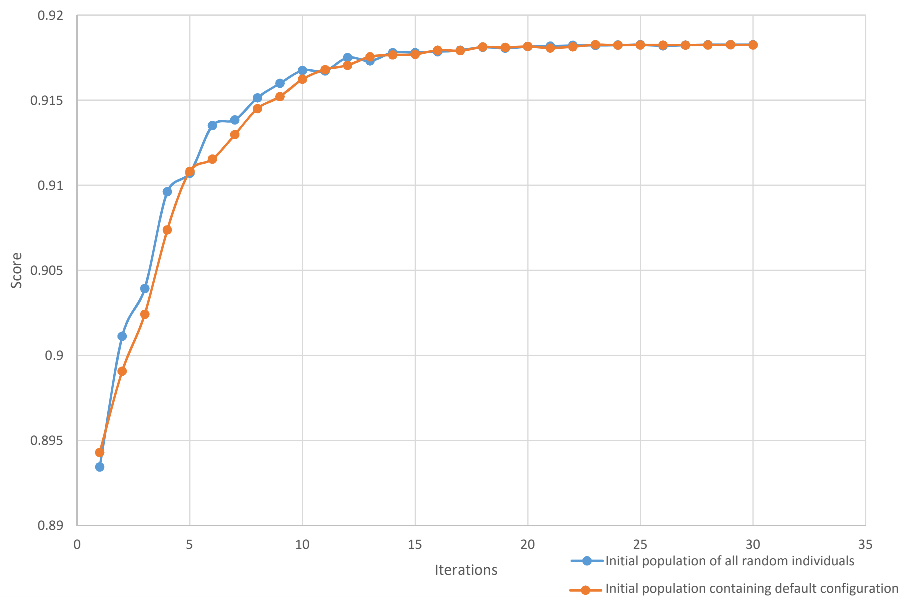

Fig. 9. Full randomly generated population vs Population including the default configuration.

This can be explained by the fact that the default configuration is basically tuned towards achieving the highest possible Frequency over all the other considered features. This justifies why the initial population is randomly generated in our case.

4.3 Establishing a population size

The population size is the other hot factor to fix when defining the initial population considered by the genetic algorithm. As can be shown in 10.a), the higher the population size, the lower the number of required iterations to reach the global maximum score. However, the number of individuals to take into consideration increases as the population size does 10.b). For instance, a total number of 90 individuals (2 individuals during 45 iterations) must be evaluated while that number grows up to around 200 individuals in the case of considering a population size of 20. As a result, one should not only focus on the number of iterations, or the number of individuals, but must find out a good compromise among them.

At the same time, one should also take into consideration the fact that the GA is running on a machine with a limited computation power that can be measured in terms of available cores, and the degree of multi-threading supported by such cores. As shown in Figures 11 and 12, since the number of available threads strongly impacts the number of individuals that can be evaluated in parallel, the

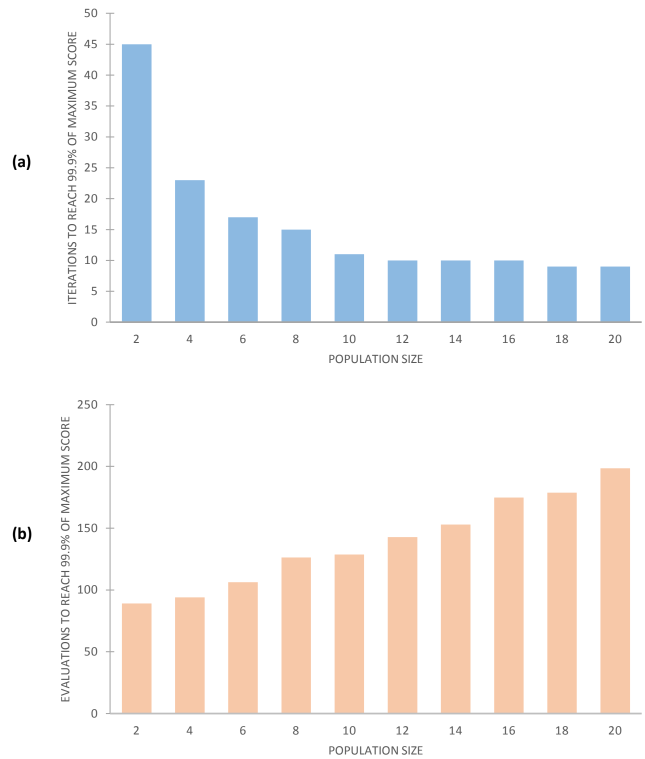

Fig. 10. Impact of population size on the number of iterations (a) and evaluations (b)

fastest convergence towards the maximum is achieved when the population size (the set of individuals considered per iteration) equals the number of available threads. This means that the number of threads will strongly condition the considered population size. In deed, in our case, the available level of parallelism of the processor used to run the experiments makes the cost of evaluating 8 individuals equivalent (from a temporal viewpoint) to the one of evaluating 2, 4 or 6 individuals.

Consequently, and taking into consideration all the previous results, the selected population size will be of 8 individuals. First, because a population size of 8 provides a good compromise between the number of individuals to evaluate and the number of iterations of the algorithm to carry out. Second, because the machine used for the experiments supports the simultaneous execution of 8 threads.

4.4 Fixing the mutation rate and crossover ratio

As previously established, the three different crossovers methods that are under consideration are the Single, Double and Uniform crossover methods. The GA

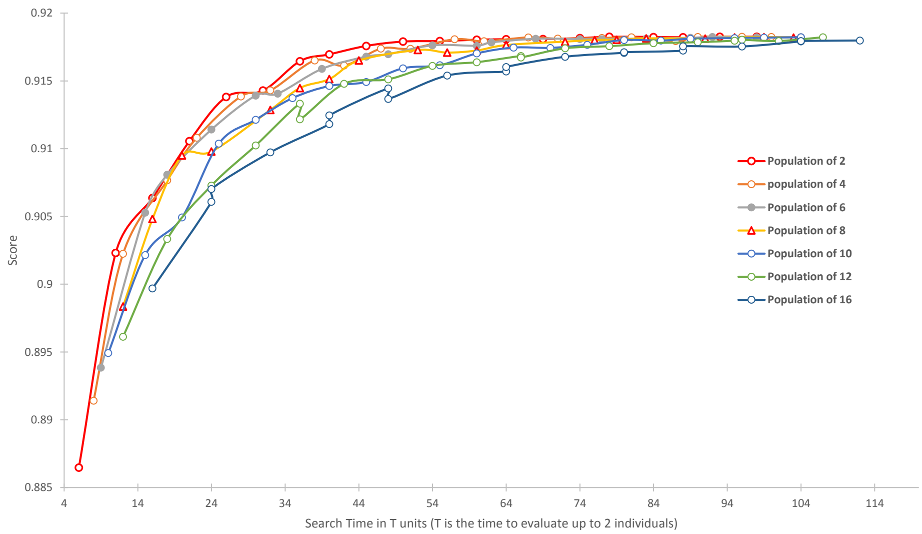

Fig. 11. Convergence speed for population sizes evaluated on a 2 thread processor

encodes the use of these methods internally using a 3-number word (b_1, b_2, b_3), where b_1 designates a value for the use of the single crossover, b_2 a value for the use of the double crossover and b_3 a value for the use of to the uniform crossover. Then, the likelihood of selection of each method is the proportion of each number over the sum of all of them. For example, an encoding of 111, means that all methods can be potentially applied with the very same probability ($\frac{1}{3}$) on a given individual, while an encoding of 231 means that the single crossover will be applied with a probability of $\frac{2}{6}$, the double crossover with a probability of $\frac{3}{6}$ and the uniform crossover with a probability of $\frac{1}{6}$. Figure 13 uses these encoding in order to show the combined impact of the selected crossover method and mutation rate. As can be seen a maximum is reached when the crossover is 001 and the mutation rate holds a value of 8.5%. It is worth mentioning that the mutation rate has been limited to bound between 3% (0.03) and 20% (0.2). As can be seen in 13, mutation rates higher than 20% decrease the score of individuals, which means that the lead to new individuals diverging from an optimal solution. This is why those values have not been taken into consideration.

4.5 Final resulting configuration for the genetic algorithm

Summing up the conclusion of all the experiments carried out, the final configuration of the proposed genetic algorithm will be the following one:

- Active population size: 8 individuals
- Crossover: only uniform
- Mutation Rate: 0.085
- Filtering identical solutions: Activated

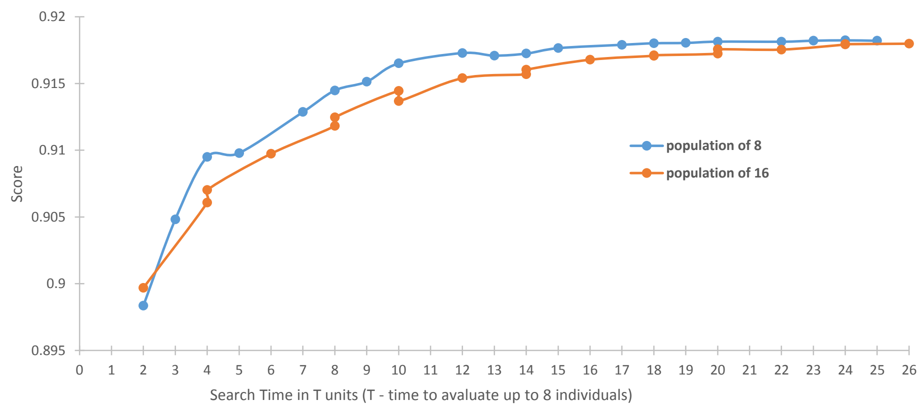

Fig. 12. Convergence speed for population sizes evaluated on a 8 thread processor

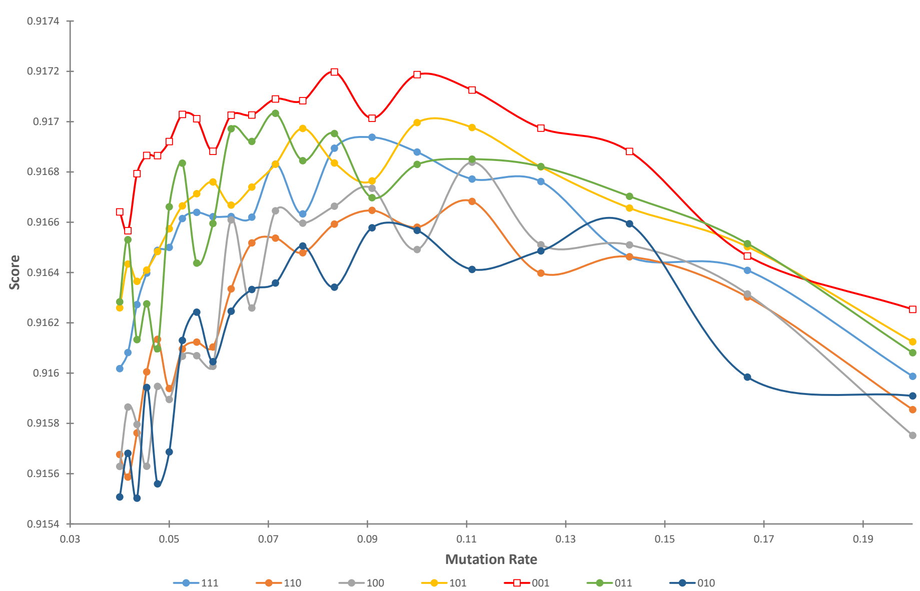

Fig. 13. Impact of Crossover Choice and Mutation Rate on score.

To estimate the efficiency of this actual parameters, the algorithm is launched, ending when the solution converges. We obtain the curve Figure 14. As can be seen, after 16 iterations (i.e. after evaluating 128 individuals) the algorithm converge towards the optimum solution.

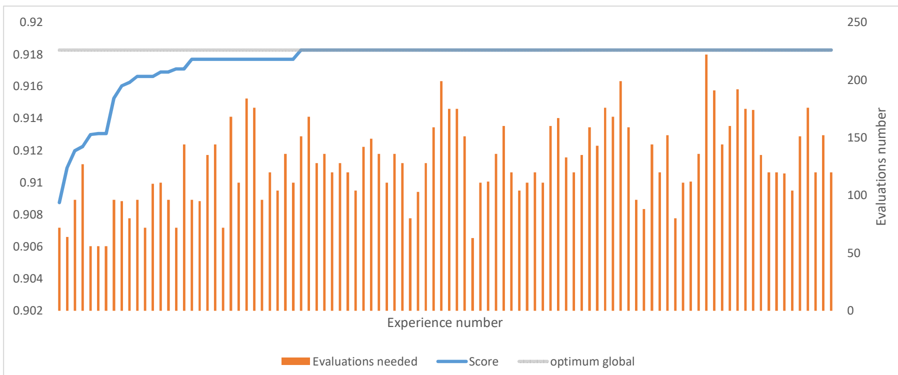

Fig. 14. 100 runs of configured Algorithm with model

5 Conclusions

This paper shows that genetic algorithms have a great potential to derive optimal configurations for EDA tools in the context of simultaneously evaluating the PPAD features of a HW design. It has been presented whole process towards the tuning of these algorithms. Result obtained are quite promising, since they show a convergence rate for the GA which is as fast as the one provided by the use of statistical methods. But, the additional benefit of the genetic algorithm is that it takes into consideration all the possible interactions among configuration parameters, which was something neglected by statistical approaches.

Next steps of this research will be focused on replacing the statistical model of the target system by the real simulation of the HW design under consideration.

Acknowledgment

This work has been partially funded by the Ministerio de Economía, Industria y Competitividad de España under grant agreement no TIN2016-81075-R, and the “Programa de Ayudas de Investigación y Desarrollo” (PAID) de la Universitat Politècnica de València.

References

1. H. Kaeslin, *Digital Integrated Circuit Design: From VLSI Architectures to CMOS Fabrication*, 1st ed. New York, NY, USA: Cambridge University Press, 2008.
2. J. Panerati, D. Sciuto, and G. Beltrame, "Optimization strategies in design space exploration," in *Handbook of Hardware/Software Codesign*, S. Ha and J. Teich, Eds. Dordrecht: Springer, 2017, ch. 6, pp. 189–217.
3. E. Aarts, J. Korst, and W. Michiels, *Simulated Annealing.* Boston, MA: Springer US, 2005, pp. 187–210.
4. G. Beltrame, L. Fossati, and D. Sciuto, "Decision-theoretic design space exploration of multiprocessor platforms," *IEEE Transactions on Computer-Aided Design of Integrated Circuits and Systems*, vol. 29, no. 7, pp. 1083–1095, 2010.
5. I. Tuzov, D. d. Andres, and J. Ruiz, "Dependability-aware design space exploration for optimal synthesis parameters tuning," in *2017 47th Annual IEEE/IFIP International Conference on Dependable Systems and Networks (DSN)*, June 2017, pp. 121–132.
6. H. Esbensen and E. S. Kuh, "Design space exploration using the genetic algorithm," in *IEEE International Symposium on Circuits and Systems (ISCAS'96).* IEEE, 1996, pp. 500–503.
7. S. K. Rethinagiri, O. Palomar, A. Cristal, O. Unsal, and M. M. Swift, "Dessert: Design space exploration tool based on power and energy at system-level," in *System-on-Chip Conference (SOCC), 2014 27th IEEE International.* IEEE, 2014, pp. 48–53.
8. T. Basten, E. Van Benthum, M. Geilen, M. Hendriks, F. Houben, G. Igna, F. Reckers, S. De Smet, L. Somers, E. Teeselink *et al.*, "Model-driven design-space exploration for embedded systems: The octopus toolset," *Leveraging Applications of Formal Methods, Verification, and Validation*, pp. 90–105, 2010.
9. C. Silvano, W. Fornaciari, G. Palermo, V. Zaccaria, F. Castro, M. Martinez, S. Bocchio, R. Zafalon, P. Avasare, G. Vanmeerbeeck, C. Ykman-Couvreur, M. Wouters, C. Kavka, L. Onesti, A. Turco, U. Bondi, G. Mariani, H. Posadas, E. Villar, C. Wu, F. Dongrui, Z. Hao, and T. Shibin, "Multicube: Multi-objective design space exploration of multi-core architectures," in *VLSI 2010 Annual Symposium*, N. Voros, A. Mukherjee, N. Sklavos, K. Masselos, and M. Huebner, Eds. Dordrecht: Springer Netherlands, 2011, pp. 47–63.
10. P. Bose, "Ensuring dependable processor performance: an experience report on pre-silicon performance validation," in *International Conference on Dependable Systems and Networks*, 2001, pp. 481–486.
11. S. Scharoba and H. T. Vierhaus, "An interactive design space exploration tool for dependable integrated circuits," in *Digital System Design (DSD), 2016 Euromicro Conference on.* IEEE, 2016, pp. 714–717.
12. I. Tuzov, D. de Andrés, and J.-C. Ruiz, "DAVOS: EDA toolkit for dependability assessment, verification, optimization and selection of hardware models," in *IEEE/IFIP Annual International Conference on Dependable System and Networks*, 2018, pp. 1–8.
13. I. Tuzov, J.-C. Ruiz, and D. de Andrés, "Accurately simulating the effects of faults in vhdl models described at the implementation-level," in *2017 13th European Dependable Computing Conference (EDCC).* IEEE, 2017, pp. 10–17.
14. I. Tuzov, J.-C. Ruiz, D. De Andrés, and P. Gil, "Speeding-up simulation-based fault injection of complex hdl models," in *Dependable Computing (LADC), 2016 Seventh Latin-American Symposium on.* IEEE, 2016, pp. 51–60.

15. C. Wu and M. Hamada, *Experiments: Planning, Analysis, and Optimization*, ser. Wiley Series in Probability and Statistics. Wiley, 2011.
16. X.-S. Yang, *Nature-inspired metaheuristic algorithms.* Luniver press, 2010.
17. S. Mashohor, J. Evans, and T. Arslan, “Elitist selection schemes for genetic algorithm based printed circuit board inspection system,” vol. 2, 10 2005, pp. 974 – 978 Vol. 2.
18. Y. Liang and K.-S. Leung, “Genetic algorithm with adaptive elitist-population strategies for multimodal function optimization,” *Applied Soft Computing*, vol. 11, no. 2, pp. 2017 – 2034, 2011, the Impact of Soft Computing for the Progress of Artificial Intelligence. [Online]. Available: http://www.sciencedirect.com/science/article/pii/S1568494610001535
19. M. Srinivas and L. M. Patnaik, “Adaptive probabilities of crossover and mutation in genetic algorithms,” *IEEE Transactions on Systems, Man, and Cybernetics*, vol. 24, no. 4, pp. 656–667, Apr 1994.
20. Xilinx Inc., “XST User Guide for Virtex-6, Spartan-6, and 7 Series Devices (v 14.5),” 2013. [Online]. Available: http://www.xilinx.com/support/documentation/sw_manuals/xilinx14_7/xst_v6s6.pdf
21. Oregano Systems GmbH, “MC8051 IP Core, Synthesizeable VHDL Microcontroller IP-Core, User Guide (V 1.2), 2013,” 2013. [Online]. Available: http://www.oreganosystems.at/download/mc8051_ug.pdf
22. D. C. Montgomery, *Design and Analysis of Experiments.* New York: John Wiley & Sons, 2000.

Energy Modeling and Analysis for IoT Sensor Devices: A DTMC-Based Approach

Canek Portillo, Jorge Martinez-Bauset, Vicent Pla and Vicente Casares-Giner

ITACA Research Insitute
Universitat Politècnica de València, Spain

Abstract. With the development of Internet of Things (IoT), opportunities for WSN have emerged through new and improved applications. In this work an analysis of the energy consumption of a WSN with a DC MAC is performed. To accomplish that, an analytical model with a two-dimensional Discrete-Time Markov Chain (2D-DTMC) is developed, and the energy consumption and energy efficiency are obtained. The analytical model exhibits excellent accuracy when compared with simulation results.

Keywords: Energy analysis, discrete-time Markov chain (DTMC) model, IoT, WSN.

1 Introduction

A feature of Internet of Things (IoT) is the application of sensors and actuator devices, which are used to monitor multiple environments [1]. In building automation, energy management, industrial or health applications, sensors collect data and transmit it to a central collector or sink. The data is further processed, analysed and used for a specific purpose. In each one of these applications, sensor devices can be considered as part of a Wireless Sensor Network (WSN) [2]. The technological evolution of sensors facilitate the integration of WSN with IoT. There are several platforms for WSN that allow smart system applications for IoT [3–7]. The study of the energy consumption in WSN is of great importance due to the energy supply limitations of the sensor nodes, which commonly are battery-supplied. We can find several energy performance studies for WSN applied to IoT. For instance, a comprehensive study of energy for WSN-based IoT applications is presented in [8, 9]. Also in [10], a study of energy consumption for IoT is developed based on WSN. However, all these studies are based on simulations, or focusing in the routing protocol and without considering the Medium Access Control (MAC) protocol properly. In [11], an energy analysis is carried out through experiments, considering an specific application scenario, but no analytical model is contemplated in the evaluation. We can find analytical models for the energy analysis of the WSN nodes, but these have been developed from a routing perspective [12] or if the MAC is considered, the models are not based on a Discrete Time Markov Chain (DTMC) [13, 14]. In [15],

C.Fernandez-Llatas and M.Guillen (Ed.):
Workshop on Innovation on
Information and Communication Technologies
(ITACA-WIICT 2018)

ISBN 978-84-09-07373-3

a stochastic analysis of energy consumption is performed, even a Markov chain is constructed, but using a generic MAC protocol and without specifying the different energy consumptions in their lifetime analysis. Examples of modeling and performance analysis applied to WSN, where the energy consumption is analised, can be found [16–19]. In those papers, the authors have modeled the MAC protocol using DTMC, but the entire transmission process is not taken into account for the calculation of energy consumption [17, 19]. In addition, these models are less systematic and less precise, as they do not consider the stationary probability distribution from the beginning, in their calculations of energy consumption [16–19]. In a previous work [19], we have evaluated the performance of a WSN that uses a duty-cycled (DC) MAC protocol, but it is a general study without focusing on energy consumption. In the present work, we include a detailed performance analysis focused on the energy consumption. The main contribution of this work is the analytical modeling and performance evaluation of the energy consumption for a DC MAC WSN. The model is based on a two-dimensional Discrete-Time Markov Chain (2D-DTMC). The calculation of energy consumption is exhaustive but more systematic and precise than those found in the literature. The different contributions to the energy consumed by a node in its transmission process are also well differentiated.

The remainder of the article is organized as follows. In section 2 the transmission model is presented, and the general scenario is described. The mathematical modeling of the system is presented in section 3. The analysis to obtain the energy performance is developed in section 4. The results and their discussion are set out in section 5. Finally, the conclusions are presented in section 6.

2 Transmission model

2.1 Duty-cycled MAC protocol

Our study is based on S-MAC, that is the first MAC protocol for WSN to implement the synchronous DC technique [20]. In S-MAC the time is divided into cycles of equal duration T, and each cycle consists of *active* and *sleep* periods. The *active* period is subdivided into two parts: the *sync* period of fixed-duration T_{sync}, where *SYNC* packets are exchanged, and the *data* period, where the *DATA* packets are exchanged. During a *sync* period, nodes choose a *sleep-awake* schedule and exchange it with its neighbours through *SYNC* packets. These packets include the address of the node that sends the packet and the start time of its next *active* period. With this information, the nodes coordinate to wake up together at the beginning of each *sync* period. *SYNC* packets are transmitted using a Carrier Sense Multiple Access with Collision Avoidance (CSMA/CA) mechanism for contention-based access to the channel. CSMA/CA is based on the generation of a random backoff time and a carrier sensing procedure. If the channel is unoccupied when the backoff timer expires, then the node transmits the *SYNC* packet. Nodes also use CSMA/CA to transmit *DATA* packets during the *data* period. They generate new backoff times at each *data* period initiation and perform carrier sense. If the channel is idle when the backoff timer expires, then nodes can transmit one *DATA* packet using the *RTS/CTS/DATA/ACK* handshake. When a winning node receives a *CTS* in response to its previous *RTS*, it transmits one *DATA* packet, and waits for the *ACK*. In S-MAC, a node goes to *sleep* until the beginning of the next *sync* period when: i) it loses the contention (hears a busy medium before its backoff expires); ii) it encounters an *RTS* collision; iii) after a successful transmission (only one packet per cycle is sent) [20].

2.2 Scenario and assumptions

We consider a WSN network with N nodes that send the packets to a *sink* node, where all nodes are reached in one hop. The scenario consists of a single cell cluster, but multiple clusters together can form a larger network. For convenience, one node is selected as reference node, *RN*. It is assumed that the *sink* node behaves like a packet absorption node, it only receives packets (never transmits *DATA* packets). A node has a buffer that can store at most Q packets, and it serves them according a FIFO discipline. The transmission of a packet by the *RN* happens when it wins the contention for medium access.

We also assume that: i) nodes are configured with infinite retransmissions, ii) all nodes contain the same initial energy; iii) the channel is error-free; iv) packets arrive to the buffer of a node following a renewal process, and the number of packets that arrive per cycle is characterized by independent and identically distributed random variables. We assume that the number of packets that arrive to a buffer follow a discrete Poisson distribution of mean λT, where λ is the packet arrival rate and T is the cycle duration. However, other distributions can be deployed.

In Fig. 1, a diagram of the transmission process is shown, where the *sync*, *data* and *sleep* periods are depicted.

3 System model

3.1 Access to the medium

The *RN* is an arbitrarily chosen node. A node is considered active when it has at least one packet in the queue. Active nodes generate a random back-off time selected from $[0, W-1]$. When the *RN* is active, it transmits a packet successfully if the other contending nodes select back-off times larger than the

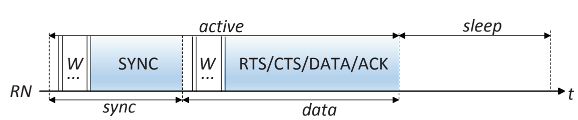

Fig. 1. Transmission process.

one chosen by the *RN*. The packet transmitted by the *RN* will fail (collide) when the *RN* and one or more of the other contending nodes choose the same backoff time, and this backoff time is the smallest among all contending nodes. If the backoff time generated by the *RN* is not the smallest among those generated by the other contending nodes, two outcomes are possible: either another node is able to transmit successfully, or other nodes collide when transmitting. Nodes that loose the contention (because they hear a busy medium before their backoff time expires) or encounter an *RTS* collision, go to *sleep* until the *sync* period of the next cycle.

N is the number of nodes. Consider a cycle where the *RN* is active and denote by $k, 0 \leq k \leq N-1$, the number of nodes that are also active in the same cycle in addition to the *RN*. Let $P_{s,k} = \sum_{i=0}^{W-1} \frac{1}{W}\left(\frac{W-1-i}{W}\right)^k, P_{sf,k} = \sum_{i=0}^{W-1} \frac{1}{W}\left(\frac{W-i}{W}\right)^k$, and $P_{f,k} = P_{sf,k} - P_{s,k} = \frac{1}{W}$, be the probabilities that the *RN* transmits a packet successfully, transmits a packet (successfully or with collision), and it transmits with failure (collision), respectively, when it contends with other k nodes. $P_{s,k}$ is the probability that the *RN* chooses a backoff value from $[0, W-1]$ and the other k nodes choose a larger value. $P_{sf,k}$ and $P_{f,k}$ can be described in similar terms. Conditioned on a successful or unsuccessful packet transmission by the *RN* when contending with other k nodes, the average backoff times are $BT_{s,k} = \frac{1}{P_{s,k}} \sum_{i=0}^{W-1} i \cdot \frac{1}{W}\left(\frac{W-1-i}{W}\right)^k, or BT_{f,k} = \sum_{i=0}^{W-1} i \cdot \left[\left(\frac{W-i}{W}\right)^k - \left(\frac{W-1-i}{W}\right)^k\right]$.

3.2 The 2D-DTMC

Here we model the evolution of the number of packets in the queue of the *RN*, and the number of active nodes in the cluster over the time, by a 2D-DTMC. The system state is represented by (i, m), where $i \leq Q$ is the number of packets in queue of *RN*, and m, is the number of active nodes other than the *RN*, in the network, $m < N$. Then, $P_{(i,m),(j,n)}$ is the transition probability from state (i, m) to state (j, n).

The 2D-DTMC describes the evolution with time of the state of the nodes. Some useful expressions and the state transition probabilities of the 2D-DTMC, are given in detail in [21, Table 1].

3.3 Solution of the 2D-DTMC

The solution of the 2D-DTMC can be obtained by solving the set of linear equations,

$$\boldsymbol{\pi}\boldsymbol{P} = \boldsymbol{\pi}, \quad \boldsymbol{\pi}\boldsymbol{e} = 1\,, \tag{1}$$

where $\boldsymbol{\pi} = [\pi(i, n)]$ is the stationary distribution, $\boldsymbol{P}$ is the transition probability matrix, whose elements are defined in [21], and $\boldsymbol{e}$ is a column vector of ones.

The average probability, P_s, that the *RN* transmits a packet successfully, conditioned on the *RN* being active, is given by,

$$P_s = \frac{1}{G} \sum_{i=1}^{Q} \sum_{k=0}^{K} \pi(i, k) \cdot P_{s,k}\,, \tag{2}$$

and $G = \sum_{i=1}^{Q} \sum_{k=0}^{K} \pi(i,k)$. By solving the set of equations (1), $\boldsymbol{\pi}(P_s)$ can be determined for a given P_s. Then, a new P_s can be obtained from (2) for a given $\boldsymbol{\pi}$. Denote by $\boldsymbol{\pi}$ the solution of this fixed-point equation, i.e., the stationary distribution at the fixed-point.

4 Energy consumption

The entire transmission process occurs during a cycle that consists of an *active* period and a *sleep* period. The *active* period is subdivided into the *sync* and *data* periods. In this section we derive expressions to determine the average energy consumed by the *RN* per cycle, considering the different periods and contributions.

4.1 Average energy consumption in the *sync* period

During the *sync* period, nodes consume energy due to the transmission of $SYNC$ packets, and also due to the reception of those packets The following expression allows us to determine the energy consumed by the *RN*, in the *sync* period, E_{sc},

$$T_{sync} = (W-1) + t_{SYNC} + D_p \, , \tag{3}$$

$$E_{sc} = \frac{1}{N_{sc}} \cdot [(t_{SYNC} \cdot P_{tx} + (T_{sync} - t_{SYNC}) \cdot P_{rx})] + \frac{N_{sc}-1}{N_{sc}} \cdot (T_{sync} \cdot P_{rx}) \ , \tag{4}$$

where T_{sync} is the duration of the *sync* period, W is the size of the contention window, t_{sync} is the duration of the transmission of a $SYNC$ packet, and D_p is the one-way propagation delay. Also, P_{rx} and P_{tx} are the reception and transmission power levels, respectively. The N_{sc} parameter indicates the periodicity in cycles of the transmission of the $SYNC$ packets. We assume that the *RN* transmits one $SYNC$ packet every N_{sc} cycles, and might receive one packet per cycle in the remaining cycles $(N_{sc}-1)$.

4.2 Average energy consumption in the *data* period

In this section we calculate the energy consumed by the *RN* in the *data* period. It should be noted that only the energy consumed by the radio frequency transceiver is studied. The energy consumed by the sensor nodes due to events related to specific sensing or monitoring tasks depends on the application and is not included here.

Let E_s^{tx} and E_f^{tx} be the energy consumption terms when the *RN* transmits successfully, and it transmits with failure (collision), respectively. Then, the average energy consumed by the *RN* during the *data* period of a cycle, is given by,

$$E_d = E_{tx,s}^d + E_{tx,f}^d \tag{5}$$

$E^{d}_{tx,s}$ is obtained by,

$$
\begin{aligned}
E^{d}_{tx,s} &= \sum_{i=1}^{Q}\sum_{k=0}^{K}\pi(i,k)P_{s,k}(E^{d}_{\mathit{1}} + BT_{s,k}P_{rx}) \\
E^{d}_{\mathit{1}} &= (t_{RTS} + t_{DATA})P_{tx} + [t_{CTS} + t_{ACK} + 4D_p]P_{rx},
\end{aligned}
\tag{6}
$$

where, $t_{RTS}, t_{DATA}, t_{CTS}$ and t_{ACK}, are the corresponding packet transmission times. $E^{d}_{tx,f}$ is given by,

$$
\begin{aligned}
E^{d}_{tx,f} &= \sum_{i=1}^{Q}\sum_{k=0}^{K}\pi(i,k)P_{f,k}(E^{d}_{\mathit{2}} + BT_{f,k}P_{rx}) \\
E^{d}_{\mathit{2}} &= t_{RTS}P_{tx} + 2D_pP_{rx},
\end{aligned}
\tag{7}
$$

4.3 Average energy consumption during *wake* cycles

In order to *listen* to *SYNC* packets from neighbour nodes, the *RN* remains *awake* in certain cycles after a successful o failed transmission. We refer to these cycles as *awake* cycles.

Let $E^{aw}_{tx,s}$, $E^{aw}_{tx,f}$ and E^{aw}_{oh} be the energy consumption terms when the *RN* transmits successfully, it transmits with failure (collision), and it *overhears* transmissions, respectively, during the *awake* cycles. Then, the average energy consumed by the *RN* during an *awake* cycle, is given by,

$$
E_{aw} = E^{aw}_{tx,s} + E^{aw}_{tx,f} + E^{aw}_{oh}\,, \tag{8}
$$

$E^{aw}_{tx,s}$ is given by,

$$
\begin{aligned}
E^{aw}_{tx,s} &= \sum_{i=1}^{Q}\sum_{k=0}^{K}\pi\left(i,k\right)P_{s,k}\left[E^{aw}_{\mathit{1}} + BT_{s,k}P_{rx}\right]\,, \\
E^{aw}_{\mathit{1}} &= \left[T - T_{sync} - \left(t_{RTS} + t_{CTS} + t_{DATA} + t_{ACK} + 4D_p\right)\right]P_{rx}\,,
\end{aligned}
\tag{9}
$$

where T is the cycle duration. $E^{aw}_{tx,f}$ is obtained by,

$$
\begin{aligned}
E^{aw}_{tx,f} &= \sum_{i=1}^{Q}\sum_{k=1}^{K}\pi\left(i,k\right)P_{f,k}\left[E^{aw}_{\mathit{2}} - BT_{f,k}P_{rx}\right]\,, \\
E^{aw}_{\mathit{2}} &= \left[T - T_{sync} - \left(t_{RTS} + 2D_p\right)\right]P_{rx}\,,
\end{aligned}
\tag{10}
$$

E_{aw}^{oh} is given by,

$$
\begin{aligned}
E_{aw}^{oh} = & \sum_{i=1}^{Q} \sum_{k=1}^{K} \pi\left(i,k\right) kP_{s,k} \left[E_{\mathit{1}}^{aw} + E_{\mathit{3}}^{aw}\right] \\
& + \sum_{k=1}^{K} \pi\left(0,k\right) kP_{s,k\text{-}\mathit{1}} \left[E_{\mathit{1}}^{aw} + E_{\mathit{3}}^{aw}\right] \\
& + \sum_{i=1}^{Q} \sum_{k=2}^{K} \pi\left(i,k\right) \widehat{P}_{f,k} \left(T - T_{sync}\right) P_{rx} \\
& + \sum_{k=2}^{K} \pi\left(0,k\right) \widehat{P}'_{f,k} \left(T - T_{sync}\right) P_{rx} + \pi\left(0,0\right) \left(T - T_{sync}\right) P_{rx} \,,
\end{aligned}
\tag{11}
$$

$$
\begin{aligned}
E_{\mathit{3}}^{aw} &= \left[t_{RTS} + D_p\right] P_{rx} + \left[t_{CTS} + t_{DATA} + t_{ACK} + 3D_p\right] P_{sl} \,, \\
\widehat{P}_{f,k} &= \sum_{i=1}^{W} \left[\sum_{n=2}^{k} \binom{k}{n} \left(\frac{1}{W}\right)^{n} \left(\frac{W-i}{W}\right)^{k-n+1} \right], \\
\widehat{P}'_{f,k} &= \sum_{i=1}^{W} \left[\sum_{n=2}^{k} \binom{k}{n} \left(\frac{1}{W}\right)^{n} \left(\frac{W-i}{W}\right)^{k-n} \right],
\end{aligned}
\tag{12}
$$

where, $\widehat{P}_{f,k}$ and $\widehat{P}'_{f,k}$, define the probabilities that one of k nodes different from the *RN*, wins the access to the channel but it transmits with collision, when the *RN* is active or inactive, respectively. P_{sl} is the *sleep* power level.

Depending on the *RN* being active or inactive during *overhearing*, different events may occur: i) one of the other k nodes transmits successfully (with probability $kP_{s,k}$ or $kP_{s,k\text{-}\mathit{1}}$); and ii) two or more of the other k nodes collide (with probability $\widehat{P}_{f,k}$ or $\widehat{P}'_{f,k}$). We assume that when *RN* is idle ($i = 0$), it listens to *RTS*, as it contains the duration of the transmission, it goes to *sleep* during the transmission, and it wakes up at the end of the transmission, and remains *awake* for the rest of the cycle.

4.4 Average energy consumption during *normal* cycles

Normally, after a successful or failed transmission, nodes go to *sleep* to save energy. We refer to these cycles as *normal* cycles. The following expressions are used to determine the power consumption of the *RN* during *normal* cycles.

Let $E_{tx,s}^{nr}$, $E_{tx,f}^{nr}$ and E_{oh}^{nr} be the energy consumption terms when the *RN* transmits successfully, it transmits with failure (collision), and it *overhears* transmissions, respectively, during a *normal* cycle. Then, the average energy consumed by the *RN* during a *normal* cycle, is given by,

$$
E_{nr} = E_{tx,s}^{nr} + E_{tx,f}^{nr} + E_{oh}^{nr} \,, \tag{13}
$$

$E^{nr}_{tx,s}$ is determined by,

$$E^{nr}_{tx,s} = \sum_{i=1}^{Q}\sum_{k=0}^{K} \pi(i,k)\, P_{s,k} \left[E^{nr}_{1} - BT_{s,k}P_{sl}\right] ,$$
$$E^{nr}_{1} = \left[T - T_{sync} - (t_{RTS} + t_{CTS} + t_{DATA} + t_{ACK} + 4D_p)\right] P_{sl} , \tag{14}$$

$E^{nr}_{tx,f}$ is given by,

$$E^{nr}_{tx,f} = \sum_{i=1}^{Q}\sum_{k=1}^{K} \pi(i,k)\, P_{f,k} \left[E^{nr}_{2} - BT_{f,k}P_{sl}\right] ,$$
$$E^{nr}_{2} = \left[T - T_{sync} - (t_{RTS} + 2D_p)\right] P_{sl} , \tag{15}$$

E^{nr}_{oh} is obtained by,

$$\begin{aligned} E^{nr}_{oh} &= \sum_{i=1}^{Q}\sum_{k=1}^{K} \pi(i,k)\, kP_{s,k} \left[(BT_{s,k} + D_p)\, P_{rx} + (E^{nr}_{3} - BT_{s,k}P_{sl})\right] \\ &+ \sum_{i=1}^{Q}\sum_{k=2}^{K} \pi(i,k)\, \widehat{P}_{f,k} \left[(BT_{f,k} + Dp)\, P_{rx} + (E^{nr}_{3} - BT_{f,k}P_{sl})\right] \\ &+ \sum_{k=0}^{K} \pi(0,k)\, (T - T_{sync})\, P_{sl} , \\ E^{nr}_{3} &= \left[T - T_{sync} - D_p\right] P_{sl} , \end{aligned} \tag{16}$$

RN sleeps when it is inactive, $i = 0$. Note that in E_{nr} we only consider the energy consumed in addition to $E^{d}_{tx,s}$ and $E^{d}_{tx,f}$, in *normal* cycles.

4.5 Total average energy consumption

To compute the total average energy, we consider that during the *sleep* period, there is a fraction of cycles where the node goes to *sleep* normally. On the other hand, there is also a fraction of cycles, where the nodes does not go to *sleep*, but stay *awake* in order to be able of *listening* a possible *SYNC* packet transmitted by other nodes in the network.

The total average energy is given by,

$$E = E_{sc} + E_d + E_{sl} . \tag{17}$$

where E_{sl} is the average energy consumed in the *sleep* period, and is determined by,

$$E_{sl} = E_{nr}\frac{(N_{aw} - 1)}{N_{aw}} + E_{aw}\frac{1}{N_{aw}} \tag{18}$$

where N_{aw} is the periodicity in cycles where there is an *awake* in the *sleep* period.

4.6 Energy efficiency

Dimensionless energy efficiency Let EE be the energy efficiency of the RN, defined as the ratio between the average energy consumption when the RN transmits successfully and the total average energy consumed by the RN during a cycle. The energy consumption, when the RN node transmits successfully, considers all the transmission process during the *data* and *sleep* periods. On the other hand, the total average energy considers also the failing transmission due to collisions, and *overhearing*. Note that the energy consumed due to signalling is omitted in the calculation.

$$EE = \left(E_{tx,s}^{d} + E_{tx,s}^{nr}\right) / \left(E_d + E_{nr}\right). \tag{19}$$

Energy efficiency (Kbytes / mJ) Let ξ be the energy efficiency of the RN, defined as the ratio between the average number of bytes successfully transmitted per cycle and the total average energy consumed in that cycle.

$$\xi = \eta \cdot S/E. \tag{20}$$

where S is the size of $DATA$ packets, and η is the node throughput, defined as the average number of packets successfully delivered by a node in a cycle, and is determined by,

$$\eta = \sum_{i=1}^{Q} \sum_{k=0}^{K} \pi(i,k) \cdot P_{s,k}. \tag{21}$$

5 Numerical results

5.1 Scenarios and parameter configuration

The analytical results are obtained from the developed 2D-DTMC model. The simulation results are obtained by means of a custom-based discrete event simulator developed in C language, where the transmission scheme is implemented. The developed simulator mimics the physical behaviour of the system. That is, at each cycle a node receives packets according to a given discrete distribution, it contends for access to the channel with other nodes if it has packets in the buffer, and if it wins, then it transmits a packet. The simulation results are completely independent of those obtained by the analytical model. That is, the calculation of the performance metrics in the simulations does not depend on the developed mathematical expressions. The WSN is configured considering the following parameters: number of sensor nodes $N = 15$, $DATA$ packet size $S = 50$ bytes, queue capacity of a node $Q = 10$ packets, packet arrival rate is $\lambda = 1.5$ packets/s, $N_{sc} = 20$, $N_{aw} = 80$, the transmission, reception and *sleep* power levels are: $P_{tx} = 52$ mW, $P_{rx} = 59$ mW and $P_{sl} = 3$ μW [22], respectively. The time parameters are summarized in Table 1. The contention window (W) is set to 128.

Table 1. Temporary parameters (milliseconds)

Duration of cycle (T)	60	Propagation delay (D_p)	0.0001
t_{RTS}, t_{CTS} and t_{ACK}	0.18	t_{SYNC}	0.18
t_{DATA}	1.716	Time slot (backoff)	0.1

In the following subsections the results of the performance parameters obtained from the analytical model and by simulation are shown. The simulation results are represented only with markers, while analytical results are represented by lines.

5.2 Average energy consumption

In Fig. 2, the total average energy consumption as a function of the arrival rate λ is shown. The energy consumed increases approximately linearly with the load, until close to $\lambda = 1.5$, then it remains constant for larger loads. The increase in λ causes a relatively rapid saturation that allows stabilization in energy consumption. A relatively large amount of energy consumed is due to *overhearing*, especially when the curve stabilizes. Recall that E is the sum of all the energy contributions considered, both in the *active* period and in the *sleep* period.

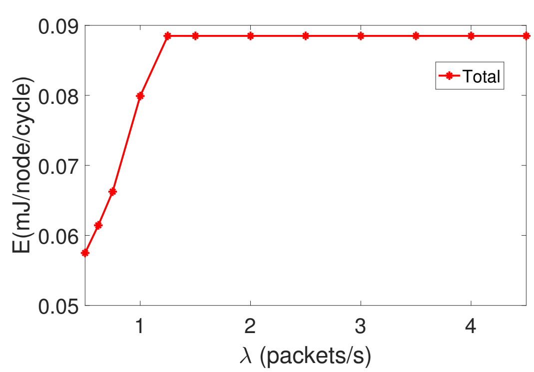

Fig. 2. Total average energy consumption. $N = 15$.

In Fig. 3, the different contributions to the total average energy consumption are shown. These include the energy consumed during the *sync* period, the *data* period, and due to *awake* cycles during the *sleep* period. The behaviour of the energy consumptions due to *sync* period and due to *awake* cycles are constant, and correspond to the energy consumed to perform signalling tasks.

From Fig. 3, note that the *data* energy consumption includes the energy consumed due to successful and failed (collision) *DATA* packet transmissions, the energy consumed due to *overhearing* because other node different from *RN* has won the contention (successfully or with collision), and the consumption in *normal* cycles during the *sleep* period, when nodes goes to *sleep*, once its activity during that cycle has finished. We can further disaggregate the consumed energy, and separate the *data* energy consumption into *data-tx* and *normal* (see Fig. 4).

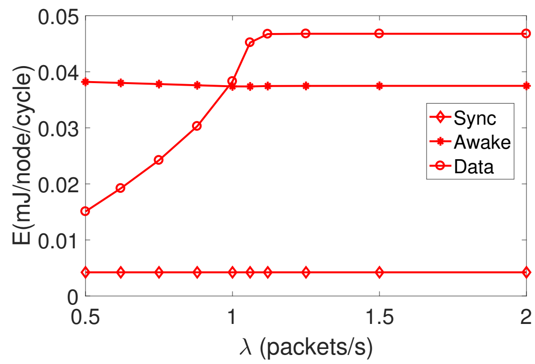

Fig. 3. Different contributions to the energy consumed by the *RN* as the data arrival rate varies, when $N = 15$.

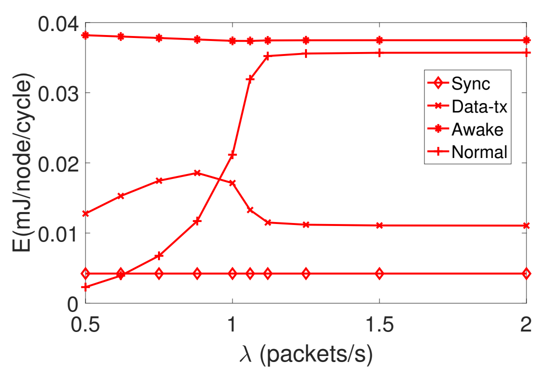

Fig. 4. Different contributions to the energy consumed by the *RN* as the data arrival rate varies, when $N = 15$. Disaggregation of data in *data-tx* and *normal*

In Fig. 4, *data-tx* represents the energy consumed during the *DATA* packet transmission, including the contention procedure and the collisions, while *normal* represents the energy consumed during the *sleep* period, and the *overhearing*. The figure shows that for low loads, the energy consumed due to the *data-tx*, reach the highest values. On the other hand, the energy consumed due to the *awake* and *normal* cycles are significantly higher in comparison with the energy consumed in *data-tx*. We must remember that the energy consumed in the *awake* and *normal* cycles, also includes the energy due to collisions and *overhearing*.

In Fig. 5, the total average energy consumption is shown as a function of the number of nodes in the network. In this case, the energy consumed increases with N until $N = 11$, then the curve decays, as more nodes are added to the network. The first part, when the curve raises, the contention for the medium access is low, therefore a significant fraction of the consumed energy is due the *DATA* packet transmissions. On the other hand, a smaller fraction of the consumed energy is due to collisions and *overhearing*. Note that the last ones mentioned consumptions are consequence of the operation of the medium access mechanism. In the second part, when the curve decays, the contention continues increasing as more nodes are added to the network. The decrease in energy consumption is explained as the channel is getting more occupied with N, and becoming busy in all cycles. Therefore, nodes have very low opportunities to transmit its packets, consuming energy in *listening* to collisions and going to *sleep*. The curve of the figure can be better understood, if the energy consumed is disaggregated.

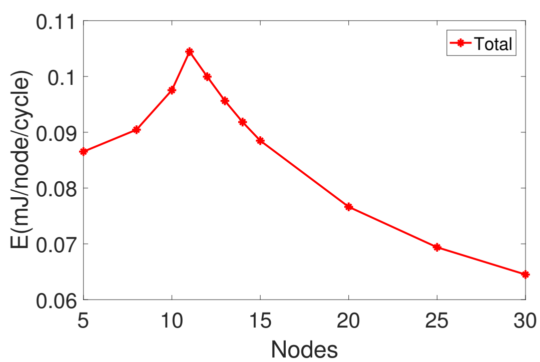

Fig. 5. Total average energy consumed by the RN as the number of nodes varies, when $\lambda = 1.5$.

In Fig. 6, the different contributions to the total average energy consumption are shown in function of the number of nodes. This figure can be explained in the same terms that we have used to explain the different energy contributions in Fig. 3.

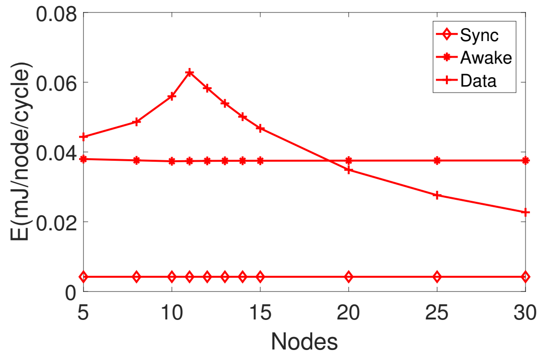

Fig. 6. Different contributions to the energy consumed by the RN as the number of nodes varies, when $\lambda = 1.5$.

In Fig. 7, a further disaggregation of the *data* energy is shown. The *data* energy is separated in its components: *data-tx* and *normal* energies. From the figure, we can confirm that the first part, when the curve raises, the consumed energy is mostly due to *data-tx* (transmission of *DATA* packets). However, in the second part, when the curve decays, *normal* is the dominant energy component.

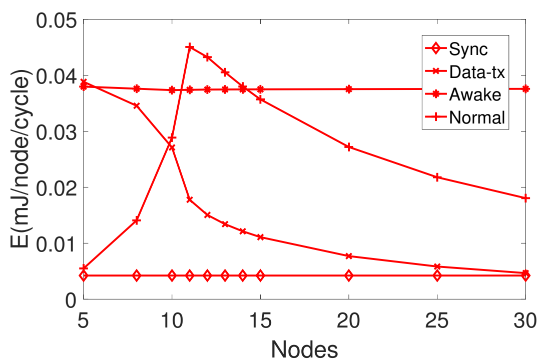

Fig. 7. Different contributions to the energy consumed by the RN as the number of nodes varies, when $\lambda = 1.5$. Disaggregation of data in *data-tx* and *normal*

From Fig. 5 and Fig. 7, note that the total average energy consumption achieved, when $N = 5$ and $N = 15$ are very close. Although the total average energy is similar, the proportion of its energy consumption components is not. For $N = 15$, the dominant energy consumed component is due to the *overhearing* and collisions ($normal$). However, in the less congested case ($N = 5$), the fraction of energy consumed in $DATA$ transmission ($data\text{-}tx$) is relatively higher.

5.3 Energy Efficiency

In Fig. 8, the dimensionless energy efficiency (EE) as a function of λ is shown, considering the variation of the contention window size $W = \{16, 64, 128, 256\}$. In general, the EE reach relative high values for low traffic. This means that, for this low traffic interval, most part of the energy consumed by the nodes is used for transmitting packets successfully. However, then the EE decreases with λ, obtaining relatively low values. When the load increases, the congestion of the network also increases, therefore the probability that a node transmits a $DATA$ packet successfully decreases significantly with λ.

Likewise, when W decreases, the probability that a node transmits successfully decreases. Therefore, EE increases with W. Remember that, this results represent the fraction of the average consumed energy during a successful transmission over the total average energy consumed (including *overhearing* and collisions) in a transmission (see equation 19).

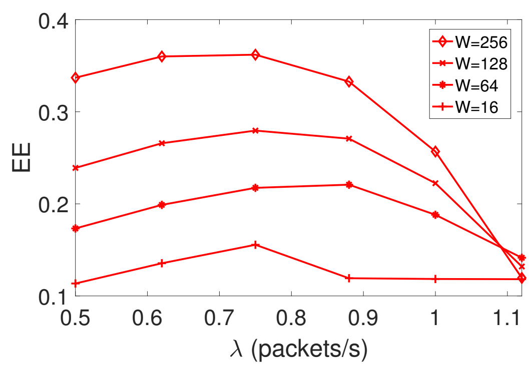

Fig. 8. Dimensionless energy efficiency as the data arrival rate varies, when $N = 15$.

In Fig. 9, the energy efficiency en terms of ($Kbytes/mJ$) as a function of λ is shown, considering different sizes of W. The figure shows that in general, for low load, more bytes per Joule can be sent by a node. Moreover, the efficiency achieved is higher as W decreases. Remember that in the calculation of ξ, the total energy consumption is considered, including the *sync* and *awake* energies, that are used for signalling purposes. Besides, the W is merely considered in the denominator of the expression (equation 20).

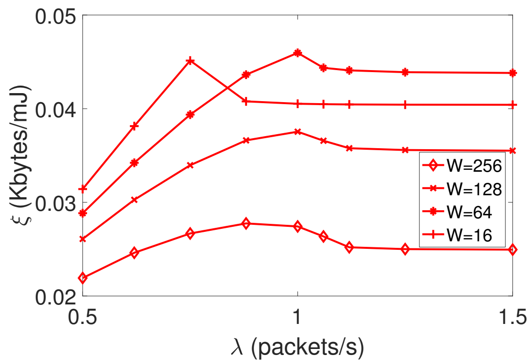

Fig. 9. Energy efficiency as the data arrival rate varies, when $N = 15$.

6 Conclusions

In this paper, we developed a 2D-DTMC-based model to analyse the energy consumption performance of sensor devices that could be used for a WSN-based IoT application. Furthermore, we derive exhaustive expressions to determine the variety of energy consumptions of the sensor nodes. The model considers a synchronous duty-cycled MAC protocol, and its solution, in terms of stationary probability distribution, is used by the expressions to evaluate the energy performance, in a more precisely and systematic way. Results of average energy consumption and energy efficiency are obtained, validated through discrete-event based simulations, and the obtained results are accurate. As a future work, we are planning to extend the model, in order to support heterogeneous scenarios, with different classes of nodes conforming the network. Also, the incorporation of an aggregated transmission scheme, is another possibility that we are contemplating.

Acknowledgement

This work has been supported by the Ministry of Economy and Competitiveness of Spain through projects TIN2013-47272-C2-1-R and TEC2015-71932-REDT. Work done as part of the Program Financed by the European Union-Action 2-Erasmus Mundus Partnerships, GRANT AGREEMENT NUMBER-2014-0870/001-001. C. Portillo also thanks the support given by SEP-SES (DSA/103.5/15/6629).

References

[1] Shu Yinbiao, Kang Lee, Peter Lanctot, F Jianbin, H Hao, B Chow, and JP Desbenoit. Internet of Things: Wireless Sensor Networks. *White Paper, International Electrotechnical Commission, http://www. iec. ch*, 2014.

[2] L. Mainetti, L. Patrono, and A. Vilei. Evolution of wireless sensor networks towards the Internet of Things: A survey. In *SoftCOM 2011, 19th International Conference on Software, Telecommunications and Computer Networks*, pages 1–6, Sept 2011.

[3] Y. W. Kuo, C. L. Li, J. H. Jhang, and S. Lin. Design of a Wireless Sensor Network-Based IoT Platform for Wide Area and Heterogeneous Applications. *IEEE Sensors Journal*, 18(12):5187–5197, June 2018.

[4] C. Z. Myint, L. Gopal, and Y. L. Aung. Reconfigurable smart water quality monitoring system in IoT environment. In *2017 IEEE/ACIS 16th International Conference on Computer and Information Science (ICIS)*, pages 435–440, May 2017.

[5] K. H. Kamaludin and W. Ismail. Water quality monitoring with internet of things (IoT). In *2017 IEEE Conference on Systems, Process and Control (ICSPC)*, pages 18–23, Dec 2017.

[6] Q. Chi, H. Yan, C. Zhang, Z. Pang, and L. D. Xu. A Reconfigurable Smart Sensor Interface for Industrial WSN in IoT Environment. *IEEE Transactions on Industrial Informatics*, 10(2):1417–1425, May 2014.

[7] M. T. Lazarescu. Design of a WSN Platform for Long-Term Environmental Monitoring for IoT Applications. *IEEE Journal on Emerging and Selected Topics in Circuits and Systems*, 3(1):45–54, March 2013.

[8] T. D. Nguyen, J. Y. Khan, and D. T. Ngo. An effective energy-harvesting-aware routing algorithm for WSN-based IoT applications. In *2017 IEEE International Conference on Communications (ICC)*, pages 1–6, May 2017.

[9] T. D. Nguyen, J. Y. Khan, and D. T. Ngo. A Self-Sustainable RF Energy Harvesting Algorithm for WSN-Based IoT Applications. In *GLOBECOM 2017 - 2017 IEEE Global Communications Conference*, pages 1–6, Dec 2017.

[10] Y. Cho, M. Kim, and S. Woo. Energy efficient IoT based on wireless sensor networks. In *2018 20th International Conference on Advanced Communication Technology (ICACT)*, pages 294–299, Feb 2018.

[11] A. S. Wander, N. Gura, H. Eberle, V. Gupta, and S. C. Shantz. Energy Analysis of Public-Key Cryptography for Wireless Sensor Networks. In *Third IEEE International Conference on Pervasive Computing and Communications*, pages 324–328, March 2005.

[12] Mari Carmen Domingo and Rui Prior. Energy Analysis of Routing Protocols for Underwater Wireless Sensor Setworks. *Computer Communications*, 31(6):1227 – 1238, 2008. Advanced Location-Based Services.

[13] MuhammadMahtab Alam, Olivier Berder, Daniel Menard, Thomas Anger, and Olivier Sentieys. A Hybrid Model for Accurate Energy Analysis of WSN Nodes. *EURASIP Journal on Embedded Systems*, 2011(1):307079, Jan 2011.

[14] Hai-Ying Zhou, Dan-Yan Luo, Yan Gao, and De-Cheng Zuo. Modeling of Node Energy Consumption for Wireless Sensor Setworks. *Wireless Sensor Network*, 3(01):18, 2011.

[15] Y. Wang, M. C. Vuran, and S. Goddard. Stochastic Analysis of Energy Consumption in Wireless Sensor Networks. In *2010 7th Annual IEEE Communications Society Conference on Sensor, Mesh and Ad Hoc Communications and Networks (SECON)*, pages 1–9, June 2010.

[16] Ou Yang and Wendi Heinzelman. Modeling and Performance Analysis for Duty-Cycled MAC Protocols with Applications to S-MAC and X-MAC. *IEEE Transactions on Mobile Computing*, 11(6):905–921, 2012.

[17] Jorge Martinez-Bauset, Lakshmikanth Guntupalli, and Frank Y Li. Performance Analysis of Synchronous Duty-Cycled MAC protocols. *IEEE Wireless Communications Letters*, 4(5):469–472, 2015.

[18] Lakshmikanth Guntupalli, Jorge Martinez-Bauset, Frank Y Li, and Mary Ann Weitnauer. Aggregated Packet Transmission in Duty-Cycled WSNs: Modeling and Performance Evaluation. *IEEE Transactions on Vehicular Technology*, 66(1):563–579, 2017.

[19] Canek Portillo, Jorge Martinez-Bauset, and Vicent Pla. Modelling of S-MAC for Heterogeneous WSN. 6th IFIP NTMS Workshop on Wireless Sensor Networks: Architectures, Deployments (WSN-ADT), 26-28 Feb. 2018, Paris, France.

[20] Wei Ye, John Heidemann, and Deborah Estrin. An Energy-Efficient MAC Protocol for Wireless Sensor Networks. In *INFOCOM 2002. Twenty-First Annual Joint Conference of the IEEE Computer and Communications Societies. Proceedings. IEEE*, volume 3, pages 1567–1576. IEEE, 2002.

[21] Canek Portillo, Jorge Martinez-Bauset, Vicente Casares-Giner, and Vicent Pla. The State Transition Probabilities of the 2D-DTMC. Technical Note. [online]. http://personales.alumno.upv.es/caporji/transprob.pdf., June 2018.

[22] Mica Data Sheet. Crossbow Technol. Inc., San Jose, CA, USA. [online]. http://edge.rit.edu.

Contribution to the Analysis of the Lifetimes of Well Functioning of Wireless Sensor Networks

Amal Chaffai, Vicente Casares-Giner
Universitat Politècnica de València, Spain
Email: amcha@doctor.upv.es , vcasares@itaca.upv.es

Abstract

Uneven energy depletion causes energy holes and leads to degraded network performance then the entire network fails. If sensors around a sink all run out of energy, the sink will be isolated from the network. Therfore the main contribution of this work is to provide a theoretical explanation of the uneven energy depletion phenomenon noticed in sink-based wireless sensor networks with a states transitions equations. And sort out the problem of maximizing network lifetime through balancing energy consumption for uniformly deployed data gathering sensor wirless networks, is the focus of the present study on advancing sophisticated of deterministic protocol for carrying out a procedure toward more flexible but equally able to be trusted distributed approaches. In addition, this paper aims to introduce the first implementation of a new protocol networks to become challenge faced to overcome the scalability issues inherent dense low power networks.

Index Terms: Energy holes, balancing energy, maximizing network lifetime.

1 Introduction

To seek the ways to avoid the creation an energy hole around the sink, we investigate the theoretical problems aspects of the uneven energy depletion phenomenon of balancing energy consumption and maximizing network lifetime for data gathering sensor networks. Similar to the models in [1–3], Olariu and Stojmenovic (2006) were unable to actually design a data gathering scheme that will reasonably balance energy based on theoretical findings. Therefore this remains an open problem [3]. The solutions presented in this study are complimentary to existing work on designing random uniform node deployment schemes [1, 2, 4]. According to [3], there are several other manner to offset the uneven energy depletion problem. The most obvious strategy is to mandate the sinks to move around in such a way that some load balancing is obtained across the deployment area [1]. This solution works especially well in autonomous sensor networks [5]. Even another solution involves establishing temporary sinks that act as ad-hoc aggregation points. However, power consumption is an important issue for this type of aggregations because the terminals of ad-hoc networks are lightweight and low capacity. The optimization in the designs to reduce the power consumption as much as possible and thus extend the lifetime of the batteries of WSNs should be take it account. Finally, as discussed in [3], a certain amount of load balancing is obtained by overlapping the disks around the sinks, although it may produce an array of ambiguous areas. Thus, our contributions also is focusing in to put forward a glimpse of the architecture system as full advantages of corona-based network division, data aggregation and hybrid-routing, the network is divided into coronas centered at the sink, and all nodes in the same corona use the same probability for direct transmission and the same probability for hop-by-hop transmission. Thereby this investigation can be lay out as follows:

- The Design purpose optimally sink organizes the sensors around it into a dynamic infrastructure. This task is referred to training as [2,6] and involves partitioning the disk D of radius R into disjoint concentric coronas. This scheme can evenly distribute energy consumption among nodes in each corona.
- To Design a new data gathering protocol, which can achieve balanced energy consumption among nodes both within one corona and among different coronas. Which it involves data gathering in terms of network lifetime.

C.Fernandez-Llatas and M.Guillen (Ed.):
Workshop on Innovation on
Information and Communication Technologies
(ITACA-WIICT 2018)

ISBN 978-84-09-07373-3

- To Design an algorithm [3,7] to calculate the optimal data distributions for all coronas in fact to balance energy consumption among nodes in different coronas, to maximize the network lifetime.

The remainder of this paper is organized as follows: Section 2 reviews related work, Section 3 addresses the aspect of basic notions concept, and Section 4 presents the system models and the statement of the problem. In section 5 we show that maximizing network lifetime is guaranteed by carefully tailoring the coronas. The contribution ends with a final discussion of the results obtained followed by a conclusion in section 6.

2 Related Work

Energy efficiency has been considered as the most important design challenge in sensor networks [8–10]. Since sensor nodes often are deployed in harsh environments, it is often difficult or impossible to recharge or replace batteries [11, 12]. The problem of the energy gap is a key factor that affects the useful life of the network [2]. There has been a good number of research works to find an effective solution to the prevention of energy depletion near the sink of a wireless sensor network. In recent years, part of the research in WSNs has been aimed at studying the potential of collaboration between the different nodes in the data collection processes and their aggregate processing data aggregation, with the main objective of minimizing the impact that the redundant transmissions have in the joint performance of the network and in the exhaustion of the battery of the nodes, reason for which the routing designed for a WSNs is centered precisely in this sense, constructing hierarchical algorithms that optimize on the one hand the distance of the resulting route and energy consumption and, on the other hand, its duration and ability. A well known hierarchical architecture addressing algorithm is LEACH [4] that uses randomization to rotate the (CHs) and achieve a significant improvement compared to a direct approximation. Nevertheless this approach allows only the grouping of (CHs) of a single hop and does not consider the problems of hot spots. Some researchers presented a mathematical model to characterize the problem of the energy gap in wireless sensor networks. Based on a traffic perspective, this analytical model examines the validity of several possible schemes that aim to mitigate or solve the problem of the energy gap [1]. It is observed that in the networks of uniformly distributed sensors, data deployment and compression of data have a positive effect [13]. Otherwise have considered the use of competition radio to produce unequal grouping, but this mechanism does not consider the density of the deployed sensors that could cause a lot of load in the (CHs) and too much overload in the communication networks. Further more, other researchers proposed an unequal grouping mode for the organization of the network that showed an unrealistic architecture because they considered that scalability is not a concern [11, 12].

3 Basic Notions Concept

Early in the evolution of the WSNs concept, system designers recognized that visualizing the two expressions lifetime network and splitting determine the essential features of the WSNs concept. It provides a glimpse of its basic key elements concept-lifetime network and splitting [14] and describes certain mathematical properties any regular approximates shape geometry system to delineate areas. Reason why it will be used a specific wedge to show how can be effected in a working system. The sensor network model consider an arbitrary wedge subtended by an angle of Θ. W is partitioned into K sectors as $A_1, A_2, \ldots, A_K$, by its intersection with K concentric circles, centered at the sink, and of monotonically increasing radii $R_1 < r$. As illutrated in the Fig. 1. Can cover a plane with no gaps or overlaps [3, 14]. To catch the point of the motivation for choosing the infrastructure discussed above, let us focus our attention on the "worst-case" points [14] in others techniques the vertices were in fact the worst-case points, the energy is concentrated in the corners and vertices and it costs to get to the center [3, 14]. Assuming that energy at sink is unlimited CHs can then be placed at strategic locations. Thereby, the features of the aggregation model proposed [5] in this study of the training sensor network is modeled here by a 2-dimensional plane with no loss of generality, we assume that the trainer is centrally located relative to all deployed nodes. The first goal of training is to establish a coordinate system, to provide the nodes location awareness in that system, and to organize the nodes into clusters to establishes a polar coordinate system.

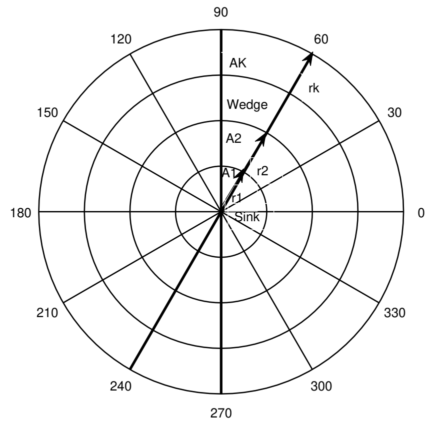

Figure 1: A wedge W partitioned into k sectors

4 Network Model and Assumptions

A fundamental assumption here is, we adopt the following general power consumption model, [15] and we will contribute to avoid the problem using a states transitions equations to know which probabilities are the best.

$$Et(d) = ad^{\alpha} + \ \ b \text{ and } Er = b, \tag{1}$$

where $a > 0$ is a constant standing for the transmitter amplifier, $b > 0$ is a constant representing energy for running electronic circuit, and the path loss α is $2 \leqslant \alpha \leqslant 6$. The sensors must work unattended as it is either impractical or infeasible to devote attention to individual sensors. They are anonymous they do not have fabrication time identities. In particular, point to point routing cannot be based on IDs of neighboring sensors. Each sensor has a non-renewable energy budget when the on board energy supply is exhausted,the sensor becomes in-operational. Each sensor has a maximum transmission range, denoted by tx, assumed to be much smaller than R, the furthest possible distance from a sensor to its closest sink [2,6].

5 Network Lifetime Maximization

To prevent undesired behavior by way of creation an energy hole around the sink, an algorithm will discuss the implementation, and break down this problem into smaller parts by first studying a typical clusters such as we can implement the areas of clustering sectors into following a states transitions equations:

$$\begin{aligned} S_i &= \frac{\Theta}{2} * (r_i^2 - r_{i-1}^2) \\ A_i &= S_i + A_{i-1} \ \ ; \ \ 1 \leqslant i \leqslant 3. \end{aligned} \tag{2}$$

The methodology to solve this equations is an iterative process for a case $\alpha > 2$ and it consist in hybrid-routing, in which each node (CHs) alternates between hop-by-hop transmission mode and direct transmission mode to report data. In direct transmission mode, each node sends its data directly to the sink without any relay [15]and this mode helps to alleviate the relay burden for the nodes close to the sink. In hop by hop transmission mode, each node forwards the data to its next hop neighbors, and this mode helps to relieve the burden of long-distance transmission for the nodes far away from the sink. Therefore, it is possible to obtain fairly even energy consumption among all nodes by properly allocating the amount of data transmitted in the two modes, as illutrated in Fig. 2. If we require energy expenditure balanced across all the coronas,

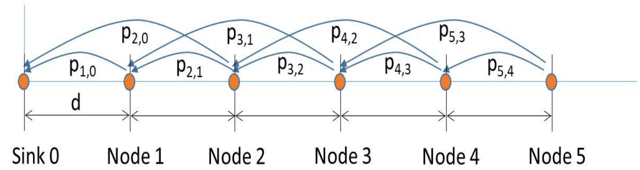

Figure 2: Hybrid routing

Table 1: Table Probabilities Routing

De\ a	0	1	2	3	4	5
0	0	0	0	0	0	0
1	1	0	0	0	0	0
2	0.875	0.125	0	0	0	0
3	0	0.6250	0.3750	0	0	0
4	0	0	0.3750	0.6250	0	0
5	0	0	0	0.1250	0.8750	0

$$E_1 = E_2 = \ldots = E_k. \tag{3}$$

We propose to determine every r_i,

$$2 \leqslant i \leqslant k, \tag{4}$$

As a function of r_1 and R. The width of each corona is,

$$\Delta_i = r_i - r_{i-1}. \tag{5}$$

The widths of the coronas must satisfy the following inequality [3]:

$$r_1 = \Delta_1 < \Delta_2 < \ldots \Delta_i < \ldots \Delta_k \leqslant tx. \tag{6}$$

And the experimental results themselves will keep as illustrated in Table 1 probabilities routing.

Indeed, as theorem 6.1 $[2,3]$ in order to minimize the total amount of energy spent on routing along a path originating at a sensor in corona A_i and ending at the sink, all the coronas must have the same width d and the optimal amount of energy is i times the energy needed to send the desired information between adjacent coronas.

5.1 Energy Expenditure Results and Analysis

The main goal of this section is to prove the above assumptions such we should set optimal deterministic value r_1 and determine r_2, r_3 ,. . . , r_k accordingly [3]. The generic computation applying the equation follow:

$$E_i = \frac{\overline{T}}{\pi\rho}[1 - \frac{r_i^2 - 1}{r_k^2}]\frac{(r_i - r_{i-1})^\alpha + c}{r_i^2 - r_{i-1}^2}; i = 1, 2, 3, \ldots \tag{7}$$

Hence, we can illustrate, E_1, E_2,. . . , E_k by a numerical example:

The system parameters are, $R = 225m$, $c = 4500$, $\alpha = 4$, density $\rho = 35$, Let $\overline{T}$ denote the number of sector-to-sink paths. Thus,$\overline{T}$ equals the total number of tasks that the wedge can handle during the lifetime of the network. And the lifetime of network is defined as the operational time of the network during which it is able to perform the dedicated task(s).

E_1, E_2,. . . , E_k. Can satisfy equation mentioned above on the last section(6). Then, the optimal value of d as theorem 6.1 [3] is suggested by deterministic value of r_1. Therfore, we have: $d = r_1$.

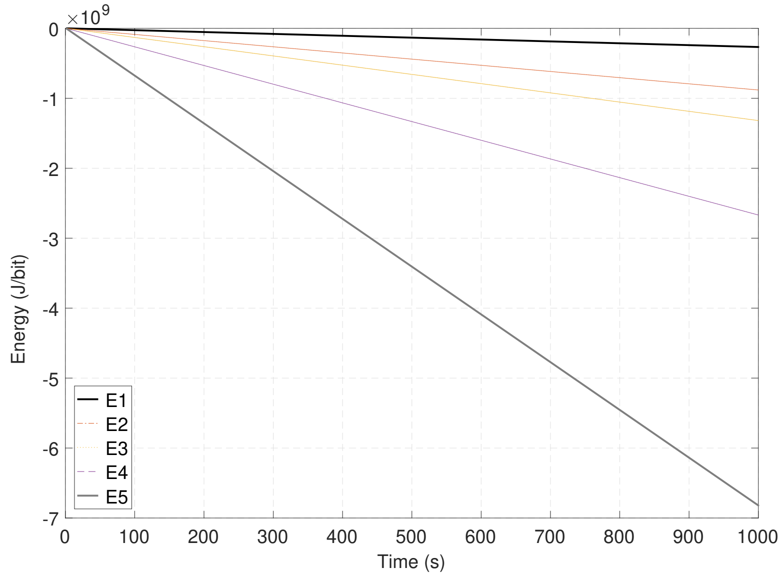

Figure 3: Expenditure energy

5.2 Network Lifetime Maximimization Framework

The objective of the NLM framework is to compute the optimal number of coronas in terms of maximizing the network lifetime. As [3, 7]determining r_2, r_3,..., r_k as a function of r_1, involved of course, $r_k = R$ and must satisfy equation(6). Then, this also indirectly, determines the number of coronas k. Therfore, $k_1 = 1 < k2 < \dots k_i \leqslant \frac{tx}{2*\Delta_{i-1}}$. The iterative process is straightforward and not presented here due to space limitations.

6 Conclusions

The method presented is investigated with regard to strategic locations of CHs, when investigating coherent effects for energy-efficient communication. We divided the monitored area into wedges comparable to the approach presented in [3]. And we made the assumptions quotes before motivated by the uniformity of the deployment and each CH is equally likely to be the source of a path to the sink. This fact must be considered [14,16] when designing the corresponding new protocol whose purpose is to avoid the energy hole around the sink. Therefore, the results prove that, the novel technique presented above is effective method to settle problems aspects of the uneven energy depletion phenomenon of balancing energy consumption and maximizing network lifetime.

References

[1] K. T. G. J.Lian, L.Chen, "Localized Routing Trees for Query Processing in Sensor Networks," *Proc. ACM Knowledge and Information Management*, vol. 1, pp. 259 – 260, October 2005.

[2] L. S.Olariu, A.Wadaa and M.Eltoweissy, "Wireless Sensor Networks: Leveraging the Virtual Infrastructure," *IEEE Network*, vol. 18, no. 4, pp. 51 – 56, 2004.

[3] I.Stojmenovic and S.Olariu, "Data- Centric Protocols for Wireless Sensor Snetworks, in:Handbook of Sensor Networks:Algorithms and Architectures," *Wiley*, pp. 417 – 456, 2005.

[4] A. W.Heinzelman and H.Balakrishnan, "An Application - Specific Protocol Architecture for Wireless Micro- Sensor Networks," *IEEE Transactions on Wireless Communications*, vol. 1, pp. 660 – 670, 2002.

[5] N.Vlajic and D.Xia, "Wireless Sensor Networks: to Cluster or not to Cluster," *University of York*, pp. 9 – 268, November 2005.

[6] L. K. A.Wadaa, S.Olariu and M.Eltoweissy, "On Training a Sensor Networks," *University of York*, no. 17, pp. 1 – 8, january 2005.

[7] H. Zhang and H. Shen, "Balancing Energy Consumption to Maximize Network Lifetime in Data - Gathering Sensor Networks," *IEEE transactions on parallel and distributed systems*, vol. 20, no. 10, pp. 15 – 26, october 2009.

[8] Y. F.Akyildiz, W.Su and E.Cayirci, "Wireless Sensor Networks:A Survey," *Computer Networks*, vol. 38, no. 4, pp. 393 – 422, 2002.

[9] D. E. D.Culler and M.Srivastava, "Overview of Sensor Networks," *IEEE Computer*, vol. 37, no. 8, pp. 41 – 49, 2004.

[10] J. K. K.Martinez and R.Ong, "Sensor Network Applications," *IEEE Computer*, vol. 37, pp. 50 – 56, 2004.

[11] C. R. V. Mhatre, "Design Guidelines for Wireless Sensor Setworks: Communication,Clustering and Aggregation," *Ad Hoc Networks*, vol. 2, pp. 45 – 63, 2004.

[12] D. R. V.Mhatre, C.Rosenberg and N.Shroff, "A minimum cost heterogeneous sensor network with a lifetime constraint," *IEEE Transactions on Mobile Computing*, vol. 4, no. 1, pp. 4 – 15, 2005.

[13] K. N. J. Lian and G. B. Agnew, "Modeling and Enhancing Data Capacity in Wireless Sensor Networks," *IEEE Monograph on Sensor Network Operations,IEEE Press*, vol. 1, pp. 660 – 670, 2004.

[14] V. DONALD, "The Cellular Concept," *BSTJ*, vol. 58, no. 10, pp. 15 – 41, January 1978.

[15] V.Rodoplu and T.Meng, "Minimum Energy Mobile Wireless Networks," *IEEE International Conference on Communications*, vol. 3, pp. 1633 – 1639, 1998.

[16] P. V.Casares and DiegoPacheco-Paramo, "Combined Contention and TDMA - Based Communication in Wireless Sensor Networks," *8th Euro - NF Conference on Next GenerationInternet (NGI),Karlskrona,Sweden*, pp. 1 – 8, 2012.

Multisensor data fusion for epileptic seizure prediction: A review of the state of the art

Adriana Leal[1], Anna Bianchi[2], Maria da Graça Ruano[1], V. Traver[3], J. Henriques[1], P. Carvalho[1] and César Teixeira[1]

[1] Centre for Informatics and Systems, University of Coimbra, DEI, Polo 2, Pinhal de Marrocos, 3030-290 Coimbra, Portugal
{aleal, mruano, jh, carvalho, cteixei}@dei.uc.pt

[2] Department of Electronics, Information and Bioengineering, Politecnico di Milano, Piazza Leonardo da Vinci 32, 20133 Milan, Italy
annamaria.bianchi@polimi.it

[3] ITACA. Univertat Politècnica de València, Camino de Vera S/N, Valencia 46022, Spain
vtraver@itaca.upv.es

Abstract. Automatic seizure detection and prediction can play a significant role in improving quality of life of patients diagnosed with epilepsy for whom no therapy has been found to be successful in ceasing seizures. Inspection of the existence of electroencephalographic patterns during seizure discharges has been long performed. Additionally, the observation of extracerebral alterations simultaneous to the changes in brain electrical activity before, during and after seizure discharges has unleashed a new era in seizure prediction characterized by the combination of information obtained from different modalities. Specifically, besides scalp and intracranial EEG data, electrocardiography, accelerometry, electromyography and electrodermal activity have also been given considerable attention in the context of seizure prediction.

To date, however, no particular data fusion methodology has yielded the best results leading scientists to believe that the development of patient-specific approaches may be the right path to follow.

This review presents an overview of the existent multisensor data fusion methods designed for seizure detection and prediction. Special emphasis is assigned to the combination of EEG- and ECG-derived information, as cardiovascular changes have been considered important biomarkers in epilepsy.

1 Introduction

Besides the explicit electroencephalogram activity, epileptic seizures have implicit manifestations on other body functions. In fact, the occurrence of epileptic seizures is often associated with dysfunction of the autonomic nervous system, reflected in the output of both the parasympathetic and sympathetic systems responses to the cardiorespiratory function. Cardiac parameters such as heart rate (HR), heart rate variability (HRV) and blood pressure were reported to change

C.Fernandez-Llatas and M.Guillen (Ed.):
Workshop on Innovation on
Information and Communication Technologies
(ITACA-WIICT 2018)

ISBN 978-84-09-07373-3

across the pre-, post- and ictal periods, along with sweat production oscillations. The occurrence of such extracerebral alterations, concurrent with the electroencephalographic profile changes, has prompted the recording of other biosignals including electrocardiogram, electrodermal activity (sweat levels) and plethysmography (blood pressure), nowadays considered important tools of epileptology. Furthermore, by monitoring these autonomic related parameters it may be possible to identify seizures which are not associated with motor symptoms as is the case of temporal lobe seizures and which may not be detected by using accelerometry and electromyography recordings. The combination of information from sensors able to capture the brain electrical activity, the autonomic regulation and the seizure-related motor signs has been reported to decrease the number of false positives and significantly improve prediction.

The present document reports an overview of the state of the art regarding the data fusion approaches used so far in seizure prediction field, with particular emphasis placed on the electroencephalogram (EEG) and electrocardiogram (ECG) multisensor schemas.

2 The Autonomic Nervous System

The autonomic nervous system (ANS) is responsible for the regulation of HR, respiration, micturition, digestion and reproduction. The parasympathetic and sympathetic reflex centres can be identified as subdivisions of the ANS acting in concert to maintain homoeostasis. Alterations in the normal autonomic function will be reflected in one or in both of the parasympathetic and sympathetic systems responses.

The ANS responses are influenced by brain structures including amygdala and hypothalamus and also anterior cingulate, insular, posterior orbito-frontal and prefrontal cortices. As the epileptic discharges can take place or propagate to these structures it is very likely that the such abnormal event can lead to disturbances in the normal autonomic function [3,4,9]. Autonomic typical symptoms include mainly cardiorespiratory and gastrointestinal abnormal parameters, palpitations, polyuria and sweating [2,19]. Specifically, when the sympathetic nervous activity is triggered during seizures, it typically results in increased HR and blood pressure and possible occurrence of tachycardia and tachypnea [3,9]. On the other hand, when the parasympathetic system response predominates, although in a significantly lower number of seizures, the normal cardiorespiratory function is altered with regards to the decreasing of heart and respiration rates and also blood pressure [3,9].

However, a wide plethora of studies has provided high variability of results regarding the individual contribution of both autonomic subsystems during epileptic seizures and the consequent changes in cardioespiratory parameters. Such variability can be mainly explained by the difficult task of isolating cardiac effects of seizures from effects of drug administration, stress condition or even from the effect of physical effort. Furthermore, the type of seizure, location and size of the brain region affected by an epileptic discharge can also help explaining differences across studies [28]. For example, although no consensus has been achieved yet, it has been hypothesized that changes in autonomic function may be more evident when the patient's seizure location is in the right hemisphere in contrast with the left one [1, 4, 23]. Additionally, lateralization of the ANS responses has been reported to change from patient to patient [2].

Nevertheless, the most common and evident cardiac parameter's alterations that have been reported include ictal tachycardia and, less frequently, ictal bradycardia [4]. It must be noticed that, postictal arrhythmias including asystole and atrioventricular block, albeit rarely occur, typically follow a convulsive seizure and are often associated with cases of near SUDEP [11].

According to these observations, HR was reported to increase during seizures in 40-100% of patients, in 35-100% of their seizures. Such high range can be explained by the heterogeneity of epileptic populations regarding the different conditions influencing seizures such as the patient's vigilance state, type of seizure, type of epilepsy, seizure-onset location lobe, lateralization, patients' age and gender, and time to diagnosis [1, 4, 18]. As an example, it is known that there is an higher increase in HR in seizures happening during sleep in comparison to the ones occurring in awake state. This difference is the consequence of the predominance of the parasympathetic system activity during sleep state.

Furthermore, the most significant findings regarding epileptic patients refer to decreased HRV reflected in the lower values of HF[4] component, SDNN[5] and RMSSD[6] when comparing to healthy subjects. Decreased HF component is typically associated with impaired parasympathetic activity in epileptic patients. A reduced HRV is often present in chronic drug resistant epilepsy patients, therefore possibly indicating parasympathetic inhibition.

A recent study presented by Piper et al. considered the interconnection between two coupled networks: the temporal lobe epilepsy (TLE) associated network and the central autonomic network. Using EEG and ECG data provided by 18 children with TLE, the research group was able to identify an increase in the coherence patterns between HRV's low frequency (HRV-LF, present in the range of 0.04-0.15 Hz) and the IMF-envelope (corresponding to delta-activity) of each EEG channel, before and after the seizure. The rise in both features indicate the occurrence of correlative coupling/synchronization, and was also found to be dependent on the lateralization of the seizure. It should be noted that the authors also considered an important aspect when analysing epileptic seizures: each seizure occurring in a given patient must be treated as unique, having specific characteristics that must be taken into account when interpreting the corresponding results [19].

ECG's morphology has also been reported to change as consequence of epileptic seizure discharges, even though in a reduced number of papers comparing to

---

[4] Frequency-domain HRV feature: high frequency spectral component (or respiratory sinus arrhythmia) that corresponds to the power in the range from 0.15 to 0.4 Hertz.

[5] Time-domain HRV feature: standard deviation of beat-to-beat (or NN) intervals.

[6] Time-domain HRV feature: square root of the mean of the squares of the successive NNs.

the other aforementioned cardiac parameters [3, 22]. Repolarization abnormalities were specifically detected during ictal tachycardia as was documented by Stollberger et. al who observed ST-segment changes in the end of ictal period in 9 out of 22 drug resistant focal epilepsy patients [23, 26].

Additionally, it was observed that the corrected QT interval diminished during the early postictal period of FOIA[7] and FBTC[8] seizures in 17 patients diagnosed with drug resistant TLE. The corrected QT interval refers to the use of methodologies to reduce the dependence of the QT interval on the HR [27]. In a dataset comprising focal and generalized seizures recorded in 81 drug resistant epileptic patients, a T wave inversion and ST elevation or depression happened in eight patients [33].

At last, it was also possible to understand that disturbances in the ANS manifested predominantly in studies involving TLE patients which is in agreement with the localization of most of the structures responsible for cardiovascular autonomic regulation being in the temporal lobe [12].

3 Multisensor data fusion in seizure prediction

The number of multimodal methodologies for seizure prediction/detection is gradually increasing as the scientific community is becoming aware of the presence of extracerebral manifestations of these events. On the one hand, there is evidence for the concurrent epileptogenic network and ANS outputs, the latter reflected in physiological parameters measurable by ECG and electrodermal activity (EDA). On the other hand, seizures associated with motor clinical symptoms can also be monitored using movement sensing devices, such accelerometry and electromyogram (EMG).

3.1 EEG and ECG fusion schemes

Based on the increasing findings regarding the changes in cardiac parameters occurring during seizures, it was possible to believe that seizure detection may benefit from the combination of time-synchronous EEG and ECG's information in a multisensor data fusion schema. Data fusion approaches can be implemented at different levels of the data processing chain [7, 10]. Namely, fusion of information from EEG and ECG in the context of epilepsy has been performed at:

(i) Feature level (or feature-in-decision-out scheme) by feeding a common classifier with features derived from different biosignals (see Figure 1) [16, 31]

(ii) Classifier level (or decision-in-decision-on scheme) by using each biosignal feature set as an input to distinct classifiers and finally by obtaining a final decision based on the output of the individual classifiers (see Figure 2) [17, 21].

[7] Focal onset impaired awareness.

[8] Focal to bilateral tonic-clonic.

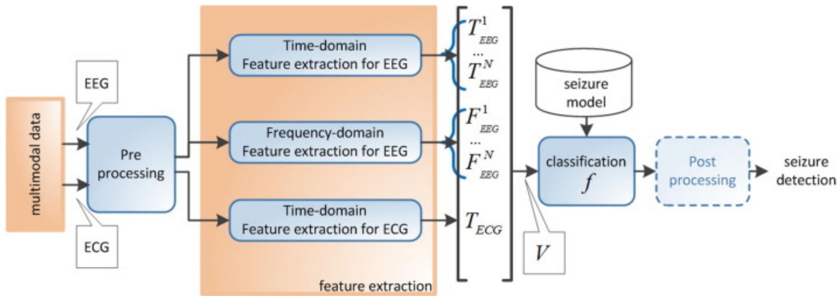

Fig. 1: Feature-level data fusion schema implemented by Mporas et al. [16].

Table 4 presents the state of the art of the existent methodologies regarding fusion in seizure detection. It is possible to observe that in the vast majority of the studies data fusion was performed at the feature level. In two studies [8,13], feature level fusion was compared with decision level, with the former returning a better performance for Greene and colleagues [8]. Results from the two types of data fusion were similar for Mesbah et al. with a slight improve in specificity by using the decision level fusion method [13].

In all the papers where the performance of fusion methodologies was compared to the results obtained by using individual detectors for each modality, the former was reported to outperform the latter. Naturally, using a set of features derived from both EEG and ECG will most likely improve classification by complementing the information provided by each sensor. The use individual detectors, even though, it has been proven to detect several types of seizures still lacks specificity [24].

Frequency features were extracted from EEG in all papers whereas in five out of eight papers authors extracted a set of features from the EEG recordings capturing time- and frequency-domain information and also the nonlinear

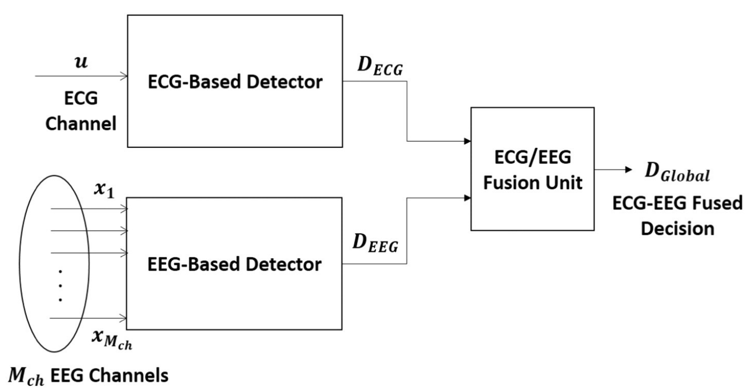

Fig. 2: Decision-in-decision-out data fusion schema implemented by Qaraqe et al. [21].

behaviour [13, 15, 16, 30, 31]. Regarding the ECG, in three articles only HRV features were computed [8, 13, 21] whereas only features derived from HR were extracted in another three papers [15, 16, 25]. Valderrama et al. on the other hand decided to analyse information derived from both HRV and HR as well as nonlinear features in their multisensor fusion methods [30, 31]. Features capturing the changes in ECG's morphology were not reported to be used in any paper, possibly due to the hardest task of segmentation of the QRS complex, especially when the ECG is contaminated with noise.

The best set of both EEG and ECG features is not evident from the analysis of the information in Table 4. In fact, besides being difficult to compare the results from different studies as different performance metrics and epileptic groups of study are considered, other confounders related to the developed methodology can impair a comparison of the final performance of the fusion method for the different types of features (e.g., different EEG feature set and different fusion methodology). Nevertheless, it is clear that a feature selection process can be useful in enlightening about the most informative features for each type of biosignal and consequently reduce the computational cost of the final seizure prediction framework. Only one study reported the application of a filter-based method for feature selection in each biosignal dataset which has lead to an increase in the performance of the prediction [13].

It is important to note however that a given feature set might be found for a specific group of patients or even for a distinct type of seizures [5, 29]. That was evidenced in Greene et al. study reporting the designing of a methodology for the detection of neonatal seizures, in which a patient-specific approach was compared with a patient-independent, with the best performance obtained for the former [8]. In fact, it is in accordance to the literature findings reporting that seizures occurring in the same patient may be associated with distinct preictal dynamics and also that different onset mechanisms can be triggered for short and long seizures [5].

SVM classifier was used in six studies to perform seizure prediction/detection [15, 16, 21, 30, 31]. Mporas et al. reported improved performance of SVM over backpropagation multilayer perceptron neural network, k-nearest neighbour algorithm and C4.5 decision tree. As one of the most popular supervised learning method it has been widely used in seizure prediction both in binary problems (seizure versus non-seizure) and in multi-class classification (interictal, preictal, ictal and postictal) as in Valderrama et al. paper [30].

In the reviewed studies, methodologies were designed to detect focal onset seizures [13, 30, 31], generalized seizures [15, 16] and focal and generalized onset seizures [8, 21, 25]. It is in line with the literature overview presented by Ulate-Campos at al. which proposes the existence of a correlation between sensor and seizure type. In fact, the individual performance of EEG- and ECG-based seizure detectors has been found to be the highest for focal onset atonic seizures [29].

Half of the studies considered in this review entail the analysis of long-term EEG and ECG recordings, with four papers reporting results obtained for the analysis of more than 12 hours of continuous data [8, 25, 30, 31]. Furthermore, no information about the recordings number and size was provided in Mporas et al. studies this way rendering the comparison of methodologies even harder [15,16]. The analysis of long-term continuous biosignals has been associated with more reliability of seizure forecasting which stands in line with the idea of the existence of a seizure propensity interval characterized by an increase of seizure discharge likelihood, according to Freestone et al, driven by "the current brain state, the phase of the body's internal rhythms (sleepwake cycle, time of the day, day of week, and month of year), and possibly environmental conditions" [5]. This change in the paradigm entails the envision of seizure prediction in light of the changes in the prediction scenario over time, including the circadian rhythms, medication intake and patient vigilance state.

3.2 Other multisensor data fusion

Similarly to the results for EEG- and ECG-based fusion detectors, combining information from both EDA and accelerometry can improve seizure detection specificity, as confounding factors, such as epilepsy non-related movements in case of accelerometry and stress states able to increase sweat, are most probability undetected by the fusion scheme [32]. On the other hand, using these motion sensors has also been shown to improve detection of motor seizures [29].

Additionally, accelerometry and EDA can be easily and practically recorded using a single wearable device such as, for example, a wrist-worn sensor (see

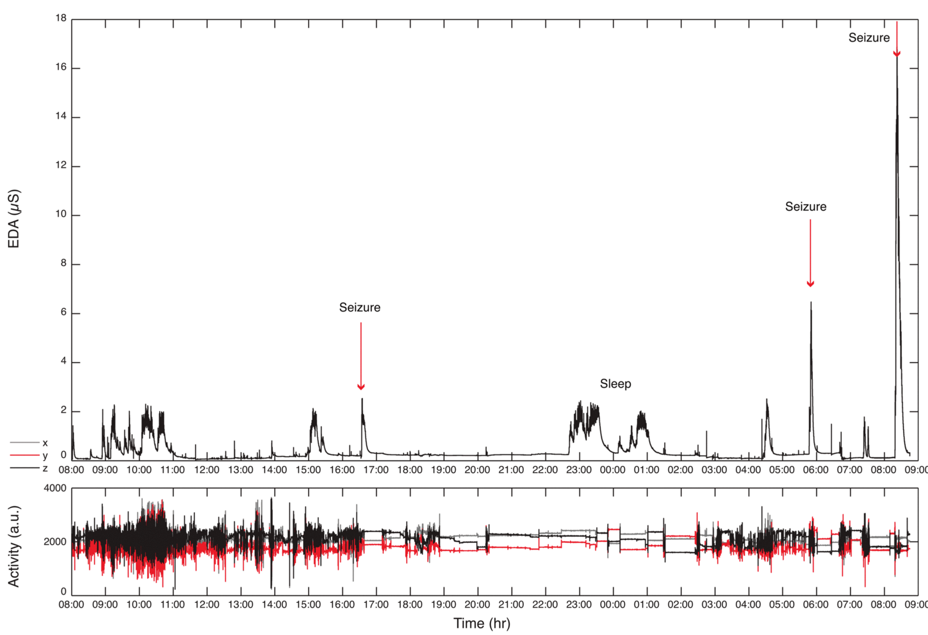

Fig. 3: Example of 24 hour EDA and accelerometry recordings during seizures. Source: Poh et al. 2010 [14].

Figure 3). The multisensor data fusion schemes are similar to the ones reported in 3.1 consisting in feature and decision level data fusion. For example, Poh et al. used SVM classifiers to obtain posterior probability estimates for each feature vector. Then a decision threshold was applied to these estimates in order to assign each epoch to one of the two classes, seizure or nonseizure. The authors developed seizure detection methodology using EDA and accelerometry data acquired in 80 patients (a total of 16 generalized tonic-clonic seizures occurring in seven patients). The algorithm was able to correctly detect 15 of those seizures (94% of sensitivity) and presented a FPR of 0.74 seizures per 24 hours. The authors also compared the performance of this EDA- and accelerometry-based detector with the one returned by a detector being fed with features derived solely from accelerometry having found a decrease in FPR (of 1.5 seizures per 24 hours) for the accelerometry alone [20].

Another interesting research paper has proposed a combination of three biosignals, EEG, ECG and EMG for the detection of 494 focal and focal to bilateral tonic-clonic seizures recorded in 92 epileptic patients (55 diagnosed with TLE and 37 diagnosed with extratemporal lobe epilepsy). Independent detectors were assigned to each modality and the final decision was obtained using OR logical operator. The study reported an overall SE of 86% and an average of 16.5 false detections per 24 h (FD/24 hour). TLE patients (284 seizures) resulted in 94% SE and 12.8 FD/24 hour. XTLE patients (210 seizures) showed a SE of 74% and 22.2 FD/24 hour. Individual detectors were outperformed by the fusion of the decisions (particularly noticeable for the ECG and EMG cases). EEG- and EMG-based detector presented similar performance when comparing to three modality detector [6].

4 Conclusion

Multimodal seizure prediction approaches have been shown to overcome single modality based ones, either by increasing sensitivity as by decreasing false detection rate. Hitherto, however, no specific sensor combination or even at the individual level has been proven to be optimal for a given type of epilepsy or seizure type, whatsoever. These findings suggests that, currently, the best approach to follow consists in designing seizure detection and prediction algorithms that are tailored to the epileptic patient's characteristics, including type of seizure and other variables related to the physiological state of the patient.

By keeping pace with the technological advances, new devices are being developed in order to simultaneously acquire different biosignals in a noninvasive way and by causing minimal discomfort. This way, models built on multimodal data fusion can be integrated in closed-loop systems and provide broad active feedback to the patient, caregiver and clinic.

Table 1: EEG and ECG data fusion papers in seizure prediction.

Paper	Demographics	Methodology	EEG Features	ECG Features	Results
Qaraqe et al. 2016 [21]	10 patients (98-280 recordings, each with 5-22 seizures). Focal, focal to bilateral tonic-clonic and generalized onset seizures. **Analysed period:** one hour.	RBF-SVM. **Fusion:** independent detectors: (i) direct fusion with final decision given by *AND* operator and (ii) override fusion based on an override feature which registers EEG-based seizure decisions. EEG-based detector decision obtained by applying *AND* and *OR* operators and majority voting to sub-band EEG-based detectors.	Delta, theta, alpha and beta frequency bands' energy.	Skewness of time-frequency distribution of HRV.	Direct fusion: 100% SE, 17-second detection latency and FPR of 0.9/h when using the *AND* EEG sub-band fusion technique. Override fusion: 100% SE, 4.2-second detection latency and FPR of 3.1/h when using the *AND* EEG sub-band fusion technique.
Mporas et al. 2014 [15]	3 patients with generalized onset seizures	Seizure or nonseizure classification using SVM (polynomial kernel function), backpropagation multilayer perceptron neural network, k-nearest neighbour algorithm and C4.5 decision tree. 10-fold cross validation. Application of post-processing smoothing window filter to the recognized labels of each epoch. **Fusion:** feature vector fed into a single detector.	Minimum and maximum values, mean, variance, standard deviation, percentiles, interquartile range, mean absolute deviation, range, skewness, kurtosis, energy, Shannon's entropy, logarithmic energy entropy, number of positive and negative peaks, zero-crossing rate; 6-th order AR coefficients, power spectral density, frequency with maximum and minimum amplitude, spectral entropy, delta-theta-alpha-beta-gamma band energy; discrete WT coefficients (with Daubechies 16 and 8 decomposition levels).	HR absolute value and variability statistics of the HR: minimum value, maximum value, mean, variance, standard deviation, percentiles (25%, 50%-median and 75%), interquartile range and mean absolute deviation range.	Best performance obtained for the SVM classifier (mean accuracy for all patients of 92.47%). Performance improved slightly to 93.16%, by applying the post-processing smoothing window (3 epochs).

TLE: temporal lobe epilepsy; EMD: empirical mode decomposition; WT: wavelet transform; RBF: radial basis function; SVM: support vector machines; HR: heart rate; HRV: heart rate variability; AR: auto regressive; SP: specificity; SE: sensitivity; FPR: false prediction rate.

Continued on next page

Paper	Demographics	Methodology	EEG Features	ECG Features	Results
Mporas et al. 2015 [16]	3 patients with generalized onset seizures	Seizure or non-seizure classification using SVM. 10-fold cross-validation. **Fusion:** feature vector fed into a single detector.	Minimum and maximum values, mean, variance, standard deviation, percentiles (25%, 50median and 75%), interquartile range, mean absolute deviation, range, skewness, kurtosis, energy, Shannons entropy, logarithmic energy entropy, number of positive and negative peaks, zero-crossing rate; 6-th order AR coefficients, power spectral density, frequency with maximum and minimum amplitude, spectral entropy, delta-theta-alpha-beta-gamma band energy; discrete WT coefficients (with Daubechies 16 and 8 decomposition levels).	HR absolute value and variability statistics of the HR, i.e. minimum value, maximum value, mean, variance, standard deviation, percentiles (25%, 50%-median and 75%), interquartile range and mean absolute deviation, range	Mean accuracy for all patients of 92.47%, mean precision for all patients of 85.27% and mean SE for all patients of 99.96% .
Valderrama et al. 2010 [31]	4 patients (mean duration of 14 days, 29 seizures and 1333-hour-long interictal). Besides scalp EEG, intracranial EEG was also recorded in one patient. Patients diagnosed with drug resistant focal epilepsy.	SVM (RBF kernel). 3-fold cross-validation. **Preictal** duration set to 10 min and **postictal** duration set to 5 min. **Fusion:** feature vector fed into a single detector.	Mean, variance, skewness, kurtosis, long term energy. Mean-squared error of estimation AR models (model order 10), relative power of spectral delta, theta, alpha, beta and gamma bands, spectral edge frequency, decorrelation time, Hjorth mobility and complexity; energy of WT coefficients (with Daubechies 4 and 6 decomposition levels)	Mean, variance, maximum and minimum of RR intervals, mean, variance, maximum and minimum HR, approximate entropy; VLF, HF and LF.	Higher performance was obtained when using information from all EEG channels and all features (comparing to the use of all features for individual channels). This was not seen for ECG channels with the analysis of individual ECG channels returning similar performance. In average, highest performance (no information regarding the metric) was obtained for preictal states (90.59 ± 6.74%) followed by postictal (89.06 ± 11.60%), interictal (85.64 ± 7.78%) and ictal (65.62 ± 16.84%) states, using all features and all channels from both EEG and ECG.

TLE: temporal lobe epilepsy; EMD: empirical mode decomposition; WT: wavelet transform; RBF: radial basis function; SVM: support vector machines; HR: heart rate; HRV: heart rate variability; AR: auto regressive; SP: specificity; SE: sensitivity; FPR: false prediction rate.

Continued on next page

Paper	Demographics	Methodology	EEG Features	ECG Features	Results
Valderrama et al. 2012 [30]	12 patients (duration range of 4-20 days, mean duration of 12 days, 108 seizures and 3178-hours of data); 12 patients have scalp EEG recordings and 6 have intracranial EEG; Patients diagnosed with drug resistant focal epilepsy.	SVM (with multi-class linear classification in order to distinguish interictal, preictal, ictal and postictal classes). 3-fold cross-validation. In-sample and out-of-sample classifications. Different **preictal** periods were tested (5, 10, 20, 30, 45 and 60 min). **Fusion:** feature vector fed into a single detector. Validation of preictal period's classification using a null model based on seizure time surrogates.	Mean, variance, skewness, kurtosis, long term energy; mean-squared error of estimation AR models (model order 10), relative power of spectral delta, theta, alpha, beta and gamma bands, spectral edge frequency and power, decorrelation time, Hjorth mobility and complexity; energy of WT coefficients (with Daubechies 4 and 6 decomposition levels).	Mean, variance, maximum and minimum of RR intervals, mean, variance, maximum and minimum HR, approximate entropy; VLF and LF.	Mean duration of preictal period was 37.5±14.5 min, ranging from 20 to 60 min. In 83% of cases the best performance was achieved when using all features. Classification performance using individual ECG channels was similar to the classification using individual EEG channels, with the highest accuracy having been achieved using single ECG channels in 58% of the patients. In-sample classification resulted in the best performance being substantially higher than out-of sample classification. In 75% of cases the accuracies obtained were statistically significant when comparing to a random surrogates. In the search for the most discriminative features for out-of-sample classification, it was possible to conclude that good performances were obtained for specific stages of sleep, which are in turn more or less susceptible to seizures.

TLE: temporal lobe epilepsy; EMD: empirical mode decomposition; WT: wavelet transform; RBF: radial basis function; SVM: support vector machines; HR: heart rate; HRV: heart rate variability; AR: auto regressive; SP: specificity; SE: sensitivity; FPR: false prediction rate.

Continued on next page

Paper	Demographics	Methodology	EEG Features	ECG Features	Results
Mesbah et al. 2012 [13]	8 newborns (8 EEG/ECG records, 13 seizures with total duration of 33 min and mean duration of 2.54 min, mean record duration of 21.22 min, 2.8 hours of data). Focal onset seizures.	Linear, quadratic, and k-NN (with k = 1, 3, and 5) classifiers using a leave-one-out cross validation. Feature selection using a fast correlation based filter. **Fusion:** (i) feature vector fed into a single detector and (ii) independent detectors for each modality and final decision given by different operators (mean, maximum, minimum, product and majority voting).	Mean, standard deviation, skewness, kurtosis, coefficient of variation, RMS, zero-crossings, Hjorth parameters and total nonlinear score; peak frequency maximum frequency, bandwidth and spectral power of the dominant spectral peak; total time-frequency (TF) energy, the largest and smallest singular values of the TF distributions (TFD) and number of TF components with prefixed minimum duration; variance of detail components of scales 2, 3, 4, 6, 7 and approximation component of scale 9 and mean of detail coefficient of scales 5, 6 and 9 obtained using WT (Daubechies 4 and 9 decomposition levels).	HRV: mean, standard deviation and Hjorth parameters; mean, standard deviation, median, RMS, minimum, maximum, coefficient of variation, skewness, and kurtosis extracted from the instantaneous frequency, instantaneous bandwidth and instantaneous amplitude of the LF, mid-frequency (MF) and HF components; energy in LF, MF, and HF components, total energy in all HRV components, LF/HF; generalized Shannon entropy of the normalized TFD.	Best overall performance obtained at (i) the feature level fusion scheme for the 1-NN classifier (SE of 95.20% and SP of 88.60%) and (ii) the decision level scheme for mean, maximum, minimum, product and sum decision rules (SE of 95.20% and SE of 94.30%). Multimodal seizure detector outperformed individual EEG and ECG classifiers. Best performances were obtained using the reduced-dimension feature sets (both for the case of individual classifiers as for the fusion classifier schemes).

TLE: temporal lobe epilepsy; EMD: empirical mode decomposition; WT: wavelet transform; RBF: radial basis function; SVM: support vector machines; HR: heart rate; HRV: heart rate variability; AR: auto regressive; SP: specificity; SE: sensitivity; FPR: false prediction rate.

Continued on next page

Paper	Demographics	Methodology	EEG Features	ECG Features	Results
Greene et al. 2007 [8]	10 newborns (12 EEG/ECG records, 633 seizures, mean seizure duration of 4.6 min, mean record duration of 12.84 hours, 154.1 hours of data). Focal and generalized onset seizures.	Linear discriminant analysis. Patient-independet and patient-dependent classifiers. **Fusion:** (i) feature vector fed into a single detector and (ii) independent detectors for each modality and final weighted (static and dynamic) decision.	Nonlinear energy, line length, dominant spectral peak, power ratio, bandwidth of dominant spectral peak and spectral entropy.	Mean and standard deviation of RR intervals, mean RR interval spectral entropy, mean change in RR interval, RR interval coefficient of variation and RR interval power spectral density.	Multimodal seizure detector outperformed individual EEG and ECG classifiers. Feature level fusion scheme returned better overall performance than decision level scheme. Dynamic weighting, by dealing with the presence of artifact, electrode drop-off and/or interference, returned best results comparing to the static weighting. The patient-specific approach was found to provide the best performance (good detection rate of 97.52%, FDR of 13.18%, SE of 74.08%, SP of 86.82%) comparing to the patient-independent.
Shoeb et al. 2009 [25]	Two patients. Patient A: focal onset impaired awareness seizures, 81 hours of data. Patient B: focal to bilateral tonic-clonic seizure, 26 hours of data.	Patient-specific approach. **Fusion:** independent detectors, SVM used for EEG and threshold-based linear classifier used for ECG.	7 overlapping frequency bands, 3 Hz wide and collectively spanning 020 Hz.	Average HR computed over the 3 minute period.	Patient A: 5/5 seizures were detected and a FPR of one false alarm every 2.5 hours. Patient B: 1/1 seizure was detected and no false alarm raised.

TLE: temporal lobe epilepsy; EMD: empirical mode decomposition; WT: wavelet transform; SVM: support vector machines; HR: heart rate; HRV: heart rate variability; AR: auto regressive; SP: specificity; SE: sensitivity; FPR: false prediction rate.

References

1. Bialer, M., Johannessen, S.I., Levy, R.H., Perucca, E., Tomson, T., White, H.S., Koepp, M.J.: Seizure detection and neuromodulation: A summary of data presented at the XIII conference on new antiepileptic drug and devices (EILAT XIII). Epilepsy Research 130, 27–36 (feb 2017), https://www.sciencedirect.com/science/article/pii/S0920121116302194?via{%}3Dihubhttp://linkinghub.elsevier.com/retrieve/pii/S0920121116302194
2. Delamont, R.S., Walker, M.C.: Pre-ictal autonomic changes. Epilepsy Research 97(3), 267–272 (dec 2011), http://www.sciencedirect.com/science/article/pii/S092012111100324Xhttp://linkinghub.elsevier.com/retrieve/pii/S092012111100324X
3. Devinsky, O.: Effects of Seizures on Autonomic and Cardiovascular Function. Epilepsy Currents 4(2), 43–46 (2004), http://www.ncbi.nlm.nih.gov/pubmed/15562299http://www.pubmedcentral.nih.gov/articlerender.fcgi?artid=PMC531654http://www.pubmedcentral.nih.gov/articlerender.fcgi?artid=531654{&}tool=pmcentrez{&}rendertype=abstract
4. Eggleston, K.S., Olin, B.D., Fisher, R.S.: Ictal tachycardia: The headheart connection. Seizure 23(7), 496–505 (aug 2014), http://linkinghub.elsevier.com/retrieve/pii/S1059131114000636
5. Freestone, D.R., Karoly, P.J., Peterson, A.D.H., Kuhlmann, L., Lai, A., Goodarzy, F., Cook, M.J.: Seizure Prediction: Science Fiction or Soon to Become Reality? (nov 2015), http://link.springer.com/10.1007/s11910-015-0596-3
6. Fürbass, F., Kampusch, S., Kaniusas, E., Koren, J., Pirker, S., Hopfengärtner, R., Stefan, H., Kluge, T., Baumgartner, C.: Automatic multimodal detection for long-term seizure documentation in epilepsy. Clinical Neurophysiology 128(8), 1466–1472 (aug 2017), http://linkinghub.elsevier.com/retrieve/pii/S1388245717301980
7. Gravina, R., Alinia, P., Ghasemzadeh, H., Fortino, G.: Multi-sensor fusion in body sensor networks: State-of-the-art and research challenges. Information Fusion 35, 68–80 (may 2017), http://www.sciencedirect.com/science/article/pii/S156625351630077Xhttp://linkinghub.elsevier.com/retrieve/pii/S156625351630077X
8. Greene, B.R., Boylan, G.B., Reilly, R.B., de Chazal, P., Connolly, S.: Combination of EEG and ECG for improved automatic neonatal seizure detection. Clinical Neurophysiology 118(6), 1348–1359 (jun 2007), http://www.sciencedirect.com/science/article/pii/S1388245707000521http://linkinghub.elsevier.com/retrieve/pii/S1388245707000521
9. Jansen, K., Lagae, L.: Cardiac changes in epilepsy. Seizure 19(8), 455–60 (oct 2010), http://www.ncbi.nlm.nih.gov/pubmed/20688543
10. Khaleghi, B., Khamis, A., Karray, F.O., Razavi, S.N.: Multisensor data fusion: A review of the state-of-the-art. Information Fusion 14(1), 28–44 (jan 2013), http://www.sciencedirect.com/science/article/pii/S1566253511000558http://linkinghub.elsevier.com/retrieve/pii/S1566253511000558
11. van der Lende, M., Surges, R., Sander, J.W., Thijs, R.D.: Cardiac arrhythmias during or after epileptic seizures. Journal of Neurology, Neurosurgery & Psychiatry 87(1), 69—-74 (jun 2015), http://jnnp.bmj.com/content/87/1/69.abstracthttp://jnnp.bmj.com/lookup/doi/10.1136/jnnp-2015-310559
12. McCraty, R.: Science of the Heart: Exploring the Role of the Heart in Human Performance Volume 2. HeartMath Institute, Boulder Creek, CA (2016), http://rgdoi.net/10.13140/RG.2.1.3873.5128

13. Mesbah, M., Balakrishnan, M., Colditz, P.B., Boashash, B.: Automatic seizure detection based on the combination of newborn multi-channel EEG and HRV information. EURASIP Journal on Advances in Signal Processing 2012(1), 215 (dec 2012), https://asp-eurasipjournals.springeropen.com/articles/10.1186/1687-6180-2012-215
14. Ming-Zher Poh, Loddenkemper, T., Swenson, N.C., Goyal, S., Madsen, J.R., Picard, R.W.: Continuous monitoring of electrodermal activity during epileptic seizures using a wearable sensor. In: 2010 Annual International Conference of the IEEE Engineering in Medicine and Biology. vol. 2010, pp. 4415–4418. IEEE (aug 2010), http://ieeexplore.ieee.org/document/5625988/http://www.ncbi.nlm.nih.gov/pubmed/21095760
15. Mporas, I., Tsirka, V., Zacharaki, E.I., Koutroumanidis, M., Megalooikonomou, V.: Online Seizure Detection from EEG and ECG Signals for Monitoring of Epileptic Patients. In: Lecture Notes in Computer Science (including subseries Lecture Notes in Artificial Intelligence and Lecture Notes in Bioinformatics), vol. 8445 LNCS, pp. 442–447. Springer, Cham (2014), http://link.springer.com/10.1007/978-3-319-07064-3{_}37
16. Mporas, I., Tsirka, V., Zacharaki, E.I., Koutroumanidis, M., Richardson, M., Megalooikonomou, V.: Seizure detection using EEG and ECG signals for computer-based monitoring, analysis and management of epileptic patients. Expert Systems with Applications 42(6), 3227–3233 (apr 2015), http://linkinghub.elsevier.com/retrieve/pii/S0957417414007763
17. Nasehi, S., Pourghassem, H.: Seizure Detection Algorithms Based on Analysis of EEG and ECG Signals: a Survey. Neurophysiology 44(2), 174–186 (jun 2012), http://link.springer.com/10.1007/s11062-012-9285-x
18. Osorio, I., Manly, B.: Probability of detection of clinical seizures using heart rate changes. Seizure 30, 120–123 (2015)
19. Piper, D., Schiecke, K., Pester, B., Benninger, F., Feucht, M., Witte, H.: Time-variant coherence between heart rate variability and EEG activity in epileptic patients: an advanced coupling analysis between physiological networks. New Journal of Physics 16(11), 115012 (nov 2014), http://stacks.iop.org/1367-2630/16/i=11/a=115012?key=crossref.e244fbb4a14679ffbf46ca2a23e26a5f
20. Poh, M.Z., Loddenkemper, T., Reinsberger, C., Swenson, N.C., Goyal, S., Sabtala, M.C., Madsen, J.R., Picard, R.W.: Convulsive seizure detection using a wrist-worn electrodermal activity and accelerometry biosensor. Epilepsia 53(5), e93–e97 (may 2012), http://doi.wiley.com/10.1111/j.1528-1167.2012.03444.x
21. Qaraqe, M., Ismail, M., Serpedin, E., Zulfi, H.: Epileptic seizure onset detection based on EEG and ECG data fusion. Epilepsy & Behavior 58, 48–60 (may 2016), http://www.sciencedirect.com/science/article/pii/S152550501600113Xhttp://linkinghub.elsevier.com/retrieve/pii/S152550501600113X
22. Rugg-Gunn, F.J., Holdright, D.: Epilepsy and the Heart. British Journal of Cardiology pp. 223–229 (2010), http://www.medscape.com/viewarticle/730022
23. Sevcencu, C., Struijk, J.J.: Autonomic alterations and cardiac changes in epilepsy. Epilepsia 51(5), 725–737 (may 2010), http://doi.wiley.com/10.1111/j.1528-1167.2009.02479.x
24. Shmuely, S., van der Lende, M., Lamberts, R., Sander, J., Thijs, R.: The heart of epilepsy: Current views and future concepts. Seizure 44, 176–183 (jan 2017), http://www.sciencedirect.com/science/article/pii/S1059131116301698http://linkinghub.elsevier.com/retrieve/pii/S1059131116301698

25. SHOEB, A., PANG, T., GUTTAG, J., SCHACHTER, S.: NON-INVASIVE COMPUTERIZED SYSTEM FOR AUTOMATICALLY INITIATING VAGUS NERVE STIMULATION FOLLOWING PATIENT-SPECIFIC DETECTION OF SEIZURES OR EPILEPTIFORM DISCHARGES. International Journal of Neural Systems 19(03), 157–172 (jun 2009), http://www.ncbi.nlm.nih.gov/pubmed/19575506http://www.pubmedcentral.nih.gov/articlerender.fcgi?artid=PMC4211613http://www.worldscientific.com/doi/abs/10.1142/S0129065709001938
26. Stollberger, C., Finsterer, J., Tigaran, S., Jaffe, A.S.: Evidence of cardiac ischemia during seizures in drug refractory epilepsy patients. Neurology 62(7), 1238–1239 (apr 2004), http://www.ncbi.nlm.nih.gov/pubmed/12578934http://www.neurology.org/cgi/doi/10.1212/WNL.62.7.1238-a
27. Surges, R., Scott, C.A., Walker, M.C.: Enhanced QT shortening and persistent tachycardia after generalized seizures. Neurology 74(5), 421–426 (feb 2010), http://www.ncbi.nlm.nih.gov/pubmed/20124208http://www.pubmedcentral.nih.gov/articlerender.fcgi?artid=PMC2872619http://www.neurology.org/cgi/doi/10.1212/WNL.0b013e3181ccc706
28. Tripathi, M., Choudhary, N.: Significance of Heart Rate Variability in Patients with Epilepsy. In: Kamath, M.V., Watanabe, M., Upton, A. (eds.) Heart Rate Variability (HRV) Signal Analysis: Clinical Applications, chap. 21, p. 513. CRC Press, Boca Raton, FL (2013), http://www.amazon.com/Heart-Rate-Variability-Signal-Analysis/dp/1439849803
29. Ulate-Campos, A., Coughlin, F., Gaínza-Lein, M., Fernández, I.S., Pearl, P., Loddenkemper, T.: Automated seizure detection systems and their effectiveness for each type of seizure. Seizure 40, 88–101 (aug 2016), https://www.sciencedirect.com/science/article/pii/S1059131116300711?{_}rdoc=1{&}{_}fmt=high{&}{_}origin=gateway{&}{_}docanchor={&}md5=b8429449ccfc9c30159a5f9aeaa92ffbhttp://linkinghub.elsevier.com/retrieve/pii/S1059131116300711
30. Valderrama, M., Alvarado, C., Nikolopoulos, S., Martinerie, J., Adam, C., Navarro, V., Le Van Quyen, M.: Identifying an increased risk of epileptic seizures using a multi-feature EEGECG classification. Biomedical Signal Processing and Control 7(3), 237–244 (may 2012), http://www.sciencedirect.com/science/article/pii/S1746809411000450http://linkinghub.elsevier.com/retrieve/pii/S1746809411000450
31. Valderrama, M., Nikolopoulos, S., Adam, C., Navarro, V., Le Van Quyen, M.: Patient-specific seizure prediction using a multi-feature and multi-modal EEG-ECG classification. In: IFMBE Proceedings. vol. 29, pp. 77–80. Springer, Berlin, Heidelberg (2010), http://link.springer.com/10.1007/978-3-642-13039-7{_}20
32. Van de Vel, A., Cuppens, K., Bonroy, B., Milosevic, M., Jansen, K., Van Huffel, S., Vanrumste, B., Cras, P., Lagae, L., Ceulemans, B.: Non-EEG seizure detection systems and potential SUDEP prevention: State of the art. Seizure 41, 141–153 (oct 2016), https://www.sciencedirect.com/science/article/pii/S1059131116301145?via{%}3Dihubhttp://linkinghub.elsevier.com/retrieve/pii/S1059131116301145
33. Zijlmans, M., Flanagan, D., Gotman, J.: Heart Rate Changes and ECG Abnormalities During Epileptic Seizures: Prevalence and Definition of an Objective Clinical Sign. Epilepsia 43(8), 847–854 (aug 2002), http://doi.wiley.com/10.1046/j.1528-1157.2002.37801.x

Cardiovascular effects of stress and emotions: a brief overview of concepts and assessment methods

Pierluigi Reali[1], Antonio Martinez-Millana[2], Paulo de Carvalho[3], and Anna Maria Bianchi[1]

[1] Politecnico di Milano, Dept. of Electronics Information and Bioengineering (DEIB), Via Golgi 39, 20133 Milano, Italy
{pierluigi.reali, annamaria.bianchi}@polimi.it
[2] Universitat Politécnica de Valencia, ITACA, Camino de Vera S/N, 46022 Valencia, Spain
anmarmil@itaca.upv.es
[3] Universidade dei Coimbra, Centre for Informatics and Systems, Polo II, 3030-290 Coimbra, Portugal
carvalho@dei.uc.pt

Abstract. Stress and emotions can cause several physiological and behavioral changes, some of which may also have a severe impact on the cardiovascular function. For this reason, an accurate assessment of stress level and emotion kind and strength should be considered important to reduce the associated cardiovascular risks. However, the use of biological parameters to reliably evaluate stress and emotions requires appropriate experimental choices and analysis methods to minimize the variability of the measures and ensure a better comparison between different subjects. The aim of the present paper is to provide a critical, though brief, overview of some of the most used biological parameters that can be considered to quantitatively assess stress and emotions.

1 Introduction

It is known that stress, in the form of many psychosocial factors [1], can greatly affect our lives and cause several changes to our body's physiology. There are, at least, two pathways involved in such changes [2]: first, a fast neuroendocrine response, characterized by the release of adrenaline from the adrenal medulla and noradrenaline from sympathetic synapses, that produces cognitive engagement and several effects on cardiovascular and respiratory systems (e.g. bronchodilation, increased blood pressure and heart rate). Second, a slower adrenocortical component that provokes the release of glucocorticoids, especially cortisol; while in the short-term, glucocorticoids are important to prepare the energy reserves required to cope with stressful situations by changing various metabolic mechanisms and increasing blood glucose level, a prolonged release of glucocorticoids can have several negative effects, including immune system suppression [2], increase in blood pressure, obesity, insulin resistance and other metabolic disfunctions [3]. Since those are also recognized cardiovascular risk

C.Fernandez-Llatas and M.Guillen (Ed.):
Workshop on Innovation on
Information and Communication Technologies
(ITACA-WIICT 2018)

ISBN 978-84-09-07373-3

factors, it follows that stress can have direct implications on the development or worsening of several cardiovascular diseases.

Stress, originally defined as "the non-specific response of the body to any noxious stimulus" (Selye, 1936) [4], can arise from very different situations. Given the difficulties of measuring the biological reaction to stress in real-life conditions, mainly related to the impossibility of recreating standardized experimental conditions [5], many studies focus their attention on creating stressful situations in laboratory settings and analyzing the biological response to them. Some tasks that are typically used to induce stress are arithmetical calculations, speech and other verbal tasks [6]. Previous laboratory studies have revealed a significant increase in heart rate and systolic blood pressure induced by arithmetical calculations [6, 7], indicating an increased sympathetic activation during moderate stress conditions. However, although a laboratory setting has the great advantage of allowing the control of many confounding factors [5] and there are evidences that the physiological stress responses elicited by the most commonly used tasks are significantly associated with stress responses experienced in real-life [8], there are also some limitations regarding this kind of laboratory studies. In particular, the use of those non-specific laboratory tasks is limited to the assessment of short-term stress response in healthy subjects [5] and cannot take into account the chronic aspects of stress, which seem to be primarily responsible for the pathophysiologic changes caused by stress and, specifically, for the association between psychosocial stress and cardiovascular diseases [3].

To account for those long-term aspects, some authors have carried out studies considering specific groups of chronically (or periodically) stressed subjects and investigating the physiological response to real-life stressors, in order to maximize the stress response of that specific group and, eventually, comparing the response between subjects with different levels of reported stress. For example, following this kind of approach, some studies have investigated the physiological stress response of university students during an examination session and compared it with measurements done during the subsequent holiday period [9]. Other studies have analyzed the physiological reaction to gambling, which is another particular form of stressor caused by the unpredictability of the result that, by definition, characterizes each kind of gamble. During gambling, increased levels of cortisol have been documented by several researches [10,11,12], suggesting the activation of the same hypothalamic-pituitary-adrenal (HPA) axis involved in reaction to other stressors. Also heart rate was found to be increased during gambling [11], suggesting an increased sympathetic activation, which is consistent with the stress response observed in other studies [7]. Some of these studies found also a significant dampening of cortisol secretion in frequent or pathological gamblers compared with recreational ones [11,12], similar to what has been observed in chronic drug consumption and other sorts of addictions.

Regarding the second main topic of this work, namely the emotions, the link between stress and emotions is well documented in the literature [13]. In particular, a better management of the emotions is considered important to cope with stress [13,14] and some findings in the field of emotional intelligence suggest a greater impact of stress on people with high emotion perception, while people with low emotion perception seems to be less sensitive to stress noxious effects [15]. From this point of view, being able to quantitatively evaluate the kind and strength of emotions felt by different categories of people while reacting to certain stimuli may be important to infer their exposure to stress effects. Also, there are evidences of a straight link between emotions and cardiovascular diseases. For instance, while it has been found that specific negative emotions, like anxiety, anger and depression, may play an important role in the development of coronary heart disease [16], positive emotions, specifically optimism, seem to have a protective function against angina and heart attacks and to positively influence physical recovery after coronary artery bypass [17].

The next section describes some of the mainly used methods and parameters for emotion and stress assessment from biological signals.

2 Methods

2.1 Experimental protocols

The most commonly used methods to quantitatively evaluate emotions relies on the presentation of a certain stimulus and the analysis of the consequent physiological response. There are several kinds of stimuli that can be used to elicit emotions, like music [18], odors [19], videos [20] and pictures. In particular, among pictures, the most commonly used in the literature come from the International Affective Picture System (IAPS) [21]. The IAPS database consists of pictures that are pre-evaluated in terms of valence (pleasant vs unpleasant), arousal (calm vs excited) and dominance (controlled vs uncontrolled), which are the three major dimensions that characterize an emotional state [22]. One of the main advantage of using IAPS pictures is that they are a standardized kind of stimuli, which means that the results obtained in different studies can be compared more easily [21]. Moreover, since they are pre-evaluated stimuli, they are one of the preferred tools for the development and tuning of emotion recognition methods based on the analysis of physiological signals. In this field, some of the main difficulties to deal with when designing experimental protocols with IAPS pictures are the timing of presentation (how much time a picture should be presented to record the physiological reaction to it?) and the sequence of presentation (e.g. is it better to use a random sequence or an arousal increasing one?). Of course, the answer to the first question primarily depends on the response time of the physiological signals under study; for example, it is known that the accurate estimation of frequency domain parameters from the heart rate variability (HRV) requires approximately 2 minutes of stationary signal [23], but showing the same picture for a time frame sufficiently long to meet this condition might produce an undesirable decrease of attention in the subject. As for the second question, it is true that random presentation sequences should be preferred to avoid any sequence-related effects between subsequent images (avoiding the emotional response elicited by the visualization of an image to be systematically affected by the previous one), but some authors seems to prefer the use of valence and arousal increasing protocols [24], probably because they are able to linearly increase and keep high the engagement of the subject during the experimental session.

2.2 Biological measures

In this section some of the most interesting biological parameters that can be used for both stress and emotion assessment are presented. These parameters are extracted from several signals, in order to obtain a multifactorial evaluation [25]: electroencephalography (EEG), electrodermal activity (EDA), heart rate variability signal (HRV), respiration.

The analyses conducted on the EEG typically focus on the computation of spectral power in alpha (from 8 to 13 Hz) [26], beta (from 13-30 Hz) [27] and theta (from 4 to 8 Hz) bands [28], that reflect different processing activities of the brain, and in the calculation of indices that consider the intrinsic relationships among these bands, like the Engagement Index [29,30]. Other authors proposed an approach based on the computation of the global field power (GFP) between specific sets of electrodes to estimate attention, memorization and pleasantness indices [31].

EDA is one of the mostly used signals to quantify sympathetic activity associated with emotion, cognition and attention [25], also because its measurement only requires two electrodes placed on the middle phalanges of index and middle fingers. There are many indices that can be extracted from EDA. The simplest one is the average value of the signal (mean EDA), calculated after a low pass filtering with cut-off frequency of 2.5 Hz, intended to remove movement and contact artifacts while preserving the useful frequency content [32]. The mean value of EDA was found to be positively correlated with the level of emotional arousal [25]. Other more complex indices proposed in the literature applies the decomposition of the EDA into a slowly-varying tonic part and a fast-varying phasic part [33], allowing for a differentiated analysis of the two components. In particular, the decomposition procedure gives the possibility to analyze the phasic component, that appears to be the mostly related to sympathetic activity, without the superposition of the previous responses that, in the raw signal, would be preserved by the tonic component [33]. By following this approach, two major indices can be calculated [33,34]: the integrated skin conductance response (ISCR), that is the time integral of the phasic driver, and the sum of the amplitude of the phasic driver peaks (AmpSum).

The HRV signal can be obtained by applying Pan-Tompkins algorithm [35] to a single ECG lead to detect R peaks and, then, by computing the temporal distance between consecutive R peaks (Fig.1). There are many parameters that can be computed from HRV signal, both in the time and frequency domains. Some of the mostly used time domain parameters in the emotion and stress assessment fields are the average value (mean RR) and the standard deviation (SDRR) of the RR intervals. In particular, a reduction of mean RR can be related with increased perceived valence [19], while a significant reduction of SDRR is commonly observed during the execution of stressful laboratory tasks compared with baseline condition [36]. The frequency domain parameters mainly considered for emotion and stress evaluation are the spectral power of the HRV signal computed in the low frequency (LF, 0.04-0.15 Hz) and high frequency (HF, 0.15-0.4 Hz) bands and the ratio between them (LF/HF); LF and HF power components are typically normalized by total spectral power minus the power calculated in the very low frequency (VLF) band [23], in order to account for variations in total power between different subjects and facilitate the comparison between baseline condition and stress phase (or between baseline and the presentation of emotional stimuli). From a physiological point of view, an increase of HF power component is typically associated with vagal activity modulation; on the other hand, an increase of LF component cannot be reliably associated with sympathetic activation, because LF component was found to reflect both sympathetic and vagal activity [23]; the LF/HF ratio, by representing the sympatho-vagal balance, is often considered a valid substitute of the LF component to assess sympathetic activation [23].

In studies related to emotion and stress assessment, the respiratory signal is usually acquired by means of a non-calibrated thoracic or abdominal elastic band and so no information about respiratory volumes is available. Of course, there are some exceptions documented in the literature, like in [37] where researchers measured, by using an inductive plethysmograph, specific breath parameters such as mean expiratory flow and minute ventilation. One of the most interesting applications of the respiratory signal is provided by its association with the HRV signal for the estimation of autoregressive (AR) bivariate models [38]. This method is used to highlight common frequency content between two different biological signals, in our case the HRV signal and the respirogram (i.e. the respiratory signal sampled in occurrence of each R peak) (Fig. 1), and allows the estimation of other two parameters for the assessment of the sympatho-vagal balance: the spectral power coherent with respiration (CRP) and the non-coherent one (NCRP).

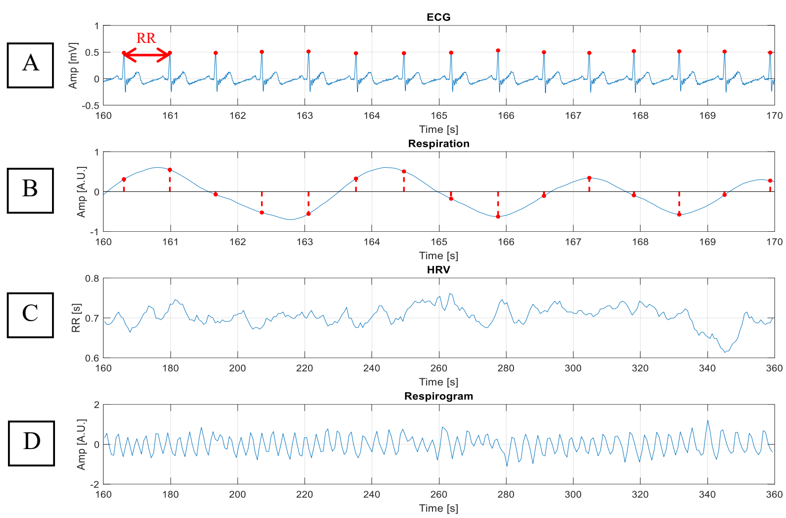

Fig. 1. Signal processing steps on ECG and respiratory signal to derive HRV and respirogram. A: ECG signal; the R peaks detected by Pan-Tompkins algorithm are marked with a red point. B: Respiratory signal; the samples considered for the respirogram are marked with a red point. C: HRV signal; the amplitude of the signal corresponds to the distances between consecutive R peaks (graphically represented in A). D: respirogram; the amplitude of the signal corresponds to the amplitude of the respiratory signal in occurrence of each R peak

An important advantage of the bivariate method over the univariate estimation of LF and HF power components is that the first does not need to recognize LF and HF frequency bands, which may vary between different subjects [38]. Both the bivariate and univariate methods have proven to be able to detect significant differences among the different phases of a stressful protocol [39].

3. Results and discussion

By using many of the parameters described in the present paper, some encouraging results, in terms of emotion evaluation, were obtained in a recent study [40]. In that study, a set of fifteen IAPS pictures was presented to fourteen healthy volunteers in random sequence and EEG, ECG and EDA were acquired during the experiments. The study aimed at developing multi-linear model for the estimation of valence, arousal and dominance levels from several biological parameters computed from those signals. By means of stepwise regression algorithm, a subset of significant features was selected and the obtained three final multi-linear regression models (one for each dimension) show an overall good performance in predicting valence, arousal and dominance of the considered IAPS pictures by using mean RR, mean EDA, EEG alpha, beta and theta power as predictor variables. It is worth noting that no frequency domain HRV parameter resulted sufficiently significant to be included in the models; this could be attributed to the fact that each stimulus (i.e. each IAPS picture) was analyzed for only 14 seconds that, as previously said, cannot be considered a sufficient time frame for an accurate estimation of LF and HF power components. Some improvements may be obtained by changing timing and presentation sequence of the IAPS images. In this sense, a hybrid approach that may provide sufficiently long time frames of analysis while maintaining enough subject's engagement, could be obtained by presenting blocks of images characterized by similar levels of arousal, valence and dominance and considering each block as a single time frame with mean arousal and valence computed among the images included in that block; each block and its pictures could be still presented in random sequence to avoid the previously described sequence-related effects.

Stress and emotion assessment studies have several potential clinical applications. As highlighted in the present and many other papers, both stress and emotion-related conditions (like depression) are associated with severe cardiovascular risks. By investigating the physiological mechanisms that underly these phenomena, it may be possible to ensure better containment of those risks, early diagnosis and improved management of dangerous stress and emotional situations. In particular, the development of reliable physiological models for emotions evaluation may improve the diagnosis and follow-up of some mental conditions, like depression [41], characterized by impaired emotion regulation (i.e. reduced capability of controlling emotions, compared with healthy subjects). Moreover, an important outcome of stress assessment studies may be the development of data processing methods for the detection of stress level at work, which may help in preventing and managing the recognized cardiovascular consequences of job-related stress, like hypertension.

References

1. Hemingway H., Marmot, M.: Psychosocial factors in the etiology and prognosis of coronary heart disease: systematic review of prospective cohort studies. The British Medical Journal, 318 (1999) 1460–1467.
2. Brunner E.: Stress and the biology of inequality. The British Medical Journal, 314 (1997) 1472-1476.
3. Fraser R., Ingram M.C., Anderson N.H., Morrison C., Davies E., Connell J.M.C.: Cortisol Effects on Body Mass, Blood Pressure, and Cholesterol in the General Population. Hypertension, 33 (1999) 1364-1368.
4. Selye, H.: A syndrome produced by diverse nocuous agents. Nature, 138 (1936) 32.
5. Chida Y., Steptoe A.: Greater Cardiovascular Responses to Laboratory Mental Stress Are Associated With Poor Subsequent Cardiovascular Risk Status. Hypertension, 55 (2010) 1026-1032.
6. Brugneraa A., Zarbo C., Tarvainen M.P., Marchettini P., Adorni R., Compare A.: Heart rate variability during acute psychosocial stress: A randomized crossover trial of verbal and non-verbal laboratory stressors. International Journal of Psychophysiology, 127 (2018) 17–25.
7. Guasti L., Simoni C., Mainardi L., Crespi C., et al.: Lack of relationship between cardiovascular reactivity to mental stress and autonomic modulation of the sinoatrial node in normotensive and hypertensive male subjects. International Journal of Psychophysiology 71 (2009) 258–263.
8. Henze G., Zänkert S., Urschler D.F., Hitl T.J., et al.: Testing the ecological validity of the Trier Social Stress Test: Association with real-life exam stress. Psychoneuroendocrinology 75 (2017) 52–55.
9. Melillo P., Bracale M., Pecchia L.: Nonlinear Heart Rate Variability features for real-life stress detection. Case study: Students under stresss due to university examination. BioMedical Engineering Online, 10:96 (2011).
10. Potenza, M.N., Fiellin D.A., Heninger G.R, Rounsaville B.J., Mazure C.M.: Gambling. An addictive behavior with health and primary care implications, J. Gen. Intern. Med., 17 (2002) 721-732.
11. Meyer G., Schwertfegerb J., Exton M.S., Janssen O.E., Knapp W., Stadler M.A., Schedlowski M., Kruger T.H.C.: Neuroendocrine response to casino gambling in problem gamblers, Psychoneuroendocrinology, 29 (2004) 1272–1280.
12. Paris J.J., Franco C., Sodano R., Frye C.A., Wulfert E.: Gambling pathology is associated with dampened cortisol response among men and women. Physiology & Behavior, 99 (2009) 230–233.
13. Lazarus R.S., FROM PSYCHOLOGICAL STRESS TO THE EMOTIONS: A History of Changing Outlooks. Annu. Rev. Psychol. 44 (1993) 1-21.
14. Bradley R.T., McCraty R., Atkinson M., Tomasino D., Daugherty A., Arguelles L.: Emotion Self-Regulation, Psychophysiological Coherence, and Test Anxiety: Results from an Experiment Using Electrophysiological Measures. Appl. Psychophysiol. Biofeedback, 35 (2010) 261–283.
15. Ciarrochi J., Deane F.P., Anderson S.: Emotional intelligence moderates the relationship between stress and mental health. Personality and individual differences, 32 (2002) 197-209.
16. Kubzansky L.D., Kawachi I.: Going to the heart of the matter: do negative emotions cause coronary heart disease?. Journal of Psychosomatic Research, 48 (2000) 323–337.
17. Tugade M.M., Fredrickson B.L., Barrett L.F.: Psychological Resilience and Positive Emotional Granularity: Examining the Benefits of Positive Emotions on Coping and Health. Journal of Personality 72 (2004) 1161-1190.

18. Kim J. and André E.: Emotion Recognition Based on Physiological Changes in Music Listening. IEEE Transactions on Pattern Analysis and Machine Intelligence, 30 (2008) 2067-2083.
19. Bensafi M., Rouby C., Farget V., Bertrand B., Vigouroux M., Holley A.: Autonomic nervous system responses to odours: the role of pleasantness and arousal. Chem. Senses, 27 (2002) 703-709.
20. Gross J.J. and Levenson R.W: Emotion elicitation using films. Cognition Emotion, 9 (1995) 87-108.
21. Lang P.J., Bradley M. M. and Cuthbert B.N.: International affective picture system (IAPS): Affective ratings of pictures and instruction manual. Technical Report A-8. University of Florida, Gainesville, FL (2008).
22. Russel J. and Mehrabian A.: Evidence for a three-factor theory of emotions. J. Research in Personality, 11 (1977) 273-294.
23. Task Force of The European Society of Cardiology and The North American Society of Pacing and Electrophysiology: Heart rate variability: standards of measurement, physiological interpretation, and clinical use. European Heart Journal, 17 (1996) 354-381.
24. Nardelli M., Valenza G., Greco A., Lanata A., Scilingo E.P.: Recognizing emotions induced by affective sounds through heart rate variability. IEEE Transactions on affective computing, 6 (2015) 385-394.
25. Granero A.C., Fuentes-Hortado F., Ornedo V.N., Provinciale J.G., Ausìn J.M., Raya M.A.: A comparison of physiological signal analysis techniques and classifiers for automatic emotional evaluation of audiovisual contents. Frontiers in Computational Neuroscience, 10 (2016).
26. Gerrard P. and Malcolm R., Mechanism of modafinil: a review of current research. Neuropsychi-atr. Dis. Treat., 3 (2007) 349–364.
27. Pfurtscheller G. and Lopes da Silva F.H., Event-related EEG/MEG synchronization and desyn-chronization: Basic principles. Clinical Neurophysiology 110 (1999) 1842–1857.
28. Sakowitz O.W., Schurmann M. and Basar E., Oscillatory frontal theta responses are increased upon bisensory stimulation. Clin. Neurophysiol., 111 (2000) 884-893.
29. Pope A.T., Bogart E.H., Bartolome D.S., Biocybernetic system evaluates indices of operator engagement in automated task. Biological Physiology, 40 (1995) 187-195.
30. Chaouachi M., Frasson C., Exploring the relationship between learner EEG mental engagement and affect, in V. Aleven, J. Kay, J. Mostow (eds) Intelligent Tutoring Systems. ITS 2010. Lecture Notes in Computer Science, vol. 6095, Springer, Berlin, Heidelberg (2010).
31. Vecchiato G., Cherubino P., Maglione A.G., Kong W., Hu S., Wei D., Colosimo A., Babiloni F., Comparison of cognitive and emotional cerebral variables in Eastern subjects watching TV advertisements: a case study. International Journal of Bioelec-tromagnetism, 14 (2012) 127 – 132.
32. Valenza G., Lanatà A. and Scilingo E.P., The Role of Nonlinear Dynamics in Affective Valence and Arousal Recognition, IEEE Transactions on Affective Computing, 3 (2012) 237-249.
33. Benedek M. and Kaernbach C., A continuous measure of phasic electrodermal activity. Journal of Neuroscience Methods, 190 (2010) 80-91.
34. Lajante M. and Droulers O., Measuring arousal in consumer research: a new EdA signal pro-cessing method. Advances in Consumer Research, 40 (2012) 763-764.
35. Pan J., Tompkins W.J.: A real-time QRS detection algorithm. IEEE Transactions on Biomedical Engineering, BME-32 (1985) 230-236.
36. Castaldo R., Melillo P., Bracale U., Caserta M., Triassi M., Pecchia, L.: Acute mental stress assessment via short term HRV analysis in healthy adults: A systematic review with meta-analysis. Biomedical Signal Processing and Control, 18 (2015) 370-377.

37. Gomez P., Zimmermann P., Guttormsen-Schär S., Danuser B.: Respiratory responses associated with affective processing of film stimuli. Biological psychology, 68 (2005) 223-235.
38. Bianchi A., Bontempi B., Cerutti S., Gianoglio P., Comi G., Natali Sora M.G.: Spectral analysis of heart rate variability signal and respiration in diabetic subjects. Med. Biol. Eng. Comput., 28 (1990) 205.
39. Magagnin V., Mauri M., Cipresso P., Mainardi L., Brown E.N., Cerutti S., Villamira M., Barbieri R.: Heart rate variability and respiratory sinus arrhythmia assessment of affective states by bivariate autoregressive spectral analysis. Comput Cardiol, 37 (2010) 145–148.
40. Reali P., Cosentini C., De Carvalho P., Traver V., Bianchi A.M.: Towards the development of physiological models for emotions evaluation, in International Conference of the IEEE Engineering in Medicine and Biology Society (2018). Accepted paper.
41. Joorman J., Gotlib H.: Emotion regulation in depression: relation to cognitive inhibition. Cognition and Emotion, 24 (2010) 281-298.

Exploratory study of applications of image analysis for time and cost saving evaluation for the artificial turf sport surfaces

Sánchez-Palop, Luis I.[1] Puigcerver-Palau, Sergio-Antonio[1] Durá-Gil, Juan-Vicente[1] Morón-Ballester, Raúl[1] Aragón-Basanta, Elisa[1] Alcántara-Alcover, Enrique[1] Asensio-Cuesta, Sabina[2] Laparra-Hernández, José[1] Mengual, Rafael[1]

[1] Instituto de Biomecánica de Valencia (IBV), Universidad Politécnica de Valencia, Camino de Vera s/n, 46022, Valencia, Spain

[2] Instituto de Tecnologías de la Información y Comunicaciones (ITACA), - Universitat Politècnica de València, Camino de Vera s/n. 46022 Valencia, Spain

Abstract. The aim of this paper is to present a simple, low cost and fast methodology to assess artificial turf conditions based on image processing. This methodology will help the facility manager to decide on the need of maintenance operations, without performing the more complex and expensive standard testing methodologies of the official institutions (FIFA, World Rugby, etc.). The methodology is based on image processing algorithms able to evaluate the infill and turf distribution and degradation, football rebound and football roll, and the correlation with player and maintenance expert's perception and standard testing methodologies. The results obtained are promising and provide a first approach for the field surface conditions with an adequate level of accuracy for an indicator that helps to decide what maintenance operations are necessary.

Keywords: Turf, Tests, Image processing.

1. Introduction and scope of the project

Previous studies have shown a lack of methodologies to assess the field conditions that could be performed fast and inexpensively [1]. The current testing methodologies are the standard used by the official institutions, such as FIFA or WorldRugby, to evaluate the quality of sport fields. These methodologies are often expensive and require the use of very specific equipment by well-trained experts.

However, it is not necessary to run the full list of tests to have an indicator of the field condition. A few properties provide enough information to decide whether a field is in a poor condition for the sports practice and to decide which maintenance operations will improve the mechanical behavior of the field [2, 3].

To address this need, there are approaches [4] that have been working on the use of image registration and processing for analysing the properties of artificial turf fields that are important for playability and player's safety: fiber and infill distribution, ball rebound and ball roll. This approach will provide a simple, fast setting and cheaper tool for the football fields' evaluation. It is important for the facility manager to know the

C.Fernandez-Llatas and M.Guillen (Ed.):
Workshop on Innovation on
Information and Communication Technologies
(ITACA-WIICT 2018)

ISBN 978-84-09-07373-3

current condition of the fields as an adequate maintenance is essential for the mechanical properties of the surface [5, 6]

The full list of FIFA testing procedures covers every aspect of the field performance: drainage, shock absorption, football behavior [7, 8], etc. Nonetheless, these tests are meant to evaluate and rate the quality of the field, and the scope of this research is to focus in the evaluation of the artificial turf conditions to decide on the maintenance operations that are necessary at that moment.

The aim of this paper is to present a simple, low cost and fast methodology to assess artificial turf conditions based on image processing.

2. Simplified testing methodology development

The methodology to assess the artificial turf conditions based on the image consists of two main algorithms: (1) Fiber and infill distribution testing algorithms; (2) Football rebound and roll testing algorithms.

2.1. Fiber and infill distribution testing algorithms

The evaluation of the fiber and infill distribution is the most complex of the developed techniques, as a further image processing is needed. The approach used consisted in the processing of pictures of football fields to apply a color discrimination technique that differentiates between the green of the turf fiber, the black of the infill and possible defects present in the field. For the defect detection, a zoom of the initial images is needed, as it is necessary a higher level of detail. Therefore, the resolution of the pictures taken has to be high enough to allow the zooming without an important loss of information.

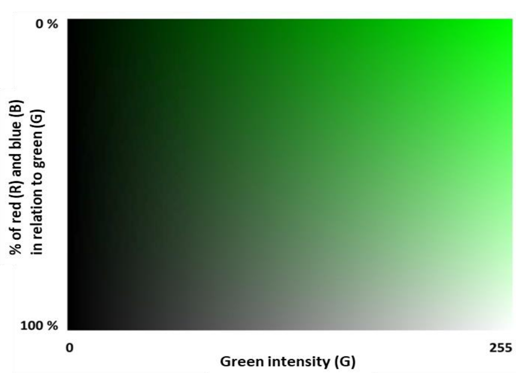

Fig. 1. RGB correlation between red (R), blue (B) and green intensity (G).

The first stage of the analysis comprised the adjustment of the different color RGB thresholds for the evaluation, with eight combinations of Red, Blue and Green intensities. Then, a series of artificial turf field pictures were analyzed using those eight combinations and the results were compared with the knowledge of selected experts.

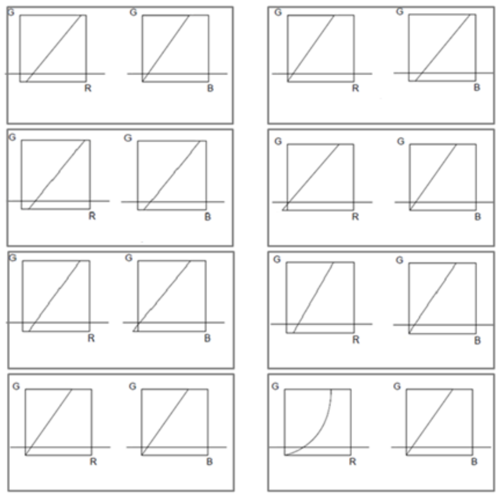

Fig. 2. Different RGB combinations tested to evaluate the artificial turf fields.

The process of picture evaluation was divided in two phases:

1. Analysis of 10 pictures of entire football fields.
2. Analysis of pictures of a detail of football fields. The pictures were obtained by zooming those from the first phase and by on-site registration.

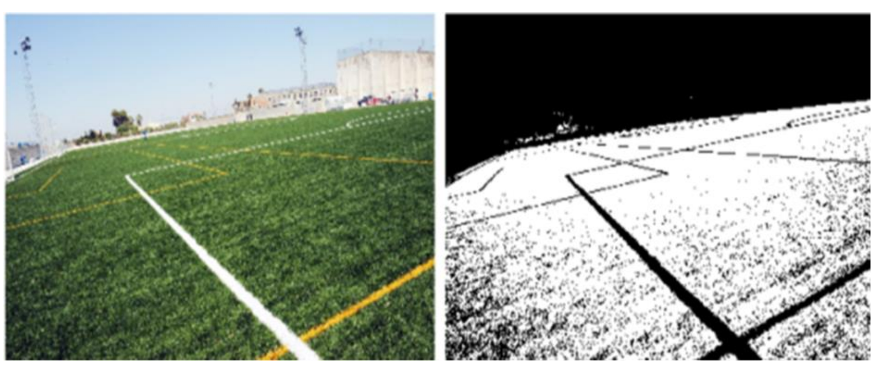

Fig. 3. Results for the analysis of a football field picture.

The results allow determining the turf field degradation and providing recommendations on what maintenance operations are necessary. In order to check the validity of the results, the verdict obtained from the image processing has been compared with the evaluation of maintenance experts and the measurements from standard methodology testing.

2.2. Football rebound and roll testing algorithms

The current testing methodology for football rebound requires special equipment to let the ball go and to measure the rebound height. An algorithm has been developed to determines the loss of energy on the rebound by measuring the height of the first rebound and calculating the height decrease on percentage, similarly to the FIFA testing.

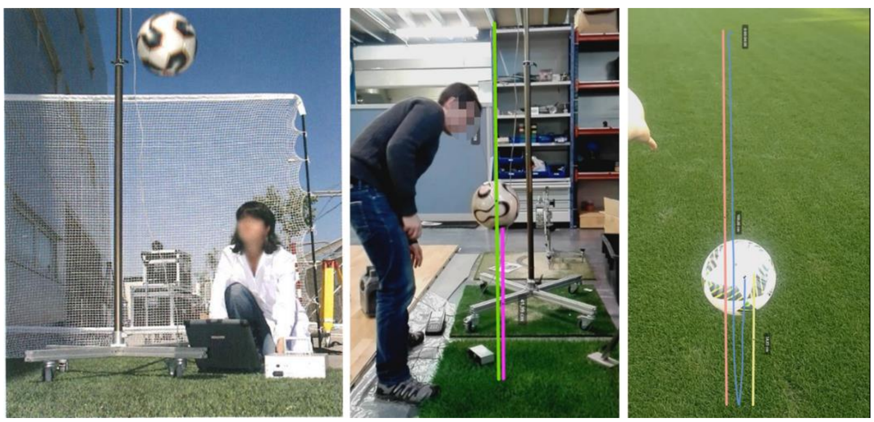

Fig. 4. Comparison between actual FIFA rebound test on the field (left) and on laboratory environment (center) and simplified rebound test (right).

The main difference between the standard test and the new methodology is that test does not require the specific equipment to measure the rebound or to release the ball. In the simplified methodology, the tester can release the ball directly from his hand, and the video registration can be done just with a mobile phone.

To validate the results obtained, the output of the algorithm has been compared with actual results of the FIFA standard methodology on different surfaces, with an average deviation of only 2%.

Table 1. Results for the algorithm developed to measure the rebound height and comparison with FIFA test results.

Surface	Release height (m)	Rebound height FIFA (m)	Percentage FIFA	Percentage algorithm	Rebound height algorithm (m)
Concrete	2,00	1,18	59,06%	59,96%	1,20
Concrete	1,85	1,10	59,25%	59,27%	1,10
Concrete	1,70	1,02	60,05%	59,70%	1,01
Concrete	1,60	0,97	60,76%	61,72%	0,99
Concrete	1,90	1,13	59,41%	60,30%	1,15
Padel	2,00	1,19	59,55%	60,44%	1,21
Padel	1,90	1,13	59,54%	60,12%	1,14
Padel	1,85	1,12	60,51%	59,77%	1,11
Padel	1,70	1,03	60,58%	60,10%	1,02
Padel	1,60	0,97	60,62%	57,43%	0,92
Football	2,00	0,87	43,29%	42,10%	0,84
Football	1,90	0,83	43,42%	42,44%	0,81
Football	1,85	0,80	43,30%	42,56%	0,79
Football	1,70	0,76	44,47%	42,44%	0,72
Football	1,60	0,70	43,70%	41,99%	0,67

For the football roll testing, the aim is also to avoid the use of specific measuring equipment and to allow the remote processing of the data gathered on field. The algorithm measures the distance travelled by the football by comparing that distance with the size of the ball.

Fig. 5. Image processed to measure the distance travelled by the football during the FIFA test.

4. Applications

4.1. Remote evaluation of field conditions

The ability to evaluate the field conditions helps reducing the costs of the maintenance operations, as it makes possible to determine the percentage of turf coverage remotely. It is important to consider that nowadays the commuting is one of the greatest costs for the inspection operations. The experts must travel from their headquarters to the field with all the equipment necessary to evaluate the field conditions on site.

This methodology allows the field managers to send the pictures taken on-site to the experts or even upload them to the web platform and receive a set of recommendations on the required maintenance operations.

4.2. History log of field conditions

The data gathered from the image processing can be recorded to create a history log of the field conditions. That information could be useful, for example, to evaluate which events are more severe to the artificial turf or estimate the tear trends of the field to optimize the maintenance with a prediction of the best time to perform the maintenance operations.

4.3. Set of simple and fast test based on mainstream technology

The official institutions such as FIFA, WorldRugby, ATP, etc. have their own standard test methodologies to rate and certificate the quality of a sports field. As mentioned before, the field certification is out of scope for this project. The main application for this work is to give the field operator a quick and economic tool to determine the field conditions on a more regular basis.

The football rebound and roll normative tests require specific equipment to measure and to let the ball go. Instead, the developed methodology simplifies the technology and equipment needed, and gives an output that can be correlated to the standard values used to rate the field conditions.

The results of the tests shall indicate if the field is adequate for the football practice, as the rebound and the roll are great indicators for the ball performance.

5. Conclusions and future work

The results for the methodology developed are quite promising considering that this is a prospective approach, and there is still room for improvement.

At this moment, the main limitations are related with the image recording conditions, especially for the fiber coverage and infill distribution analysis. The pictures shall be taken with natural light and in good weather conditions to obtain good results with the algorithm developed. However, the algorithm is at a preliminary stage, and it is expected to work with lower quality images in the future. We are currently working in the use of convolutional networks to train the algorithms and allow the methodology to be more versatile and work in different environmental conditions.

Although the set of tools have been developed and tested on football fields, the protocols and algorithms can be modified to work with different sports and surfaces. For example, the ball rebound test was also used on concrete and wooden floors, and therefore can be easily adapted for indoor sports such as futsal, handball or basketball.

As a conclusion, it is possible to simplify the current testing methodologies to evaluate the surface condition and its suitability for sport practice. Even if it will be still mandatory to perform the complete standard tests to certificate the quality of the fields, the outputs of the image processing will be a powerful tool for the daily management of sports facilities and the decision-making process for maintenance operations.

References

1. Seguridad y mantenimiento de los campos de fútbol de césped artificial. Publicaciones del Consejo Superior de Deportes INESPORT (2012)
2. How to maintain football turf. FIFA quality program for football turf. (2013)
3. McLaren, NJ., Fleming, PR., Forrester, S.: Artificial Grass: A longitudinal study on ball roll and free pile height. Procedia Engineering. Elsevier (2014)
4. Fleming, PR.: Artificial turf systems for sport surfaces: current knowledge and research needs. Proceedings of the Institution of Mechanical Engineers, Part P: Journal of Sports Engineering and Technology Vol 225, Issue 2, 43-63 (2011)
5. Sanchís, M., Alcántara, E., Rosa, D.: Efecto de las operaciones de mantenimiento sobre las propiedades de campos de césped artificial. Revista de biomecánica del Instituto de Biomecánica de Valencia, Issue 45, 27-30 (2006)
6. James, IT., McLeod, AJ.: The effect of maintenance on the performance of sand-filled synthetic turf surfaces. Sports Technology, 3(1), 43-51 (2010)
7. Handbook of test methods. FIFA quality program for football turf. (2015)
8. Guidelines for synthetic turf performance. Synthetic Turf Council (2011)

Structure and Evaluation of a Social Networking Healthcare Platform: The Case of Huzuni

Harold Kazungu-Woods[1], Sabina Asensio-Cuesta[1], Juan Miguel García-Gómez[1]

[1] ITACA Institute - Universitat Politècnica de València, Camino de Vera s/n. 46022 Valencia, Spain

hawooka@doctor.upv.es, sasensio@dpi.upv.es, juanmig@ibime.upv.es

Abstract. The Huzuni platform is designed as social networking platform for people with mental health disorders. It integrates social networking, e-learning and healthcare sub-platforms. User experience related changes play a crucial part in the user-technology interactions. Mere functionality of product-service is insufficient since now users view products as artefacts of pleasure, enjoyment, engagement and embodiment. In interface design while interactions with technology are evolving rapidly, our perception of how the user's needs have evolved has not been equally as fast and remained constrained to certain limits within the design process. This paper presents the structure and functionality of the Huzuni Social Networking Healthcare Platform. Evaluation through participatory design research and usability studies with targeted users for better user-centered design is described. This research gives insights into an alternative perspective of product user-experience, both expected and designed, from the point of the targeted audience, the future user.

Keywords: platform, ergonomics, user experience, usability, participatory design

1 Introduction

The structure and information architecture of an interface makes navigation and understanding information easy for users [1,2,3]. To archive this goal, different approaches and methods can be adopted to ensure that the structure and information is designed to the targeted users' needs [2,3]. Many user experience design and research methods exist [4,5,6,7] as the selection of the most appropriate one for each phase of the design process is very important. A hybrid of user experience and user-centered methods were applied in the concept, design and research of the Huzuni platform design, especially participatory design. Participatory design, also often referred to as co-design or co-operative design [8,9], as the name suggests, is rather a process than a result, in that, it is divided into 3 phases of; (1) understanding and problem definition; (2) creating potential solutions and; (3) testing these ideas through engaging potential targeted future users of the intended product-service during the design process [9,10]. The aim is to change the mindsets, attitudes and behaviour of the involved targeted

C.Fernandez-Llatas and M.Guillen (Ed.): Workshop on Innovation on Information and Communication Technologies (ITACA-WIICT 2018)

ISBN 978-84-09-07373-3

users or participants through mindful, playful, thoughtful and engaging innovative and experimental processes that uncover insights [10]. Insights about possible "pain points"[1] present where change is necessary at an early stage within the Huzuni platform design process.

Whereas variations exist in the way participatory design is executed across different domains [9,11,12], including healthcare design, the variations have to; (1) engage with potential targeted users, whether real users or hypothetical personas, which will be affected by the product-service design and the outcomes of the design process; and (2) operate within the boundaries of the core principles of co-design [9,10,12];

(a) Inclusive: for better results in simulations and testing solution, it should be inclusive and a representation of all groups that will be impacted by the product-service and harness the resulting decisions, thought process, experiences and feedback.

(b) Participative: the process must be open, empathetic and responsive with a high degree of engagement by participants to interact and shared gained knowledge from lived experience and generate thoughts and ideas through workshops, simulations, exercises, activities, chats, etc.

(c) Iterative: continuous re-evaluation and testing of ideas and solutions throughout the process, adapting to changes as the emerge from new scenarios with openness to creativity and exploration, and the possibility of failure during numerous attempts. Effectiveness of the interaction stages and engagement can be tested for effectiveness and pools of ideas-solutions fine-tuned to context and their potential impact based on the original objective of the task.

(d) Equivalent: all attending participants are regarded equal in expertise of their experience with set strategies applied to eliminate inequality because the product-service experience by the user is always a true value of its own experience with varying levels of ease or understanding, regardless of novice or expertise.

(e) Goal Oriented: regardless of the intention of the process, whether to design, or evaluate something existing its set to achieve a set of outcomes where the most promising of solutions can be revisited and tested or experimented in successive phases of the participatory process.

In recent years, the users' desire beyond just functionality and into the realm of experience has led to the creation of delightful and engaging user experiences. This has made user experience the norm for industry standards as a response from companies as opposed previous years when commodities held greater value [13,14]. Design trends and demand are now on products that can integrate and take into account the users' everyday lives as opposed to products that simply support the user's everyday tasks

[1] Pain points user interactions that cause a negative experience.

[15] because functionality alone can no longer compete with experiences of engagement, embodiment and pleasure [16,17]. Consequently, designers and companies have to adapt to the rising demand for user experience and its integration in the product-service-system design to stay competitive. User experience is an inevitable design goal in product-interact design [18] and a success measure for the user [19]. This has made user experience the pinnacle of product design, research and industry today which highlights the relevance of this research.

This paper presents the structure and functionality; and some of the evaluation approaches undertaken through participatory design research and usability studies with targeted future users for better user-centered design for digital health. This research gives insights into an alternative perspective of product usability and user-experience, both expected and designed, from the point of the targeted audience, the future user. The research is driven by the need to close the information gap of knowledge about expected user experiences in the early design stages to inform better digital health design decisions for the Huzuni platform.

2 Methods and Approaches

The design and development of the Huzuni platform project can be divided in two phases: concept design and concept evaluation. Six concepts were designed conceived and later discussed through inclusive participatory design with target users based on the outcomes of multiple sessions, user interviews, surveys etc. The original concept was a social networking platform geared towards mental health. Two additional concepts; (1) Health Integration, and (2) E-Learning Integration resulted from the targeted user participation. Several users and experts evaluated the platform concepts for relevance and need. These user evaluations and a feasibility analysis at different stages of the platform design served as input for an overall evaluation and discussion during the projects progression through the different stages that followed.

With usability and user experience in mind, the studies employed a selection of the most appropriate research methods available. These included methods that are previously tried-and-tested methods, e.g. usability studies to recent approaches, e.g. unmoderated online user experience assessments. The project benefited from the application of combined hybrid of multiple research methods determined by need and time – “what to do and when?” [20]. The combination of methods helped the project cover all aspects of user experience and usability with three (3) foci [20,21];

- Context of use – anticipated context of the platform usage
- Attitudinal vs. Behavioral – what people say versus what they do.
- Qualitative vs. Quantitative – quality aspects versus quantifiable analysis metrics

Each of the project’s experiments comprised either a hybrid or a combination of these three aspects at different stages. In this approach, several different methods complementarily compensate for the possible limitations of any other single method

[22,23]. For example, interpretation of data from one method can be validated in another method. Quantitative metrics data that didn't offer a user values, attitude and anticipation can be compensated with qualitative methods like user feedback and emotions.

The concepts and designs of the platform were evaluated through participatory design sessions (n=6) and usability studies (n=1) with university students (n=110) at Universitat Politècnica de València (UPV). The participants in participatory sessions were verbally guided through the storyboards and could ask questions about how specific anticipated features would work. After each session reviews were made about why, what they liked most and least, and to whom they would recommend the platform. After a series of design concepts and scenarios were shown, experimented and discussed, the participant got to choose which design concept and features were preferable. This was performed at the end of early stage concept participatory sessions and surveys though votes with; votes for favoured concept (F), unfavoured concept (U) and indecision (Z), as shown in Table 1 (below). Further discussion gave insight of preferences for a hybrid platform that combined some of the individual concepts.

Table 1. Platform concepts vote statistics and favourable concept percentages.

Concepts	**F**	**U**	**Z**	**Total Favourable Vote (%)**
Social Networking	60	5	2	89.5%
E-Learning	57	0	10	85%
Health	65	2	0	97%
Gaming	18	36	13	26.8%
Hybrid	51	7	9	76.1%

3 Design Tools

With the increase in technology, a variety of design tools and techniques have rapidly become available with each offering its own unique advantages and disadvantages. The choice of tool therefore depends on the intended task for a particular phase of the project development. The Huzuni platform was researched and designed using a hybrid of methods and design tools. In the initial design stage, prototypes of the platform were explored and designed first through simple sketches and paper prototypes. These were later developed into low-fidelity digital wireframes after a variation of idea and design concept iterations. The high-fidelity and detailed design prototypes were interchangeably developed using a combination of Sketch App [24] and Adobe Experience Design (Adobe XD) [25]. High-fidelity prototypes were imported into Invision [26] to add interactivity and test the anticipated interaction between the users and the platform.

In the evaluation phase, the high-fidelity interactive prototypes were later used to evaluate interaction, information architecture, user experience and usability with five groups of students at UPV (n=110) through usability tests and scenarios designed in Morae [27].

4 Structure and Functionality

4.1 Structure

As a structured information system, the platform design involves the determination of interdependent variables [28]. Therefore, the precedence structuring for the platform functionalities of determining these variables involves information design for better user experience. Efficient usability and user experience is founded on good information architecture [1, 2, 29]. The platform structure was developed for implementing the design in four categories:

(1) Social – a social networking sub-platform for patient users, supporters, professionals and relevant organizations
(2) Health - a healthcare sub-platform for interaction between patient users and healthcare professional and providers
(3) E-Learning – an e-Learning sub-platform for educational material, projects, programs and information
(4) Cloud – a cloud storage service for ease access of shared patient-doctor information, and user-service provider e.g. educational material, insurance, etc.

Each category is further subdivided into its individual subcategories or functionalities. Many techniques have been developed in cognitive psychology [30, 31] to help effectively apply psychological principles to design e.g. including Gestalt principles and recognition patterns which explore the users' visual perception of elements in relation to each other. This helps users be oriented in the structure [30, 31, 32].

Fig. 1. Huzuni structure typology and features by category; plus, universal features available in all 4 categories. (*see, next page*)

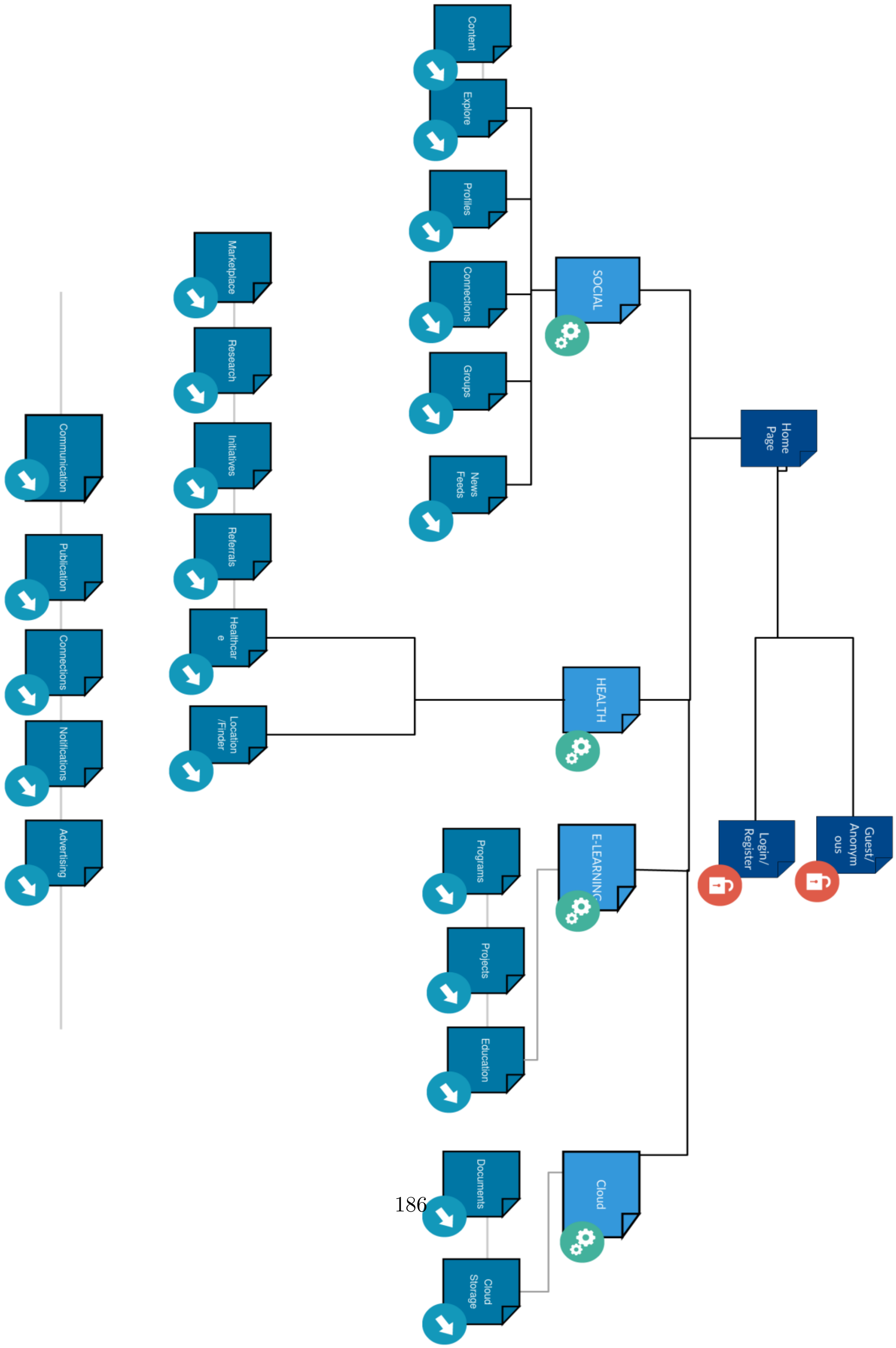
Home Page
Login/ Register
Guest/ Anonymous
SOCIAL
Content
Explore
Profiles
Connections
Groups
News Feeds
HEALTH
Marketplace
Research
Initiatives
Referrals
Healthcare
Location /Finder
E-LEARNING
Programs
Projects
Education
Cloud
Documents
Cloud Storage
Communication
Publication
Connections
Notifications
Advertising

4.2 Functionality

Information interaction is the *"process by which interact with an information system as a blueprint and navigational aid."* [33]. As such information architecture performs an important supporting role in interactivity in articulating the user, content and system, illustrating the context for information architecture [33]. After the design, performance and structure requirements were specified, the subcategories of functionalities and platform features were determined within the four main structure categories; (1) social, (2) health, (3) e-learning, and (4) cloud as briefly described below.

4.2.1 Social

The social networking sub-platform includes the following features and functions:

- Explore – for exploring content within the main platform
- Profile – for personalization within the platform or anonymity in cases of privacy and stigma
- Connections – for friends, supporters, and influencers within the platform
- Experiences – shared moments, places, lessons, etc. to inspire others
- Publications – Articles, Stories, videos, podcasts on mental health
- Groups and Communities – to identify with support and mutual interests
- News Feed – customizable updates feed based on settings
- Content – Shared content; text, photos, audio and video
- Communication - Chat/Messenger, Call (audio and video – Live Streaming)
- Engagement - likes (reactions), shares, comments and support
- Initiatives - crowd-Sourced social causes and support initiatives
- Advertising (Business) – paid feature for business and extending mental health relevant information to the community e.g. paid courses etc.
- Recommendations - Content and Experiences shared, places or recommendable healthcare professionals, mental health insurance companies etc.
- Research – content database and participant recruitments for mental health research.
- Notification

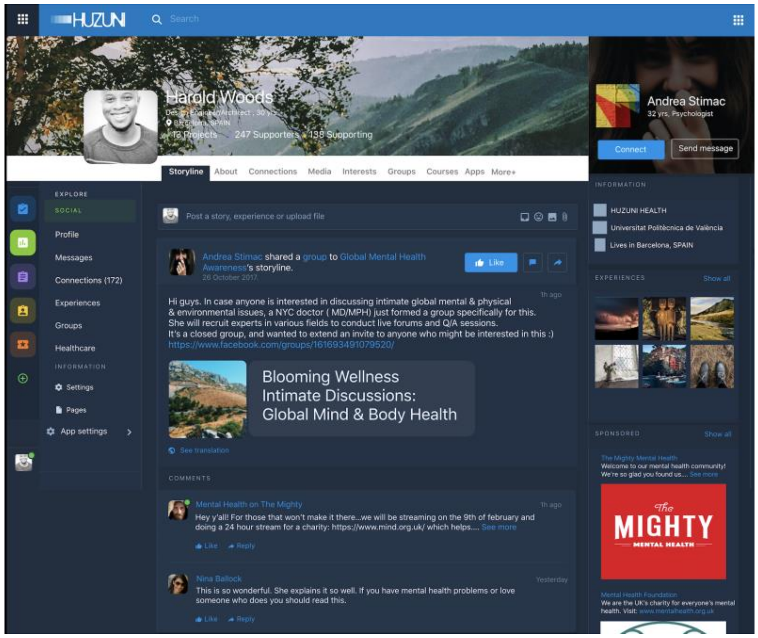

Fig. 2. Huzuni social profile feature.

4.2.2 Health

The health sub-platform includes the following features and functions:

(a) Publications Platform (Mental Health) – Articles, Stories, videos
(b) Health Care Professional Database and Rankings
(c) Connections - supporters, influencers, survivors and well wishers
(d) Finder or Locator - for on demand healthcare services
(e) Marketplace - Patient-Doctor content platform, product and products peer-to-peer sharing or sale, mental health insurance etc.

4.2.3 E-Learning

The he-learning sub-platform includes the following features and functions that are of an educational and informational nature:

- Virtual Classrooms – training and course listing by different sources
- Programs and Projects - Personal and Organizational

4.2.4 Cloud

The cloud sub-platform includes the following features and functions:

- Cloud – documents and files cloud storage that syncs with all the other 3 categories for easy access and sharing of content e.g. educational content.

Certain features are universal within the platform and available within all 4 sub platform categories. For purposes of readability this are no repeated into each category.

- Content – Shared content; text, photos, audio and video
- Communication - Chat/Messenger, Call (audio and video – Live Streaming)
- Engagement - likes (reactions), shares, comments and support
- Initiatives - crowd-Sourced social causes and support initiatives
- Advertising (Business) – paid feature for business and extending mental health relevant information to the community e.g. paid courses etc.
- Recommendations - Content and Experiences shared, places or recommendable healthcare professionals, mental health insurance companies etc.
- Research – content database and participant recruitments for mental health research.
- Notifications

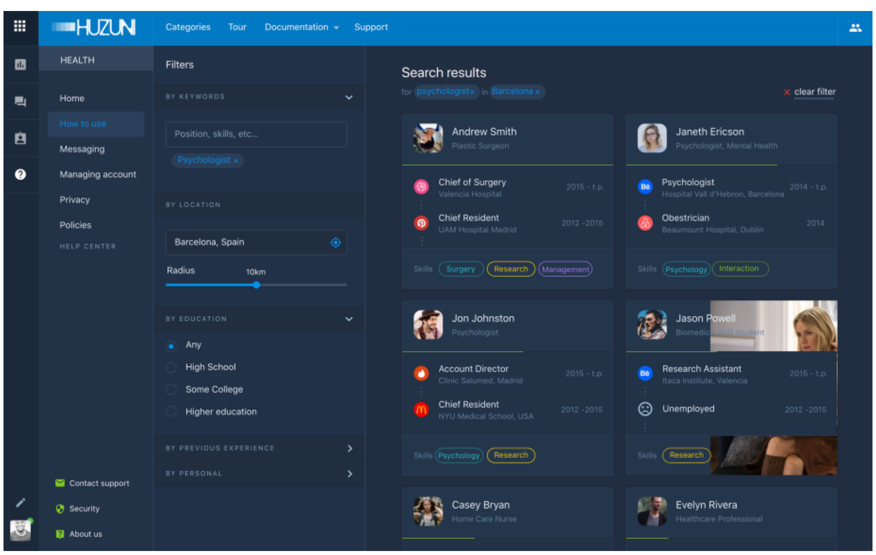

Fig. 3. Huzuni location finder feature for identifying mental healthcare professional by proximity and qualification.

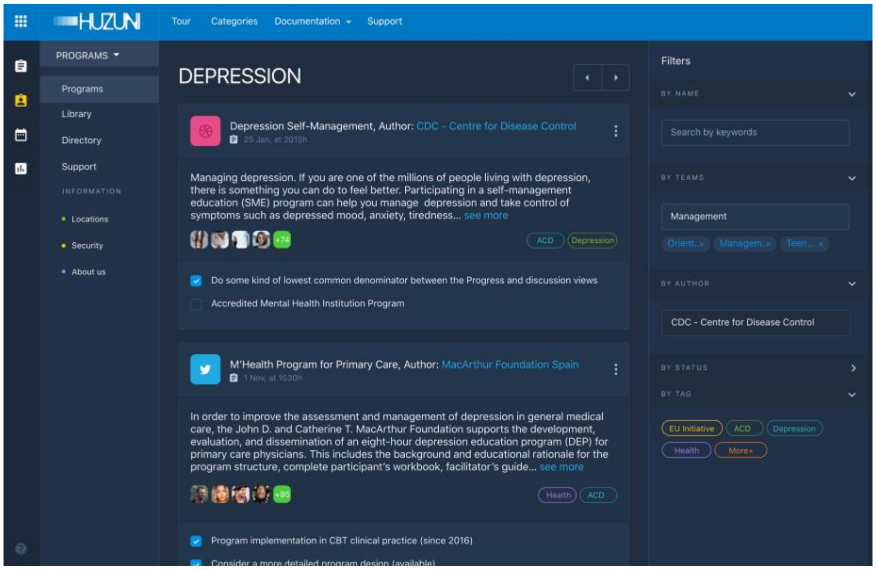

Fig. 4. Huzuni platform screenshot showing recommended and verified educational and information programs about depression.

4.3 Participatory Design in Defining Huzuni Platform Features

To achieve the goal of usability and user experience, the different design and project development stages of the platform applied user-centered methodologies and approaches from the earlies phases to-date. These methodologies were applied across all stages and often revisited for discussion and re-evaluation because the design did not take a linear process.

(a) **Co-Design and Co-Discovery.** Partnered in pairs and under observation, participants collaboratively explored the Huzuni concept design thus far as part of the co-discovery engagement and its use-cases [17] which enhanced thought processes and decisions. This is also proved in previous studies. According to [34, 35] collaborative communication is more natural than thinking out loud in isolation and is a source of design insight [35]. Participants were treated as masters or experts of their own experiences – this disqualifies any prior knowledge of the product-service that any user might have had or similar and there was no novice versus expert complex, which made all engagements and responses equally valuable.

(b) **Personas**[2] **and Character Profiles** were used as a sampling method to capture a wider spectrum of representation among targeted users. The targeted users, mostly youths, possess a wide variation in habits, preferences and behavioral patterns. Personas that represent the features of an existing targeted user group helped us define the design specifications and functionality requirements of the platform with reflection on needs, habits, trends and contextual setting [36]. This included surveys and interviews with students and the academic community, young adults and other target user profiles for observation and analysis to create meaningful personas that represented all future user profiles.

(c) **Simulations (Role Play).** Hypothetical simulations of potentially possible scenarios within the product-service were enacted by users that assume hypothetical personas as performers to understand the product-service experience. Where possible variations existed, e.g. how to get from an online course calendar to enrolling in a program. They were performed with interchanged performers undertaking the same task to better understand the product-service evolution and perception across different user profiles. For example, to better understand the information design and flow of the Huzuni platform users were asked to envision and engage information design discovery within the platform in low-fidelity paper prototypes, with 4 objectives; (1) Placeability – the ease and amenability of where functionalities could be located; (2) Findability – the ease with which a newcomer not involved in the placeability can identify or locate any given function; (3) Interaction between users performing roles and decisions in isolation versus those interacting with others; and (4) the interaction between groups scenarios versus individual scenarios. And then different groups were required to analyze the above aspects and tasks as performed by their preceding group. Users performing tasks in isolation manifested different task patterns as opposed to when in interaction with other users or in group settings due to external influence and stimuli form other members that took the form of both; (1) assisted performance for tasks and; (2) group influence. Collective group

[2] Research-based fictional characters to represent a spectrum of user types for the study.

certainty of how a task(s) should be performed often impeded the certainty of an individual within the group, even in user-cases where the group might have been misguided e.g. how to share content privately.

(d) **Group Sketching**. During sessions this helped in developing and clarifying ideas while concurrently sharing insights amidst participating teams and groups [37] to find mutual acceptance in user case and product-service performances. Idea generation and discussion of preferences led to voting for the most preferred and favored features that should be included in the Huzuni platform (*see, Section 2. Table 1*)

(e) **Mockups** through diverse media including illustration, post-its, cards, and collages among others were created and used at different stages of the project participatory design process in replication of the existing conditions of the problem(s) to be tackled, the goal, similar product-services and initiatives. Mockups between social networking, e-learning, gaming and healthcare during brainstorming and design thinking sessions gave a visual insight into other ideas. For example, we aimed to reduce both public stigma and self-stigmatization among members of the university community, both students and academic staff, suffering from mental health disorders. This prompted us to explore new concepts of maintaining anonymity where required without compromising openness where needed whilst users still benefit from the platform with great engaging user experiences equally regardless of the choice taken(s). This resulted into an anonymous or guest user section on the platform.

(f) **Experience prototypes.** In successive phases with varying fidelities these helped us to witness real use-case scenarios and potential problems within the anticipated user experience of the product-service. Insights gained from early-stage comparisons between the intended designed product-service's experience versus the real anticipated users and their expected user experience informed later decisions. For example, design and user experience deficiencies e.g. gaming features that were detected in the early paper prototypes and low-fidelity prototypes were excluded in the high-fidelity prototypes. As a simulation of the product-service to user experience the high-fidelity prototypes were even later used in further studies including interaction and usability tests with students at UPV. Creating user scenarios and interactive experience prototypes of different fidelities aided the simulation of the real product-service anticipated interaction and user-experience.

Interaction design, "*the design of the interaction between users and products*" [38] tools, methodologies and studies like interactive paper prototyping and Framer were applied to understand the interactive response experience that would create engagement between the user and the service, product or interface [39]. Identifying the dimensions of interaction within a product-service gave insight into user behavior, information architecture, visual design and the relationships between the user-product. However due to certain limitations in the tools available, for example limited interaction features in Invision software, certain feature could not be tested in high-fidelity.

5 Evaluation

5.1 Usability and Experience Design

Usability is a *"quality attribute that assesses how easy user interfaces are to use"* [40]. Usability is measured by qualitative and quantitative attitudes [41, 42] because it focuses on tasks, goals, and performances. Usability has always been the standard measure for great product or system design interactivity until in recent years when user experiences became the differentiating factor due to existence of similarities between products. Thus, product design and development for interaction now has to go beyond usability into the realm of user experience – by understanding users' everyday human needs [43]. According to Väänänen-Vainio-Mattila et al., two fundamental aspects require consideration when design for pleasure and engagement [43];

(1) An understanding of the user needs is vital to experience-centered design for interactive products [43,44]. These needs could be both pragmatic and hedonic qualities. Pragmatic quality refers to *"a product's perceived ability to support the achievement of behavioural goals"* (related to usability and functionality); while hedonic quality refers to *"a product's perceived ability to support the fulfilment of basic psychological needs such as stimulation, enjoyment, identification, and engagement"* [44,45].

(2) Great user experience design considerations require continuous iterative evaluations throughout the stages of product design and development [46].

Providing positive user experience, therefore, has become a key factor in product design and development [43, 47, 19, 48]. This means that user experience assessment and improvement need to be considered from the early phases of the design process and to be inclusive of aspects beyond just usability. Therefore, though the initial stage of the study was more focused on usability to rectify deficiencies, the next studies and tests respond to aspects beyond usability.

5.2 Usability Tests (Morae)

To understand the platform functionalities versus the user needs, evaluation is inevitable. Evaluation tests to study the usability of the Huzuni platform prototype were designed and conducted in Morae – the current industry leading software for usability testing (web, and mobile), mobile device and hardware testing; and market research [27]. Morae has the capability to integrate synchronized screen captures, audio and video recordings of users while they interact with the platform during the usability study, but the audio and video recordings were disregarded in the study (*see, Section 5.3.1*, *Fig. 5*)

5.3 Morae Usability Study Design

This study recruited a study population matching the intended and anticipated end users of the Huzuni platform – the young adults in an academic environment. During the study design, various considerations were taken into account;

(a) Objective: To investigate the perceived usability of the Huzuni platform prototype
(b) Type of Study: Observational study.
(c) Setting: Design Computer Room (Japan) with Morae in Valencia, Spain.
(d) Participants: 110 ergonomics and human factors third year design students (age 18-31) who had previous theoretical training in usability testing.
(e) Intervention: Participants were photographed, and video recorded during the study. Participants were assisted only in technical issues during the study.
(f) Main outcome measure: Difference in observer ratings of perceived usability, ease and user experience of navigation

5.3.1 Tasks and Scenarios

The study design was provided in two (2) languages; (1) English and (2) Spanish to avoid any miscommunication and language barrier challenges. Equally, all instructions and questions were in both languages. Participants were given a quick tutorial of how the Morae usability testing software works to get familiar with its user interface. The participants were split into four (4) groups, each with an average duration of 45-60 minutes per group. The study was setup into two (2) parts;

(a) Tasks and scenarios – 10 tasks and scenarios which depicted one end what the observer wanted to achieve, whilst portraying a scenario for the participant so that they would perform the task with the tools and Huzuni interactive interface available to them;

  (1) Scenario - You are a new user on the Huzuni platform. Goal - Find the Signup page.
  (2) Scenario - You are a returning user on the Huzuni platform. Goal - Find the sign in page.
  (3) Scenario - You're planning to take an online/e-learning course on Wednesday afternoon. Goal - Go to the Huzuni platform (prototype) and see what suitable course options you have available.

(4) Scenario – Use the Huzuni platform prototype to find mentorship tasks you'd be interested in attending tomorrow afternoon and newly updated tasks for the week of July 27th. Goal - Find tasks and presentation/attendance times.
(5) Scenario – You have been using the platform together with your psychologist and group support. Goal - Look up the results and progress of your mental health.
(6) Scenario – Who is the mental health psychologist closest to your location in Barcelona and how much do they charge per hour? Goal - Using the finder tool to find healthcare professionals and locations
(7) Scenario – Contact the located psychologist by chat to make an inquiry. Goal - Send a private message to a psychologist (messenger & email.
(8) Scenario – A psychologist you follow, Dr. Clare Kambamettu shared an article that shows in your updates. Locate the article and read its full contents. Goal - Access of the home, profile and content sharing feature.
(9) Scenario – Finding what projects exist about exercising when under depression. Goal - Find information about a project.
(10) Scenario – Find the available programs on depression provided by the CDC - Centre for Disease Control and MacArthur Foundation Spain. Goal - Finding programs about depression.

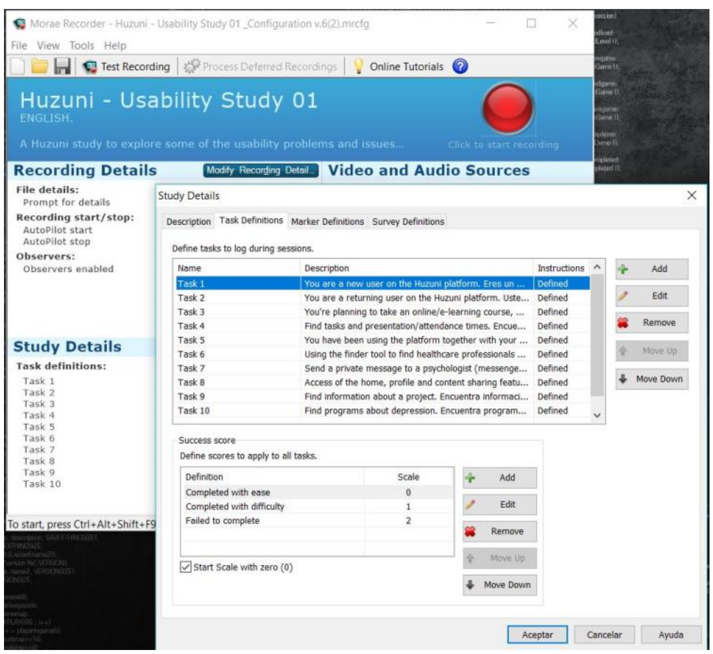

Fig. 5. Screenshot of Huzuni usability test study 01 tasks and scenarios setup.

(b) Survey – an automated survey at the end of the tasks and scenarios in form of multiple choice questions with answers to select from; one response (S) or multiple responses (M); and freedom responses (F) that gave the participant free text responses. For research and statistical purposes, please complete the short survey below. The survey questions were categorized to collect information regarding; (1) Age range; (2) Languages spoken; (3) preferred duration of intervention or online self-help; (4) preferred mode treatment and online self-help; (5) preferred mode of delivery; and (6) design suggestions. This was designed to get more insight that might have not been attained the previous options.

(1) S - What's your age range?
(2) M - What languages do you speak? (select all that apply)
(3) F - What do you think is the purpose of this platform/website/prototype?
(4) F - What would be your desired duration of intervention or help for a session with a psychologist and/or online self-help respectively? Please indicate preference (psychologist vs. online self-help) and duration preferred.
(5) M - If you were a user, what would be your preferred mode of treatment and help?
(6) M - What would be your preferred mode of delivery for the Huzuni platform?
(7) F - Although this is an incomplete prototype and you have only tested a few planned features, speaking from the perspective of both a user and designer, please make suggestions related to design, aesthetics, additional functionalities, features, content, usability, etc. for the platform.

5.3.2 General Study Results

The average duration in minutes of the study ($45< t > 60$) greatly exceeded the designed study duration ($t=20$). Anticipated interaction between the user and the platform met expected standards however is limited to the limitations of the tools used during the usability study. Interactive prototypes in Invision currently have many limitations just like in other design and interaction for usability tools. Achieving the desired usability, interaction and experience would require a tiresome and lengthy use of many different tools interchangeably. With this interchange between tools, errors and loss of information structure occurs. During the study, incidents occurred where a small number (n=4, 3.6%) of the participants viewed a shortcut or “backdoor” displaying all screens versus 106 (96.3%) who interacted with the platform directly as intended. Some tasks (n=2) needed to be redesigned or rephrased for clarity because they were unclear to certain participants. The detailed results of this study are out of the scope of this paper.

7 Discussion and Results

It was discovered that a relationship exists between users' categories and groups in a user-case scenario whether individually versus in a team or inter-group scenarios. It was observed that; (1) higher levels of certainty in performing tasks as well experience problem scenarios exist individually as opposed to group settings; (2) Individual certainty of task execution on average almost often decreases in acceptance and favour of group perspectives. Insights of previously unimagined scenarios, use-cases and functionalities emerged due to the diverse personal profiles and more inclusive categories. The user-centered approaches like the participatory design process strengthened the understanding of the necessity to re-invent contemporary design approaches and methodologies by investing more time and effort in user centric co-design with target user audiences. Just like great toys would be designed by adults only when they have the involvement and engagement of children, desired healthcare design solutions exist at the intersection of the participatory product-service design with the intended end-users or patients for greater usability, more delightful and engaging experiences. According to Hick's law and the universal principles of design, the more options users are exposed to, the longer it takes them to make a decision [49]. This was evidenced in the different design phases – participatory design. The more options the participants had, the more time and energy it takes to make a decision about the next step forward in their participation. The individual software programs and design tools had to be retrofitted to work together to achieve the platform's user interface design specifications. The underlying product platform for Huzuni and its tests on interaction and usability thus also evolved in this manner. In either instance, the net result is a collection of programs and tools that share some common methodologies and functions.

In recent years, Usability has been intensively challenged user experience enthusiasts for its limitations as a physical and cognitive approach to understanding user-product interaction [50, 51]. As a result, a shift towards user experience has erupted in favour of designing product-services that are not merely usable and functional but also aesthetic, enjoyable, pleasurable and engaging. Although it's a recent field and its definition has not yet reached a solid state, there has been wide agreement that user experience deals with more than functionality and usability [52, 53, 54, 43, 7]. Therefore, term 'user experience' has become synonymous with human-computer interaction (HCI) and product-service design as it pushes the task-based, goal-oriented boundaries of usability that are focused solely on behavioural performances [55,56,57] experience integrates positive experiences through emotions, attitudes, and meanings, and values as the outcomes of the interaction with a product or system (56,58]. Its argued that usability has evolved from a 'satisfier' into a 'dissatisfier' product attribute [17] that no longer address all the hierarchies of human needs and product-user relationships if not integrated with user experience [17,59] beyond functionality and usability to a higher-level user need – the need for pleasure. This view is supported by many researchers who have pointed to the limitations of traditional usability modern age applications [60, 61] for example in design for entertainment and enjoyment [61] and design for emotions [60, 62]. Its nearly a requirement to integrate user experience in design with a focus on a holistic approach on all aspects of interactive product-services [18]. Future research and the following design stages of the Huzuni platform further explore the theme of user experience in detail.

8 Conclusions and Future Work

The platform's approach and structure for combining social networking with health and e-learning gained great appreciation from the participants. It was perceived as a positive approach towards leveraging social networking platforms to help improve health, awareness, support and engagement for people with mental health disorders. On the contrary, the StateOfMind [63,64,65] report by the Royal Society for Public Health [65] showed that social networking alone has been ranked a great cause of deteriorated mental health with Facebook, Youtube and Instagram received greatest criticism [66]. Social networks are synonymous with use by the public but to a lesser extent by individuals with severe mental illness [67, 68, 69, 70] though enhanced social support networks for people with mental illness is an important and a proven thrust for support and motivation [71].

The platform can help shape structure and functionality as organized through interaction and information architecture. This structure forms the core of usability and user experience as users perform their day-to-day tasks. The user-centered design approach with multiple participatory design strategies and evaluation stages has enabled us to choose the most promising and user-anticipated experiences from the different options that existed. Certain features and functionalities of the platform were chosen for further re-designing and development because the target audience was either less-motivated to engage with them or did not create the expected user experience for the participants. To achieve this, a hybrid combination of established user experience design and usability evaluation methods were applied as discussed in this paper e.g. participatory design, controlled experiment, heuristic evaluation, workshops or sessions, performance measure, thinking-aloud, observation, questionnaire and surveys, interview, focus group, and user feedback [42, 34, 72]. Future research, experiments and the following design stages of the Huzuni platform will further explore the theme of both usability and user experience in detail.

References

1. Usability.Gov: User Interface Design Basics (2015) (accessed, 2017-03-15) https://www.usability.gov/what-and-why/user-interface-design.html
2. Nielson Norman Group: Top 10 Information Architecture (AI) Mistakes (2009) (accessed, 2018-06-3) https://www.nngroup.com/articles/top-10-ia-mistakes/
3. Nielson Norman Group: Low Findability and Discoverability: Four Testing Methods to Identify the Causes (2014) (accessed, 2018-06-3) https://www.nngroup.com/articles/navigation-ia-tests/

4. Nielson Norman Group: When to Use Which User Experience Research Methods (2014) (accessed, 2018-04-21) https://www.nngroup.com/articles/which-ux-research-methods/
5. Nielson Norman Group: Quantitative User-Research Methodologies: An Overview (2014) (accessed, 2018-05-13) https://www.nngroup.com/articles/quantitative-user-research-methods/
6. Interaction Design Foundation: 7 Great, Tried and Tested UX Research Techniques (2018) (accessed, 2018-05-13) https://www.interaction-design.org/literature/article/7-great-tried-and-tested-ux-research-techniques
7. Vermeeren, A., Law, L., Roto, V., Obrist, M., Hoonhout, J., Väänänen, K.: User experience evaluation methods: Current state and development needs. Extending Boundaries - Proceedings of the 6th Nordic Conference on Human-Computer Interaction. NordiCHI 2010: (2010) 521-530. 10.1145/1868914.1868973.
8. Merritt, S., Stolterman, E.: Cultural hybridity in participatory design. Proceedings of the 12th Participatory Design Conference: Vol. 2. Exploratory Papers, Workshop Descriptions, Industry Cases (2012) 73–76
9. Spinuzzi, C.: The Methodology of Participatory Design. Technical Communication. Vol. 52. (2005) 163-174 (accessed, 2018-06-3) https://repositories.lib.utexas.edu/bitstream/handle/2152/28277/SpinuzziTheMethodologyOfParticipatoryDesign.pdf
10. Roto, V., Obrist, M., Väänänen, K.: User Experience Evaluation Methods in Academic and Industrial Contexts. (2018)
11. Tone, B.: Methods and Techniques in Participatory Design. Department of Informatics, University of Oslo. Inf5722 (2017) http://www.uio.no/studier/emner/matnat/ifi/INF5722/h17/lectures/pd-metoder-teknikker-inf5722-2017.pdf
12. Barcellini, F., Prost, L., Marianne, C.: Designers' and users' roles in participatory design: What is actually co-designed by participants? Applied Ergonomics. Vol. 50. (2015) 31-40. ISSN 0003-6870. https://doi.org/10.1016/j.apergo.2015.02.005.
13. Pine, B. J., and Gilmore, J. H.: Welcome to the experience economy. Harvard Business Review (1998) 76(4), 97-105
14. Pine, B. J., and Gilmore, J. H.: The experience economy (Updated ed.). Boston, Massachusetts: Harvard Business Review Press (2011)
15. Kort, J., Vermeeren, A. P. O. S., and Fokker, J. E.: Conceptualizing and measuring user experience. In E. Law, A. P. O. S. Vermeeren, M. Hassenzahl (2007)
16. Blythe, M. A., Overbeeke, K., Monk, A. F., and Wright, P. C. (Eds.): Funology: From usability to enjoyment. Dordrecht; Boston; London: Kluwer Academic Publishers (2004)
17. Jordan, P. W.: Designing pleasurable products: An introduction to the new human factors. Taylor & Francis, London (2000)
18. Mahlke, S.: Understanding users' experience of interaction. In Proceedings of the Annual Conference on European Association of Cognitive Ergonomics - EACE'05 Chania, University of Athens,Greece (2005) 251-254
19. Sward, D., and Macarthur, G.: Making user experience a business strategy. In E. Law, A. P. O. S. Vermeeren, M. Hassenzahl and M. A. Blythe (Eds.), Proceedings of the COST294-MAUSE Affiliated Workshop: Toward a UX Manifesto. Lancaster, UK (2007) 35-42
20. Nielson Norman Group: When to Use Which User Experience Research Methods (2014) (accessed, 2018-06-3) https://www.nngroup.com/articles/which-ux-research-methods/

21. Nielson Norman Group: User Research Methods: From Strategy to Requirements to Design (2017) (accessed, 2018-04-7) https://www.nngroup.com/courses/research-beyond-user-testing/
22. Flick, U.: An introduction to qualitative research (4th ed.). Sage Publications, London (2009)
23. Potter, W. J.: An analysis of thinking and research about qualitative methods. Lawrence Erlbaum Associates, Inc. Mahwah, New Jersey (1996)
24. Sketch: The Digital Design Toolkit (2018) (accessed, 2018-06-3) https://www.sketchapp.com/
25. Adobe: The Future of Experience Design (2018) (accessed, 2018-06-3) https://www.adobe.com/products/xd.html?promoid=PYPVQ3HN&mv=other
26. Invision: Design Better. Faster. Together (2018) (accessed, 2018-06-3) https://www.invisionapp.com/
27. Morae: Usability Testing with Morae (2018) (accessed, 2018-06-3) https://www.techsmith.com/morae.html
28. Steward, D.: The Design Structure System: A Method for Managing the Design of Complex Systems. Engineering Management, IEEE Transactions on. EM-28. 10.1109/TEM.1981.6448589. (1981)
29. Kensing, F., and Blomberg, J.: Participatory Design: Issues and Concerns. Computer Supported Cooperative Work. Kluwer Academic Publishers. Netherlands (1998) 7: 167–185. (accessed, 2018-06-3) http://citeseerx.ist.psu.edu/viewdoc/download?doi=10.1.1.124.9929&rep=rep1&type=pdf
30. Zimbardo, P.G., and Gerrig, R.J.: "Perception", In: D.J. Levitin (ed.), Foundations of cognitive psychology, MIT Press, Cambridge (2002) 133-188.
31. Chen, J.: Flow in Games (and Everything Else). Commun ACM. 50, 31-34 (2007)
32. Jeff Johnson.: Designing with the Mind in Mind. Simple Guide to Understanding User Interface Design Guidelines. Ed. 2. Elsevier (2014)
33. Toms, E.G.: Information Interaction: Providing a Framework for Information Architecture. Journal of the Association for Information Science and Technology. Vol. 53. Issue 10 (2002) 855-862 (accessed, 2018-06-3) https://onlinelibrary.wiley.com/doi/full/10.1002/asi.10094
34. Nielsen, J.: Usability engineering. Academic Press, Inc. San Diego, USA (1993)
35. Dumas, J. S., and Redish, J.: A practical guide to usability testing. Exeter, Intellect Books, England (1999)
36. Frank, L.: Real or Imaginary: The effectiveness of using personas in product design, research paper published in the Irish Ergonomics Review, Proceedings of the IES Conference 2009, Dublin (2009)
37. Saul, G., Mark, R., David, W.: Group Sketch, paper, Department of Computer Science, University of Calgary, Canada (2006)
38. Siang, T.: The Interaction Design Foundation: What is Interaction Design? (2014) (accessed, 2018-06-3) https://www.interaction-design.org/literature/article/what-is-interaction-design
39. Carroll, J.: Designing Interaction: Psychology at the Human-Computer Interface, Cambridge University Press, England (1991)
40. Nielsen, J.: Usability Inspection Methods, John Wiley & Sons, (1994) ISBN 0-471-01877-5
41. ISO 9241-11.: Ergonomic requirements for office work with visual display terminals (VDTs) - Part 11: Guidance on usability. International Organization for Standardization (ISO). Switzerland (1998)
42. Jordan, P. W.: An introduction to usability. Taylor & Francis, London (1998)

43. Väänänen-Vainio-Mattila, K., Roto, V., and Hassenzahl, M.: Now let's do it in practice: User experience evaluation methods in product development. In Extended Abstracts of the International Conference on Human Factors in Computing Systems - CHI'08. ACM Press, New York (2008) 3961-3964
44. Hassenzahl, M.: The thing and I: Understanding the relationship between user and product. In M. A. Blythe, K. Overbeeke, A. F. Monk and P. C. Wright (Eds.), Funology: from usability to enjoyment. Kluwer Academic Publishers, Dordrecht; Boston; London (2003) 31-42)
45. Hassenzahl, M.: User experience (UX): Towards an experiential perspective on product quality. In Proceedings of the 20th International Conference of the Association Francophone d'Interaction Homme-Machine - IHM'08. ACM Press, New York (2008) 11-15
46. ISO 13407.: Human-centred design processes for interactive systems. International Organization for Standardization (ISO). Switzerland (1999)
47. Obrist, M., Roto, V., and Väänänen-Vainio-Mattila, K.: User experience evaluation: Do you know which method to use? In Extended Abstracts of the 27th International Conference on Human Factors in Computing Systems - CHI'09. ACM Press, New York (2009) 2763-2766
48. Pine, B. J., and Gilmore, J. H.: The experience economy: Work is theatre and every business a stage. Harvard Business School Press, Boston (1999)
49. Lidwell, W., Holden, K., Butler, J.: Universal Principles of Design. (2003)
50. Blythe, M. A., Overbeeke, K., Monk, A. F., and Wright, P. C. (Eds.).: Funology: From usability to enjoyment. Kluwer Academic Publishers. Dordrecht; Boston; London (2004)
51. Green, W. S., and Jordan, P. W. (Eds.).: Pleasure with products: Beyond usability. Taylor & Francis. London; New York (2002)
52. Alben, L.: Quality of experience: Defining the criteria for effective interaction design. Interactions, (1996) 3(3), 11-15.
53. Bevan, N.: UX, usability and ISO standards. In Extended Abstracts of the International Conference on Human Factors in Computing Systems - CHI'08. ACM Press, New York (2008)
54. Hassenzahl, M., and Tractinsky, N.: User experience - A research agenda. Behaviour and Information Technology, (2006) 25(2), 91-97.
55. Bargas-Avila, J. A., and Hornbæk, K.: Foci and blind spots in user experience research. Interactions (2012) 19(6), 24-27.
56. Law, E., Roto, V., Hassenzahl, M., Vermeeren, A. P. O. S., and Kort, J.: Understanding, scoping and defining user experience: A survey approach. In Proceedings of the 27th International Conference on Human Factors in Computing Systems - CHI'09. ACM Press, New York (2009) 719-728
57. Law, E., Roto, V., Vermeeren, A. P. O. S., Kort, J., and Hassenzahl, M.: Towards a shared definition of user experience. In Extended Abstracts of the International Conference on Human Factors in Computing Systems - CHI'08. ACM Press, New York (2008) 2395-2398
58. Zimmermann, P. G.: Beyond usability - measuring aspects of user experience. Unpublished Doctoral Dissertation, Swiss Federal Institute of Technology Zurich, Switzerland (2008)
59. Jordan, P. W.: Pleasure with products: Human factors for body, mind and soul. In W. S. Green and P. W. Jordan (Eds.), Human factors in product design: Current practice and future trends. Taylor & Francis. London; Philadelphia (1999) 206-217
60. Dormann, C.: Affective experiences in the home: Measuring emotion. In Proceedings of the International Conference on Home-Oriented Informatics and Telematics - HOIT'03. California, USA (2003)

61. Mandryk, R. L., Inkpen, K. M., and Calvert, T. W.: Using psychophysiological techniques to measure user experience with entertainment technologies. Behaviour and Information Technology (2006) 25(2), 141-158
62. Zimmermann, P. G., Gomez, P., Danuser, B., and Schär, S. G.: Extending usability: Putting affect into the user-experience. In E. Law, E. T. Hvannberg and M. Hassenzahl (Eds.), Proceedings of the 2nd COST294-MAUSE International Open Workshop on User Experience: Towards a Unified View. Oslo, Norway (2006) 27-32
63. Royal Society for Public Health. (accessed, 2016-10-15) https://www.rsph.org.uk/our-work/campaigns/status-of-mind.html
64. Royal Society for Public Health: State of Mind (accessed, 2016-10-16) https://www.rsph.org.uk/uploads/assets/uploaded/62be270a-a55f-4719-ad668c2ec7a74c2a.pdf
65. Royal Society for Public Health. (accessed, 2018-06-3) https://www.rsph.org.uk/
66. PsychAlive: Which is Worst for Your Mental Health: Instagram, Facebook or Youtube? (2016) (accessed, 2017-08-21) https://www.psychalive.org/worst-mental-health-instagram-facebook-youtube/
67. Vaughan, C.E. & Leff, J.P.: The influence of family and social factors on the course of schizophrenic and depressed neurotic patients. British Journal of Psychiatry. (1976) 129, 123-137.
68. Kuo, W., & Tsai, Y.: Social Networking, Hardiness and Immigrant's Mental Health. Journal of Health and Social Behavior (1986) 27(2), 133-149. Retrieved from http://www.jstor.org/stable/2136312
69. Fiori, K.L., Antonucci C.T., Cortina, K.S.: Social Network Typologies and Mental Health Among Older Adults, The Journals of Gerontology: Series B, Vol. 61. Issue 1, 1 January 2006 (2006) 25–32. https://doi.org/10.1093/geronb/61.1.P25
70. Thornicroft, G. and Breakey, W.R.: The COSTAR programme 1: Improving social networks of the long-term mentally ill. British Journal of Psychiatry (1991) 159, 245-249
71. Siegel, D., Tracy, E.M., Corvo, K.N.: Strengthening Social Networks: Intervention Strategies for Mental Health Case Managers, Health & Social Work, Volume 19, Issue 3, 1 August 1994 (1994) 206–216 https://doi.org/10.1093/hsw/19.3.206
72. Popovic, V.: Product evaluation methods and their importance in designing interactive artifacts. In W. S. Green and P. W. Jordan (Eds.), Human factors in product design: Current practice and future trends. Taylor & Francis. London; Philadelphia (1999) 26-35

Extended Access Barring in Cellular-based Machine-Type Communications: Practical Implementation and Impact of Paging Timing *

Luis Tello-Oquendo, José Ramón Vidal, Vicent Pla, Jorge Martinez-Bauset

Instituto ITACA, Universitat Politècnica de València, Valencia 46022, Spain

Abstract. Machine-Type Communication (MTC) is expanding rapidly and is expected to play an essential role within the upcoming 5th generation (5G) wireless systems. The main challenge in MTC is the scalable and efficient connectivity for a massive number of devices which fundamentally causes signaling overload in the random access channel. Extended access barring (EAB) is one mechanism suggested by the 3GPP for congestion control. The network activates or deactivates EAB through a congestion coefficient. In this paper, we propose a realistic way to implement the congestion coefficient so that EAB can operate and handle congestion episodes in MTC scenarios. We study the performance of EAB under different MTC traffic loads using our proposed congestion coefficient implementation and evaluate the impact of the paging timing on the EAB operation in terms of network key performance indicators (KPIs). Numerical results show the accuracy of our method to implement the congestion coefficient. In addition, we show that increasing the value of the paging cycle configuration influence on the network performance under EAB by improving the successful access probability at the cost of longer access delay while reducing the number of preamble transmissions in light-loaded MTC scenarios which translates in energy savings for power-constrained MTC devices.

1 Introduction

Internet of Things (IoT) is one of the most transformative and disruptive technologies of the upcoming wireless systems that has the potential to radically change the world around us. It is predicted that 1.5 billion of IoT devices use cellular connections by 2022 [10]. Machine-type communication (MTC) is becoming the dominant communication paradigm for a wide range of emerging IoT applications including healthcare, smart cities, smart grids, smart transportation, and environmental monitoring. In this kind of applications a vast number of devices are deployed aiming at provisioning ubiquitous services with minimal (or without) human intervention. The 5th generation (5G) cellular networks will be in charge of supporting this huge number of devices generating sporadic small packets at random times. In this context, the random access channel (RACH) is generally used to initiate the communication sessions, aimed at delivering this kind of traffic.

* This work was supported in part by the Ministry of Economy and Competitiveness of Spain under Grants TIN2013-47272-C2-1-R and TEC2015-71932-REDT.

C.Fernandez-Llatas and M.Guillen (Ed.):
Workshop on Innovation on
Information and Communication Technologies
(ITACA-WIICT 2018)

ISBN 978-84-09-07373-3

The RACH is accessed by means of a four-message handshake contention-based procedure. First, the devices (named UEs herein) wait to the next random access opportunity (RAO) and sends a *Msg1* using a randomly chosen preamble from a pool of available preambles. *Msg1* is detected at the eNodeB if the preamble is chosen by just one UE in the current RAO; if not, a collision occurs. For each detected preamble, the eNodeB sends a random access response (RAR) message, *Msg2*, which includes one uplink grant, from a limited number of grants available. *Msg2* is used to assign time-frequency resources to the UEs for the transmission of the connection request. UEs that received an uplink grant send their connection request message, *Msg3*, using the resources specified by the eNodeB. Finally, the eNodeB responds to each *Msg3* transmission with a contention resolution message, *Msg4*. The interested reader is referred to [3,4,6,15] for further details. A fundamental issue is the efficient management of network resources in overload situations produced when many MTC devices react to the same event which results in signaling congestion in the RACH.

The 3GPP proposes the extended access barring (EAB) as one of the mechanisms for congestion control in current cellular systems [7]. EAB selectively restricts the attempts of UEs to access the RACH. Each UE configured for EAB is allocated an access class (AC) in the range 0–9. When the network determines that it is appropriate to apply EAB (by means of a congestion coefficient), it barres all UEs in a given set of ACs, and broadcasts a sistem information block type 14 (SIB14) containing a 10-bit barring bitmap. The barring is of simple on/off type, where access to each AC is either allowed or not. EAB may be effective whenever the congestion occurs sparingly and during short periods of time (in the order of a several seconds). This fact goes in line with the bursty traffic behavior of MTC described in [1].

In the literature, several studies address the EAB mechanism. On the one hand, there are studies that misinterpret the EAB behavior or do not conform with 3GPP specifications [11,12]. On the other hand, studies such as [9,13,14,16] analyze EAB mainly in terms of access success probability and access delay. In such studies, a practical way to implement the congestion coefficient remains unclear since the number of preamble transmissions is not known at the eNodeB.

In this paper, we propose a realistic method to implement the congestion coefficient for the proper functioning of EAB. Then, we conduct a thorough performance analysis of this mechanism and evaluate the impact of paging timing on EAB performance. Our main contributions are summarized as follows

- We implement and evaluate the EAB scheme in massive MTC scenarios following the 3GPP directives for this kind of studies.
- We propose a method to estimate the congestion coefficient from the number of used preambles at every RAO, which is effectively known at the eNodeB so that our proposed solution conforms the network specifications [2,4,6,7] and can be successfully integrated into the system.
- We evaluate the impact of the paging timing on the EAB performance in a realistic situation in which the congestion coefficient is estimated as mentioned above.

Simulation results show that a limiting factor of EAB as defined by the 3GPP is that, when a barred AC is released, its UEs initiate their access procedure in bursts of periodicity T_{SIB14}. These bursts cause many preamble collisions during the first RAOs, deteriorating overall performance. On the other hand, increasing the paging cycle rises the successful access probability at the cost of longer access delay while diminishing the number of preamble transmissions in light-loaded MTC scenarios which results in energy savings for power-constrained devices.

The rest of the paper is organized as follows. In Section 2, we first present the operation mode of EAB, then we propose a method to compute the congestion coefficient used to turn on or off this mechanism and present the paging timing according with current network specifications. In Section 3, we analyze in-depth the performance of EAB in terms of network key performance indicators (KPIs) and evaluate the impact of the paging timing. Finally, in Section 4 we present our conclusions.

2 Extended Access Barring Mechanism

In the following, we first present the operation mode of EAB. Then, we propose a method to implement the EAB congestion coefficient for its proper functioning and present the paging timing for information update.

2.1 EAB operation mode

EAB is activated when congestion is detected. For this purpose, the 3GPP defines a congestion coefficient (CC_W) for a moving time-window of W ms, as detailed in Section 2.2. With a periodicity given by a *modification period* parameter, CC_Ws are used to update the EAB state. If CC_W for $W = 1000$ ms exceeds 0.4, EAB is turned on and all ACs except one are barred. From here, every time that CC_W for $W = 500$ ms is under 0.4, barring state is released for one AC. The release of ACs proceeds in cycle order until all ACs are unbarred. Then, if CC_W for $W = 1000$ ms is under 0.2, EAB is turned off.

The SIB14 contains the bitmap of barred ACs; the eNodeB broadcasts messages containing SIB14s with a periodicity of $T_{SIB14} \in \{80, 160, 320, 640, 1\,280, 2\,560, 5120\}$ ms [7]. Every time the bitmap has to be changed, the eNodeB notifies it to the UEs through a *system information change* parameter contained in the paging messages [8]. Paging messages are sent at specific radio frames and subframes, namely paging frames (PF)s and paging occasions (PO)s, within a paging cycle (T_P). UEs in idle state wake up at their respective PO and read the paging message. UEs calculate their POs from their local identifiers, in order that the POs of the different UEs are distributed homogeneously throughout T_P (see Section 2.3). When a UE reads a paging message with *system information change* set to on, it reads the next message containing the SIB14. To make sure that all UEs are notified of all changes and have a chance to update their EAB information, the *modification period* is set to the maximum of T_P and T_{SIB14}, and changes on the bitmap are notified when they are produced but the SIB14 update is delayed up to the next *modification period*. When a UE has to access to the RACH, it checks its barring state from the bitmap contained in the latest updated SIB14.

2.2 Congestion Coefficient Implementation

The CC_W is defined as [17]

$$CC_W = 1 - \frac{nRAR_W}{nPT_W}, \tag{1}$$

where $nRAR_W$ is the number of RARs sent during W ms and nPT_W is the number of preamble transmissions during W ms.

To calculate CC_W and therefore update its value at every RAO, the eNodeB would need to know the number of preamble transmissions at each RAO. But in the commonly assumed collision model defined by the 3GPP, this number is unknown, because those preambles transmitted by more than one UE are not decoded. Therefore, the value of nPT_W defined in (1) should be estimated from the number of preambles used (by at least one UE) at each RAO. In our study, we have obtained this estimation as follows.

Let $Y_j(i) \in \{0, 1\}$ be the random variable that denotes the transmission of preamble j at RAO(i) given that the total number of preamble transmissions at RAO(i) is $n_t(i)$. Then, $Y_j(i) = 0$ when the preamble j has not been transmitted by any UE at RAO(i), and $Y_j(i) = 1$ otherwise. Its probabilities are

$$\begin{cases} \mathbb{P}\{Y_j(i) = 0\} = \left(1 - \frac{1}{R}\right)^{n_t(i)}, \\ \mathbb{P}\{Y_j(j) = 1\} = 1 - \left(1 - \frac{1}{R}\right)^{n_t(i)}, \end{cases} \tag{2}$$

where R is the number of available preambles, and

$$\mathbb{E}\{Y_j(i)\} = 1 - \left(1 - \frac{1}{R}\right)^{n_t(i)}. \tag{3}$$

Then, the number of used preambles at RAO(i), $n_u(i)$, is

$$n_u(i) = \sum_{j=0}^{R} Y_j(i), \tag{4}$$

and its expected value is

$$\mathbb{E}\{n_u(i)\} = R\left[1 - \left(1 - \frac{1}{R}\right)^{n_t(i)}\right]. \tag{5}$$

Since $n_u(i)$ is known at he eNodeB, and assuming that $\mathbb{E}\{n_u(i)\}$ changes slowly, it can be estimated from a short term time average of $n_u(i)$. Let $\hat{n}_u(i)$ be an estimate of $\mathbb{E}\{n_u(i)\}$ at RAO(i) obtained by exponential smoothing of $n_u(i)$,

$$\hat{n}_u(i) = \alpha\, \hat{n}_u(i-1) + (1-\alpha)\, n_u(i), \tag{6}$$

with $\alpha < 1$. Finally, from Eq. (5), the estimated value of the number of transmitted preambles used to calculate CC_W is

$$n_t(i) = \frac{\log\left(1 - \frac{\hat{n}_u(i)}{R}\right)}{\log\left(1 - \frac{1}{R}\right)}. \tag{7}$$

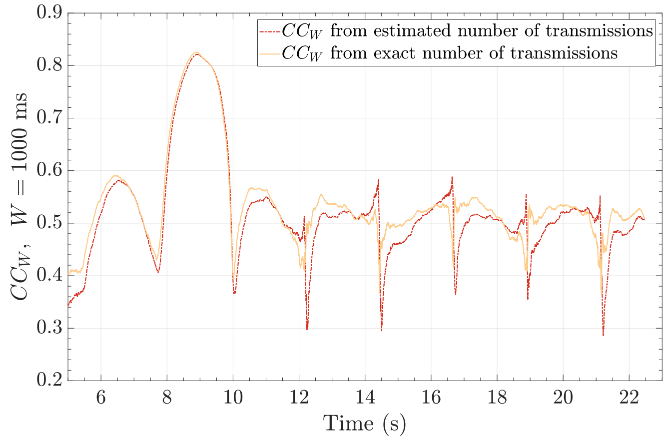

Fig. 1. CC_W operation. $N_M = 30\,000; (T_P, T_{SIB14}) = (2560, 320)$ ms.

We have checked through simulations that the values of CC_W obtained by means of this estimator are very close to those obtained using the real number of preambles transmitted. Fig. 1 illustrates an example of the values of CC_W for $W = 1000$ ms during a congestion episode induced by the MTC traffic benchmark described in Section III with $N_M = 30\,000$ MTC UEs arrivals and $(T_P, T_{SIB14}) = (2560, 320)$ ms. The CC_W obtained from the estimated number of transmissions is compared with the obtained from the exact value of transmissions. As can be seen, the error in the estimated CC_W is minimal.

2.3 Paging Timing

The UE can be in two RRC states: connected or idle. The UE is in connected state after successfully performing the random access procedure. The UE is in idle state during inactivity periods and may use DRX to reduce power consumption and receive system information changes notifications from the eNodeB. In idle state, the DRX cycle can be allocated by either the upper layers or the eNodeB. If it is allocated by the upper layers, the DRX is specific per UE, and a *specificDRX* value is set. Otherwise, the DRX cycle is allocated by the eNodeB through the paging cycle parameter and the *defaultPagingCycle*, broadcast through SIB2, is set. Note that a UE can also use a extended DRX value, $eDRX \triangleq 512$ radio frames.

The paging message is used to inform UEs in idle state about a change of system information and/or provide notifications such as the Earthquake Tsunami Warning System (ETWS). The eNodeB initiates the paging procedure by transmitting the paging message at the UE's paging occasion, PO, as specified in [8].

The exact timing of the paging message for both eNodeB and UE is a function of two parameters: PF, and PO. One PF is one radio frame, which may contain one or multiple POs. When DRX is used, the UE needs only to monitor one PO per DRX cycle.

Table 1. Subframe Patterns for PO mapping [8]

Ns	PO when $\mathtt{i\_s} = 0$	PO when $\mathtt{i\_s} = 1$	PO when $\mathtt{i\_s} = 2$	PO when $\mathtt{i\_s} = 3$
1	9	N/A	N/A	N/A
2	4	9	N/A	N/A
4	0	4	5	9

For computing above parameters, let T_P be the paging cycle used in the system as

$$T_P \triangleq \min(\mathit{defaultPagingCycle}, \mathit{specificDRX}). \tag{8}$$

Note that if *eDRX* is used by the UE, $T_P = 512$ radio frames.

Then, PF is given by the following equation

$$PF = (\mathtt{SFN} \bmod T_P) = (T_P \text{ div } \mathtt{N}) * (\mathrm{UE_{ID}} \bmod \mathtt{N}), \tag{9}$$

where $\mathtt{SFN}$ is the system frame number, $\mathtt{N} = \min(T_P, \mathtt{nB})$ indicates the number of PFs within the paging cycle, $\mathtt{nB} \in \{4T_P, 2T_P, T_P, \frac{T_P}{2}, \frac{T_P}{4}, \frac{T_P}{8}, \frac{T_P}{16}, \frac{T_P}{32}, \frac{T_P}{64}, \frac{T_P}{128}, \frac{T_P}{256}\}$ is broadcast in SIB2, and $\mathrm{UE_{ID}} = \mathtt{IMSI} \bmod 1024$; $\mathtt{IMSI}$ is the international mobile subscriber identity given as a sequence of six up to 21 digits.

Accordingly, the parameter PO is mapped using Table 1 and the index $\mathtt{i\_s}$ computed as

$$\mathtt{i\_s} = \lfloor \mathrm{UE_{ID}}/\mathtt{N} \rfloor \bmod \mathtt{Ns}, \tag{10}$$

where $\mathtt{Ns} = \max(1, \mathtt{nB}/T_P)$ indicates the number of POs per PF.

3 Performance Analysis

A single cell environment is assumed in which the access requests of MTC UEs follow a $Beta(3, 4)$ distribution over a period of 10 s, according to the traffic model 2 specified by the 3GPP in [1]. This traffic model can be seen as an extreme scenario in which a vast number of MTC UE arrivals (ranging from 5 000 to 30 000) occur in a highly synchronized manner (e.g., after an alarm that activates them).

We measure three network KPIs, namely the probability to successfully complete the random access procedure, P_s; the mean number of preamble transmissions needed by the UEs to successfully complete the random access procedure, K; and the access delay (mean and percentiles) of the successful accesses, D. These KPIs are in conformance with the 3GPP directives [1] to assess the efficiency of the LTE-A random access procedure with MTC.

To obtain the above KPIs, we developed a discrete-event simulator that fully reproduces the behavior of UEs, eNodeB, and RACH during the random access procedure. We assume a typical PRACH configuration, *prach-ConfigIndex 6* [5], where the subframe length is 1 ms and the periodicity of RAOs is 5 ms. $R = 54$ out of the 64 available preambles are used for the contention-based random

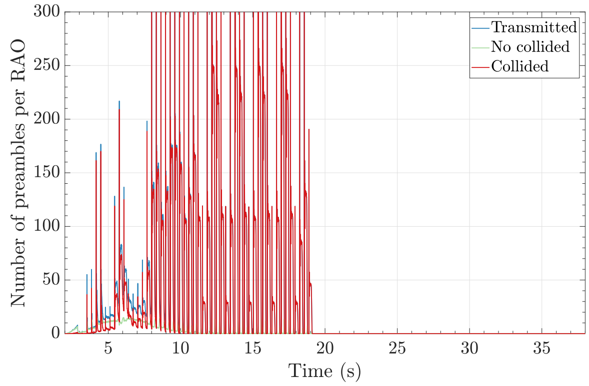

(a)

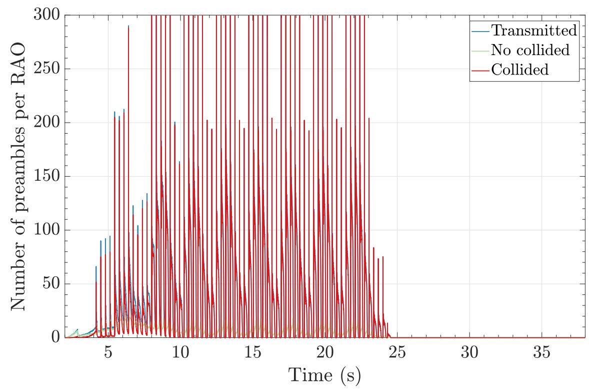

(b)

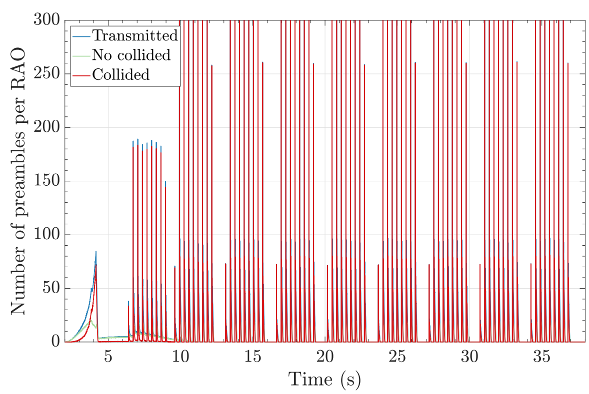

(c)

Fig. 2. UE access attempts. (a) $T_P = 640\,\mathrm{ms}$. (b) $T_P = 1280\,\mathrm{ms}$. (c) $T_P = 2560\,\mathrm{ms}$.

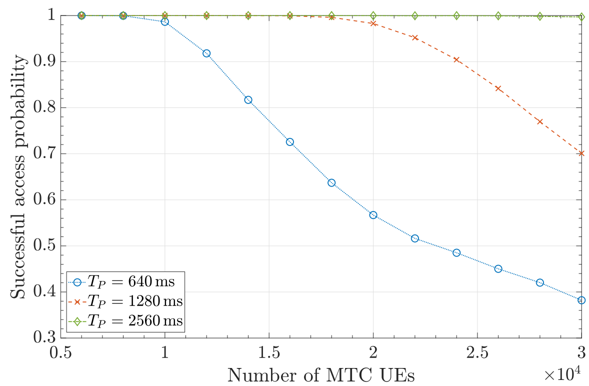

(a)

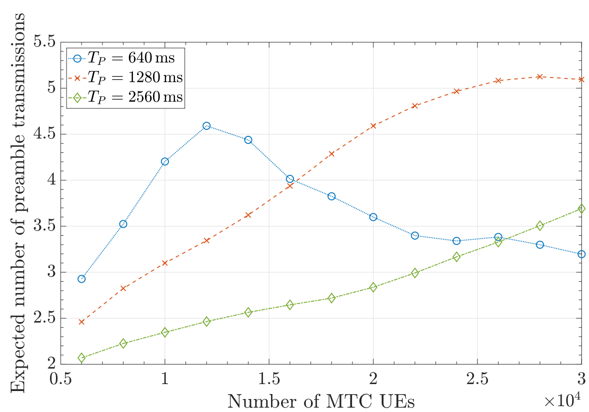

(b)

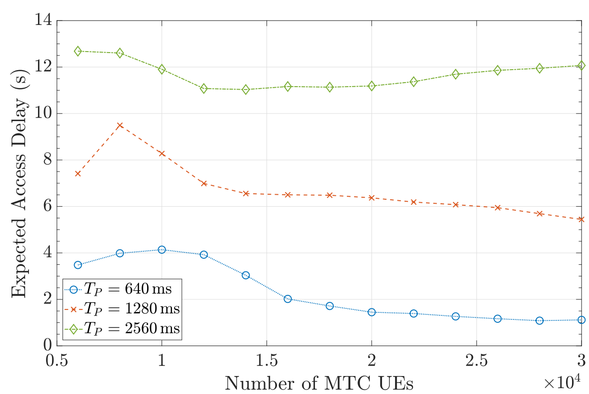

(c)

Fig. 3. Key performance indicators. (a) Successful access probability. (b) Preamble transmissions. (c) Access Delay.

access procedure and the maximum number of preamble transmissions of each UE, *preambleTransMax*, is set to 10. Additional system configuration parameters can be found in [15, Table III].

First we show in detail how the standard EAB mechanism handles congestion episodes. Fig. 2 plots the temporal distribution of preamble transmissions during a congestion episode of $N_M = 30\,000$ MTC UEs and $(T_P, T_{SIB14}) = (\{640, 1280, 2560\}, 320)$ ms. It can be seen that, when congestion builds up, at $t \approx 4$ s, EAB is enabled. Then, ACs start to be unbarred, one at a time, with a periodicity of *modification period* $= T_P$. Every time that an AC is unbarred, a number of UEs access the RACH in bursts of periodicity $T_{SIB14} = 320$ ms. Each burst corresponds to those UEs whose POs are between two consecutive broadcasts of the SIB14; these UEs access the RACH simultaneously because they update their SIB14 simultaneously. As the T_P configuration value increases, the time required to relieve a congestion episode is longer (e.g., with $T_P = 2560$ ms, the network handles $N_M = 30\,000$ access requests in ≈ 37 s whereas ≈ 19 s are required with $T_P = 640$ ms.)

In Fig. 3, we present the network KPI results for different configurations of T_P. Considering feasible parameter values in the LTE-A standard, we tested several configurations for the combination of T_P and T_{SIB14} and we verified that, as in [9,17], combinations in which $T_P < T_{SIB14}$, result in very poor performance in terms of P_s (we omit these results because of lack of space). Hence, we show the results for $T_P \in \{640, 1280, 2560\}$ ms and $T_{SIB14} = 320$ ms. In Fig. 3a, we can see that the access success probability increases as the T_P duration increases. This is because the greater the T_P, the greater the number of information updates per T_P, which results in lower intensity of the traffic burst after each SIB14 update. However, the cost of increasing T_P is that ACs are unbarred at a slower rate (one AC per T_P), thus increasing the access delay as can be seen in Fig 3c. In terms of expected number of preamble transmissions, increasing T_P reduces this metric particularly in light-loaded scenarios (i.e., $N_M < 16\,000$) thus decreasing the energy consumption; however, in heavy-loaded scenarios (i.e., $16\,000 \leq N_M$) this metric increases gradually as T_P increases; this is because the delay caused by the paging mechanism: long paging cycle limits the performance of the barring phase. As a result, some devices cannot receive the EAB updated information on time and their accesses will probably fail; therefore, they should start the access attempt again.

To sum up, increasing T_P rises the successful access probability at the cost of longer access delay while diminishing the number of preamble transmissions in light-loaded MTC scenarios which translates in energy savings for power-constrained MTC devices.

4 Conclusion

In this paper, we have proposed a practical method to implement the congestion coefficient used by extended access barring for handling congestion in massive machine-type communication scenarios. Through extensive discrete-event simulations, we analyzed the EAB scheme using our proposed congestion coefficient implementation and studied the impact of the paging timing on the performance of EAB. Numerical results show that setting a higher paging cycle value increases the successful access probability in the network at the cost of longer access delay while diminishing the number of preamble transmissions in light-loaded MTC scenarios. This results in energy savings that is useful for the rather power-constrained devices in MTC applications.

References

1. 3GPP: Study on RAN Improvements for Machine Type Communications. 3GPP, TR 37.868 (Sep 2011)
2. 3GPP: Physical layer procedures. 3GPP, TS 36.213 (Dec 2014)
3. 3GPP: Feasibility Study for Further Advancements for E-UTRA. 3GPP, TR 36.912 (Mar 2017)
4. 3GPP: Medium Access Control (MAC) Protocol Specification. 3GPP, TS 36.321 (Sep 2017)
5. 3GPP: Physical Channels and Modulation. 3GPP, TS 36.211 (Sep 2017)
6. 3GPP: Radio Resource Control (RRC), Protocol specification. 3GPP, TS 36.331 (Sep 2017)
7. 3GPP: Service Accessibility. 3GPP, TS 22.011 (Sep 2017)
8. 3GPP: TS 36.304, V14.4.0, User Equipment (UE) procedures in idle mode (Sep 2017)
9. Cheng, R.G., Chen, J., Chen, D.W., Wei, C.H.: Modeling and analysis of an extended access barring algorithm for machine-type communications in LTE-A networks 14(6), 2956–2968 (June 2015)
10. Ericsson: Ericsson mobility report/internet of things forecast (Nov 2017), https://www.ericsson.com/en/mobility-report/internet-of-things-forecast
11. Hwang, R.H., Huang, C.F., Lin, H.W., Wu, J.J.: Uplink access control for machine-type communications in LTE-A networks. Personal and Ubiquitous Computing 20(6), 851–862 (Nov 2016)
12. Kim, H., Lee, S.S., Lee, S.: Dynamic extended access barring for improved M2M communication in LTE-A networks. In: Proc. IEEE SMC. pp. 2742–2747 (Oct 2017)
13. Larmo, A., Susitaival, R.: RAN overload control for Machine Type Communications in LTE. In: IEEE Globecom Workshops. pp. 1626–1631 (Dec 2012)
14. Phuyal, U., Koc, A.T., Fong, M.H., Vannithamby, R.: Controlling access overload and signaling congestion in M2M networks. In: Proc. IEEE ASILOMAR. pp. 591–595 (Nov 2012)
15. Tello-Oquendo, L., Leyva-Mayorga, I., Pla, V., Martinez-Bauset, J., Vidal, J.R., Casares-Giner, V., Guijarro, L.: Performance Analysis and Optimal Access Class Barring Parameter Configuration in LTE-A Networks With Massive M2M Traffic 67(4), 3505–3520 (April 2018)
16. Toor, W.T., Jin, H.: Comparative study of access class barring and extended access barring for machine type communications. In: Proc. IEEE ICTC. pp. 604–609 (Oct 2017)
17. WG2, G.T.R.: Further performance evaluation of EAB information update mechanisms. Meeting N. 77 R2-120270, 3rd Generation Partnership Project (3GPP) (Feb 2012)

Systematic Review on Support Systems for Cancer Patient: Nutritional Assessment and Educative Strategy Improve Patient's QOL

Lucia A Carrasco-Ribelles[1], Ana Rojo-Agusti[1], Carlos Antequera-Sanchez[1], Gema Ibanez-Sanchez[1], Aurora Perla[2], Eva Domínguez[2], Luis Cabañas[3], Isidro Jarque[4]

[1] Universitat Politècnica de València, 46022 Valencia, Spain
{geibsan@upvnet.upv.es}
[2] Instituto de Investigación Sanitaria La Fe
[3] Universidad de Valencia,
[4] Hospital Universitario y Politécnico La Fe

Abstract. Background: There is an increasing trend on using support systems for improving the quality of life (QoL) of people with concrete diseases such as diabetes, cholesterol, cancer among others. This review is focused on cancer, especially in multiple myeloma, where almost all support systems are focused in a unique aspect, such as nutrition, education or physical activity. Purpose: To determine the features of newly support systems for cancer patients, in order to improve patient care. Data sources: PUBMED, GoogleScholar, Annals of Oncology, European Journal of Oncology and Blood since January 2010. Study selection criteria: Researchers independently screened reports to identify studies published in English or Spanish of support systems for cancer patients which described sort of educational programs or nutritional and physical assessments as main determinant in the supportive treatment. That were implemented in clinical settings, carried out an educative strategy or reported nutritional, physical, functional and psychosocial status outcomes. Data extraction and synthesis: Of the 348108 articles that were found containing the combinations of keywords in any of their fields in any date, 68 were selected by means of filters of publication dates (2010-2018) and criteria of keyword searching fields (Title/Abstract). Post-duplicates elimination, 66 articles were screened and only 12 of them were preferred as relevant, fitting the inclusion-exclusion requirements. Its exhaustive analysis revealed that a total of 8 studies (67%) focused their support field on assessing QoL or Symptom burden; at least 5 studies (41.8%) measured nutritional status, physical activity and patient knowledge; only 3 studies (25%) evaluated emotional status. On average, trials considered at least 3 of these items. A comparative of PICOS parameters is attained for 10 studies (83.3%) which offered quantitative outcomes, therefore researcher obtained data about study design, participants' characteristics, patient assistance, intervention modalities and outcomes. Conclusion: None selected study address patient support from all approaches described. The nutritional follow-up systems and disease education programs are highlighted as essential core of effective support systems. Funding source: Publication made within the framework of the project *Diseño de servicios para mejora del factor humano en pacientes con Mieloma - NuMielo* funded by the *Comisión Mixta de Evaluación Ayudas UPV-LA FE 2017*

C.Fernandez-Llatas and M.Guillen (Ed.):
Workshop on Innovation on
Information and Communication Technologies
(ITACA-WIICT 2018)

ISBN 978-84-09-07373-3

1 Introduction

1.1 Background

Multiple Myeloma (MM) is a clonal plasma cell disorder responsible of 1% of all cancers and 10% of hematologic malignancies [1]. The second most common hematologic malignancy, it is an estimated worldwide incidence of 114,000 new cases and 80,000 deaths in 2012 [73]. In the United States (US), the estimated annual incidence in 2015 was 26,850 new cases and 11,240 deaths [74]. In Europe, the estimated annual incidence in 2012 was 38,900 new cases and 24,300 deaths.

Multiple myeloma is largely a disease of older people. The median age at diagnosis is 69 years, and approximately 2/3 of people are over age of 65 at the time of diagnosis [75], [2] whereas average survival is approximately 5-7 years, it varies depending on host factors, tumour burden (stage), cytogenetic abnormalities and response to therapy [3]. The incidence of MM is increasing slowly; this may be related to an aging population, as well as to increasing obesity rates. However, deaths from MM are decreasing year-on-year: the 5-year survival rate in the US was 27% in 1975 compared to 53% from 2008 to 2010 [76], and in Europe was approximately 40% between 2006 and 2008.

Local MM treatments consist in multiple cycles of radiation therapy or surgery, which are more likely to be useful for earlier stage cancers. For more advanced cancer drug therapy, biophosphonates therapy, stem cells transplant and supportive treatments or a combination thereof accounts for the systemic treatments commonly used. The MM, its related-treatment side-effects and extended hospital stays reduce quality of life (QOL) due to the increased immobility, the physical deconditioning and weakness [4] [77] [79] and the loss of appetite and worsening of nutritional status.

In MM health care, symptoms of the disease, as well as related-treatment side effects, are addressed with the palliative care treatments. Nevertheless, support systems aimed at empowering the patient and recovering its QoL are founded on integrated care methodologies on diverse domains: educative, nutritional, symptomatology, physical and emotional status [78].

Research has shown that both, educative and coaching programs present positive effects in patient's attitude towards overcoming the disease. It is considered that monitoring nutritional and symptomatology status of the patient will provide relevant clinical information [80]. Furthermore, the visualization of the user results will enhance system adherence and increase the patient empowerment. It is hoped that clinical therapies combined with support systems will result in a quality care aid for the multiple myeloma patient. A logic model for Support System and QoL outcomes can be seen in Figure 1. This model shows a graphic representation of the potential mechanism of action for improving cancer patients' life. It was taken into consideration for carrying out the systematic review and focusing it on specific knowledge targets.

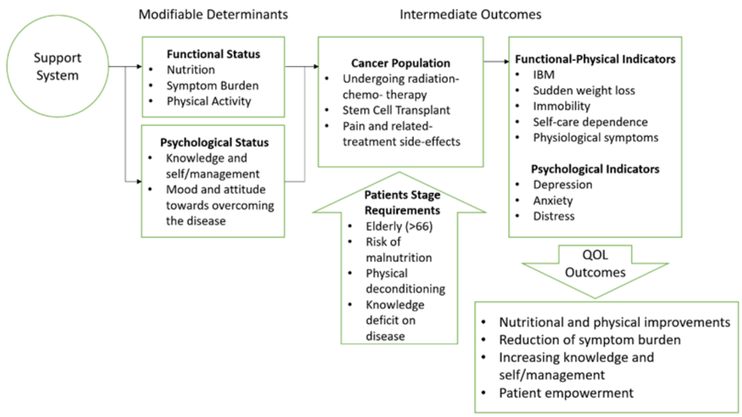

Fig. 1. Logic Model for Support System and QoL Outcomes.

1.2 Objectives

In order to check the most effective cancer support systems used from 2010 to date PRISMA guidelines are followed. Given the vast heterogeneity of supporting care systems in cancer, this review focuses on searching support systems for cancer patients driven at medical institutions which assessing patient nutritional status or leading an educational strategy. Selected studies are evaluated following PICOS methodology and the impact that these systems have on patients' QOL, the domain of intervention, and the patient assistance are parameters compared among all the studies. Accordingly, this meta-analysis search to submit the optimal support system for multiple myeloma patients.

2 Methods

2.1 Protocol

The methodology employed for this systematic review follows the Preferred Reporting Items for Systematic Reviews and Meta-Analyses (PRISMA) statement for reporting systematic reviews that evaluate health care interventions [5]. In addition, the PRISMA reporting guidelines [6] has been consulted for writing this paper.

2.2 Information Sources and Search

The search was conducted in PubMed and GoogleScholar databases and in the journals Annals of Oncology, European Journal of Oncology and Blood, including every article since 2010. The search took place from the 6th to the 8th of June 2018. Selected keywords were: (1) Cancer AND Nutrition AND Education for patients, (2) Cancer AND Nutrition AND Empowerment, (3) Myeloma AND Nutrition AND Support, (4), Myeloma AND Nutrition AND Smartphone. All the studies that included one of these combinations of keywords in their title or abstract were selected to further inspection.

Table 1. Search criteria in the different scientific databases.

Keywords/ Databases	PubMed	Google Scholar	Annals of Oncology	European Journal of Oncology	Blood – American Society of Haematology Journal
Cancer AND Nutrition AND Empowerment	"abstract, title"	"title"	"title"	"abstract, title"	"abstract, title"
Cancer AND Nutrition AND Education for patients	"abstract, title"	"title"	"title"	"abstract, title"	"abstract, title"
Myeloma AND Nutrition AND Support	"abstract, title"	"title"	"title"	"abstract, title"	"abstract, title"
Myeloma AND Nutrition AND Smartphone	"abstract, title"	"title"	"title"	"abstract, title"	"abstract, title"

2.3 Eligibility Criteria and Study Selection

Inclusion and exclusion criteria was defined for the systematic review, so the studies included must meet at least one of the inclusion criteria and none of the exclusion. The inclusion criteria are: (1) the study describes a support system for cancer patients, (2) the study describes an educational strategy for cancer patients, (3) the main object of the study is cancer patients' nutrition. The exclusion criteria are: (1) the study is not written in English or Spanish, (2) the main beneficiaries of the study are not cancer patients, (3) the study does not include a support system, (4) the study is not developed or validated in a health organization or health facility. These criteria are chosen as it is the most related with the main research question. The identification and further selection of papers was guided by the PRISMA flow diagram [5], to properly remove those who were duplicated or irrelevant according to eligibility criteria.

2.4 Data Items Collection Process

The following items were collected for all papers that fitted eligibility criteria: (1) title, (2) assistance modality, (3) assistance frequency (4) cancer kind, (5) users involved, (6) number of patients, (7) evaluated parameters during the study, (8) evaluating method, (9) results. This data was collected independently by some authors and then cross checked for consistency.

2.5 Synthesis of results

The results will be organized in a summary table where the main topics will be shown (Table 1). The parameters of papers (Table 2) which describe sort of similar support systems will be compared amongst them, as most of them described quite different systems. Chosen parameters could seem very generalist but that allows a comparison between the studies.

3. Results

3.1 Study Selection

The general search included all the published articles that collected the defined keywords in their content resulted in 348.108 findings in any date. As cancer is a popular topic, the clear majority of these papers only mentioned cancer in their introduction or in their conclusion, so they were not working directly in cancer. Those papers that did not include any of the four before-mentioned combination of keywords in their title or abstract were removed, as the papers published before 2010. After that, there were only 68 articles left. At this point, the number of studies were sixty-six, after deleting duplications. Then, inclusion and exclusion criteria were applied to screen them and obtain the essential evidence. After that, fifty-four studies were excluded and twelve were assessed for eligibility. Finally, ten of them were selected for a quantitative analysis and seven were selected for a qualitative analysis due to the parameters assessed in each study. All the process was guided by the flow diagram proposed by PRISMA statement [5] and it can be seen in Figure 2.

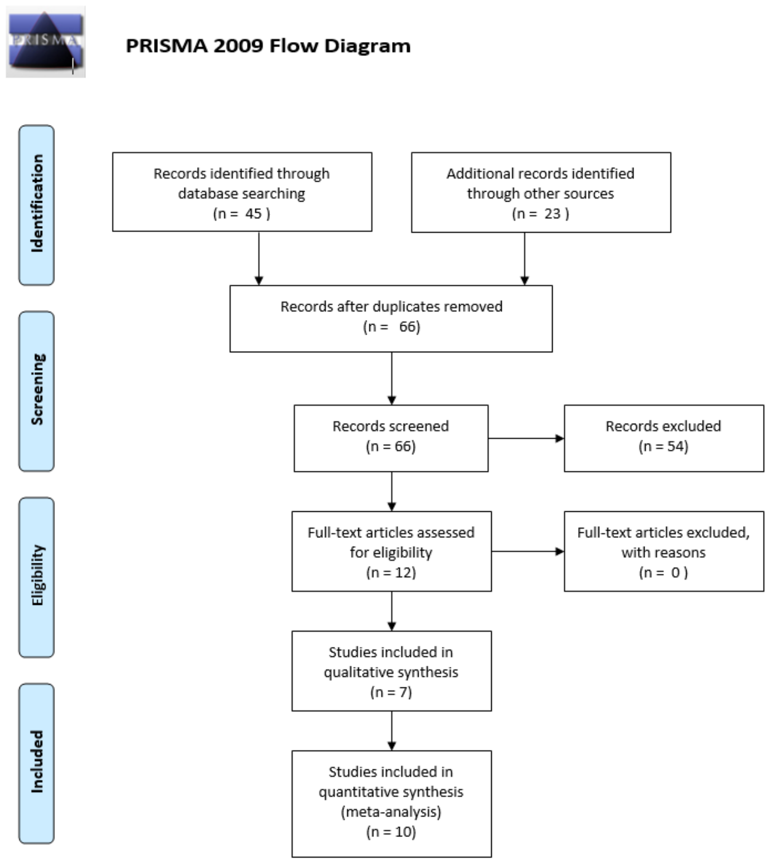

Fig. 2. ***Four-phase PRISMA flow diagram, already filled.***

3.2 Characteristics of Included Studies

The included studies resulted focused on emphasizing patient's QoL by carrying out four different care approaches or a combination of them, these were: (5) nutritional status, (8) symptomatic burden/therapy-related side-effects, (5) physical activity, (3) emotional well-being, (5) disease understanding and self-management, (8) quality of life. On average, these studies analysed at least 3 of these items. A total of 10 (83.3%) assessed clinical quantitate outcomes, of which 6 collected qualitative outcomes; 2 (16.7%) studies showed only qualitative evaluations. The participant samples included adult populations that were cancer patients, 5 trials included myeloma, lymphoma and hematological malignancies participants, 2 consisted of cancer survivor's participants, and 5 conformed by general cancer participants. The assistance methodologies followed are classified as (1) Training sessions, (2) Distance assistance and (9) Educational meetings or symposiums, both of which required attendance. In general, training programs and digital care systems were carried out during the chemotherapy treatment, even lasting between 3 to 9 months with high and continue frequency of patient care assistance, while educational programs implemented as short talks or arranged sessions lasted few weeks.

3.3 Individual Results

A summary of the main topics of each study can be seen in Table 1. Almost every paper has QoL as one of their main topics, and they are usually focused in 3-4 different fields, such as the followings:

3.3.1 Physical Activity

Four studies included physical activity therapies or the assessment of movement coordination. The immobility associated to chemotherapy and lymphoma/myeloma patients' balance control were improved with exercise programs consisting of sensorimotor-, endurance-, strength- training. The sensorimotor training developed by F.Streckmann et. al is the only study in this review to directly test motion tasks [7]. Several studies provide care systems in which monitoring physical activity is combined with other supportive therapies. Following-up the physical activity of the patient receiving palliative care takes part of rehabilitation and education programs implemented on a mobile care system with self-monitoring features [7]. Similarly, the enrolment to mobile health apps allow patients to communicate in real time with health providers to receive complete health coach and set small weekly goals. This supportive health tool reported satisfactory improvements on patients' QoL, particularly among physical, functional and emotional domains. [9] Despite of the previous results, physical fitness reveals no significant score at multidisciplinary education program based on decrease fatigue in lung cancer patients. [10]

Overall, physical activity contributes to better physical well-being, as long as exercise routine is established, and it's combined with other supportive therapies.

3.3.2 Symptom Burden

In total, eight studies included the assessment of patients' symptom burden. This is usually an additional barrier for patients that suffer such a complicated disease like cancer. For the first study, [7] it is demonstrated that following an exercise program during cancer therapy period could reduce side-effects. Moreover, complementary and alternative medicine (CAM) based on nutrition, exercise, herbs, psychological, social and spiritual health, aromatherapy, massages, acupuncture or music showed their possibilities as complements to conventional cancer therapies by proving symptoms' reduction after their application. [11] Additionally, educational programs about self-care on lung cancer patients could improve fatigue levels as shows. [11] That is not the only example of applying education for reducing side-effects, [12] manifests that multimedia information could be another way to improve patients' education about managing nutrition-related chemotherapy side-effects. Another study showed that a follow-up of colorectal cancer patient's nutrition highly reduces radiotherapy toxicity, the principal side-effects of radiotherapy. [13] Also, new technology tools such as smartphone could be an option for complementary therapies. In fact, [9] Chen C.E. et. al study shows that a virtual smartphone-based health coaching significantly improves physical and functional domains of cancer patients after chemotherapy. On the other hand, educational symposium could not be enough to make a significant improvement on knowledge about side-effects, [14, 15] although this knowledge should be increased to insure a complete assistance.

To sum up, cancer side effects could be faced from different scope, however the most economical and feasible option may be an educational system that support the cancer patient using new technologies.

3.3.3 Disease Understanding and Self-management

Educational intervention has two main purposes: to deepen disease knowledge and to change lifestyle to perceive benefit of nutrition and physical activity, self-efficacy in handling side-effects. Both goals are pursued in the Lawn S. et al. study [16] with a tailored 12-week intervention to determine optimal strategies for achieving self-management-based nutrition and physical activity for cancer survivors with fortnightly progress reviews showed a trend toward significant improvement in self-management capability and psychological impact. Shorter educational interventions are found as useful as long-term programs about increasing patient knowledge. Thompson J. et. al [12] measured the impact of an early education multimedia intervention in managing nutrition and related chemotherapy side-effects which reveal significant changes in perceived health beliefs. Leslie Padrnos et. al [14,15] through implementing an educational symposium and the evaluation of patients' quality of life before and three months after the symposium has also confirmed that improving the patient's knowledge deficit on cancer has its effect on the quality of life and health care compliance of the patient. Educational programs for post-transplant patients and their caregivers were helpful to increase knowledge of care and precautions that are required post-discharge as well as coping with life after transplant and positively evaluated. [17]

The aim of educational talks or coaching meetings is to enhance self-management and empower the patient through providing powerful information about how to battle related chemotherapy side-effects and handle their daily routine. Education intervention provides health and psychosocial benefits, it betters the mindset and attitude of the patient towards the disease and ultimately, his quality of life.

3.3.4 Emotional Well-being

In general, cancer treatments are probably one of the most complicated medical procedures that a patient must face. However, not enough attention is paid to emotional problems related to this illness. Complementary and alternative medicine can take part in the Marchand L trial [11] by improving emotional well-being through physical exercises and mindfulness-based stress reduction programs. Some of the cancer patients usually suffer depression, caused by the suffering associated to this illness. Moreover, this problem is not as easy to get over as others, a simple education program cannot improve a depression status on these patients. [10] However, a more constant follow-up could improve these situations, as [9] showed.

3.3.5 Nutritional Status

Questionnaires for assessing the cancer patients' nutritional status allow health care providers or dietitians to determine the overall risk of malnutrition and to change the patients' dietary intakes to improve their health status. Pei-Chun Chao et al [18] have determined a 4 steps strategy-based MUST to improve dietary intake in cancer patients. As first step, the Malnutrition Universal Screening Tool (MUST) scores the risk of malnutrition of the patient as 0, 1 or 2. Next steps are about Nutritional assessment, Nutritional intervention and Nutritional monitoring, which allows measuring and comparing different levels between before and after nutrition education of patient's energy and protein intake. The study of a long-term follow-up randomized controlled trial of individualized nutritional therapy conducted by Ravasco P et. al [13] conveys the effectiveness of early individualized nutritional counselling and education at improving long-term prognosis in colorectal cancer. Clear evidences are obtained of the Thompson J et. al pilot study [12] which endorse primarily to increase skills related to managing nutrition-related chemotherapy side effects as useful component of counselling services for those patients and Wangnum K et. al [10] relates, among other causal factors, the nutritional status of lung cancer patients with their fatigue side-effect. Latest mobile health app for cancer patients includes nutrition support as one of major clinical goals to be monitored. Sog JY et. al [8] based its screening nutrition tool on the PG-SGA questionnaire.

In summary, it is strongly supported that an effective measure to bring about favorable prognosis in chemotherapy patients and cancer survivors is to provide nutritional intervention and education.

3.3.6 QoL

Most of the systems that are assessed take into consideration the relevance of the quality of life among cancer patients. For instance, it is confirmed that exercise trainings could improve patient's quality of life by reducing immobility, muscular deconditioning and loss of physical control. [7] Besides, complementary therapies are another option for improving the quality of life of these patients. Another study reveals that a good nutrition with controlled exercise increases QoL as well as mindfulness-based stress reduction program could help patients with breast cancer who are post-surgery, chemo and radiation therapy. [11] Music therapy and acupuncture has exhibited improvements on quality of life parameters of cancer patients. There are different points of view for developing new methodologies for facing low quality of life, in fact, some studies based their methodologies on new technologies. [8] In this case, they developed a mobile care system that offers a self-monitoring app that facilitate the patients' assistance. Other study considers the self-management a crucial point for increase the survival by addressing nutrition and physical activity needs. [16] In this way, it was obtained an improvement in quality of life. Paying individualized and personalized attention to this patient could be another crucial point, therefore individualized follow-up of nutritional therapy on these patients significantly increases their quality of life. [13] Joining coaching and new technologies (smartphones), it is proved that digital health coaching may help post hematopoietic stem cell transplant patients improve QoL. [9] Besides, it should be considered the relevance of being informed about cancer to ensure a minimum QoL. [14,15]

In conclusion, exercise, a good nutrition, education and following-up either by traditional or technological methods could make a difference in improvement of quality of life in cancer patients.

Table 2. Main topics of each study.

Reference	Disease understanding and self-management	Emotional well-being	Nutritional status	Physical Activity	QoL	Symptom burden
7				x	x	x
8			x	x	x	
9		x		x	x	x
10		x	x	x		x
11		x			x	x
12	x		x			x
13			x		x	x
14	x				x	x
15	x				x	x
16	x			x	x	
17	x					
18			x			
Total	5	3	5	5	8	8

Table 3. Parameters of each study.

Reference	Assistance modality	Assistance frequency	Cancer kind	Users involved	Number of patients	Evaluated parameters during the study	Results
7	On-site assistance: 1-hour sessions.	Twice a week, 36 weeks.	Lymphoma	Patients, sport supervisors and physiotherapists	122	QoL , resistance, strength and motor coordination and reduction of side effects	The exercise program has had a positive impact on the QoL increase of patients during the whole therapy, although this improvement cannot be attributed to the improvement of the PNP or loss of balance control. Reducing pain, increasing sensitivity, reducing loss of balance control and reducing the risk of falling considerably increases QoL, allows dose reduction or even administration of a looser pharmacological therapy and increases survival.
8	Telemedicine assistance	Daily, 4 months	Colon and stomach cancer	Patients, 6 oncologists, 1 nurse, 2 physiologists and 2 nutritionists specialized in cancer	203	QoL, physical activity, risk of malnutrition and stress and satisfaction levels of the patient with the developed system (Likert scale) and the response to	These remote assistance and monitoring systems can maintain the quality of continuous daily care for patients with long-term chemotherapy or early chemotherapy and provide accurate information based on clinical and professional knowledge. Patients can

						clinical measures	easily access varied information related to cancer and health experts provide information in real time based on experience. The online management of cancer patients with a mobile application is demonstrated and the quality of their interfaces and contents motivates the patient, empowers them in their treatment and increases their quality of life.
9	Mobile-app	Daily for 3 months	50% myeloma, 20% lymphoma, 30% hematological malignities	Patients and health coaches	62	QoL and number of messages with their virtual adviser	68% of the patients sent at least one message to the advisor, with an average of 29 messages sent from the patient to the advisor in the 3 months that follow-up lasts. The results of the test improved considerably after counseling with 27% in physical well-being, 53% in functional well-being and 40% emotional well-being.
10	On-site assistance	Once consultation each 2 weeks during 9 weeks + initial consultation.	Lung	Patients and nurses		60	The average level of fatigue of the group receiving education on self-care was a point lower than the mean of the control group. The results of the nutritional status were better for the group that followed the self-care program than the group that did not, however the results of weight, albumin, physical form and depression were not significantly different between both groups.
11	Alternative medicine sessions	Depending on the therapy and the length of the standard treatment	Any	Patients and professionals depending on the therapy	85	Wellness (mental, emotional and symptomatic) and QoL	The results of the survey on the characteristics of the patients who followed the CAM therapy were compared with the results 6 months later. The results indicated that infections and hospitalizations were significantly reduced with the use of CAM. Many CAM therapies such as music, aromatherapy, exercise, relaxation, and mindfulness practices were cheap, accessible, effective,

							and easily incorporated into the holistic and integrated into treatment plans in conventional cancer centers and in palliative care services
12	15 minutes video on-site and brochure to take home	Unique	Any	Recently diagnosed patients	14	Knowledge about chemotherapy and health	The score in the four items on knowledge increased significantly in the two weeks after watching the DVD. This shows that a DVD on the nutritional effects of chemotherapy along with a brochure on the subject, increases short-term knowledge. No significant differences were found on the opinion of the importance of nutrition or the belief of being responsible handling side effects. The patients showed significant increases in the efficacy of themselves perceived after the nutritional education with respect to the starting point. They also showed an increase in perceived knowledge and skills related to the management of the side effects of chemotherapy. This means that the DVD and the booklet could provide a benefit in improving confidence when dealing with these side effects.
13	On-site assistance	Unspecified	Any	Patients, nutritionists and health professionals	37	Daily protein and energy requirements, adherence to the regulated diet, treatment toxicity and quality of life	This study concludes the effectiveness of nutrition in the long-term diagnostic improvement of colorectal cancer if early and individualized nutritional counseling is offered to the patient during radiotherapy.
14	Symposium	Unique	Hematological malignancies (50), multiple myeloma (24), lymphoma	Patients and coaches	79	Knowledge about the disease, symptoms burden and QoL	The topics of knowledge with higher results (more knowledge) were: illness (80%), screening tests (74%), and monitoring tools (72%). The topics of least knowledge were financial management (13%), legal problems (13%)

			(17), leukemia (6), myeloproliferative neoplasia / myelodysplastic syndrome (3), solid tumors (77)				and pain management (35%). There was a significant increase in the understanding of disease (from 80% to 92%), in treatment options (from 60% to 76%), nutrition (from 68% to 84%) and legal problems (15% to 32%)).
15	Symposium	Unique	Myeloid diseases, myeloma, lymphoma, chronic lymphocytic leukemia, breast cancer, lung cancer, cutaneous malignancy, colon cancer and prostate cancer	Patients and coaches	115	QoL	Most of the attendees understood their illness a little (54%) or a lot (29%). The majority of the respondents showed at least a little understanding about treatment options (84%), symptomatology (74%), screening modalities (83%) and side effects of cancer (71%). Those interviewed showed less knowledge about their illness about related stress (49%), risk factors (49%), management of illness related to fatigue (41%) and legal problems related to illness or treatment (27 %).
16	On-site assistance	Depending on the patient	Any	Patients, caregivers and family members	25	QoL and self-sufficiency.	Survivors of cancer, in the active phase of treatment or in its later phase, found this program acceptable to help carry out its nutritional and physical activity objectives according to the interviews and the questionnaires and the anthropomorphic results.
17	Education face-to-face and printed copies	Once a month	Myeloma	Patients, caregivers and family members	138 attendees	Usefulness of the given information, patient safety at discharge and suggestions for improvement	The post-transplant education groups improved the education of patients and caregivers, increasing their confidence and knowledge and has become a useful tool in group orientations. The patients and caregivers suggested adding a

							dietitian which was considered for the improvement of the nutritional information provided.
18	On-site assistance	Unspecified	Any	Patients, caregivers, nurses and dietitians/nutritionists.	444	BMI, the percentage of weight lost in the last 3 months, the decrease in appetite and the adherence to the tracking system.	The limitations related to nutrition education sessions are recognized, such as attitude, family support, access to food and changes in eating habits. The short time of study of the program is recognized to achieve consistent and extrapolatable results. It is concluded that nutrition education and patient follow-up improves protein and energy intakes in hospitalized malnourished patients, reduces the risk of infections and accelerates patient recovery.

4. Discussion

4.1 Evidence Summary

As a result, the following evidence has been collected. For instance, exercise, especially sensorimotor training, [7] and movement interventions are promising complements to cancer therapies. [11] They help patients by improving their QoL, balance control, mobility and by reducing side-effects, symptom burden, overall costs of care, recurrence and mortality in some cancers. Additionally, several studies reported that good nutritional status is vital for patients with cancer. [13] A good nutrition can improve long-term prognosis [13]. Besides, malnutrition increases the duration of the hospital stay, reduce the cost-benefit and risk-benefit ratios of cancer treatments and is related with excess mortality among cancer patients [17]. However, a minor fraction of cancer patients receives any counselling about nutrition-management, but simple oral nutritional interventions could significantly improve the nutritional status and the quality of the diet consumed of cancer patients. [18] Besides of mentioned above, several studies described some education programmes on health, daily life, self-management, nutrition or self-care. It should be noticed that they obtained remarkable results which reveal that these interventions are feasible, useful and appreciated [14] for different patients with cancer [16,10]. These programmes enhanced the education of patients and caregivers, increasing their confidence and knowledge, [17] as well as empowering cancer patients [15]. Other studies noted unnecessary a face-to-face interaction or even an interaction to provide education for cancer patients. An educational multimedia information about nutrition-related side effects could lead to increased knowledge and skills related to managing that side effects of chemotherapy. [12] Also, mobile care systems have been implemented with success, providing health education and self-management features [8] or allowing virtual coaching, with a real caregiver on the other side. [9] As a result, they enabled patients to obtain personalized healthcare, a remote monitoring and information based on clinical and professional knowledge. [8] All of that, followed by an improvement of QoL.

4.2 Limitations

It should be aware that the conclusion of a systematic review must be taken within the context of the search. Therefore, some limitations were found during its study. Firstly, due to the variety of sources, it has not been possible to apply exact search filters and restrictions on each data source. Secondly, ideally, the selected studies should have been focused on multiple myeloma. As not enough findings were obtained, the search was broadened accepting more flexible criteria. Thirdly, despite the effort that studies make to being inferable, any research is constraint to being focused on a specific patient population. Consequently, each result is highly bound to its context. Finally, some of the journals did not allow to access to full report preventing from consulting some relevant information.

4.3 Conclusions

As this systematic review's results show, there are several ways to improve cancer patients' QoL in addition to their regular treatment. These proposals are usually developed as tests, so they are not prolonged in time or extended to other hospitals either, preventing more patients could benefit from them. Most of the papers included in this report only study the effect of a unique support system type, while the combination of some of them could be interesting and improve even more patients' QoL. From the evidence, it can be said that nutrition-centred support systems can better cancer patients' daily life easily and from the first interventions. It can also be said that most patients appreciate being given some education about their disease, how it can change their life and how to adapt themselves to these changes. Finally, the success of app cancer patients support systems has been demonstrated in some studies. Having a support system developed as a mobile could help to make it more reachable to a greater number of patients, as almost everybody has a smartphone nowadays. Considering that cancer is a high prevalence disease and that it does affect a wide and disparate range of people, having a care support system reachable to everybody regardless of their purchase power would make cancer treatment fairer and more equitable.

4.4 Fundings

Publication made within the framework of the project Diseño de servicios para mejora del factor humano en pacientes con Mieloma - NuMielo funded by the Comisión Mixta de Evaluación Ayudas UPV-LA FE 2017.

5. References

1. National Comprehensive Cancer Network (last access: 25/09/2018) https://www.nccn.org/professionals/physician_gls/default.aspx

2. Kyle, R. A., Gertz, M. A., Witzig, T. E., Lust, J. A., Lacy, M. Q., Dispenzieri, A., Fonseca, R., Rajkumar, S. V., Offord, J. R., Larson, D. R., Plevak, M. E., Therneau, T. M., Greipp, P. R. Review of 1027 patients with newly diagnosed multiple myeloma. Mayo Clin Proc. 2003 Jan; 78(1):21-33.

3. Russell, S. J., Rajkumar, S. V. Multiple myeloma and the road to personalised medicine. The Lancet Oncology. 2011; 12: 617–619

4. Newton, R. U., Galvao, D. A. Exercise in prevention and management of cancer, Curr Treat Options Oncol, 2008, vol. 9: 135-146

5. Liberati, A., Altman, D. G., Tetzlaff, J., Mulrow, C., Gøtzsche, P. C., et al. (2009) The PRISMA Statement for Reporting Systematic Reviews and Meta-Analyses of Studies That Evaluate Health Care Interventions: Explanation and Elaboration. PLoS Med 6(7): e1000100. doi:10.1371/journal.pmed.1000100

6. Welch, V., Petticrew, M., Tugwell, P., Moher, D., O'Neill, J., et al. (2012) PRISMA-Equity 2012 Extension: Reporting Guidelines for Systematic Reviews with a Focus on Health Equity. PLoS Med 9(10): e1001333. doi:10.1371/journal.pmed.1001333

7. Streckmann, F., Kneis, S., Leifert, J. A., Baumann, F. T., Kleber, M., Ihorst, G., L. Herich, Grüssinger, V., Gollhofer, A., Bertz, H.; Exercise program improves therapy-related side-effects and quality of life in lymphoma patients undergoing therapy, Annals of Oncology, Volume 25, Issue 2, 1 February 2014, Pages 493–499, https://doi.org/10.1093/annonc/mdt568

8. Soh, J. Y., Cha, W. C., Chang, D. K., Hwang, J. H., Kim, K., Rha, M., Kwon, H. Development and Validation of a Multidisciplinary Mobile Care System for Patients With Advanced Gastrointestinal Cancer: Interventional Observation Study. JMIR Mhealth Uhealth 2018;6(5):e115. DOI: 10.2196/mhealth.9363. PMID: 29735478

9. Chen, C. E., Mao, A. Y., Murray, J. G., Oran, B., Qazilbash, M. H., Shah, N., Ahmed, S., Bashir, Q., Hosing, C., Shpall, E. J., Steele, J. R., Champlin, R. E., & Parmar, S. (2016). Feasibility of a Smartphone-Based Health Coaching Intervention for Patient Self-Management of Nutrition in the Post-Chemotherapy Setting. Blood, 128(22), 3554. Accessed July 18, 2018. Retrieved from http://www.bloodjournal.org/content/128/22/3554.

10. Wangnum, Kotchukorn & Thanarojanawanich, Thanyaluck & Chinwatanachai, Kwanta & Jamprasert, Lawan & Maleehuan, Onarmon & Janthakun, Vachira. (2013). Impact of the multidisciplinary education program in self-care on fatigue in lung cancer patients receiving chemotherapy. Journal of the Medical Association of Thailand = Chotmaihet thangphaet. 96. 1601-8.

11. Marchand L. Integrative and complementary therapies for patients with advanced cancer. Ann Palliat Med 2014;3(3):161-171. doi: 10.3978/j.issn.2224-5820.2014.07.01

12. Thompson, J., Silliman, K., & Clifford, D. E. (2013). Impact of an early education multimedia intervention in managing nutrition-related chemotherapy side effects: a pilot study. *SpringerPlus*, *2*, 179. http://doi.org/10.1186/2193-1801-2-179

13. Paula Ravasco, Isabel Monteiro-Grillo, Maria Camilo; Individualized nutrition intervention is of major benefit to colorectal cancer patients: long-term follow-up of a randomized controlled trial of nutritional therapy, The American Journal of Clinical Nutrition, Volume 96, Issue 6, 1 December 2012, Pages 1346–1353, https://doi.org/10.3945/ajcn.111.018838

14. Padrnos, L., Mikhael, J., Bennett, R., Kosiorek, H., Dueck, A. C., Northfelt, D. W., Tibes, R., Khera, N., & Mesa, R. A. (2015). Living with Cancer: An Educational Intervention in Cancer Patients Can Improve Knowledge Deficit. Blood, 126(23), 3321. Accessed July 17, 2018. Retrieved from http://www.bloodjournal.org/content/126/23/3321.

15. Padrnos, L., Dueck, A. C., Bennett, R. M., Emanuel, R. M., Mesa, R. A., Northfelt, D., Mikhael, J. R., Glassley, P., & Stigge, R. (2013). Living With Cancer: Assessing The Educational, Symptomatic, and Quality Of Life Impact Of a Comprehensive Patient Symposia On Cancer Patients. Blood, 122(21), 2955. Accessed July 18, 2018. Retrieved from http://www.bloodjournal.org/content/122/21/2955.

16. Lawn, S., Zrim, S., Leggett, S., Miller, M., Woodman, R., Jones, L., Kichenadasse, G., Sukumaran, S., Karapetis, C. and Koczwara, B. (2015), Is self-management feasible and acceptable for addressing nutrition and physical activity needs of cancer survivors?. Health Expect, 18: 3358-3373. doi:10.1111/hex.12327

17. Dabney, J., Bernhard, L., Cherni, K., Kosar, J., Serafin, M., McLellan, L., Visnosky, M., Loejos, L., Curtis, J., & Bolwell, B. (2006). Post-Transplant Education Group Increases Patient Knowledge and Confidence.. Blood, 108(11), 3325. Accessed July 17, 2018. Retrieved from http://www.bloodjournal.org/content/108/11/3325.

18. Chao, Pei-Chun & Chuang, Hui-Ju & Tsao, Li-Yen & Chen, Pei-Ying & Hsu, Chia-Fen & Lin, Hsing-Chun & Chang, Chiu-Yueh & Lin, Cheau-Feng. (2015). The Malnutrition Universal Screening Tool (MUST) and a nutrition education program for high risk cancer patients: strategies to improve dietary intake in cancer patients. BioMedicine. 5. 17. 10.7603/s40681-015-0017-6.

19. Rajkumar, S. V., & Kyle, R. A. (2005). Multiple myeloma: Diagnosis and treatment. Mayo Clinic Proceedings, 80(10), 1371–1382. https://doi.org/10.4065/80.10.1371

20. Boyle, P., Boffetta, P., & Autier, P. (2008). Diet, nutrition and cancer: Public, media and scientific confusion. Annals of Oncology, 19(10), 1665–1667. https://doi.org/10.1093/annonc/mdn561

21. Macaulay, V. M., Middleton, M. R., Protheroe, A. S., Tolcher, A., Dieras, V., Sessa, C., … Soria, J. C. (2013). Phase I study of humanized monoclonal antibody AVE1642 directed against the type 1 insulin-like growth factor receptor (IGF-1R), administered in combination with anticancer therapies to patients with advanced solid tumors. Annals of Oncology, 24(3), 784–791. https://doi.org/10.1093/annonc/mds511

22. Espinoza, M., Perelli, J., Olmos, R., Bertin, P., Jara, V., & Ramírez, P. (2016). Nutritional assessment as predictor of complications after hematopoietic stem cell transplantation. Revista Brasileira de Hematologia e Hemoterapia, 38(1), 7–14. https://doi.org/10.1016/j.bjhh.2015.10.002

23. Patel, A. V., Hildebrand, J. S., Campbell, P. T., Teras, L. R., Craft, L. L., McCullough, M. L., & Gapstur, S. M. (2015). Leisure-time spent sitting and site-specific cancer incidence in a large U.S. Cohort. Cancer Epidemiology Biomarkers and Prevention, 24(9), 1350–1359. https://doi.org/10.1158/1055-9965.EPI-15-0237

24. McCullough, M. L., Teras, L. R., Shah, R., Diver, W. R., Gaudet, M. M., & Gapstur, S. M. (2014). Artificially and sugar-sweetened carbonated beverage consumption is not associated with risk of lymphoid neoplasms in older men and women. Journal of Nutrition, 144(12), 2041–2049 9p. https://doi.org/10.3945/jn.114.197475

25. Teras, L. R., Gaudet, M. M., Blase, J. L., & Gapstur, S. M. (2015). Parental Age at Birth and Risk of Hematological Malignancies in Older Adults. American Journal of Epidemiology, 182(1), 41–48. https://doi.org/10.1093/aje/kwu487

26. Sheean, P. M., Kilkus, J. M., Liu, D., Maciejewski, J., & Braunschweig, C. A. (2017). Incident hyperglycemia, parenteral nutrition administration and adverse outcomes in patients with myeloma admitted for initial autologous stem cell transplant, 48(8), 39–46. https://doi.org/10.1016/j.bbi.2015.08.015.Chronic

27. Miwa, A. (2012). Integrated supportive therapy for multiple myeloma-bone disease treatment, myeloma kidney treatment, cryotherapy, nutrition support team. Nihon Rinsho Geka Gakkai Zasshi. 70 Suppl 2:603-27. Accessed July 26, 2018. Retrieved from https://www.ncbi.nlm.nih.gov/pubmed/23134022

28. Britton, Julie A., Khan, A. E., Rohrmann, S., Becker, N., Linseisen, J., Nieters, A., Kaaks, R., Tjønneland, A., Halkjær, J., Severinsen, M. T., Overvad, K., Pischon, T., Boeing, H., Trichopoulou, A., Kalapothaki, V., Trichopoulos, D., Mattiello, A., Tagliabue, G., Sacerdote, C., Peeters, P. H. M., Bueno-de-Mesquita, H. Bas, Ardanaz, E., Navarro, C., Jakszyn, P., Altzibar, J. M., Hallmans, G., Malmer, B., Berglund, G., Manjer, J., Allen, N., Key, T., Bingham, S., Besson, H., Ferrari, P., Jenab, M., Boffetta, P., Vineis, P., Riboli, E. (2008). Anthropometric characteristics and non-Hodgkin's lymphoma and multiple myeloma risk in the European Prospective Investigation into Cancer and Nutrition (EPIC). Haematologica, 93(11), 1666–1677. https://doi.org/10.3324/haematol.13078

29. Aoyama, T., Imataki, O., Inoue, N., Katsumata, M., Katsuta, T., Kataoka, T., Yoshida, T., Mochizuki, T., Motokawa, S., Tamai, Y., Hagiwara, S., Kawakami, K. (2007) Nutritional pathway for autologous stem cell transplantation. Gan to Kagaku Ryoho. Cancer & Chemotherapy. 34(8):1249-1253. Accessed July 26, 2018. Retrieved from http://www.pieronline.jp/content/article/0385-0684/34080/1249;jsessionid=6u0nb3hheraag.x-sunmedia-live-01

30. Iversen, P. O., Wisløff, F., & Gulbrandsen, N. (2010). Reduced nutritional status among multiple myeloma patients during treatment with high-dose chemotherapy and autologous stem cell support. Clinical Nutrition, 29(4), 488–491. https://doi.org/10.1016/j.clnu.2009.12.002

31. Cueva, K., Cueva, M., Revels, L., & Dignan, M. (2018). Culturally-Relevant Online Education Improves Health Workers' Capacity and Intent to Address Cancer. Journal of Community Health, 0(0), 1–7. https://doi.org/10.1007/s10900-018-0465-5

32. Légaré, F., Stacey, D., Forest, P. G., Coutu, M. F., Archambault, P., Boland, L., Witteman, H. O., LeBlanc, A., Lewis, K. B., Giguere, A. M. C. (2017). Milestones, Barriers and Beacons: Shared Decision Making in Canada Inches Ahead. Zeitschrift Fur Evidenz, Fortbildung Und Qualitat Im Gesundheitswesen, 123–124, 23–27. https://doi.org/10.1016/j.zefq.2017.05.020

33. Kienle, G. S., Mussler, M., Fuchs, D., & Kiene, H. (2016). Individualized Integrative Cancer Care in Anthroposophic Medicine: A Qualitative Study of the Concepts and Procedures of Expert Doctors. Integrative Cancer Therapies, 15(4), 478–494. https://doi.org/10.1177/1534735416640091

34. Ohashi, K. (2015). Empowerment approach to the management of comorbid diabetes and cancer. Nihon Rinsho. Japanese Journal of Clinical Medicine. 73(12):2141-2147. Accessed July 26, 2018. Retrieved from https://europepmc.org/abstract/med/26666166

35. Azétsop, J., & Joy, T. R. (2013). Access to nutritious food, socioeconomic individualism and public health ethics in the USA: A common good approach. Philosophy,

Ethics, and Humanities in Medicine, 8(1), 1–13. https://doi.org/10.1186/1747-5341-8-16

36. Hansra Damien, Ramdial Jeremy, Martinez Gianni, Farooq Faheem, Alfredo Torres, Saravia Diana, Ashwin Mehta and Eugene Ahn. Disparities Between Patient and Hematology/Oncology Physician Expectations for Integrative Oncology in an Ethnically Diverse Population. Blood 2014. 124:2641.

37. Bultijnck R, Van de Caveye I, Rammant E, Everaert S, Lumen N, Decaestecker K, Fonteyne V, Deforche B, Ost P. Clinical pathway improves implementation of evidence-based strategies for the management of androgen deprivation therapy-induced side effects in men with prostate cancer. BJU Int. 2018 Apr;121(4):610-618. doi: 10.1111/bju.

38. Shimizu N, Hatao F, Fukatsu K, Aikou S, Yamagata Y, Mori K, Yamashita H, Nomura S, Seto Y. Results of a nationwide questionnaire-based survey on nutrition management following gastric cancer resection in Japan. Surg Today. 2017 Dec;47(12):1460-1468. doi: 10.1007/s00595-017-1552-4.

39. Zhou Y. Era of enhanced recovery after surgery and robotic gastric cancer surgery. Zhonghua Wei Chang Ke Za Zhi. 2017 May 25; 20(5):495-499.

40. Payne C, Wiffen PJ, Martin S. WITHDRAWN: Interventions for fatigue and weight loss in adults with advanced progressive illness. Cochrane Datanase Syst Rev. 2017 Apr /; 4: CD008427. doi: 10.1002/14651858.CD008427.pub3.

41. Choi AH, O'Leary MP, Merchant SJ, Sun V, Chao J, Raz DJ. Kim JY, Kim J. Complications of feeding Jejunostomy Tubes in Patients with Gastroesophageal Cancer. J Gastrointest Surg. 2017 Feb; 21(2):259-265. doi: 10.1007/s11605-016-3297-6.

42. Parker PA, Banerjee SC, Matasar MJ, Bylund CL, Franco K, Li Y, Levin TT, Jacobsen PB, Astrow AB, Leventhal H, Horwitz S, Kissane DW. Protocol for a cluster randomised trial of a communication skills intervention for physicians to facilitate survivorship transition in patients with lymphoma. BMJ Open. 2016 Jun 28;6(6): e011581. doi: 10.1136/bmjopen-2016-011581.

43. An H, Nho JH, Yoo S, Kim H, Nho M, Yoo H. Effects of Lifestyle Intervention on Fatigue, Nutritional Status and Quality of Life in Patients with Gynecologic Cancer. J Korean Acad Nurs. 2015 Dec; 45(6):812-22. doi: 10.4040/jkan.2015.45.6.812.

44. Beach WA, Dozier DM, Buller MK, Gutzmer K, Fluharty L, Myers VH, Buller DB. The Conversations About Cancer (CAC) Project-Phase II: National findings from viewing When Cancer Calls…and implications for Entertainment-Education (E-E). Patient Educ Couns. 2016 Mar; 99(3):393-399. doi: 10.1016/j.pec.2015.10.008.

45. Hui D, Dev R, Bruera E. The last days of life: symptom burden and impact on nutrition and hydration in patients. Curr Opin Support Palliat Care. 2015 Dec;9(4):346-54. doi: 10.1097/SPC.0000000000000171.

46. Karvinen K, Bruner B, Truant T. The Teachable Moment After Cancer Diagnosis: Perceptions from Oncology Nurses. Oncol Nurs Forum. 2015 Nov; 42(6):602-9. doi: 10.1188/15.ONF.602-609.

47. Flodgren G, Rachas A, Farmer AJ, Inzitari M, Shepperd S. Interactive telemedicine: effects on professional practice and health care outcomes. Cochrane Database Syst Rev. 2015 Sept 7; (9):CD002098. doi: 10.1002/14651858.CD002098.pub2.

48. Suk H, Kwon OK, Yu W. Preoperative Quality of Life in Patients with Gastric Cancer. J Gastric Cancer. 2015 Jun;15(2):121-6. doi: 10.5230/jgc.2015.15.2.121.

49. Gschwendtner KM, Klein G, Güthlin C, Holmberg C, Horneber M, Weis J. Importance of complementary medicine approaches for patients with prostate cancer. Urologe A. 2014 Nov; 53(11):1600-9. doi: 10.1007/s00120-014-3613-2.

50. Adams J, Sibbritt D, Lui CW, Broom A, Wardle J. {Omega}-3 fatty acid supplement use in the 45 and Up Study Cohort. BMJ Open 2013 April 11; 3 (4). pii: e002292. doi: 10.1136/bmjopen-2012-002292. Print 2013.

51. Millar, H., & Davison, J. (2012). Nutrition Education for Osteoporosis Prevention in Men With Prostate Cancer Initiating Androgen Deprivation Therapy. Clinical Journal Of Oncology Nursing, 16(5), 497-503. doi: 10.1188/12.cjon.497-503

52. Del Ferraro, C., Grant, M., Koczywas, M., & Dorr-Uyemura, L. (2012). Management of Anorexia-Cachexia in Late-Stage Lung Cancer Patients. Journal Of Hospice & Palliative Nursing, 14(6), 397-402. doi: 10.1097/njh.0b013e31825f3470

53. Payne, C., Martin, S., & Wiffen, P. (2010). Interventions for fatigue and weight loss in adults with advanced progressive illness. Cochrane Database Of Systematic Reviews. doi: 10.1002/14651858.cd008427

54. Wang, C., Wang, H., Pang, Y., & Yeh, K. (2011). Early nutritional support in non-metastatic stage IV oral cavity cancer patients undergoing adjuvant concurrent chemoradiotherapy: analysis of treatment tolerance and outcome in an area endemic for betel quid chewing. Supportive Care In Cancer, 20(6), 1169-1174. doi: 10.1007/s00520-011-1192-y

55. Teichgräber, U., Pfitzmann, R., & Hofmann, H. (2011). Central Venous Port Systems as an Integral Part of Chemotherapy. Deutsches Aerzteblatt Online. doi: 10.3238/arztebl.2011.0147

56. Kuhnley, R., & Cueva, M. (2011). Learning About Cancer Has Brightened My Light: Cancer Education for Alaska Community Health Aides and Community Health Practitioners (CHA/Ps). Journal Of Cancer Education, 26(3), 522-529. doi: 10.1007/s13187-011-0207-1

57. Farrington, M., Cullen, L., & Dawson, C. (2010). Assessment of oral mucositis in adult and pediatric oncology patients: an evidence-based approach. ORL Head Neck Nurs, 2010 Summer(28(3), 8-15.

58. Brauer, J., El Sehamy, A., Metz, J., & Mao, J. (2010). Complementary and Alternative Medicine and Supportive Care at Leading Cancer Centers: A Systematic Analysis of Websites. The Journal Of Alternative And Complementary Medicine, 16(2), 183-186. doi: 10.1089/acm.2009.0354

59. Wu, X., Wang, Y., Wu, Q., Cheng, W., Liu, W., & Zhao, Y. et al. (2014). HFE interacts with the BMP type I receptor ALK3 to regulate hepcidin expression. Blood, 124(8), 1335-1343. doi: 10.1182/blood-2014-01-552281

60. Omwanghe, O. A., Kwon, S., Muntz, D. S., Montgomery, S., Kemiki, O., Hsu, L. L., Thompson, A. A., & Liem, R. I. (2014). Habitual Physical Activity and Exercise Patterns in Children and Adolescents with Sickle Cell Disease. Blood, 124(21), 4099. Accessed July 26, 2018. Retrieved from http://www.bloodjournal.org/content/124/21/4099.

61. Lee, J., Bang, S., Choi, H. S., Ahn, S., & Lee, J. H. (2012). Prevalence and Risk Factors of Iron Deficiency Anemia in Korea: The Fifth Korean Health and Nutrition Examination Survey (KNHANES V-1). Blood, 120(21), 5170. Accessed July 26, 2018. Retrieved from http://www.bloodjournal.org/content/120/21/5170.

55. Teichgräber, U., Pfitzmann, R., & Hofmann, H. (2011). Central Venous Port Systems as an Integral Part of Chemotherapy. Deutsches Aerzteblatt Online. doi: 10.3238/arztebl.2011.0147

56. Kuhnley, R., & Cueva, M. (2011). Learning About Cancer Has Brightened My Light: Cancer Education for Alaska Community Health Aides and Community Health Practitioners (CHA/Ps). Journal Of Cancer Education, 26(3), 522-529. doi: 10.1007/s13187-011-0207-1

57. Farrington, M., Cullen, L., & Dawson, C. (2010). Assessment of oral mucositis in adult and pediatric oncology patients: an evidence-based approach. ORL Head Neck Nurs, 2010 Summer(28(3), 8-15.

58. Brauer, J., El Sehamy, A., Metz, J., & Mao, J. (2010). Complementary and Alternative Medicine and Supportive Care at Leading Cancer Centers: A Systematic Analysis of Websites. The Journal Of Alternative And Complementary Medicine, 16(2), 183-186. doi: 10.1089/acm.2009.0354

59. Wu, X., Wang, Y., Wu, Q., Cheng, W., Liu, W., & Zhao, Y. et al. (2014). HFE interacts with the BMP type I receptor ALK3 to regulate hepcidin expression. Blood, 124(8), 1335-1343. doi: 10.1182/blood-2014-01-552281

60. Omwanghe, O. A., Kwon, S., Muntz, D. S., Montgomery, S., Kemiki, O., Hsu, L. L., Thompson, A. A., & Liem, R. I. (2014). Habitual Physical Activity and Exercise Patterns in Children and Adolescents with Sickle Cell Disease. Blood, 124(21), 4099. Accessed July 26, 2018. Retrieved from http://www.bloodjournal.org/content/124/21/4099.

61. Lee, J., Bang, S., Choi, H. S., Ahn, S., & Lee, J. H. (2012). Prevalence and Risk Factors of Iron Deficiency Anemia in Korea: The Fifth Korean Health and Nutrition Examination Survey (KNHANES V-1). Blood, 120(21), 5170. Accessed July 26, 2018. Retrieved from http://www.bloodjournal.org/content/120/21/5170.

62. Merkel, D., Balicer, R., Davidovitch, N., Grotto, I., Zarka, S., & Huerta, M. (2007). Population-Based Prevalence of Anemia, Iron, Folic Acid and Vitamin B12 Deficiency among Young Adults in Israel.. Blood, 110(11), 3754. Accessed July 26, 2018. Retrieved from http://www.bloodjournal.org/content/110/11/3754.

63. Peric, Z., Botti, S., Krawczyk, J., van der Werf, S., van Biezen, A., Aljurf, M., Murray, J., Stringer, J., Liptrott, S. J., Greenfield, D. M., Duarte, R. F., Ruutu, T., & Basak, G. W. (2017). Variability of Nutritional Practices in Peritransplant Period after Allogeneic Hematopoietic Stem Cell Transplantation: A Survey By the Complications and Quality of Life Working Party of the EBMT. Blood, 130(Suppl 1), 1954. Accessed July 26, 2018. Retrieved from http://www.bloodjournal.org/content/130/Suppl_1/1954.

64. Padrnos, L. J., Wu, Q., Scherber, R. M., Northfelt, D. W., Mikhael, J. R., Bennett, R. M., Dueck, A. C., & Mesa, R. (2014). Understanding and Information in Cancer Patients: The Impact of a Cancer Symposia on Patient Knowledge. Blood, 124(21), 6011. Accessed July 26, 2018. Retrieved from http://www.bloodjournal.org/content/124/21/6011.

65. Hollenbeak, C., Spackman, E., Page, M. J., Ben-Joseph3, R., & Williamson3, T. (2005). The Prevalence of Metabolic Syndrome in an NHANES Population.. Blood, 106(11), 5589. Accessed July 25, 2018. Retrieved from http://www.bloodjournal.org/content/106/11/5589.

66. Mesa, R. A., Huang, J., Schwager, S., Pardanani, A., Hussein, K., Dingli, D., Jensen, M., Haglind, E., & Tefferi, A. (2007). Hypocholesterolemia Is Independently

Associated with Decreased Survival in Patients with Primary Myelofibrosis: An Analysis of Lipid Profiles in 558 Myeloproliferative Patients.. Blood, 110(11), 2548. Accessed July 25, 2018. Retrieved from http://www.bloodjournal.org/content/110/11/2548.

67. Motyckova, G., Sherman, A. E., Fega, K. R., DeAngelo, D. J., Abel, G. A., Steensma, D., Wadleigh, M., Stone, R. M., & Driver, J. A. (2012). Prospective Cohort Study of Geriatric Assessment in Older Patients with Acute Myeloid Leukemia. Blood, 120(21), 4285. Accessed July 26, 2018. Retrieved from http://www.bloodjournal.org/content/120/21/4285.

68. Lama, B., Jones, R., Barlow, N., & Keenan, R. D. (2016). Geophagia: A Scientific Approach to a Historical Practice to Sustainably Treat Endemic Iron Deficiency in a Rural Community in Nepal. Blood, 128(22), 2346. Accessed July 26, 2018. Retrieved from http://www.bloodjournal.org/content/128/22/2346.

69. Scherber, R. M., Langlais, B. T., Geyer, H., Dueck, A., Kosoriek, H., Johnston, C., Padrnos, L., Palmer, J., Fleischman, A. G., & Mesa, R. A. (2017). Nutrition and Supplement Use Characteristics in the Myeloproliferative Neoplasms: Results from the Nutrient Survey. Blood, 130(Suppl 1), 2193. Accessed July 26, 2018. Retrieved from http://www.bloodjournal.org/content/130/Suppl_1/2193.

70. Aljitawi, O. S., Radel, J., Kimler, B., Eskew, J., Parelkar, N., Swink, M., Garimella, R., Dong, L. I., McGuirk, J., & Vielhauer, G. (2011). The Novel Use of Hyperbaric Oxygen Therapy to Improve Umbilical Cord Blood Stem Cell Engraftment in Irradiated NOD/SCID Mice: What Did We Learn?. Blood, 118(21), 4695. Accessed July 26, 2018. Retrieved from http://www.bloodjournal.org/content/118/21/4695.

71. Suh, K. J., Shin, D., Kim, I., Yoon, S., Lee, J., Bang, S., Kim, K. H., Park, J. H., Park, S. M., Kim, Y., Yun, Y. H., & Koh, Y. (2016). Quality-of-Life and Health Behaviors in Survivors of Acute Leukemia Compared with the General Population: A Population-Based Matched Case-Control Study. Blood, 128(22), 5981. Accessed July 25, 2018. Retrieved from http://www.bloodjournal.org/content/128/22/5981.

72. Motyckova, G., Fega, K. R., Sherman, A. E., DeAngelo, D. J., Abel, G. A., Steensma, D., Wadleigh, M., Stone, R. M., & Driver, J. A. (2012). Geriatric Assessment Variables Add Prognostic Value to the International Prognostic Scoring System. Blood, 120(21), 4933. Accessed July 26, 2018. Retrieved from http://www.bloodjournal.org/content/120/21/4933.

73.Ferlay, J., E. Steliarova-Foucher, J. Lortet-Tieulent, S. Rosso, J. W. W. Coebergh, H. Comber, D. Forman, y F. Bray. «Cancer Incidence and Mortality Patterns in Europe: Estimates for 40 Countries in 2012». *European Journal of Cancer (Oxford, England: 1990)* 49, n.º 6 (abril de 2013): 1374-1403. https://doi.org/10.1016/j.ejca.2012.12.027.

74. National Cancer Institute. https://www.cancer.gov/ last access: 25/09/2018

75. Ailawadhi, Sikander, Pooja Advani, Dongyun Yang, Radhika Ghosh, Abhisek Swaika, Vivek Roy, James Foran, Gerardo Colon-Otero, y Asher Chanan-Khan. «Impact of Access to NCI- and NCCN-Designated Cancer Centers on Outcomes for Multiple Myeloma Patients: A SEER Registry Analysis». Cancer 122, n.º 4 (15 de febrero de 2016): 618-25. https://doi.org/10.1002/cncr.29771.

76. Pulte, Dianne, Adam Gondos, y Hermann Brenner. «Improvement in Survival of Older Adults with Multiple Myeloma: Results of an Updated Period Analysis of SEER Data». The Oncologist 16, n.º 11 (11 de enero de 2011): 1600-1603. https://doi.org/10.1634/theoncologist.2011-0229.

77. Baz R, Lin HM, Hui AM, Harvey RD, Colson K, Gallop K et al. Development of a conceptual model to illustrate the impact of multiple myeloma and its treatment on health-related quality of life. Support Care Cancer. 2015 Feb 24.

78. Jordan K, Proskorovsky I, Lewis P, Ishak J, Payne K, Lordan N et al. Effect of general symptom level, specific adverse events, treatment patterns, and patient characteristics on health-related quality of life in patients with multiple myeloma: results of a European, multicenter cohort study. Support Care Cancer. 2014 Feb;22(2):417-26.

79. Efficace F, Baccarani M, Breccia M, Cottone F, Alimena G, Deliliers GL et al. Chronic fatigue is the most important factor limiting health-related quality of life of chronic myeloid leukemia patients treated with imatinib. Leukemia 2013; 27: 1511–1519.

80. Osborne TR, Ramsenthaler C., de Wolf-Linder S., Schey S, Siegert R, Edmonds P et al. Understanding what matters most to people with multiple myeloma: a qualitative study of views on quality of life. BMC Cancer 2014,14:496

The ITACA-WIICT'18 is a meeting forum for scientifics, technicians and other professionals who are dedicated to Information and communication technologies study and research. Its fundamental scope is to promote the contact among scientific and professionals, improving the cooperation as well as the technological transfer among professionals.

Institute ITACA
Information and Communication Technologies

978-84-09-07373-3